Universität Bonn

Physikalisches Institut

Particle Physics from Singular Geometries

Paul-Konstantin Oehlmann

We study string compactifications on spaces that are either partial or fully singular and analyze the symmetries in the effective theories that they generically give rise to. In the heterotic case we consider orbifolds and their fully singular Landau-Ginzburg phase. Using mirror symmetry we deform back to the orbifold and smooth spaces while keeping track of all enhanced Landau-Ginzburg symmetries and their breakdown. In this way we provide a new tool to calculate R-and non R-symmetries for geometries where the usual methods are hard to apply. We also consider the $\mathbb{Z}_2 \times \mathbb{Z}_4$ orbifold and its properties for phenomenological applications in detail. Analyzing the symmetries of the theory and the effects of Wilson lines provides a generic pattern for the locations of MSSM matter in the orbifold space in order to exhibit phenomenological necessary properties. In the F-theory framework the singularities appear not in the physical compactification but as singularities of elliptic fibrations. We analyze the special of additional sections and multi-sections of the elliptic fibrations that give rise to gauged U(1) and discrete gauge symmetries. We are establishing a link between various fiber realizations and the resulting symmetries and their breakdown in the effective theories. By doing so we reveal new geometries and their properties that yield U(1) symmetries with novel features as well as discrete symmetries. By engineering additional SU(5) singularities in addition to two U(1) symmetries we consider F-theory GUT models relevant for phenomenology. The gauge group is broken down to the standard model with matter parity and the spectrum matches that of the MSSM.

Physikalisches Institut der
Universität Bonn
Nussallee 12
D-53115 Bonn

BONN-IR-2016-02
February 2016
ISSN-0172-8741

Particle Physics from Singular Geometries

Dissertation
zur
Erlangung des Doktorgrades (Dr. rer. nat.)
der
Mathematisch-Naturwissenschaftlichen Fakultät
der
Rheinischen Friedrich-Wilhelms-Universität Bonn

von
Paul-Konstantin Oehlmann
aus
Leipzig

Bonn, 09.03.2015

Dieser Forschungsbericht wurde als Dissertation von der Mathematisch-Naturwissenschaftlichen Fakultät der Universität Bonn angenommen und ist auf dem Hochschulschriftenserver der ULB Bonn http://hss.ulb.uni-bonn.de/diss_online elektronisch publiziert.

1. Gutachter:	Prof. Dr. Hans Peter Nilles
2. Gutachter:	Priv. Doz Dr. Stefan Förste
Tag der Promotion:	19.05.2015
Erscheinungsjahr:	2016

Abstract

We study string compactifications on spaces that are either partial or fully singular and analyze the symmetries in the effective theories that they generically give rise to. In the heterotic case we consider orbifolds and their fully singular Landau-Ginzburg phase. Using mirror symmetry we deform back to the orbifold and smooth spaces while keeping track of all enhanced Landau-Ginzburg symmetries and their breakdown. In this way we provide a new tool to calculate R-and non R-symmetries for geometries where the usual methods are hard to apply. We also consider the $\mathbb{Z}_2 \times \mathbb{Z}_4$ orbifold and its properties for phenomenological applications in detail. Analyzing the symmetries of the theory and the effects of Wilson lines provides a generic pattern for the locations of MSSM matter in the orbifold space in order to exhibit phenomenological necessary properties. In the F-theory framework the singularities appear not in the physical compactification but as singularities of elliptic fibrations. We analyze the special of additional sections and multi-sections of the elliptic fibrations that give rise to gauged U(1) and discrete gauge symmetries. We are establishing a link between various fiber realizations and the resulting symmetries and their breakdown in the effective theories. By doing so we reveal new geometries and their properties that yield U(1) symmetries with novel features as well as discrete symmetries. By engineering additional SU(5) singularities in addition to two U(1) symmetries we consider F-theory GUT models relevant for phenomenology. The gauge group is broken down to the standard model with matter parity and the spectrum matches that of the MSSM.

Acknowledgements

First of all I would like to thank my supervisor Prof. Hans Peter Nilles for giving me the opportunity to work in this extraordinarily fascinating field of physics. In particular I am grateful for the opportunity of writing my master and doctoral thesis in his research group. Since the early stages of my masters he formed my scientific picture considerably by his lectures and views on physics. Moreover I have always enjoyed the rich and open minded atmosphere in his group and the conferences that he allowed me to attend. I also thank Priv. Doz. Stefan Förste for being my second advisor.

I would also like to thank Michael Blaszczyk, Fabian Rühle, Sven Krippendorf, Damian Mayorga, Jonas Reuter, Denis Klevers, Hernan Piragua and Mirjam Cvetič for the nice and fruitful collaborations. Moreover I would like to thank Damian Mayorga, Thorsten Schimannek, Jonas Reuter, Rolf Schneeweiß, Michael Blaszczyk, Annika Reinert and Christoph Liyanage for proof reading the manuscript of this thesis. I am also deeply grateful to all former and current members of the BCTP for providing such an friendly and inspiring atmosphere throughout all years. In that regard I must thank Andreas Wisskirchen and our secretaries Dagmar Fassbender, Petra Weiss, Partricia Zündorf and Christa Börsch for all their hard work to keep the BCTP running. I am especially happy to thank Matthias Schmitz, Damian Mayorga and Michael Blaszczyk for their friendship and great times in and outside of the institute.

However, my biggest thanks go to my family for all their trust and in particular to my mother Illi as well as Heiko for all their support and advices throughout my life and study.

Contents

CHAPTER 1

Introduction

In der Beschränkung zeigt sich erst der Meister,
Und das Gesetz nur kann uns Freiheit geben.

-J.W. von Goethe, Das Sonett

Motivation

One of the most fundamental guidelines of physics is the concept of symmetry. Its success results in connecting seemingly unrelated phenomena by symmetry transformations and hence in the simplification of our physical models. This not only reduces the amount of parameters and makes the theory more elegant but reveals its fundamental entities. The predictive power of the new theory lies then in the possibility to investigate the symmetry *orbit* of the new entities for new phenomena that can be tested in experiments. In the last consequence having revealed these entities form our fundamental picture of nature and its origin.

The concept of symmetries lies at the heart of today's two main pillars of theoretical physics: General relativity (GR) and quantum field theories (QFT).
In special relativity, Einstein first demanded invariance of the speed of light within all reference frames that are connected via Lorentz transformations. This led to the formulation of four-dimensional Minkowski space-time and theories invariant under Lorentz transformations. Generalizing this idea he demanded further that the physical observables should be invariant under general local coordinate transformations as well. In this way the flat Minkowski background was promoted to a dynamical space-time in which gravity emerges from its curvature. Today this theory is extraordinarily well tested and it is the main ingredient underlying models of interstellar and cosmic physics.
In the formulation of microscopic theories of physics, symmetries play an even more crucial role. At such small scales quantum mechanical fluctuations become dominant and symmetries are a necessary way to constrain the fluctuations of the degrees of freedom. In this way we can speak of particles in a quantum theory only properly if they are irreducible representations of the Lorentz group. The representations are labeled by spin 0 and $1/2$ for scalar and fermionic matter fields as well as spin 1 for the force carrier fields.
Including perturbative interactions in a QFT increases the problem of the quantum fluctuations even more severely. Here already the first quantum correction of a process such as electron scattering be-

comes infinitely large.

In the year 1971 t'Hooft showed that these divergences can be treated in a reasonable manner [1] if they can be *renormalized*. In this ground breaking work he showed that renormalization can only be done in a sensible way if the mass of the spin 1 vector bosons that carry the interaction, are protected by a local gauge symmetry. However, it was puzzling how the massive $W^{\pm}$ and Z vector bosons that are the messengers of the electro-weak force could be described. The concept of *spontaneous symmetry breaking* helped out: It says that the theory possesses a symmetry at the fundamental level but the ground state does not. The symmetry breakdown is triggered by the Higgs boson [2] that obtains a vacuum expectation value (VEV) giving mass both to the vector bosons [3] and to fermions. Hence the detection of the Higgs boson in July 2012 at the LHC [4, 5] confirmed not only our conceptual understanding of symmetries and their breakdown but also revealed the last missing piece of the standard model of particle physics.

The standard model of particle physics [6, 7, 8] (SM) is one of the most successful and beautiful theories we have. It is given by the gauge groups

$$\mathrm{SU(3)_C} \times \mathrm{SU(2)_L} \times \mathrm{U(1)_Y}\,.$$

The matter content comes in three copies of massless chiral fermions and the scalar Higgs boson in the representations:

Q	$\bar{u}$	$\bar{d}$	L_i	$\bar{e}$
$(\mathbf{3},\mathbf{2})_{1/6}$	$(\bar{\mathbf{3}},\mathbf{1})_{-2/3}$	$(\bar{\mathbf{3}},\mathbf{1})_{1/3}$	$(\mathbf{1},\mathbf{2})_{-1/2}$	$(\mathbf{1},\mathbf{1})_{1}$

H
$(\mathbf{1},\mathbf{2})_{1/2}$

The 19 parameters that fix the model are consistent with 250 pages of experimental [9] data obtained by the particle physics group to a remarkable degree.

However also the standard model possesses many open questions that need to be answered. First there is the observed neutrino oscillation [10] that cannot be explained with the massless neutrinos of the standard model alone. Moreover there is the problem of the Higgs mass in the standard model: Although this term is renormalizable it undergoes huge quadratic quantum corrections pushing its size to scales close to the Planck scale $\sim 10^{19}$ GeV. Explaining the Higgs mass of ~ 125 GeV requires a very strong tuning of canceling effects that are very unnatural if they could not be explained by the virtue of a symmetry. Furthermore there is evidence that our visible matter is not the only kind of matter in our universe but contains a dark component as well. One evidence for this hypothesis comes from galactic observations: It was found that the rotational velocity of galaxies does not fall off like the visible matter distribution as expected but stays flat, suggesting a large non-baryonic matter component. Further evidence comes from the gravitational lensing effects near colliding galaxies. There the lensing effect revealed huge matter densities away from the visible ones. Another hint comes from the measurement of the temperature fluctuations in the cosmic microwave background (CMB). These fluctuations are extremely sensitive to the the cosmic constituents of the early universe. The perturbations have recently been measured by the PLANCK collaboration [11] to an impressive degree of precision and are well described in the cosmological Λ_{CDM} model. In this model our visible matter accounts only for 4 % of the universes energy density. On the other hand 70 % is contributed by a dark energy and 25 % percent by dark matter.
In addition to the unsatisfactory fact to describe the minor 4 % of the universe's energy density we can ask more questions: Why do we have exactly this gauge group? Why do we have exactly three copies

Gauge group	$SU(3)_C \times SU(2)_L \times U(1)_Y$	$\supset$ SU(5)	$\supset$ SO(10)	$\supset$ E_6
Matter Representation	$Q : (\mathbf{3},\mathbf{2})_{1/6}\,, \overline{u} : (\bar{\mathbf{3}},\mathbf{1})_{-2/3}\,, \nu : (\mathbf{1},\mathbf{1})_1$	**10**	$\overline{\mathbf{16}}$	**27**
	$\overline{d} : (\bar{3},\mathbf{1})_{1/3}\,, L : (\mathbf{1},\mathbf{2})_{-1/2}$	$\overline{\mathbf{5}}$		
	$\nu_r : \mathbf{1}$	**1**		
Higgs Representation	$H_u : (\mathbf{1},\mathbf{2})_{1/2}\,, H_d : (\mathbf{1},\mathbf{2})_{-1/2}$	$\mathbf{5}\,, \overline{\mathbf{5}}$	**10**	

Table 1.1: Unification chain of gauge groups and representations.

of families with so different masses and why do we live in four dimensions? But in addition to those questions one issue is particularly important and hard to answer: What is the microscopic origin of gravity and why is it so much weaker than the other forces?

Up to now it is not possible to turn gravity into a consistent QFT. When we take the flat Minkowski background and quantize the perturbations this implies that gravity is a spin 2 field. However interacting gravity theories cannot be properly renormalized [12]. Thus the notorious divergences cannot be sufficiently controlled which makes it impossible to quantize gravity in the same way as gauge theories. But there are phenomena that need a quantum formulation of gravity: To understand the microscopic nature of black holes makes a quantum gravity necessary. Moreover from the red-shift of nearby galaxies we know that our universe is undergoing an accelerated expansion [13]. First of all this implies that there must have been a point in time when the universe was extremely dense and the quantum nature of gravity was important. Moreover this cosmological expansion can only be caused by a vacuum energy. Calculating such a term does not make any sense in an ordinary quantum field theory where ground state energies are typically around the Planck scale. However the value of the cosmological constant is measured to be 10^{-120} times smaller than the expected Planck scale which is an enormous hierarchy.

There have been many attempts of answering the questions above. The neutrino oscillation can be explained by introducing a right handed neutrino that is uncharged under the standard model gauge group with a a mass around $\sim 10^{16}$ GeV. The problem of the Higgs mass can be alleviated by introducing a new type of symmetry that is supersymmetry (SUSY). SUSY is the unique extension of the Lorentz group that establishes a symmetry between fermions and bosons and unifies these two very different kinds of particles. Thus to enhance the standard model to its minimal SUSY extension (MSSM) we need to more than double the amount of particles: First we need to introduce all SUSY partners for the SM particles but we also need a second Higgs for phenomenological reasons and anomaly freedom of the theory. However SUSY can naturally support a dark matter candidate as the lightest supersymmetric particle. In addition the introduction of SUSY modifies the running of all gauge coupling parameters in the standard model such that they meet at a scale of $\sim 10^{16}$ GeV almost perfectly. This is a hint to another unification of all three gauge groups into one common group such as SU(5) [14] and coincides with the right handed neutrino mass. This unification can indeed answer the question why we have exactly this structure of gauge groups and matter in the SM:
Gauge group unification comes with a partial family unification, whereas one family of the SM is represented by a **10** and one $\overline{\mathbf{5}}$-plet representation. The chain of unification can be pushed even more forward to SO(10) where one complete family plus the right handed neutrino can be described in one representation and full unification of matter and Higgses is realized in a **27**-plet of E_6 depicted in Table 1.1. The above picture also comes with its own problems. First of all grand unified groups predict the existence of operators that lead to fast proton decay that can only be controlled by invoking additional symmetries.

Then SUSY has not been observed yet and thus must be spontaneously broken. The breaking of SUSY however is not unique and should be explained by an additional extension of the theory. Moreover the masses term of the two Higgses, relevant for triggering the electro-weak symmetry is the only mass scale in addition to the Planck scale in the theory. Hence again there is a hierarchy between two widely separated scales. In addition we find more tensions in the unified picture of such SUSY GUTs: From the matter table 1.1 it becomes clear that the MSSM Higgses descent from **5** and $\bar{\mathbf{5}}$-plets of SU(5) that also contribute additional triplet states. These triplets lead to proton decay if they do not get a large mass. However they descend from the same multiplet as the Higgses and hence should have the same mass as them which contradicts our requirement for light Higgses. Hence we need a way to treat those triplets differently than the Higgs doublets although they come from the same representation.

All of above attempts center around the unification of the gauge interactions only but have nothing to say about gravity. The introduction of (exact) SUSY implies the vanishing of the ground state energy which removes the UV divergence. There are general arguments about quantum theories of gravity that state that all global symmetries should be gauged [15, 16, 17] and that gravity can only be renormalized by the inclusion of an infinite tower of higher massive spin fields (e.g. see [18]. Hence when we found SUSY for example in the upcoming LHC run then we knew that in a theory of quantum gravity it should be gauged. Doing so yields theories that includes spin 3/2 and a spin 2 super partner and are called super gravities (SUGRA) (i.e. see [19]). Although these theories are still not renormalizable it shows the natural role of SUSY in a quantum theory of gravity.

The invention of string theory is the closest to a quantum gravity we have come so far. It results from promoting the point like particle to a two dimensional string. The two dimensional string world sheet is by consistency a supersymmetric and conformal field theory (CFT). It is also consistency that fixes the target space dimensionality to be ten and a massless spin two field is automatically included in the spectrum. In flat space we have full control over the conformal field theory (CFT) and we can compute the whole massless and infinite tower of massive string states as demanded by a theory of quantum gravity. In the perturbative regime we have five different string theories whereas the cancellation of anomalies includes gauge interactions [20] for the heterotic string theories directly.

In the year 1995 Witten [21, 22] showed that all of these string theories are connected via a web of dualities. For example weakly coupled Type IIA string theory can look exactly like strongly coupled Type IIB. Furthermore he showed that these theories descend from an eleven dimensional theory called M-theory. M-theory is believed to be a theory of M2 and M5 branes that are even higher dimensional generalizations of strings. However, a perturbative formulation is not known but only the eleven dimensional SUGRA limit when the branes are shrunk to point like objects. Hence we should think of strings not as the fundamental objects but as the appearing dominant degrees of freedom in certain regimes of the M-theory star, depicted in Figure 1.1. In 1996 [23] Vafa formulated F-theory in which non-perturbative aspects of Type IIB string theory and partially the heterotic string are encoded in the geometry of an auxiliary torus. In that sense F-theory is located in the bulk of the M-theory star and allows us to investigate strongly coupled string theories.

However, to connect the ten dimensional string theory to our four dimensional world we have to deal with the six residual ones. The standard approach goes back to the idea of Kaluza and Klein in which a fifth dimensions was compactified on a circle with small radius. But taking the simplest alternative for string theory i.e. compactification on six circles would lead to theories that have more than one super symmetry generator which implies a non-chiral theory. But thanks to the build in dynamics of gravity

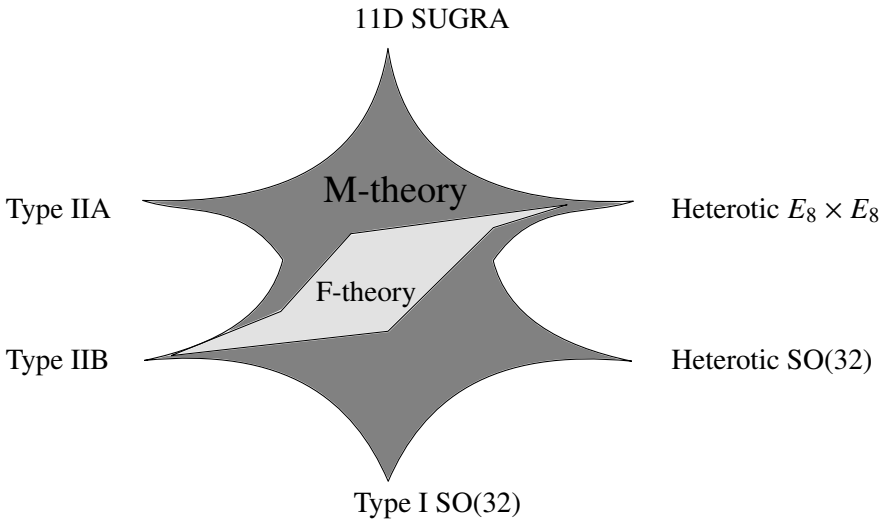

Figure 1.1: The M-theory theory star and the string theories at corners boundaries.

and thus geometry into string theory there is a one to one correspondence between properties of the compactification space and the resulting symmetries of the four dimensional theory.
To obtain a supersymmetric theory that includes chiral fermions we need to compactify on Calabi-Yau (CY) spaces. However, this is by far not a unique choice and hence the landscape of four dimensional compactifications is extremely huge.
Hence a major program in string theory is to understand the properties of that string landscape and to find the spot that can describe our world i.e. the SM model.

For particle model building the $E_8 \times E_8$ heterotic string theory is particularly well suited as the two exceptional group factors naturally provide a subgroup for grand unified gauge factors. However it is very hard to quantize the heterotic string on these spaces, such that only the SUGRA approximation of the string can be used. Certain (partially) singular limits of smooth CY spaces called orbifolds are an alternative as they are essentially flat apart from some singularities. This makes it possible to quantize the string and to use the powerful CFT techniques.
Another interesting starting point for models of particle physics is F-theory. There the grand unified group can be engineered as a stack of branes on which strings can stretch along giving rise to gauge group and matter. Due to its similarity to the heterotic string it is also possible to obtain exceptional group structures that are not possible in perturbative Type IIB models. Actually one can show that these structures are needed even if only SU(5) grand unified theories are considered in order to generate a large top-quark Yukawa coupling.

Outline

This thesis considers two patches of the M-theory star: The first half centers around the heterotic string while the second one focuses on F-theory. The heterotic string on orbifolds is of great interest due to its CFT description that gives access to the full string theory spectrum and offers a wide range of continuous and discrete symmetries which can help to control interactions of phenomenologically relevant models. In computer based searches many models with interesting phenomenology for particle physics

have been constructed within the $\mathbb{Z}_{6-II}$ geometry the so called Mini-Landscape [24]. In particular the construction of all orbifold spaces and the refined analysis of R-symmetries on these spaces were an active field of research in the past years[25, 26, 27]. In our approach we want to consider particle model building on orbifolds in a more systematic way and analyze whether there are general patterns of orbifold models that descend from phenomenological requirements and apply them to the $\mathbb{Z}_2 \times \mathbb{Z}_4$ geometry. In addition we want to investigate orbifold models from a very different perspective: Using the gauged linear sigma model description we can smoothly interpolate between various different geometrical and non-geometrical regimes. In particular in the Landau-Ginzburg phase the whole geometry is completely singular. There we can compute the full massless spectrum and its symmetries to get additional insights into the origin of discrete symmetries and their breakdown in various geometric regimes.
In a similar context we want to consider F-theory and its potential for model building. Here we want to consider the possibility for additional symmetries such as U(1) or discrete remnants thereof that are generically much harder to understand in F-theory as the non-Abelian gauge factors. By using various techniques of algebraic geometry we want to analyze the structures that allow for these additional symmetries in F-theory. After having investigated possibilities to engineer SU(5) theories we explore them and the resulting particle phenomenological properties.

Chapter 2 is intended as an introduction to the heterotic string theory. We first give the ten dimensional heterotic string theory and its spectrum, introduce Calabi-Yau compactifications and their properties as well as details of orbifold compactifications. We highlight the orbifold singularities and how string states get localized at these points. Moreover we comment on symmetries such as discrete non-Abelian flavor symmetries and R-symmetries. We exemplify this in the simple $\mathbb{Z}_3$ orbifold example that we reconsider from a different perspective in Section 4.2.4 again.
In **Chapter 3** we are interested in particle physics model building on the $\mathbb{Z}_2 \times \mathbb{Z}_4$ geometry that has not been considered before. In order to do so we introduce its geometry and give particular emphasis to its discrete symmetry structure. Using the automorphisms of the E_8 gauge lattice we construct all inequivalent gauge embeddings systematically. Additionally we give a qualitative analysis of Wilson line effects at each fixed point that specify the string model. This analysis is the starting point to which we add phenomenological constraints such as three families, a large top-quark Yukawa coupling and the requirement for light Higgses.
This approach results in a general pattern of where the MSSM matter should be localized in the geometry that we exemplify in a concrete toy model. These results are very general and explain the findings of the computer based Mini Landscape searches.
With the orbifolds we have discussed spaces that are partially singular. In **Chapter 4** we are considering spaces that are fully singular but have a description as so called Landau-Ginzburg Orbifolds (LGO). To consider those spaces we first introduce them by considering Gauged Linear Sigma Models (GLSM) that can be seen as an effective UV description of the string world sheet theory. In a first example we consider a GLSM that exhibits the $\mathbb{Z}_3$ orbifold phase and then interpolate further down to the LGO phase. There we shortly review the methods [28, 29] used to calculate the full massless spectrum. After that we generalize the results from [30] to obtain the R-symmetry of the four dimensional theory and provide a new method to obtain all other discrete and gauge symmetries of the four dimensional effective field theory. Furthermore we perform a full scan over all A_1^9 Gepner models and construct their full massless spectrum. We encounter the phenomenon of mirror symmetry and find models with various amounts of super symmetries that all satisfy a common relation. After that we go back to the $\mathbb{Z}_3$ example and use mirror symmetry to describe the $\mathbb{Z}_3$ orbifold phase as a deformation of the mirror dual LGO. We match the spectrum both from the deformation of the world sheet theory and by Higgsing the four dimensional effective theory where the VEV parametrizes the orbifold size. Finally we give a more exotic example

that describes a $\mathbb{Z}_3$ orbifold on an E_6 lattice in the geometric regime. Here we show the breaking of the R-symmetry as we go to the orbifold point. Moreover we show that two non-R symmetries survive the transition to the smooth Calabi-Yau phase.

In the second part of this work we turn to F-theory compactifications. Here the physical space is smooth but the non-trivial gauge interactions and matter content is completely encoded in the singularity structure of the auxiliary torus which is going to be the main object of our considerations. **Chapter 5** again serves as an introduction in which we review the general construction of the torus and how gauge interactions, matter spectrum and Yukawa couplings are obtained. To do that we have a look at the torus structure or more generally the elliptic curve and its constructions as hypersurfaces in various ambient spaces. We give specific emphasis to the rational points and multi-points of the elliptic curve and show how the first ones lead to U(1) gauge symmetries when the elliptic curve is promoted to a fibration. All introduced techniques and concepts are made clear throughout this chapter by considering the example of the elliptic curve in $BL_3\mathbb{P}^2$ over a general base. In the end we arrive at a six dimensional $\mathcal{N} = 1$ SUGRA that has the exact MSSM gauge group and particle representations of the MSSM. Furthermore we give all six dimensional anomaly constraints that the model obeys, and check explicitly for gravitational ones. Moreover we review various constructions to engineer additional higher gauge symmetries, i.e. SU(5) groups first within the local approach of the spectral cover but also the so called *tops*.
In **Chapter 6** we consider specific transitions between F-theory models and their corresponding SUGRA theories. We introduce a network structure between F-theory compactifications in which the fiber is realized as a hypersurface in one of the 16 classic 2D reflexive polyhedra. We first introduce the notion of a *toric Higgsing* in which we make the geometric and physical transitions explicit. To be completely concrete we stick to a specific base in which we perform the actual Higgsing. We use this approach in order to describe geometries with novel features: First we find models with a non-toric rational section leading to matter that carries three charge quanta of a U(1) for the first time in F-theory. We also show that our Higgsing chain leads to models with discrete symmetries. We show the connection of multi-sections to discrete symmetries of the SUGRA theory and propose a way to calculate the charges geometrically. Finally we comment on the full structure of the network in which it appears that mirror symmetry in the fiber interchanges the role of discrete and quotient symmetry factors.

In **Chapter 7** we then turn to phenomenological applications of F-theory SU(5) models with additional U(1) symmetries. After giving an overview of the approaches in the literature we sum up our model building search strategy by scanning over different flux configurations. We use these fluxes to break down to the standard model and generate a chiral 4D spectrum constrained by 4D anomaly considerations. We discuss models with up to two U(1) gauge factors and compare those obtained from the spectral cover as well as models from SU(5) *top* constructions. We find models with the precise matter spectrum of the standard model and nice phenomenological features that can be explained by the $\mathbb{Z}_2$ matter parity that we have in our VEV configuration.
In **Chapter 8** we sum up the results of this thesis and state the open problems and directions for future research.

List of publications

Parts of this work have been published in scientific Journals

- D. K. M. Pena, H. P. Nilles and P. K. Oehlmann, "A Zip-code for Quarks, Leptons and Higgs Bosons," JHEP **1212** (2012) 024 [arXiv:1209.6041 [hep-th]].
- D. Kaloni Mayorga Pena and P. K. Oehlmann, "Lessons from an Extended Heterotic Mini-Landscape," PoS Corfu **2012** (2013) 096 [arXiv:1305.0566 [hep-th]].
- S. Krippendorf, D. K. Mayorga Pena, P. K. Oehlmann and F. Ruehle, "Rational F-Theory GUTs without exotics", JHEP **1407** (2014) 013 [arXiv:1401.5084 [hep-th]].
- D. Klevers, D. K. M. Pena, P. K. Oehlmann, H. Piragua, J. Reuter, "F-Theory on all Toric Hypersurface Fibrations and its Higgs Branches", arXiv: 1408.4808 [hep-th]

CHAPTER 2

Particle Physics from the Orbifolded Heterotic String

In this chapter we review the basic concepts of the heterotic string in ten dimensions that we introduce in chapter 2.1. To make contact with four dimensional theories that exhibit $\mathcal{N} = 1$ supersymmetry we consider Calabi-Yau (CY) compactifications and introduce their properties in section 2.2. However our main attention is devoted to orbifold spaces which are much easier to control than smooth Calabi-Yau spaces because they are limits where non-trivial curvature is concentrated to certain fixed points of an otherwise flat space. Although this space has singular points string theory is well defined on those spaces. Orbifolds will be our first example of a partially singular space and its relation to enhanced symmetries.
In section 2.3 we give special attention to orbifolds and their fixed point structure as well as the particle physics and symmetries that can be obtained from them in order to lay the grounds for the subsequent chapters.

2.1 The Heterotic String in 10 D

In string theory the point like particles are promoted to two dimensional strings. Hence also the particles world line when embedded into a given target space is promoted to a two dimensional world sheet (WS). The world sheet theory gives a super conformal field theory (SCFT) specified by the two WS coordinates σ and τ that are combined into light-cone coordinates $\sigma_\pm = \sigma \pm \tau$, and a bosonic and fermionic field content X^J and ψ^K that depend on the light cone coordinates. The heterotic string is a closed string theory with the following WS action in the bosonic formulation

$$S = \frac{1}{\pi}\int d^2\sigma (2\partial_+ X^\mu \partial_- X_\mu + i\psi^\mu_+ \partial_- \psi_{\mu,+} + \partial_+ X^I_- \partial_- X_{I,-}) \,, \tag{2.1}$$

with $\mu = 0,\ldots,9$ and $I = 1,\ldots,16$. In the above action we have already used, that we can split up the WS fields into a left and right moving parts that only depend on the former light cone coordinate,

supported by the following equation of motion

$$\partial_+\partial_-\frac{1}{2}\left(X_+(\sigma_+)+X_-(\sigma_-)\right)=0\,,$$
$$\partial_-\psi_+(\sigma_+)=0\,.$$

The characterizing feature of the heterotic string is that we have only ten Majorana-Weil fermions $\psi_+(\sigma_-)$ and bosons $X^\mu_+(\sigma_-)$ that are related by WS supersymmetry on the right hand side but 26 bosons on the left handed one. The heterotic string has its name precisely from the combination of the two different dimensional theories on left and right moving side. Left and right moving bosonic coordinates recombine to ten target space coordinates X^μ that give the embedding of the WS into the target space whereas the residual 16 are not dynamical and specify the gauge sector from the target space perspective. The WS coordinates are subject to the closed string boundary conditions that read

$$X^\mu(\sigma+2\pi)=X^\mu(\sigma)\,,$$
$$\psi^I(\sigma+2\pi)=\pm\,\psi^I(\sigma)\,,$$

with positive Ramond (R) and negative Neveu-Schwarz (NS) fermion boundary conditions. The residual 16 left-moving bosonic degrees of freedom need to be compactified on a sixteen torus constructed by modding out a lattice Λ_{16}. The WS only needs to close upon a lattice translation $X^I_-(\sigma_+ + 2\pi) = X^I_-(\sigma_+) + \lambda$ with $\lambda \in \Lambda_{16}$. By single valuedness of the wave function, that comes with a factor of e^{iPX}, we find that also the internal momenta P must be quantized in the dual lattice Λ^*. Modularity of the one-loop partition function constrains the lattice to be even, uni-modular and selfdual. It is a fascinating fact that those constraints can only be satisfied by the $E_8 \times E_8$ and SO(32) root lattices.
In the following we concentrate on the case of $E_8 \times E_8$ as a gauge group. There the momenta P lie in the E_8 lattice given by

$$P\in(n_1,n_2,n_3,n_4,n_5,n_6,n_7,n_8)\,,\quad P\in(n_1+\frac{1}{2},n_2+\frac{1}{2},n_3+\frac{1}{2},n_4+\frac{1}{2},n_5+\frac{1}{2},n_6+\frac{1}{2},n_7+\frac{1}{2},n_8+\frac{1}{2})\,,$$

with the n_i satisfying

$$n_i\in\mathbb{Z}\,,\sum_i n_i=0 \bmod 2\,.$$

The left and right moving bosonic modes can be written in a Fourier expansion as

$$X^\mu_\pm=\frac{1}{2}x^\mu+\frac{1}{2}p^\mu(\sigma\pm\tau)+\frac{i}{2}\sum_{n\in\mathbb{Z},n\neq0}\frac{1}{n}\alpha_n e^{2\pi i\sigma_\pm}\,, \tag{2.2}$$

and similarly in the Ramond and Neveu-Schwarz sector we have the fermion expansions of the form

$$\begin{array}{lll}\psi^\mu_+ = & \sum_{n\in\mathbb{Z}} & d^\mu_n e^{-2\pi i\sigma_+}\quad (R)\,,\\ \psi^\mu_+ = & \sum_{n+1/2\in\mathbb{Z}} & b^\mu_n e^{-2\pi i\sigma_+}\quad (NS)\,.\end{array} \tag{2.3}$$

Upon quantization we promote the oszillator modes to operators satisfying the following (anti-)commutation relations:

$$\left[\alpha^{\mu}_{m,\pm}, \alpha^{\nu}_{n,\pm}\right] = m\delta_{m+n,0}\eta^{\mu,\nu}\delta_{\pm,\pm}\,, \tag{2.4}$$

$$\left\{d^{\mu}_{m}, d^{\nu}_{n}\right\} = m\delta_{m+n,0}\eta^{\mu,\nu}\,, \tag{2.5}$$

$$\left\{b^{\mu}_{m}, b^{\nu}_{n}\right\} = m\delta_{m+n,0}\eta^{\mu,\nu}\,. \tag{2.6}$$

In the two dimensional $\mathcal{N} = (0,1)$ theory the Fourier modes of the energy momentum tensor $L_{n,\pm}$ and the modes of the the right moving supercurrent in F_s and G_t for R and NS boundary conditions respectively generate the super Virasoro algebra. It is specified in the Ramond sector as

$$[L_m, , L_n] = (m-n)L_{m+n} + \frac{D}{8}m^3\delta_{m+n,0}\,, \tag{2.7}$$

$$[L_m, F_n] = \left(\frac{m}{2} - n\right)F_{m+n}\,, \tag{2.8}$$

$$\{F_m, F_n\} = 2L_{m+n} + \frac{D}{2}m^2\delta_{m+m,0}\,, \tag{2.9}$$

and in the NS sector

$$[L_m, , L_n] = (m-n)L_{m+n} + \frac{(D-2)}{8}m(m^2-1)\delta_{m+n,0}\,, \tag{2.10}$$

$$[L_m, G_t] = \left(\frac{m}{2} - t\right)F_{m+n}\,, \tag{2.11}$$

$$\{G_s, G_t\} = 2L_{s+t} + \frac{(D-2)}{2}(s^2 - \frac{1}{4})\delta_{m+m,0}\,. \tag{2.12}$$

Absence of spurious states in the spectrum fixes the amount of contributing fields D to be fixed to 26 left moving bosons and 10 for the supersymmetric right movers, which we took as the Ansatz in the construction of the heterotic action.

Physical states

In the following we construct physical states by choosing all negative oscillator modes of the WS fields as creation operators that act on the vacuum for left and right moving parts of the theory independently. A physical state then has to obey the constraint that it is annihilated by all positive modes of all the above operators. As the L modes are the modes of the energy momentum tensor their zero mode L_0 can be interpreted as the WS Hamiltonian. [1]

The right movers give the ten dimensional space-time representations of a physical state. As we are interested in massless states mainly, we choose light cone gauge for the target space coordinates to fix two target space coordinates $X^{\pm} = X^0 \pm X^1$. The residual 8 coordinates transform in the vector representation of the SO(8) little group of the target space. Note however that the Ramond ground state forms a spinor representation[2] while the NS one is bosonic. In the following we write the bosonic and

[1] Quantization leads to a normal ordering ambiguity that leads to a shift in the L_0 modes for the NS sector.

[2] This can be seen by noting that the Ramond ground state is an eigenstate of the fermionic zero modes that precisely satisfy, up to a scaling the 10D Clifford algebra.

fermionic modes of the two sectors as convenient SO(8) weight vectors

$$q_s = (\pm\frac{1}{2}, \pm\frac{1}{2}, \pm\frac{1}{2}, \pm\frac{1}{2}), \tag{2.13}$$

$$q_v = (\underline{\pm 1, 0, 0, 0}), \tag{2.14}$$

whereas the spinor representation has an even amount of negative signs and the underline specifies the permutation of all vector representation entries. Finally a physical state is given by the tensor product of left and right moving states that both have to obey the left and right moving mass equations i.e. to be a zero mode of the $L_{0,\pm}$ operator:

$$\frac{M_-^2}{4} = \frac{P^2}{2} + N_- - 1 = 0, \tag{2.15}$$

$$\frac{M_+^2}{4} = \frac{q^2}{2} + N_+ - \frac{1}{2} = 0 \tag{2.16}$$

In the above mass equation the left and right moving oszillator number operators appear that have the usual form

$$N_- = \sum_{n=1}^{\infty} \alpha^{\mu}_{-n,-}\alpha_{n,\nu,-} + \alpha^{I}_{-n,-}\alpha_{n,I,-}, \tag{2.17}$$

$$N_+ = \sum_{n=1}^{\infty} \alpha^{\mu}_{-n,+}\alpha_{n,\nu,+}. \tag{2.18}$$

By the commutation relation each negative oszillator α^{μ}_{-n} contributes n quanta of energy.
In this way we can construct on the left and right moving side of the theory the states and compute their individual mass contribution. A physical state must be a direct product of the two sectors and fulfill the following requirements:

- As the combination of the Virasoro modes $L_{0,-} - L_{0,+}$ are the generators of WS rotations. As we have a closed string theory each state should be annihilated by this operators. As the L_0 is the WS Hamiltonian this means that each state has to contribute the same energy from the left and right moving side, called *level matching condition*. In particular for a string state at rest, the masses on each side have to agree $M_+ = M_-$.

- In two dimensions we have the possibility to take two WS fermions and combine them into a WS boson, called bosonization. In order for a state to respect that symmetry we have to project onto states with an even number of fermion modes $(-1)^F$ which is the GSO projection. This projection ensures space-time super symmetry.

The ten dimensional spectrum
In the following we give the resulting massless spectrum of the ten dimensional $E_8 \times E_8$ heterotic string in terms of string states. The space time $\mathcal{N} = 1$ SUGRA multiplet is given as

$$|q_v\rangle \otimes \alpha_{-1,\mu}|0\rangle \begin{cases} g_{\mu\nu} & \text{graviton} \\ B_{\mu\nu} & \text{two form field} \\ \phi & \text{dilaton} \end{cases}, \qquad |q_s\rangle \otimes \alpha_{-1,\mu}|0\rangle \begin{cases} \Psi_\mu & \text{gravitino} \\ \psi & \text{dilatino} \end{cases}$$

and the super Yang-Mills multiplet

$$\left.\begin{matrix}|q_v\rangle \otimes \alpha^I_{-1}|0\rangle \\ |q_v\rangle \otimes |P\rangle\end{matrix}\right\} A_\mu \quad \text{gauge bosons}\,, \qquad \left.\begin{matrix}|q_s\rangle \otimes \alpha^I_{-1}|0\rangle \\ |q_s\rangle \otimes |P\rangle\end{matrix}\right\} \lambda \quad \text{gauginos}$$

We note that we do not have any chiral states in the spectrum but only the SUGRA and pure $E_8 \times E_8$ super Yang-Mills multiplet.

This ten dimensional theory is going to be the underlying theory that we want to compactify down to four dimensions. We start by giving the simplest way of doing so by taking the simple six circle reduction. First we observe the decomposition of the SO(8) little group into the space-time part and the internal part:

$$\mathrm{SO}(8) \to \mathrm{U}(1) \times \mathrm{SU}(4)_\mathrm{R}\,. \tag{2.19}$$

The U(1) factor can be identified with the helicity of the uncompactified spacetime directions but in addition we are left with an $\mathrm{SU}(4)_R$R-symmetry. From the decomposition of non-trivial SO(8) representations we can easily find the non-trivial decompostion into non-trivial $\mathrm{SU}(4)_\mathrm{R}$ representations as well that makes up the $\mathcal{N} = 4$ SUSY representations in four dimensions.
When we consider the four dimensional gravitino Ψ_μ with helicity $\pm\frac{3}{2}$ we find the following combinations descending from the ten dimensional one

$$q_{\text{gravitino}}: \pm(\frac{3}{2}; \pm\underline{\left(\frac{1}{2}, \frac{1}{2}\right)}, \frac{1}{2})\,. \tag{2.20}$$

Hence there are actually four gravitini in four dimensions which results in $\mathcal{N} = 4$ SUGRA. Similarly we find for the $N = 1$, 10D vector multiplets given by the weight $q_v = (\underline{\pm 1, 0, 0, 0})$ that it breaks to one vector and six scalars in 4D forming the bosonic components of the $\mathcal{N} = 4$ super Yang-Mills vector multiplet. We have seen that the $\mathrm{SU}(4)_\mathrm{R}$ plays the role of the four dimensional R-symmetry of the $\mathcal{N} = 4$ theory. To arrive at a theory with chiral fermions we have to reduce the theory to at least $\mathcal{N} = 1$. Such a theory can at most have an Abelian R-symmetry and hence we have to reduce the internal symmetries considerably to arrive at such a theory. A way to achieve that is by compactification on a Calabi-Yau manifold that we want to discuss in the following section.

2.2 Calabi-Yau manifolds

In this section we want to introduce some more formal aspects of smooth Calabi-Yau manifolds one- , two- and tree folds and their properties. Although we do not always consider smooth spaces throughout this thesis they oftentimes share important properties with smooth counterparts.

Calabi-Yau properties
In general a Calabi-Yau manifold is defined to be a complex n-dimensional manifold Y_n which is Kähler and possesses a unique nowhere vanishing closed $(n, 0)$-form. Due to that we can write the total space as a direct product $Y \times \{\mathbb{1}\}$ that has a global nowhere vanishing (n,0) form that we call Ω. However we can always write a $(n, 0)$ as a product $f\Omega$) with f being a function on Y. In the case that the function is holomorphic and Y is compact f can only be the constant function [31]. Hence the space of holomorphic (n,0) forms on Y must be one dimensional. However, it can be shown that there exist many definitions

that are equivalent to the one above.
It can be shown [31] that any manifold with nowhere vanishing $(n, 0)$-form has to have a vanishing first Chern class $c_1 = 0$ that is defined as

$$c_1(Y_n) = \frac{1}{2\pi}\mathcal{R}\,, \tag{2.21}$$

with $\mathcal{R}$ being the $(1, 1)$ Ricci tensor. The vanishing of the first Chern class implies that the space has to be Ricci flat. Note that $c_1(Y_n)$ is in general defined as its canonical class and hence a Calabi-Yau has to have a trivial canonical class.
The Ricci tensor on the other hand can be constructed using the Levi-Cevita connection, that generates the parallel transport when moving along the manifold. As we deal with complex manifolds, the connection generates parallel-transports within the U(n) group that preserves the complex structure of the space. Vanishing Ricci tensor implies that we have to restrict on the traceless part of the connection that is SU(n). The group in which a vector field on a manifold can be rotated by parallel transport is called holonomy hence it is said that a CY must have SU(n) holonomy. The holonomy is the best way to see the connection to the $\mathcal{N} = 1$ condition that we demanded in the beginning: There we have seen that the 10D gravitino is a spinor field in the internal components. However demanding SU(3) holonomy for a three fold results in the breaking of SU(4) to its SU(3) commutant group which can be at most a U(1). Hence only one gravitino is invariant i.e. *covariantly constant* which results in $\mathcal{N}$=1 SUSY[3].

In the following we want to consider the conditions and relations of CY manifolds a bit more:
We start by introducing the space of r-dimensional differential forms that are closed i.e. annihilated by a total derivative. But we want to restrict ourselves to those closed forms that are equivalent up to an exact form i.e. those that are total derivatives of $r - 1$ forms. Those forms are a topological quantitiy of the manifold they are living in measured by the de Rham cohomology

$$H^r(Y) = \frac{\text{set of closed } r\text{-forms}}{\text{set of exact } r\text{-forms}}\,. \tag{2.22}$$

If the space admits a complex structure we can split up the forms above into a holomorphic p and anti-holomorphic part q. We can then introduce the Dolbeault cohomology in the same sense as above:

$$H^{p,q}Y = \frac{\text{set of closed } (p,q)\text{-forms}}{\text{set of exact } (p,q)\text{-forms}}\,, \tag{2.23}$$

where such a form carries p holomorphic and q holomorphic indices. The dimension of the cohomology above is given by the Hodge numbers $h^{p,q}$ which are related to the total dimension as $r = p + q$ forms via the Betti numbers of Y_n as follows

$$b_r(Y) = \sum_{p+q=r} h^{p,q}(Y)\,. \tag{2.24}$$

Next we want to deduce all Hodge numbers of a general Calabi-Yau. We can complex conjugate differential forms leading to the relation of the the Hodge numbers $h^{p,q} = h^{q,p}$. We can further use duality transformation to restrict the Hodge numbers more: There is the Hodge star operation $*$ that gives an isomorphism between (p,q) and $(n - q, n - q)$-forms and hence $h^{p,q} = h^{n-p,n-q}$. For more details on the

[3] If we take a manifold with the SO(6) holonomy we could also break all gravitini, as in the case of a six-sphere. However this space is not Ricci-flat.

action of the Hodge star, see [31]. We first demand the CY to be simply connected which is the same as $b_1 = 0$.[4] By using (2.24) we find $h^{1,0} = h^{0,1} = 0$. Furthermore we can use more duality transformation to restrict the Hodge numbers more: First we have the Hodge star operation $*$ that gives an isomorphism between (p,q) and $(n-p, n-q)$ forms and hence $h^{p,q} = h^{n-p,n-q}$. By complex conjugation we can also obtain $h^{p,q} = h^{q,p}$.
At next we can use *Serre duality* to deduce more Hodge numbers: This duality relates the bundles E over Y_n as

$$H^p(Y_n, E) = H^{n-p}(Y, E \times K_Y^*)\,, \tag{2.25}$$

whereas K_Y is the canonical class of Y. As the canonical class of a CY is trivial, we find $h^{p,0} = h^{0,n-p}$.

These operations make it possible to deduce the full form of the Hodge diamond. In the following we want to discuss which Hodge structures we can expect for CY one, two and three-folds. Lets consider first the unique CY manifolds in one and two dimensions. For $n = 1$ the unique CY is the torus. As we have $h^{1,0} = 1$ we also must have $h^{0,0} = h^{0,1} = h^{1,1} = 1$.

For the complex two dimensional case there is the K3 manifold which is also unique. Here by the same arguments $h^{2,0} = h^{0,2} = 1$. By using that a K3 is simply connected it follows that $h^{1,0} = h^{0,1} = 0$. Then we find again that all but $h^{1,1}$ is fixed by the above dualities. However by introducing a bit more technology we can fix this Hodge numbers as well. At first we introduce the *Chern character* of a bundle E given by the exponentiation of its form F that we can expand in the formal sum of classes

$$c(E) = e^{\frac{iF}{2\pi}} = 1 + c_1(E) + c_2(E) + c_3(E) + ... \tag{2.26}$$

with the c_i being the i-th Chern class. Each Chern class corresponds to a sum of (i,i)-forms.
Throughout this work we use the fact that we can describe a CY manifold Y_n as the restriction of an embedding space X onto a subspace of it using polynomial constraints $P_Y = 0$. In this case we can calculate the Chern classes using the *adjunction formula* given by

$$c(Y) = \frac{c(X)}{1 + c(\mathcal{O}(P_Y))}\,, \tag{2.27}$$

whereas we divide the Chern class of the space X by the class of the bundle $\mathcal{O}$ in which the polynomial equation transforms in. By expanding the above formulas in the numerator and denominator we can read off the Chern classes of the total space. By doing so we find that $c_1(Y) = c_1(X) - c_1(\mathcal{O}(P_Y))$. Hence in order to ensure that the whole space has vanishing first Chern class we have to demand that the defining Polynomial P_Y transforms in the canonical bundle of the ambient space X. At next we introduce the Euler number χ. The Euler number can be calculated from the top Chern class, i.e. the integration over the highest non-vanishing Chern class. Furthermore, the Euler number can be computed from the betty numbers b_i as

$$\chi(M) = \sum_{i=0}^{n} (-1)^i b_i\,. \tag{2.28}$$

Using that technology we can fix all Hodge numbers of the $K3$ manifold. First we can integrate the top

[4] We demand this in order to ensure that there are not graviphoton modes in the low energy theory. However it is possible that the CY may have a non trivial first fundamental class that can be finite. Then the space is not simply connected but still does not contribute b_1's.

Chern class which results in the Euler number $\chi_{K3} = 24$ as one can easily verify (i.e. see [32]). Using that $b_0 = 1$ and that $b_1 = 0$ we find $b_2 = 22$. From $h^{2,0} = h^{0,2} = 1$ we find $h^{1,1} = 20$. The Hodge diamond is given in Figure 2.1.

$$\begin{array}{ccccc} & & h^{0,0} & & \\ & h^{1,0} & & h^{0,1} & \\ h^{2,0} & & h^{1,1} & & h^{0,2} \\ & h^{1,2} & & h^{2,1} & \\ & & h^{2,2} & & \end{array} \quad = \quad \begin{array}{ccccc} & & 1 & & \\ & 0 & & 0 & \\ 1 & & 20 & & 1 \\ & 0 & & 0 & \\ & & 1 & & \end{array}$$

Figure 2.1: The Hodge diamond of K3, the unique CY two-fold.

Finally we come to the three dimensional case. By the definition there is $h^{3,0} = 1$. By the usual line of argumentation we can deduce all but two Hodge numbers that are $h^{1,1}$ and $h^{2,1}$. Furthermore by using (2.28) we can infer

$$\chi = 2(h^{1,1} - h^{2,1}) \,. \tag{2.29}$$

Lets finally get back and have a closer look at heterotic $E_8 \times E_8$ Calabi-Yau compactifications on a CY. In the heterotic case we have the field strength H of the antisymmetric B-field that is constructed from the ten dimensional gravity multiplet. Due to gravitational and gauge anomalies [33] the H field strength is corrected to

$$H = dB + \omega_{3,\text{Spin}} - \omega_{3,\text{Gauge}} \,, \tag{2.30}$$

that has the Bianchi identity

$$dH = \text{Tr}(R \wedge R) - \text{Tr}(F \wedge F) = 0 \,, \tag{2.31}$$

where F is the field strength of the internal gauge fields. The above constraint is the low energy version of the stringy requirement to preserve modularity of the one-loop partition function that we encounter in the next section. The general solution to the Bianchi identity is hard to solve but there is an easy solution by simply setting $\omega_{3,\text{Spin}} = \omega_{3,\text{Gauge}}$. This solution is called the *standard embedding* and it implies that we embed the SU(3) holonomy valued spin connection as a vector bundle into one E_8 gauge factor. By this embedding the E_8 is broken to its SU(3) commutant that is E_6. To obtain information about the representations we can expand the E_8 adjoint into its $E_6 \times SU(3)$ subgroup:

$$\mathbf{248} \to (\mathbf{78}, \mathbf{1}) \oplus (\mathbf{1}, \mathbf{8}) \oplus (\mathbf{27}, \mathbf{3}) \oplus (\overline{\mathbf{27}}, \overline{\mathbf{3}}). \tag{2.32}$$

Here we see that the $\overline{\mathbf{27}}$ transforms as the fundamentals of the SU(3) and the $\mathbf{27}$ in the anti-fundamental. Remembering that we have set the SU(3) gauge bundle *equal* to the tangent bundle TY and that $h^{1,1}$ is the dimension of

$$H^1(Y, TY) \,, \tag{2.33}$$

and that TY transformed in the SU(3) gauge structure. Hence we find that the number of chiral $(\mathbf{27}, \mathbf{3})$ representations is given by the Hodge numbers $h^{1,1}$. Similarly we find that $h^{1,2}$ is given by two powers

of the SU(3) bundle (and its antisymmetrization)

$$H^1(Y,(TY)^2)\,. \tag{2.34}$$

Antisymmetrization of the SU(3) fundamentals gives exactly the anti-fundamental representation such that $h^{2,1}$ counts exactly the $(\overline{\mathbf{27}},\overline{\mathbf{3}})$ representation. Hence in the standard embedding, the CY geometry completely fixes the chiral spectrum that transforms non-trivially under the E_6. We should keep this correspondence always in mind in particular when we consider spaces that are not smooth anymore and thus the above methods do, strictly speaking not apply anymore. However these singular spaces are often connected to the smooth ones in a way that keeps the chiral E_6 representations invariant. Hence these representations give us an idea on what the underlying smooth or partial singular phase of a given space is going to be. Furthermore we encounter in Chapter 4 the phenomenon of *mirror-symmetry* that interchanges the Hodge numbers $h^{1,1}$ and $h^{2,1}$ along with the interpretation of Kähler and complex structure moduli.

2.3 Heterotic Strings on Orbifolds

As general smooth CY spaces are usually very complicated and in most of the cases the metric is not known making it impossible to quantize string theory on these spaces. The fact that they are basically flat apart from exceptional points is a main benefit of orbifolds over smooth CY spaces [34].
An orbifold can be obtained as the second step after the torus compactification by taking the quotient with a point group $\mathcal{P}$ of the torus lattice Λ_6 to

$$\mathbb{R}^6 \xrightarrow{\text{Compactification}} \frac{\mathbb{R}^6}{\Lambda_6} \xrightarrow{\text{Orbifolding}} \frac{\mathbb{R}^6}{\Lambda_6 \ltimes \mathcal{P}} = \frac{\mathbb{R}^6}{\mathbb{S}}\,, \tag{2.35}$$

where we have defined the space group $\mathbb{S}$. The main constraint on the twistings $\theta \in \mathbb{P}$ that we mod out is to lie within a subgroup of the SU(3) holonomy that we have mentioned before. When we complexify $\mathbb{R}^6$ to $\mathbb{C}^3$ the coordinates are given by $z^a = X^{2a-1} + iX^{2a}$ and coordinates are identified upon $g \in \mathbb{S}$ acting as

$$gz = \theta z + n_a e_a\,, \tag{2.36}$$

where $e_a \in \Lambda_6$ and θ is a twisting. The twist can be diagonal embedded into the Cartan subalgebra of SU(3) to

$$\theta = \mathrm{diag}(e^{2\pi i v_N^1}, e^{2\pi i v_N^2}, e^{2\pi i v_N^3})\,. \tag{2.37}$$

To guarantee a discrete action and to have determinant one, we get the constraints on the shift vectors v^i:

$$N v_N \in \mathbb{Z}\,, \quad v_N^1 + v_N^2 + v_N^3 \in \mathbb{Z}\,. \tag{2.38}$$

The second constraint fixes one of the shift components implying that we can mod out only two independent $\mathbb{Z}_N$ actions at a time.[5] But also note, that by writing the coordinates into three complex coordinates we have already implied a factorized form of the orbifold action. However the orbifold actions do not necessarily need to act diagonally in the three complex directions. These orbifolds are

[5] Of course both shift actions then need to be compatible with each other.

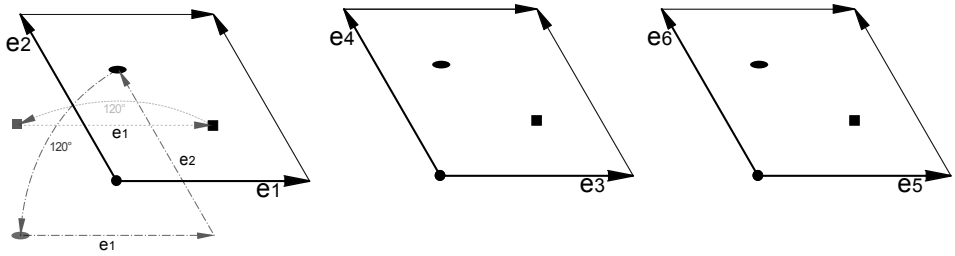

Figure 2.2: The 27 inequivalent fixed points of the $\mathbb{Z}_3$ orbifold. In the first torus we have depicted the action of the space group on the fixed points as well.

called *non-factorizable* and their treatment especially of the CFT is more involved as one can not use the holomorphicity of the coordinates.
In addition we can have lattice translations accompanied by a twist, so called *Roto-translations* that have been fully classified only recently [25]. Single twist orbifolds generically can have orders $N = 2, 3, 4, 6, 7, 8$ and 12, whereas two twist orbifolds have orders

$$(N, M) \in (2,2), (2,4), (2,6), (3,3), (3,6), (4,4), (6,6)\,.$$

As a first example, that will also reappear in Chapter 4, we consider the classic example [34, 35] of the $T^6/\mathbb{Z}_3$ orbifold. We choose the factorisable $SU(3)^3$ root lattice with the shift vector $v_3 = (\frac{1}{3}, \frac{1}{3}, -\frac{2}{3})$. The twist action is a 120^o rotation in all tori. The orbifolding procedure is depicted in Figure 2.2 as well as the action of the space group that leaves the fixed points of the first torus invariant. A main feature of orbifolds is the appearance of fixed points under the space group action defined by

$$z_f = g z_f\,, \tag{2.39}$$

$$\Leftrightarrow z_f = (\mathbb{1} - \theta^k)^{-1} n_a e_a,\,. \tag{2.40}$$

The last equation shows that a fixed point can equivalently be represented by a generating space group element $g(\theta^k, n_a e_a)$. Furthermore one can show that a fixed point results in a deficit angle given by the difference to the orbifold twist

$$2\pi(\mathbb{1} - \theta)\,. \tag{2.41}$$

This in particular tells us, that the fixed point is a curvature singularity and hence a first example of a singular space.
However string theory is well defined on such spaces. The overall flat structure makes it still possible to quantize the string on orbifolds and gives access to the full CFT description.
Identification of points upon an space group element $g(\theta^k, n_a e_a)$ naturally induces new sectors, where strings can close upon space group twistings

$$Z^i(\tau, \sigma + 2\pi) = \left(g(\theta^k, n_a e_a) Z\right)^i (\tau, \sigma) \tag{2.42}$$

$$= z_f^i + \frac{i}{2} \sum_{n \neq 0} \left(\frac{1}{n + k v^i} \alpha^i_{n + k v^i, +} e^{i(n + k v^i)\sigma_+} + \frac{1}{n - k v^i} \alpha^i_{n - k v^i, +} e^{i(n - k v^i)\sigma_-} \right). \tag{2.43}$$

and similar for the left moving fermions:

$$\psi^i_+(\theta, \sigma_+ + 2\pi) = \left(g(\theta^k, n_a e_a)Z\right)^i (\tau, \sigma_+) \tag{2.44}$$

$$= \sum_{m\in\mathbb{Z}} \left(\omega^i_{m+kv^i} e^{-i(m+v^i)\sigma_+}\right) , \tag{2.45}$$

in the Ramond sector and with m being half integer in the NS sector. There are several important things we have to note here: First the identification acting on the center of mass coordinates enforces the string to stay at a fixed point/plane and the momentum to vanish. Hence we can interpret the *twisted string* to be wound around a fixed point. The other important observation is the twisting of the bosonic and fermion oscillator modes. The (anti-)commutators of the modes are still the same

$$\left[\alpha^i_{n+kv^i}, \alpha^j_{m-kv^j}\right] = \delta^{i,j}(n + kv^i)\delta_{m+n,0} , \tag{2.46}$$

$$\left\{\omega^i_{n+kv^i}, \omega^j_{m-kv^j}\right\} = \delta^{i,j}\delta_{m+n,0} , \tag{2.47}$$

but with an additional shift in the energy contribution.
The above shifting proceeds completely analogous to the additional 16 left moving bosons. This embedding on the other hand is not arbitrary but required by consistency of the theory. Invariance of the one-loop partition function under modular transformations demands the embedding of the space group $\mathbb{S}$ into the gauge degrees of freedom $\mathbb{S} \hookrightarrow \mathcal{G}$:

$$g(\theta^k, n_a e_a) \hookrightarrow (kV_N, n_a A_\alpha) , \tag{2.48}$$

that acts on the 16 bosons as the following shift[6]

$$X^I(\sigma_+ + 2\pi) = X^I(\sigma_+) + kV^I_N + n_a A_a . \tag{2.49}$$

The shift vector V_N is associated to the the twists, whereas the A_a are called *Wilson lines* as they are associated with a gauge twist by going around a non-contractible cycle of the torus. The embedding must be a proper homomorphism and as such, we have the conditions on the twists that follow from the embedding:

$$g(\theta, 0)^N = g(\mathbb{1}, 0) \quad \hookrightarrow \quad NV_N \in \Lambda_{\mathrm{E}_8\times\mathrm{E}_8} , \tag{2.50a}$$

$$g(\theta, 0) \cdot g(\mathbb{1}, e_\beta) = g(\theta, e_\alpha) \quad \hookrightarrow \quad A_\alpha = A_\beta , \tag{2.50b}$$

$$g(\theta, e_\alpha)^{K_\alpha} \stackrel{!}{=} g(\theta^{K_\alpha}, 0) \quad \hookrightarrow \quad K_\alpha A_\alpha \in \Lambda_{\mathrm{E}_8\times\mathrm{E}_8} . \tag{2.50c}$$

The first equation restricts the shifts to be an N fractional of an $\mathrm{E}_8 \times \mathrm{E}_8$ lattice vector. In the second equation we find, that Wilson lines get identified when lattice vectors gets mapped onto each other by

[6] Note that also non-shift embeddings are possible [36].

an orbifold rotation. The modularity conditions on the Wilson lines and shifts are summarized as

$$N(V_N^2 - v^2) = 0 \bmod 2\,, \tag{2.51a}$$
$$M(V_M^2 - w^2) = 0 \bmod 2\,, \tag{2.51b}$$
$$M(V_N V_M - v \cdot w) = 0 \bmod 2\,, \tag{2.51c}$$
$$K_\alpha(A_\alpha \cdot V_{N/M}) = 0 \bmod 2\,, \tag{2.51d}$$
$$K_\alpha A_\alpha^2 = 0 \bmod 2\,, \tag{2.51e}$$
$$\gcd(K_\alpha, K_\beta)(A_\alpha \cdot A_\beta) = 0 \bmod 2 \text{ for } \alpha \neq \beta\,. \tag{2.51f}$$

There is a particular embedding that we discuss in some detail in the following, the standard embedding given by setting the geometric shift equal the three components of the gauge shift:

$$V_N = (v_N^i, 0^5)(O^8)\,. \tag{2.52}$$

In Chapter 4 we use that these compactifications can be described by a world sheet theory with enhanced $(2,2)$ supersymmetry that yields generically an unbroken $\mathrm{E}_6 \times \mathrm{E}_8$ gauge symmetry in the target space. Having specified the geometric and gauge shift v_N, w_M and V_N, V_M we can give the shifted mass equation for a state in the twisted sector corresponding to an element $g(\theta^k \cdot \omega^l\, n_a e_a)$ to be

$$\frac{M_+^2}{8} = \frac{1}{2}(\underbrace{P + kV_N + lV_M + n_a A_a}_{P_{\mathrm{sh}}})^2 + \tilde{N} - 1 + \delta_c\,, \tag{2.53}$$
$$\frac{M_-^2}{8} = \frac{1}{2}(\underbrace{q + kv_N + lw_M}_{q_{\mathrm{sh}}})^2 - \frac{1}{2} + \delta_c\,, \tag{2.54}$$

with the vacuum energy contribution

$$\delta_c = \frac{1}{2}\sum_i^3 w_i(1 - w_i), \text{ using } w^i = kv^i \bmod 1 \text{ with } 0 \leq w^i \leq 1\,. \tag{2.55}$$

By the above formulas we can arrange the massless left-and right-movers again as a direct product space of the two Hilbert spaces, $|q_{\mathrm{sh}}\rangle \otimes \alpha^i_{n-\omega}|P_{\mathrm{sh}}\rangle = |g\rangle$ that we call $\mathcal{H}_g$ emphasizing the generating element $g \in \mathbb{S}$.
However, a string with twisted boundary conditions

$$Z(\tau, \sigma + 2\pi) = gZ(\tau, \sigma)\,, \tag{2.56}$$

might also satisfy the same condition, after multiplying by another space group element $h \in \mathbb{S}$

$$hZ(\tau, \sigma + 2\pi) = g(hZ)(\tau, \sigma)\,, \tag{2.57}$$

if $[h, g] = 0$. Hence the mode expansion is exactly the same and we find states, that satisfy the same mass equation. This state must belong to the same Hilbert space, however it can lead to a non-trivial *orbifold phase* that removes the state: From rewriting a state as a vertex operator we can observe the

following shift of a state upon conjugation by an h element with a phase ϕ that is given by

$$\phi = e^{2\pi i(P_{\text{sh}}\cdot V_h - (q_{\text{sh}} - N + \tilde{N})\cdot v_h)} \underbrace{e^{-\pi i\left(V_g\cdot V_h - v_g\cdot v_h\right)}}_{\phi_{\text{vac}}} . \tag{2.58}$$

Here V_h and v_h are the combined shifts depending on the order of (possibly multiple) twists of the conjugation element. We have also highlighted the specific contribution of the vacuum phase ϕ_{vac}. Such a phase is induced by all elements of the centralizer of a given constructing element

$$\mathcal{Z}_g = \{h \,|\, [h, g] = 0 \,\forall h \in \mathbb{S}\} \,, \tag{2.59}$$

and a physical state must have a trivial phase under all those elements.

2.3.1 Orbifold symmetries

As the orbifold is a free CFT it is possible, at least in principle, to compute all n-point correlation functions. We are interested in the ones who can be interpreted as Yukawa couplings. These correlators have been analyzed in [37]. Generically the correlator splits into multiple parts that can be identified with field theory selection rules.

- **Gauge invariance** is enforced by

$$\sum_i^n = P_{\text{sh},i} = 0 \,, \tag{2.60}$$

  where i labels the i-th particles shifted gauge momentum.

- **Space group invariance** is encoded by checking

$$(\mathbb{1}, 0) \in \prod_r^n [g_r] \,. \tag{2.61}$$

  We note that checking for the above condition might be a bit more involved, because we can equally take any constructing element g_r of a constructing element conjugated by any element of the space group $h \in \mathbb{S}$ with $hgh^{-}1 \in [g]$. Generically the above constraint gives a discrete symmetry. But in many cases it happens, that fixed points are equivalent when Wilson lines are switched off. In the case when fixed points are equivalent this induces an additional permutation symmetry. This permutation symmetry enhances the discrete symmetry to a non-Abelian group. In the following and in Chapter 3 we give examples of the flavor symmetry in the $\mathbb{Z}_3$ and $\mathbb{Z}_2 \times \mathbb{Z}_4$ orbifold geometries. In some examples it was shown in [38] that the flavor symmetry can be extracted from gauged U(1) symmetries that gets broken by the orbifold procedure. In Chapter 4 we see, how the flavor symmetries can be obtained from gauged symmetries[7].

- **H-Momentum Conservation** enforces to have a conserved q_{sh} in each orbifold plane and reads

$$\sum_{r=1}^{n} \left(q_{\text{sh},r}^{i,\text{bos}}\right) = -1 + N_+^i \quad \text{for } i = 1, 2, 3 \,, \tag{2.62}$$

[7] There are general arguments that in a consistent theory of quantum gravity that all global symmetries must descend from gauged symmetries [39]

with N_+^i the right moving oszillator number. However H-momentum conservation is a specific property of a correlation function itself and does not directly allow to assign a certain quantum number to a state.

- **R-charge conservation** can be understood as a remnant of the internal 6D Lorentz symmetry that might be preserved by the compactification. These are usually interpreted as sub lattice rotations. In the case of factorizable orbifolds, these sub lattice rotations are most conveniently written into a block diagonal form, very similar to the orbifold action:

$$\rho = \mathrm{diag}(e^{2\pi i\zeta^1}, e^{2\pi i\zeta^2}, e^{2\pi i\zeta^3})\,. \tag{2.63}$$

A string n-point correlator can be conjugated by the above element but only when the states satisfy

$$\sum_{r=1}^{n}\left(\sum_{i=1}^{3}\zeta^i\left(q^{i,\mathrm{bos}}_{\mathrm{sh},r} - N^i_r + \overline{N}^i_r\right) - \gamma_{h_{gr}}\right) = -\sum_{i=1}^{3}\zeta^i \bmod 1\,. \tag{2.64}$$

For $\sum_{i=1}^{3}\zeta^i \neq 0$ the above condition looks precisely like an R-symmetry. Note that we sum over the quantum numbers of the bosonic-superpartner of the left-chiral states and hence, $-\sum_{i=1}^{3}\zeta^i$ determines the R-charge of the 4D superpotential.
It is worth mentioning, that the R-charge is not only determined by the pure geometric part of the orbifold but is corrected by the $\gamma_{h_{gr}}$-phase of a state which also includes non-trivial information about gauge quantum numbers. This fact was observed in [26, 27] and results in an anomaly universal R-charge.

2.3.2 An example: the $\mathbb{Z}_3$ orbifold

Before we turn to the $\mathbb{Z}_2\times\mathbb{Z}_4$ orbifold in the next chapter, we complete the discussion on the $\mathbb{Z}_3$ orbifold which is one of the most classic string compactification[34, 35] space. We choose the $\mathrm{SU}(3)^3$ root lattice as the torus lattice and the orbifold twist and gauge twist to be given as

$$v_3 = (\frac{1}{3},\frac{1}{3},-\frac{2}{3}) \quad V_3 = (\frac{1}{3},\frac{1}{3},-\frac{2}{3},0^5)(0^8)\,, \tag{2.65}$$

where we have chosen the standard embedding. Due to the identifications

$$\mathrm{e}^{2\pi i v^a} e_{2a-1} = e_{2a} \quad \text{for } a = 1,2,3\,, \tag{2.66}$$

we can switch on one order three Wilson line in the a-th torus which however would bring us away from the standard embedding. We find only one independent twisted sector generated by $g(\theta,0)$ because the second twisted sector is simply the inverse $g'(\theta^2,0) = g^{-1}$ and carries the CPT conjugated states of the first one.
In the untwisted sector the mass equation is not shifted and this corresponds to the original 10D theory reduced by the orbifold projection. We have summarized the states that survive the projection in Table 2.1. We find indeed only one gravitino as we expect for an $\mathcal{N}=1$ theory. We note that there are 9 moduli. In particular the three diagonal moduli that are given when the -1 in q is at the j-th position,parametrize continuous deformations of the three torus radii. Furthermore we find six more *off-diagonal* Kähler

D=10 state	projection condition	resulting states	Name
$\|q\rangle \otimes \alpha^i_{-1}\|0\rangle$	$q \cdot v_3 = 0 \bmod 1$	$\| \pm 1,0,0,0\rangle \otimes \alpha^\mu_{-1}\|0\rangle$	Gravity Multiplet
		$\pm\|\frac{1}{2},\frac{1}{2},\frac{1}{2},\frac{1}{2}\rangle \otimes \alpha^\mu_{-1}\|0\rangle$	Gravitino
		$\|0,\underline{-1,0,0}\rangle \otimes \alpha^j_{-1}\|0\rangle$	9 (bosonic) Kähler moduli
		$\|-\frac{1}{2},\underline{-\frac{1}{2},\frac{1}{2},\frac{1}{2}}\|0\rangle \otimes \alpha^j_{-1}\|0\rangle$	9 (fermionic) Kähler moduli

Table 2.1: Orbifold of the 10D SUGRA multiplet.

deformations that correspond to lattice deformations that respect the $\mathbb{Z}_3$ orbifold action[8]. Also note that there are no complex structure moduli corresponding to $|0,\underline{1,0,0}\rangle \otimes \alpha^j_{-1}|0\rangle$ fields.
When we turn to the gauge group we observe that a 4D vector state $q_v = (\pm 1,0,0,0)$ has only one SUSY partner $q_s = \pm(\frac{1}{2},\frac{1}{2},\frac{1}{2},\frac{1}{2})$ on the left movers side, hence we confirm that the gauge multiplet contains only one gaugino, as we expect it from an $\mathcal{N}=1$ theory in 4D. The projection on the right moving states is given by the additional constraint $V_3 \cdot P = 0 \bmod 1$ and leads to the following states:

$$
\begin{aligned}
|q_v\rangle \otimes \alpha^I_{-1}|0\rangle \quad & 16 \text{ Cartan Elements}\,, \\
|q_v\rangle \otimes |P_1\rangle \quad & 6 \text{ SU(3) roots with } P_1 = (\underline{1,-1,0},0^5)\,, \\
|q_v\rangle \otimes |P_1\rangle \quad & 40 \text{ roots with } P_1 = ((0,0,0),\underline{(\pm 1,\pm 1,0,0,0)})\,, \\
|q_v\rangle \otimes |\tilde{P}_1\rangle \quad & 32 \text{ roots with } \tilde{P}_1 = (\pm(\frac{1}{2},\frac{1}{2},\frac{1}{2}),(\pm\frac{1}{2})^5)\,, \\
|q_v\rangle \otimes |P_2\rangle \quad & P_2 \text{ 240 roots of } E_8^2\,.
\end{aligned}
$$

In total the first E_8 breaks down to $SU(3) \times E_6$ while the second one stays intact.
The untwisted chiral matter on the other hand is obtained from the right-mover $q_s = (\underline{-\frac{1}{2},-\frac{1}{2},\frac{1}{2},\frac{1}{2}})$ states that have a non-trivial weight P to satisfy for the constraint $q \cdot v - P \cdot V_3 = 0 \bmod 1$. The resulting states and their quantum numbers are summarized in Table 2.2.
We can proceed in a similar manner for the twisted sector states that have the constructing elements $g(\theta, n_a e_a)$. As there is no Wilson line, we find the same shift, and the same projection conditions for every fixed point and hence we find the same spectrum at every fixed point. The invariant left moving shifts are given as

$$
q^{\text{bos}}_{\text{sh}} = (0,\frac{1}{3},\frac{1}{3},\frac{1}{3})\,, \quad q^{\text{fer}}_{\text{sh}} = (\frac{1}{2},-\frac{1}{6},-\frac{1}{6},-\frac{1}{6})\,. \tag{2.67}
$$

The positive first factor in $q^{\text{fer}}_{\text{sh}}$ indicates that we have found a right-handed fermion and its bosonic superpartner. For the above right mover, we find 27 left movers that survive the orbifold projection making up a $(\overline{\mathbf{27}},\mathbf{1},\mathbf{1})$ representation. Furthermore there are three oszillator solutions involving three P_{sh} solutions that survive the orbifold projection. These states lead to three $(\mathbf{1},\overline{\mathbf{3}},\mathbf{1})$ states.
Before we sum up all the states, we also discuss the flavor symmetry along the lines of [40]. For this it is sufficient to consider only one $T^2/\mathbb{Z}_3$ plane. Lets consider first states from the first twisted sector. Here a state corresponds to an constructing element $g(\theta, ne_1)_r$ and from the point group element it becomes clear that an invariant coupling must involve at least three of them in order to be allowed. In the following it is convenient to rewrite the generating elements as sublattice $(\mathbb{1} - \theta)\Lambda$ equivalent vectors. As Λ is generated by e_1 and e_2 the sublattice is generated by $e_1 - e_2$ and $3e_2$. Hence we can

[8] The CPT complementary states are given by an overall sign change of the states.

represent the three fixed point generating elements as $g(\theta,0)$, $g(\theta,e_1)$ and $g(\theta,e_1+e_2)$ just via $g(\theta,me_1)$ with m=0,1,2.
At next we take the product of n constructing elements of states

$$\prod_r^n g(\theta,m^r e_1) = g(\theta^n,\sum_r^n m^r e_1)\,, \tag{2.68}$$

where the lattice part can only be trivial when $\sum_i^n = 0 \bmod 3$ and hence we also get a $\mathbb{Z}_3$ family symmetry here. By the above rewriting, we give the fixed points a label i.e. a family quantum number. But when there is no Wilson line switched on, all fixed points are equivalent up to permutations. This is why we have to take the *semi-direct* product with the permutation group S_3. Hence we find the resulting group

$$S_3 \ltimes (\mathbb{Z}_3 \times \mathbb{Z}_3) = \Delta(54)\,. \tag{2.69}$$

The untwisted sector fields give trivial **1** representations and the twisted ones form triplet states **3**. Similarly as for SU(3) [9] there is an invariant combination $\mathbf{1} \in \mathbf{3}\cdot\mathbf{3}\cdot\mathbf{3}$ given by an anti-symmetrization. The total flavor group is obtained by recombining the parts of each orbifold plane. Hence we obtain three $\Delta(54)$ factors. However we have to remember that there is only one independent $\mathbb{Z}_3$ orbifold rotation. Thus we have to divide by two of them such that the total flavor group is given by $\Delta(54)^3/\mathbb{Z}_3^2$ that lie in the centers of the $\Delta 54$. The final part is the R-symmetry that is generated by the individual sub lattice rotations $e^{\frac{2i\pi}{3}}$ in each torus, demanding the 4D super potential to have R-symmetry charge

$$Q_R(\mathcal{W}) = (-1,-1,-1) \bmod 3\,. \tag{2.70}$$

However, we note that in 4D there is only one independent R-charge and that the orbifold identification should remove one discrete symmetry that one can choose for example as the diagonal sum of the three symmetries. Then there are two residual non-R symmetries whereas one is redundant by the orbifold action. The whole spectrum, including all quantum numbers is summarized in Table 2.2. Clearly the

$E_6 \times SU(3) \times E_8$ rep.	$\Delta(54)^3/\mathbb{Z}_3$ flavor Rep.	R-charge
$(\mathbf{27},\bar{\mathbf{3}},\mathbf{1})$	$(\mathbf{1},\mathbf{1},\mathbf{1})$	$(-1,0,0)$
$(\mathbf{27},\bar{\mathbf{3}},\mathbf{1})$	$(\mathbf{1},\mathbf{1},\mathbf{1})$	$(0,-1,0)$
$(\mathbf{27},\bar{\mathbf{3}},\mathbf{1})$	$(\mathbf{1},\mathbf{1},\mathbf{1})$	$(0,0,-1)$
$(\mathbf{27},\mathbf{1},\mathbf{1})$	$(\bar{\mathbf{3}},\bar{\mathbf{3}},\bar{\mathbf{3}})$	$(-\frac{1}{3},-\frac{1}{3},-\frac{1}{3})$
$(\mathbf{1},\mathbf{3},\mathbf{1})$	$(\bar{\mathbf{3}},\bar{\mathbf{3}},\bar{\mathbf{3}})$	$(\frac{2}{3},-\frac{1}{3},-\frac{1}{3})$
$(\mathbf{1},\mathbf{3},\mathbf{1})$	$(\bar{\mathbf{3}},\bar{\mathbf{3}},\bar{\mathbf{3}})$	$(-\frac{1}{3},\frac{2}{3},-\frac{1}{3})$
$(\mathbf{1},\mathbf{3},\mathbf{1})$	$(\bar{\mathbf{3}},\bar{\mathbf{3}},\bar{\mathbf{3}})$	$(-\frac{1}{3},-\frac{1}{3},\frac{2}{3})$

Table 2.2: Summary of the charged spectrum of the standard embedding $\mathbb{Z}_3$ orbifold.

above spectrum and geometry is very simple which makes this orbifold a nice playground to study the heterotic string and its features. In Chapter 4 we come back to this particular geometry and study its Landau-Ginzburg Phase.
However this simple example provides already all kinds of symmetries that are interesting for particle physics, like flavor-and R-symmetries. Especially we have learned, that the number of family represent-

[9] Note that $\Delta(54)$ is a discrete subgroup of SU(3).

ation i.e. the **27**'s are strongly coupled to the amount of fixed points and that certain Yukawa couplings can be invoked by the localization properties of the fields i.e. untwisted (*bulk*) fields VS. twisted (*localized*) fields. However, for (semi-) realistic string model building purposes, the above geometry is clearly unsuitable: There are way to many families and the E_6 gauge group has to be broken down to the one of the standard model. By all these reasons it is necessary, to consider other orbifold geometries and to leave the standard embedding by considering shifts and Wilson lines that break directly down a standard model gauge factor and breaks the fixed point degeneracy in a suitable way. These (semi-) realistic model building attempts will be the topic of the next chapter with an particular focus on the $\mathbb{Z}_2 \times \mathbb{Z}_4$ orbifold geometry.

CHAPTER 3

Particle physics from orbifolds: The mini-Landscape and its extensions

The vast amount of symmetries and the enormous computational control of the orbifold CFT made it a very fruitful playground to explore and obtain realistic models of particle physics. In particular, when the computer power grew there have been efforts to systematically scan over all orbifold geometries and gauge embeddings using the C++ orbifolder [41]. The first systematic searches, made in the $\mathbb{Z}_{6-II}$ orbifold made it possible to explicitly construct $O(200)$ string vacua with the features of the MSSM, the so called Mini-Landscape[24]. Another orbifold worth mentioning is based on the $\mathbb{Z}_2 \times \mathbb{Z}_2$ orbifold [42]. In this orbifold, the Wilson line associated to a *freely acting involution* was used to break the SU(5) GUT group to that of the standard model but keeping the GUT structure at the fixed points. In this section we carry on with this program and consider model building on the $\mathbb{Z}_2 \times \mathbb{Z}_4$ orbifold geometry and concentrate on its phenomenological properties.

In order to do so it is inevitable to first introduce the compactification geometry and its symmetries in Section 3.1. We have seen in the chapter before that we have to embed the space group action into the gauge degrees of freedom. To anticipate the full potential of that geometry we cannot only rely on the standard embedding and hence we perform a full classification of all shift embeddings in Section 3.1.3. Finally we work out a combinatorial strategy that incorporates phenomenological requirements with the geometric properties that we have classified before in Section 3.2. We highlight the validity of our strategy that can also explain the findings of the Mini-Landscape searches a posteriori with a Benchmark.

3.1 The $\mathbb{Z}_2 \times \mathbb{Z}_4$ orbifolded String

To lay the grounds for model building in the next section we discuss the heterotic string on this orbifold in some detail. We start by introducing the geometry itself including an extensive discussion of all twisted sectors and their fixed points. After that we can discuss the flavor structure induced by the fixed points as well as the R-symmetries. Finally we give a discussion on how we obtaine all gauge embeddings and give an exploration of the action of Wilson lines for all fixed points.

3.1.1 The $\mathbb{Z}_2 \times \mathbb{Z}_4$ geometry

In this section we introduce the $\mathbb{Z}_2 \times \mathbb{Z}_4$ geometry in mode detail. The lattice we choose for this action is the $SU(2)^2 \times SO(4) \times SO(4)$ root lattice. The shift vectors for the two independent twists we specify to be

$$v_2 = (0, \frac{1}{2}, -\frac{1}{2}, 0)\,, \quad v_4 = (0, 0, \frac{1}{4}, -\frac{1}{4})\,. \tag{3.1}$$

The corresponding space group elements are obtained by the exponentiation of the shifts that is $\theta = e^{2\pi i v_2}$ and $\omega = e^{2\pi i v_4}$. Both shifts together do not leave any torus invariant and hence lead to $\mathcal{N} = 1$ in 4D. In general we can then write a space group element as

$$g(\theta^k \cdot \omega^l, n_a e_a)\,. \tag{3.2}$$

Due to the two twistings we specify a twisted sector by $T_{(k,l)}$ with k the $\mathbb{Z}_2$ and l the $\mathbb{Z}_4$ twist respectively. We present the fixed point structure in some detail in the following. Due to the two twistings we have fixed planes under the space group in $T_{(k,0)}$ and $T_{(0,l)}$ sectors as well as in $T_{1,2}$. But additionally there are also fixed points in the $T_{1,1/3}$ sectors.
Comparing the fixed point structure with that of the simple $\mathbb{Z}_3$ orbifold we find already more structure. The non-prime nature of the twists leads to fixed points whose generating elements are not independent but equivalent up to conjugation under other space group elements. Lets pick for example the $T_{(1,0)}$ sector depicted in Figure 3.3: Here we have four fixed points in the first torus that get tensored with the other four fixed points of the second torus generated by the $\mathbb{Z}_4$ twist element that identifies two generating elements by

$$g(\theta, n_i e_i + e_4) \xrightarrow{\text{conjugation: } h(\omega,0)} h^{-1} g(\theta, n_i e_i + e_4) h = g(\theta, n_i e_i + e_3)\,, \tag{3.3}$$

with $i = 1, 2$. Hence there is a reduction to only 12 independent fixed planes. Due to the non-trivial behavior also the centralizer of those elements is larger than for the constructing elements of other fixed points. Indeed for the above elements we find, that only a projection with space group elements of the form $h(\omega^2, n_a e_a)$ can commute with these four fixed points. For the corresponding states this means, that we have relaxed projection conditions induced by the ω twists and thus the degeneracy of the fixed tori is enlarged. Due to this feature, we call these fixed planes/points *special*.

3.1.2 Symmetries of the $\mathbb{Z}_2 \times \mathbb{Z}_4$ Geometry

Similarly as in the $\mathbb{Z}_3$ case we summarize the discrete symmetries. We start with the discrete flavor symmetry obtained from the fixed point/plane structure along the lines of [40]. First we find that the $\mathbb{Z}_2$ and $\mathbb{Z}_4$ twists contribute two discrete symmetries of the same orders.
The lattice part of the selection rule on the other hand contribute in total 4 $\mathbb{Z}_2$ symmetries. The charge of each fixed point is summarized in Table 3.6 and consistent with the labels for the fixed points given in figures 3.1-3.5. We find, that there are two independent $\mathbb{Z}_2$ factors appearing in the first torus, that come from the uncorrelated orbifold action on the two lattice vectors e_1 and e_2. In the case of no Wilson line all (but the *special* fixed points) are degenerate and the discrete group gets enhanced by an additional permutation element. In the case of the first torus each of the $\frac{\mathbb{S}^1}{\mathbb{Z}_2}$ orbicircles gets an enhanced flavor

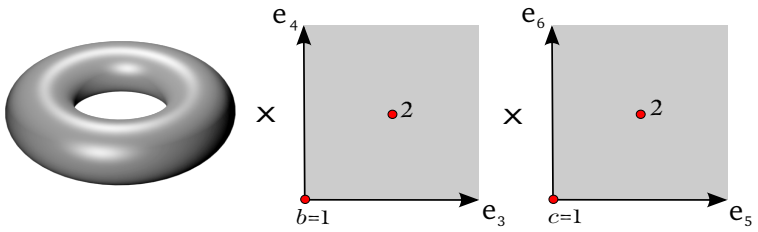

$T_{(0,1)}$

b \ c	1	2
1	0	e_6
2	e_3	$e_3 + e_6$

$T_{(0,3)}$

b \ c	1	2
1	0	e_5
2	e_4	$e_4 + e_5$

Table 3.1: Fixed tori of the $T_{(0,1)}$ and $T_{(0,3)}$ sectors. The tables below help to deduce the generating element of each fixed torus. Consider a fixed torus located at the position b and c in the last two planes, such fixed torus is generated by a space group element (ω, λ_{bc}) if the fixed torus belongs to the $T_{(1,0)}$ sector, or $(\omega^3, \lambda'_{bc})$ for $T_{(0,3)}$. The lattice vectors λ_{bc} and λ'_{bc} can be found in the bc-th entry of the left and right tables below the picture.

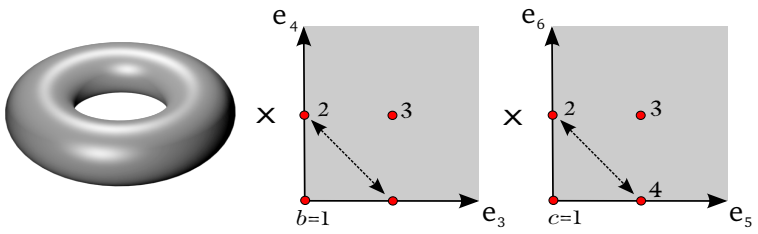

$T_{(0,2)}$

b \ c	1	2	3	4
1	0	$e_5 + e_6$	e_6	
2	$e_3 + e_4$	$e_3 + e_4 + e_5 + e_6$	$e_3 + e_4 + e_5 + e_6$	
3	e_4	$e_4 + e_5 + e_6$	$e_4 + e_6$	$e_4 + e_5$

Table 3.2: Fixed tori of $T_{(0,2)}$. Arrows in the last two planes indicate $\mathbb{Z}_4$ identifications. Similarly as in table 3.1, the generating elements can be found below the picture. Those entries which are left blank do not correspond to additional inequivalences. Special fixed tori are denoted as shaded boxes.

symmetry to

$$S_2 \ltimes \left(\mathbb{Z}_2^P \times \mathbb{Z}_2^l\right) = D_4 \,. \tag{3.4}$$

At next we consider the representations of twisted and untwisted sector states. The untwisted states transform in the trivial representation of D_4 that we call A_1. Note that D_4 contains four one dimensional representation that we label as A_i but only A_1 transforms trivially under all generators. Twisted sector states however transform as a two dimensional representation D due to the non-trivial behavior under

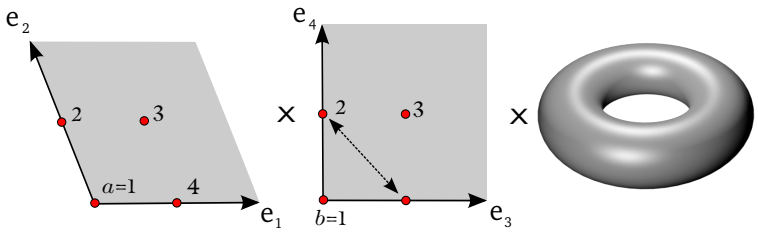

$T_{(1,0)}$

a \ b	1	2	3
1	0	$e_3 + e_4$	e_4
2	e_2	$e_2 + e_3 + e_4$	$e_2 + e_4$
3	$e_1 + e_2$	$e_1 + e_2 + e_3 + e_4$	$e_1 + e_2 + e_4$
4	e_1	$e_1 + e_3 + e_4$	$e_1 + e_4$

Table 3.3: Fixed tori of the $T_{(1,0)}$ sector. The third torus is left invariant under the $\mathbb{Z}_2$ action and the $\mathbb{Z}_4$ element identifies two fixed points in the second torus. The special fixed tori are associated to the shaded cells in the table.

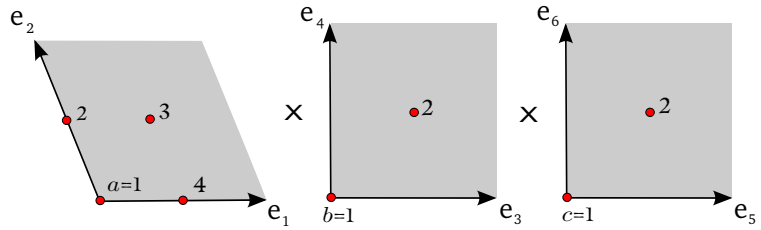

$T_{(1,1)}$

a \ bc	11	12	21	22
1	0	e_6	e_4	$e_4 + e_6$
2	e_2	$e_2 + e_6$	$e_2 + e_4$	$e_2 + e_4 + e_6$
3	$e_1 + e_2$	$e_1 + e_2 + e_6$	$e_1 + e_2 + e_4$	$e_1 + e_2 + e_4 + e_6$
4	e_1	$e_1 + e_6$	$e_1 + e_4$	$e_1 + e_4 + e_6$

$T_{(1,3)}$

a \ bc	11	12	21	22
1	0	e_5	e_3	$e_3 + e_5$
2	e_2	$e_2 + e_5$	$e_2 + e_3$	$e_2 + e_3 + e_5$
3	$e_1 + e_2$	$e_1 + e_2 + e_5$	$e_1 + e_2 + e_3$	$e_1 + e_2 + e_3 + e_5$
4	e_1	$e_1 + e_5$	$e_1 + e_3$	$e_1 + e_3 + e_5$

Table 3.4: Fixed points of the sectors $T_{(1,1)}$ and $T_{(1,3)}$.

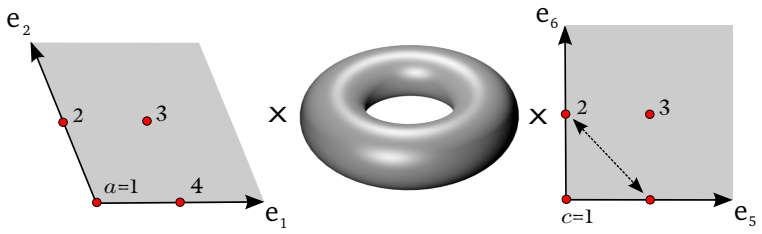

$T_{(1,2)}$

a \ c	1	2	3
1	0	$e_5 + e_6$	e_6
2	e_2	$e_2 + e_5 + e_6$	$e_2 + e_6$
3	$e_1 + e_2$	$e_1 + e_2 + e_5 + e_6$	$e_1 + e_2 + e_6$
4	e_1	$e_1 + e_5 + e_6$	$e_1 + e_6$

Table 3.5: Fixed tori of $T_{(1,2)}$ with similar fixed point topography as sector $T_{(1,0)}$

	$a=1$	$a=2$	$a=3$	$a=4$	$b=1,2$	$b=3$	$c=1,2$	$c=3,4$
$\mathbb{Z}_2^1$	0	1	1	0				
$\mathbb{Z}_2^{1'}$	0	0	1	1				
$\mathbb{Z}_2^2$					0	1		
$\mathbb{Z}_2^3$							0	1

Table 3.6: Symmetries resulting quantum numbers for the lattice parts of the space group selection rule. $\mathbb{Z}_2^1$ and $\mathbb{Z}_2^{1'}$ result from the first complex plane, $\mathbb{Z}_2^2$ and $\mathbb{Z}_2^3$ from the second and third, respectively. The indices a, b, c label the fixed points according to the notation in Figure 3.1 to 3.5.

the permutation element in S_2. Recombining the two circles back to a torus, we get the factor

$$\frac{S_2 \ltimes (\mathbb{Z}_2^p \times \mathbb{Z}_2^l) \times S_2 \ltimes (\mathbb{Z}_2^p \times \mathbb{Z}_2^{l,\prime})}{\mathbb{Z}_2^p} = \frac{D_4 \times D_4}{\mathbb{Z}_2^p} \,. \tag{3.5}$$

Note that we had to divide by the $\mathbb{Z}_2^p$ factor to counter account for the appearance in the second orbicircle. The analysis in the $\mathbb{Z}_4$ twisted sector is very similar. The two fixed points get also enhanced to a D_4 flavor factor according to

$$\mathbb{S}_2 \ltimes (\mathbb{Z}_4^p \times \mathbb{Z}_2^l) \to \frac{D_4 \times \mathbb{Z}_4}{\mathbb{Z}_2} \,. \tag{3.6}$$

Again we had to divide by a $\mathbb{Z}_2$ factor in order account for the $\mathbb{Z}_2$ factor in the numerator that becomes part of the D_4. The residual $\mathbb{Z}_4$ factor accounts for the twist sector number of the state.
By inspecting equation 3.6 we find that the two fixed points in a ω twisted torus are again D_4 representations and have the same $\mathbb{Z}_2$ lattice charge that gets combined into a D_4 doublet D while untwisted states are again neutral singlets A_1. In ω^2 twisted sectors, states with fixed point label $b = 1, 2$ (compare Table 3.6) have the same lattice charge. However two states say $|b = 1\rangle$ and $|b = 2\rangle$ get combined

into a symmetric and antisymmetric singlet combination A_1 and A_2. The $b = 3$ state is exactly the one, that gets combined as a linear combination of the two states, that transforms non-trivially among each other under the ω element. Depending on the gauge quantum numbers such a combination can be either symmetric or antisymmetric that we call A_3 or A_4.[1] To check if certain couplings exist it is worth mentioning that the product of two doublet representations can be decomposed into a sum of all singlet state representations.

$$D \cdot D = \sum_{i=1}^{4} A_i \,. \tag{3.7}$$

The overall flavor group can again be built by combining the building blocks of all three tori to

$$G_{\text{Flavor}} = \frac{\left(\frac{D_4 \times D_4}{\mathbb{Z}_2}\right) \times \left(\frac{D_4 \times \mathbb{Z}_4}{\mathbb{Z}_2}\right) \times \left(\frac{D_4 \times \mathbb{Z}_4}{\mathbb{Z}_2}\right)}{\mathbb{Z}_2 \times \mathbb{Z}_4} = \frac{D_4^4 \times \mathbb{Z}_4}{\mathbb{Z}_2^4} \,. \tag{3.8}$$

Note that we end up with only one $\mathbb{Z}_4$ factor that gives the ω twist and four $\mathbb{Z}_2$ factors that fix the relative ordering of the D_4 flavor factors. Hence without any Wilson lines, states transform in a given twisted sector transform in the $(\mathbf{R}, \mathbf{R}, \mathbf{R}, \mathbf{R})_n$ representation of the above flavor group. I.e. states in the $T_{(1,3)}$ twisted sector transform in the $(D, D, D, D)_3$ representation. All other flavor representations can be found in the Appendix A.
Finally the last geometric symmetry are the R-symmetries that give a $\mathbb{Z}_2^R$ in the first and two $\mathbb{Z}_4^R$ symmetries in the last torus.

3.1.3 Gauge embeddings

Having fixed the geometry of the $\mathbb{Z}_2 \times \mathbb{Z}_4$ we have to consider its gauge embedding. In our attempt to systematically search for realistic models, it is desirable to know all gauge embeddings for all shifts and Wilson lines. However constructing systematically all inequivalent Wilson lines and shifts is a goal which is far from trivial and we will reduce our ambition to construct all inequivalent shift embeddings only.
In the following we consider two shifts as equivalent, if there exists an isometry i.e. a transformation on the lattice vectors that leave the scalar product among any $(P \cdot V)$ invariant. We are actually looking for the automorphism of the $G = \mathrm{E}_8 \times \mathrm{E}_8$ lattice, $\mathrm{Aut}(\Lambda_G)$. These can be decomposed into the lattice automorphisms of the single E_8's and inner automorphisms. However, up to the permutation of the two E_8 factors there are no lattice automorphisms and we can stick to inner automorphisms.
The inner automorphism are generated by the Weyl group of the E_8 lattice. As the Weyl group of the two E_8 groups factorizes, it is sufficient to consider only one E_8 factor for now but keeping in mind, that all inequivalent vectors have to be merged to give modular invariant vectors in both E_8's later.
But even restricting to one gauge factors is far from trivial as the E_8 Weyl group has the order $4!6!8! \approx 7 \cdot 10^8$ due to the high symmetry of the E_8 lattice. However the Weyl group itself is generated by Weyl reflections σ_α that act in terms of the simple roots of the E_8 lattice α on a vector V as

$$\sigma_\alpha V = V - 2\frac{\alpha \cdot V}{\alpha \cdot \alpha}\alpha \,, \tag{3.9}$$

[1] Usually only one of these representations is present as an invariant combination and the non-invariant one only as a tensor with another non-invariant representation in a different torus.

which can geometrically interpreted as the the reflection along a plane perpendicular to the root α. Hence our goal is to effectively find all pairs of shifts (V_2, V_4) that cannot be related by any combinations of Weyl reflections given above. In our approach we use that the $\mathbb{Z}_4$ shifts have already been classified to only ten inequivalent ones in [43] and then find all inequivalent V_2 vectors to each one of them. This can be done by constructing all V_2 vectors as a linear combination of the E_8 positive simple roots

$$V_2 = \sum_{i=1}^{8} \frac{n_i \alpha_i}{2} \quad \text{with} \quad (2V_2)^2 \leq 8\,. \tag{3.10}$$

We have restricted to norms smaller 8 as this is the maximal norm of shifts that do not differ by lattice vectors. This becomes clear by investigating the two maximal norm shifts $V_{1,max} = \sum_{i=1}^{4} 1/2(\alpha_{2i})$ and $V_{2,max} = \sum_{i=1}^{4} 1/2\alpha_{2i-1}$. By the above argument it is clear that at norm 10 we construct a set of vectors that can be reduced by subtracting a full lattice vector to one of the smaller sets. The reason why we do not consider the (infinite) set of shifts that differ by lattice vectors we point out at the end. For a fixed V_4 two shifts are equivalent $\tilde{V}_2 \sim V_2$ if

$$\tilde{V}_2 = \sigma_\alpha V + P\,, \tag{3.11}$$

with $P \in \Lambda_{E_8}$ and $\sigma_\alpha V_4 = V_4$. In this way we reduce the system to a tractable amount. Finally we recombine the vectors to full $E_8 \times E_8$ vectors satisfying all modularity conditions given in (2.51a). Note that we can relax the third condition to

$$2(V_2 V_4 - v_2 \cdot w_4) = 0 \bmod \frac{1}{2}\,, \tag{3.12}$$

as we can use a lattice shift $V_2 \to V_2 + P$ to satisfy the strong modularity constraint.
The reason why we have chosen to mod out the action of the lattice vectors becomes clear when considering the GSO projection phase of a given twisted state. The result of a lattice shift can at most result in a (-1) factor in the projection phase. Hence for one shift representation (V_2, V_4) there only exists one other lattice shifted representative that can result in another model. These models are called *brother models* as they have the same untwisted content but only differ in the content of some twisted sectors.

In total we have obtained *144* shift pairs (V_2, V_4) and their brother models. This gives us an optimal starting point for our model building approaches. In particular in the next section we are interested in grand unified model building hence shifts that contain E_6, SO(10) or SU(5) gauge factors. The amount of shifts containing such a factor are summarized in Table 3.7 At next we consider the effects of Wilson

GUT Gauge Group	Number of models
E_6	26
SO(10)	35
SU(5)	25

Table 3.7: Summary of GUT gauge factors for the 144 inequivalent shift embeddings.

lines. First we observe that we can have in total up to four Wilson lines switched on: In the first torus there is no relation among the two basis vectors $e_{1,2}$ apart from $\theta e_{1,2} + e_{1,2} = 0$. Hence we can switch on two independent Wilson lines and by (2.51a) we find that both must be of order two. In the second

and third torus we have the identifications

$$\begin{aligned} \omega e_3 &= e_4\,, & \theta e_6 &= e_5\,, \\ \omega^2 e_3 + e_3 &= 0\,, & \omega^2 e_5 + e_5 &= 0\,. \end{aligned} \tag{3.13}$$

From the first equation we find that only one Wilson line per torus is allowed and by the second that both are of order two. To study the full landscape systematically one would have to construct all inequivalent Wilson lines and then pick one combination and perform the reduction procedure of the spectrum. We will not attempt such a classification at this point because it is out of reach of today's computer power. But we want to get a geometric intuition for the action of the Wilson lines at each fixed point.
Generically we distinguish between three different effects that a Wilson line can have on a given fixed point: First we have *invariant fixed points* where the matter does not feel the effect of the Wilson line at all and the spectrum stays in a complete GUT representation. Secondly we have *Split fixed points* where Wilson lines act only as projectors of the GUT matter. Here we lose part of control as we cannot say a priori which parts get projected out. *Split fixed points* usually appear in twisted sectors where the Wilson line is switched on along a fixed torus. Finally there are *unshielded* fixed points where the Wilson line appears in the mass equation and introduces completely new matter states where we do not have under control at all.
Without constructing a concrete Wilson line, we have computed the effects of all possible Wilson line configurations on every fixed point in every sector by a careful analysis of the respective centralizers. After that we grouped them into the three classes of fixed points. The result is summarized in Table 3.8 This table will help to deduce, if there exists a Wilson line configuration that can lift a certain fixed point degeneracy. Lifting this degeneracy also breaks the $\mathbb{S}_2$ permutation among fixed points that we used in order to construct the non-Abelian lift of the discrete flavor symmetries. Hence we can deduce, that a Wilson line in the respective sectors breaks a given D_4 factor down to an Abelian $\mathbb{Z}_2 \times \mathbb{Z}_2$ factor.

3.2 $\mathbb{Z}_2 \times \mathbb{Z}_4$ model building

Having settled the formal preliminaries of the orbifold we use that knowledge in the following for realistic model building. For that we will first discuss our model building strategy and how we translate phenomenological requirements into geometric ones that we have discussed in the section before. Combining pieces leads us to a clear picture of how a model should look and in particular to a specific pattern where the MSSM fields should be located that we support with a toy model.

3.2.1 Model building searches

In the following we present the list of phenomenological constraints we want to impose for our models. In formulating the phenomenological constraints we orient ourselves at the ones that have been imposed in the Mini-Landscape searches within the $\mathbb{Z}_{6-\mathrm{II}}$ geometry [24]. Our goal is to arrive at a model that has the SM gauge group with exactly three families. Furthermore we want to have at least one pair of Higgses that are light and a reasonable Yukawa structure. In particular we a top-quark Yukawa coupling of order one.

- We impose an **SO(10) GUT structure** on as many families as possible. This means that we select a shift embedding leading to an E_6 or SO(10) gauge group. This reduces our choices to one of the 35 shifts and their brother models, however we want to focus on the SO(10) shifts in the following. In Table B.1 of Appendix B we list the SO(10) matter spectrum and the contribution from each fixed point. This list is going to be the starting point for our model search.

Config.	1	2	3	4	5	6	7	8	9	10	11	12	13	14	15	16
W_1		✓				✓	✓	✓				✓	✓	✓		✓
W_2			✓			✓			✓	✓		✓	✓		✓	✓
W_3				✓			✓		✓		✓	✓		✓	✓	✓
W_4					✓			✓		✓	✓		✓	✓	✓	✓

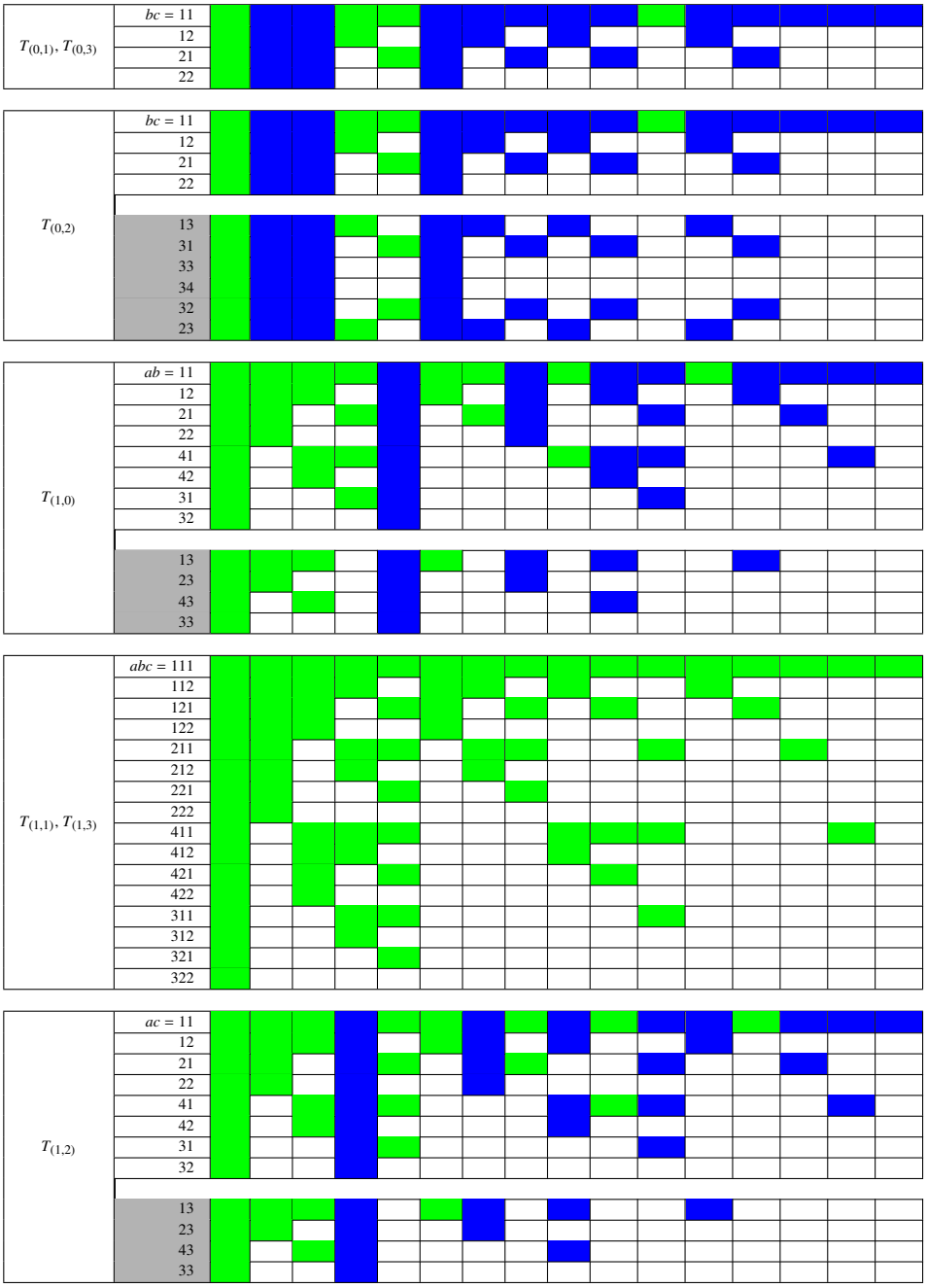

Table 3.8: Invariant (green) and split (blue) fixed points under different Wilson line configurations. All other fixed points are unshielded and we cannot infer the spectrum from the shift embedding.

- The **GUT group is broken** down to the standard model gauge group plus additional gauge factors by the use of Wilson lines. Shifts and Wilson lines do not change the rank of the gauge group. The

additional gauge factors however, can be broken when assigning VEVs to MSSM singlet fields, which we are not doing at this point.

- We need to find a **Wilson line configuration** that breaks the fixed point degeneracy in such a way that as many families as possible stay complete GUT multiplets. This can be obtained by consulting Figure 3.8 that summarizes all possible Wilson line effects at each fixed point. Combining Table 3.8 with the spectrum helps to determine at which fixed points we should look for families that have the chance to stay complete upon Wilson line breaking. For example we see Wilson line configuration six exactly leaves three fixed points in sector $T_{(1,0)}$ invariant, which hence would be a first starting point to look for families at the SO(10) level.

- We have to face the **doublet-triplet splitting** problem of the Higgs-representation. When the Higgs is a full GUT representation it is in general hard to lift the exotic triplet states while keeping the Higgses light. We address this problem by enforcing that the Higgs representation sits in a sector where the Wilson line can act as a non-trivial projector on the exotics, by comparison with Table 3.8.

- **The top-quark mass** in the standard model is of the order of the electro-weak scale and hence its Yukawa coupling is of order one. Thus we have to realize the Yukawa coupling already at the GUT level at trilinear order. By the selection rules presented before only the tree-level couplings in Table 3.9 are allowed. In the table we have used that no left-chiral field in the $T_{(1,3)}$ sector can solve for the mass equation. Moreover no coupling of the form $T_{(0,1)}T_{(0,1)}T_{(0,2)}$ and $T_{(0,3)}T_{(0,3)}T_{(0,2)}$ is allowed by H-momentum conservation. This in turn fixes the location of the top-quark constituents relative to the Higgs representation.

Couplings involving untwisted Fields	Couplings involving twisted fields only
1. $T_{(0,2)}T_{(0,2)}U_1$	6. $T_{(0,2)}T_{(1,2)}T_{(1,0)}$
2. $T_{(1,0)}T_{(1,0)}U_3$	7. $T_{(1,1)}T_{(1,1)}T_{(0,2)}$
3. $T_{(1,2)}T_{(1,2)}U_2$	8. $T_{(1,1)}T_{(0,1)}T_{(1,2)}$
4. $T_{(0,1)}T_{(0,3)}U_1$	9. $T_{(1,1)}T_{(0,3)}T_{(1,0)}$
5. $U_1U_2U_3$	

Table 3.9: The combination of twisted sector fields for all trilinear couplings in the $\mathbb{Z}_2 \times \mathbb{Z}_4$ orbifold. The sector $T_{(1,3)}$ is not listed as it cannot support left chiral

Now we have to combine all the above constraints and filter the shifts that can allow for all of them.
We start by demanding three complete families. In general we find, that there is only one shift and one Wilson line configuration that permits that: the shift 68_1 and 78 that both have families in the sector $T_{(1,2)}$. Switching on two Wilson lines in the first torus (configuration six) reduces the degeneracy to exactly three families. It follows that the top-quark Yukawa must fall into the coupling scheme 3: $T_{(1,2}T_{(1,2)}U$. As the SO(10) Yukawa is of the form $\mathbf{16} \cdot \mathbf{16} \cdot \mathbf{10}$ a Higgs $\mathbf{10}$-plet must be located in the untwisted sector. Also this constraint is satisfied. However, we could confirm that this coupling is **not** invariant under the residual gauge symmetries for the two shift embeddings. Moreover we should keep in mind, that all families have the same coupling an hence all three families would be similarly heavy. Hence we can rule out the simplest scenario that all families should stay complete and we learn, that the third family should have a different location then the light ones to realize the right mass hierarchy.
The next step is to relax completeness of the families, however it is not clear which one this should be.

If the third family is complete, the $\mathbf{16}_3\mathbf{16}_3\mathbf{10}_H$ coupling always constraints the the origin of their twisted sectors to be of the form $T_{(k,l)}T_{(k,l)}T_{(0,2l)}$ and therefore constraints the possibilities for the locations considerably. Actually we find, that there are no SO(10) models where the third family can satisfy that constraint combined with the requirement of three families.
Hence it makes sense to relax that constraint and allow the third family to come from multiple sectors where the Wilson line acts as a projector and only the two light families stay complete **16**-plets. In this scenario, the top-quark and Higgses have to come from a sector, where the degeneracy is broken down to one and the Wilson lines act as projectors. From the Table 3.8 we find, that this is never the case for fields in the $T_{(1,1/3)}$ sector and hence this sector should never be involved. Hence now we can go through the residual six trilinear Yukawa couplings and look for a Wilson line configuration that breaks degeneracy in the given sectors down to one and acts as a projector. This in turn fixes the sectors where complete families should sit by considering the Table 3.8 again. In the end, we only have to find a shift embedding that allows for families at exactly those locations. The analysis is summarized in Table 3.10. This analysis reveals that all but one scenario is ruled out: The one where the top-quark and the Higgs

Coupling	WL config.	Sectors of Light Families	Shift Embedding
$T_{(0,1)}T_{(0,3)}U_1$	14,15	$T_{(1,3)}$	No Model available
$T_{(0,2)}T_{(0,2)}U_1$	14,15	$T_{(1,3)}$	No Model available
$T_{(1,0)}T_{(1,0)}U_3$	None	–	-
$T_{(1,2)}T_{(1,2)}U_2$	None	-	-
$T_{(1,0)}T_{(0,2)}T_{(1,2)}$	None	-	-
$U_1U_2U_3$	6-15	Depends on WL config.	At least one per WL config.

Table 3.10: Wilson öline configurations and shift embeddings consistent with a unique renormalizable coupling that becomes the top-quark Yukawa. All criteria can be fulfilled simultaneously when top quark and higgs comes from the untwisted sector only.

is located in the untwisted sector. Indeed we find that in 75% of all SO(10) shifts this coupling exists and are favored by our line of argumentation. As both the Higgses and the top-quark descend from the adjoint representation of the underlying E_8 we have a combined scenario of gauge-Higgs unification [44, 45] and gauge-top unification [46].

Our reasoning has skipped the task to find actual Wilson lines that break the GUT group in a desired way and project out the correct pieces of the multiplets. In the next section we give a toy model that has all these features and that we discuss the role of the R-symmetry for the Higgs multiplets.

U	$1\ (\mathbf{16},\mathbf{2},\mathbf{1},\mathbf{1})_{0,-1}$
	$1\ (\mathbf{16},\mathbf{1},\mathbf{2},\mathbf{1})_{0,1}$
	$1\ (\mathbf{10},\mathbf{2},\mathbf{2},\mathbf{1})_{0,0}$
	$1\ (\mathbf{1},\mathbf{1},\mathbf{1},\mathbf{1})_{-12,0}$
	$1\ (\mathbf{1},\mathbf{1},\mathbf{1},\mathbf{1})_{12,0}$
	$1\ (\mathbf{1},\mathbf{1},\mathbf{1},\mathbf{28})_{6,0}$
	$1\ (\mathbf{1},\mathbf{1},\mathbf{1},\overline{\mathbf{28}})_{6,0}$

$T_{(0,1)}$	$4\ (\mathbf{1},\mathbf{1},\mathbf{1},\mathbf{8})_{6,1}$
	$4\ (\mathbf{1},\mathbf{1},\mathbf{1},\overline{\mathbf{8}})_{0,1}$
$T_{(0,2)}$	$10\ (\mathbf{1},\mathbf{2},\mathbf{2},\mathbf{1})_{6,0}$
	$10\ (\mathbf{10},\mathbf{1},\mathbf{1},\mathbf{1})_{-6,0}$
	$6\ (\mathbf{1},\mathbf{1},\mathbf{1},\mathbf{1})_{-6,-2}$
	$6\ (\mathbf{1},\mathbf{1},\mathbf{1},\mathbf{1})_{-6,2}$

$T_{(0,3)}$	$4\ (\mathbf{1},\mathbf{1},\mathbf{1},\overline{\mathbf{8}})_{6,-1}$
	$4\ (\mathbf{1},\mathbf{1},\mathbf{1},\mathbf{8})_{0,-1}$
$T_{(1,0)}$	$4\ (\mathbf{1},\mathbf{1},\mathbf{2},\mathbf{8})_{-3,0}$
$T_{(1,1)}$	-
$T_{(1,2)}$	$4\ (\mathbf{1},\mathbf{2},\mathbf{1},\overline{\mathbf{8}})_{-3,0}$
$T_{(1,3)}$	$16(\mathbf{16},\mathbf{1},\mathbf{1},\mathbf{1})_{3,0}$
	$16\ (\mathbf{1},\mathbf{2},\mathbf{1},\mathbf{1})_{3,1}$
	$16\ (\mathbf{1},\mathbf{1},\mathbf{2},\mathbf{1})_{3,-1}$

Table 3.11: Matter spectrum of the SO(10) × SU(2) × SU(2) × SU(8) toy model.

3.3 A concrete Toy Model

Our toy model is specified by the shifts

$$V_2 = \left(1,-\frac{1}{2},0,0,0,-\frac{1}{2},0,0\right)\left(\frac{5}{4},-\frac{1}{4},\frac{3}{4},\frac{3}{4},\frac{3}{4},\frac{3}{4},-\frac{1}{4},\frac{1}{4}\right),$$
$$V_4 = \left(\frac{1}{2},0,0,0,0,0,0,0\right)\left(\frac{5}{4},-\frac{1}{4},-\frac{1}{4},-\frac{1}{4},-\frac{1}{4},-\frac{1}{4},\frac{1}{2},-\frac{1}{2}\right),$$

leading to the gauge symmetry $[\mathrm{SO}(10)\times\mathrm{SU}(2)^2\times\mathrm{U}(1)]\times[\mathrm{SU}(8)\times\mathrm{U}(1)]$. The spectrum at the GUT level is given by in Table 3.11. Lets first inspect the trilinear coupling from the untwisted sector

$$(\mathbf{10},\mathbf{2},\mathbf{2},\mathbf{1})_{0,0}\cdot(\mathbf{16},\mathbf{2},\mathbf{1},\mathbf{1})_{0,-1}\cdot(\mathbf{16},\mathbf{1},\mathbf{2},\mathbf{1})_{0,1}\,, \tag{3.14}$$

that has R-charge: $(0,-1,-1,-1)$ and hence is allowed by all selection rules. It is worth noting, that the **10**-plet has its R-charge weight in the first torus, which is the one that is twisted by the $\mathbb{Z}_2$ action and in addition belongs to a real representation. Actually it is easy to see, that all states that have the oscillator in the $\mathbb{Z}_2$ twisted torus are vector-like i.e. real representation or come with an additional conjugate representation. Note that such as state has the transformation phase

$$e^{2\pi i\left(p\dot{V}_{2/4}-q\cdot v_{2/4}\right)}|q|P\rangle\,, \tag{3.15}$$

that has to be trivial. For a (bosonic) state with $q=(0,-1,0,0)$ we have

$$q\cdot v_2 = \frac{1}{2} \to \pm P\cdot V_2 = \frac{1}{2} \mod 1\,, \tag{3.16}$$
$$q\cdot v_4 = 0 \to \pm P\cdot V_4 = 0 \mod 1\,, \tag{3.17}$$

and hence it is clear that for every invariant state $|q\rangle\otimes|P\rangle$ there must also exist another state $|q\rangle\otimes|-P\rangle$. In our next step we choose the Wilson line configuration 14 of Table 3.8 given concretely by

$$W_1 = \left(-\tfrac{1}{2},\tfrac{1}{2},-\tfrac{3}{2},-\tfrac{1}{2},0,-1,-1,2\right)\left(-\tfrac{3}{4},-\tfrac{7}{4},-\tfrac{1}{4},-\tfrac{1}{4},-\tfrac{1}{4},\tfrac{7}{4},\tfrac{3}{4},\tfrac{3}{4}\right),$$
$$W_3 = \left(-1,\tfrac{3}{2},-\tfrac{1}{2},\tfrac{1}{2},0,\tfrac{1}{2},0,2\right)\left(-\tfrac{1}{2},1,-2,0,\tfrac{3}{2},-1,-\tfrac{3}{2},-\tfrac{3}{2}\right),$$
$$W_4 = \left(-\tfrac{5}{4},\tfrac{5}{4},\tfrac{1}{4},-\tfrac{1}{4},\tfrac{3}{4},-\tfrac{1}{4},\tfrac{5}{4},\tfrac{9}{4}\right)\left(0,1,1,2,-1,-\tfrac{1}{2},2,\tfrac{3}{2}\right),$$

that we have found with the help of the $C++$ orbifolder [41]. This breaks the gauge group to $G_{\rm SM} \times G_{\rm Hidden} \times \mathrm{U}(1)^9$, where $G_{\rm Hidden} = \mathrm{SU}(3) \times \mathrm{SU}(2)$ is a subgroup from the SU(8) in the second E_8. By this choice it is also clear, that exactly two **16**-plets in the $T_{(1,3)}$ sector stay complete. The resulting spectrum gives exactly three generations and all the other representation are vector-like with respect to the SM gauge group as summarized in Table C.1 of Appendix C. We want to concentrate in particular on the top-quark Yukawa coupling that precisely gets projected under the Wilson lines in the following way

$$\begin{aligned}
(\mathbf{10},\mathbf{2},\mathbf{2},\mathbf{1})_{0,0} &\to \overbrace{(\mathbf{1},\mathbf{2})_{-1/2,\cdots}}^{H_u} + \overbrace{(\mathbf{1},\mathbf{2})_{1/2,\cdots}}^{H_d} + \dots\,, \\
(\mathbf{16},\mathbf{2},\mathbf{1},\mathbf{1})_{0,-1} &\to (\mathbf{1},\mathbf{1})_{-1,\cdots} + \underbrace{(\bar{\mathbf{3}},\mathbf{1})_{1/3,\cdots}}_{U} + \dots\,, \\
(\mathbf{16},\mathbf{1},\mathbf{2},\mathbf{1})_{0,1} &\to \underbrace{(\mathbf{3},\mathbf{2})_{-1/6,\cdots}}_{Q} + \dots\,,
\end{aligned} \tag{3.18}$$

making the top quark Yukawa the only surviving coupling at tree-level. Furthermore we note, that the Higgs are a vector-like pair but the bilinear

$$(\mathbf{10},\mathbf{2},\mathbf{2},\mathbf{1})_{0,0} \cdot (\mathbf{10},\mathbf{2},\mathbf{2},\mathbf{1})_{0,0} \to H_u \cdot H_d\,, \tag{3.19}$$

is forbidden by the $\mathbb{Z}_2$ R-symmetry and hence the μ-term problem is solved.
Finally, we would like to mention, that this toy model lacks a few phenomenological requirements. At first we cannot find a VEV configuration that induces all Yukawa couplings, decouples all vector like exotic fields but still keeps the Higgses light. Another requirement is that the hidden gauge groups might become strongly coupled at low energies and trigger a gaugino condensate that breaks SUSY [47, 48] . However for this mechanism to work one usually requires hidden sector gauge factors of rank greater four [49]. These factors get broken completely by our VEV configuration leaving no chance for gaugino condensation to occur.

3.4 A Zip-Code and the orbifold Landscape

Although there are phenomenological problems in the toy model presented above our argumentation gives us a way to understand the results of the computer based searches in the $\mathbb{Z}_{6-\mathrm{II}}$ geometry which is fixed by the orbifold shift $v_6 = (\frac{1}{6}, \frac{1}{3}, -\frac{1}{2})$ on a $G_2 \times \mathrm{SU}(3) \times \mathrm{SU}(2)^2$ lattice. Here $O(200)$ models have been found that have the localization properties we have presented above. We have seen that the locations of the MSSM fields, their *Zip-Code* within the orbifold space is very important for phenomenological relevance of the model. Here we want to summarize the lessons that we have learned:

- The Higgs fields H_u and H_d reside in the untwisted sector and form a vector-like pair under all selection rules. The μ-term between them is forbidden by an R-symmetry. As untwisted fields, the Higgses descend directly from the adjoint of the E_8 gauge group, called gauge-Higgs unification.
- To allow for a large-top quark the quark constituents should live in the untwisted sector as well. This implies that the third family is not a complete GUT representation and the missing pieces are of the family are completed from fields distributed among various fixed points.
- The first two families come from complete SO(10) GUT families and are located at two equivalent fixed points in the compactification and transform as a doublet under a D_4 family symmetry. This

implies that there exists no trilinear Yukawa with the untwisted Higgs and avoids the problem of flavor changing neutral currents.

- The last lesson concerns the specific breakdown of SUSY observed in these models. One source for SUSY breakdown is gaugino condensation in the Hidden sector that usually appears in a multi-TeV range after fixing the dilaton at a GUT value. The combination of moduli stabilization and down-lifting the vacuum energy to obtain a small cosmological constant results in a SUSY breaking pattern called mirage mediation [50]. The resulting soft SUSY masses of the fields then crucially depend on their locations. For example fields in the bulk feel remnants of the $\mathcal{N} = 4$ SUSY that protects their soft masses. Hence we find a picture of very light *stop* and Higgsino masses known as natural SUSY [51].

Finally we want to note that the $\mathbb{Z}_2$ twisted torus plays a huge role in the compactification and the lessons we have presented above. It supports a $\mathbb{Z}_2$-R-symmetry[2] and leads automatically to vector-like but massless fields in the untwisted sector. Furthermore it supports an D_4 flavor factor under which the two light families form a doublet representation and that stay complete SO(10) **16**-plets upon the Wilson line breaking.

In comparison we have seen that the $\mathbb{Z}_2 \times \mathbb{Z}_4$ geometry posses more possibilities for realistic GUT embeddings than the $\mathbb{Z}_{6-\mathrm{II}}$-geometry and hence we expect, that this geometry should have the possibility to contribute a sizable addition to the Mini-Landscape models. Indeed in [52] a full search over all orbifold geometries has been performed and it was found that the $\mathbb{Z}_2 \times \mathbb{Z}_4$ orbifold geometry possesses $O(3000)$ MSSM like models, more than in any other geometry. Moreover standard model orbifold searches have also been performed within non-supersymmetric heterotic string theories.[3] It was found that also there, the $\mathbb{Z}_2 \times \mathbb{Z}_4$ geometry supported most of the realistic models [53].

[2] Taken the bosonic oszillators in account we should rather speak of a $\mathbb{Z}_4$ R-symmetry.
[3] In this heterotic string theory a $\mathbb{Z}_2$ twist breaks the E_8 symmetries to SO(16) factors together with the supersymmetry.

CHAPTER 4

Going more singular: The Landau-Ginzburg Phase

In this chapter we take a different perspective towards heterotic compactifications than in the chapter before. We consider first the gauged linear sigma model (GLSM) in Section 4.1 that can be thought of as an effective world sheet theory that allows to smoothly interpolate between different geometric phases of the theory via some parameters. We go from a smooth geometry to the orbifold phase where certain points get blow-down and consider the phase where the geometry is completely singular: The Landau-Ginzburg Orbifold (LGO) phase. We study this phase in more detail in Section 4.2 and techniques of [28] to calculate the whole massless spectrum, including additional vectors and singlets and all of their charges in terms of world sheet fields. We then perform a full scan over a closed set of models that correspond to all kinds of $\mathbb{Z}_3$ orbifolds in the geometric regime. However we discuss also many compactifications that do not support a geometric phase. We find, that the whole set of models is closed under mirror-symmetry: A symmetry that interchanges the role of Kähler and complex structure in the geometric regime as well as the Hodge numbers $h^{2,1}$ and $h^{1,1}$. This makes it particularly interesting to construct mirror-Calabi-Yaus of *rigid* geometries e.g. the standard $\mathbb{Z}_3$ orbifold that do not possess a geometric description at all which we do in Section 4.2.4.

Finally we show the power of the LGO precisely in constructing the mirror of two geometries that have a $\mathbb{Z}_3$ orbifold phase. We go down to the Fermat LGO point and construct their mirror dual. There we compute the whole spectrum and all its enhanced symmetries in terms of the world sheet fields. We then perform a world-sheet super potential deformation. There we are still at the LGO point and can compute the spectrum exactly. However in the mirror we are at finite torus volume i.e. the orbifold phase.

We use that knowledge to identify the fields that acquire a VEV in the four dimensional field theory and identify those as the Kähler moduli. In that way we can track the breakdown of all symmetries, such as discrete R- and non-R symmetries as well as the flavor symmetry in terms of the world sheet deformation. As the Kähler moduli come from a charged multiplet we can compute all higher order corrections to the Yukawa couplings simply from gauge invariance at the LGO point in the spirit of the Frogatt-Nielsen mechanism [54]. This is only possible because we know the whole structure of the Kähler moduli space and its symmetries.

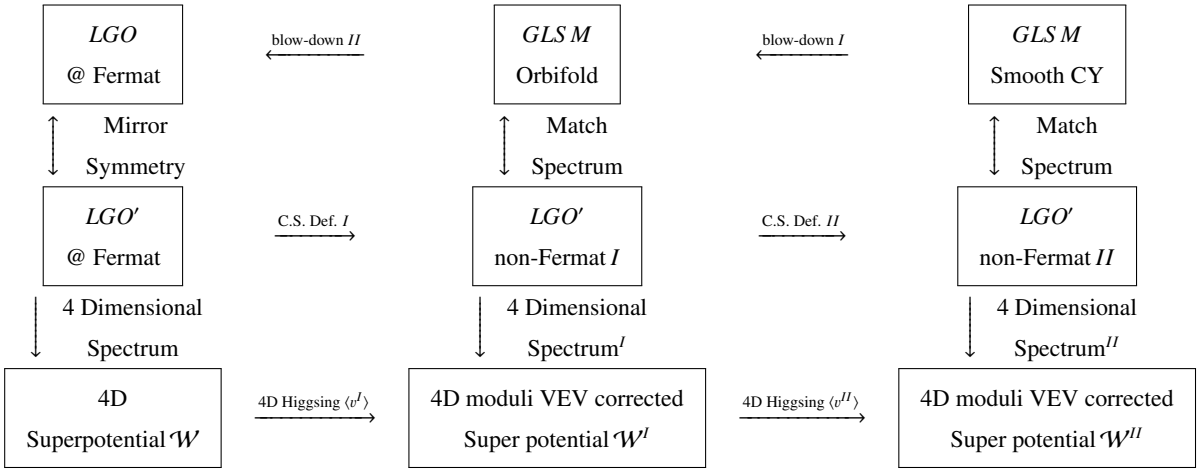

Figure 4.1: Schematic Diagram of how to obtain the whole 4D spectrum of a GLSM using mirror symmetry. We start from a GLSM and go to its LGO phase by consecutive blow-downs to the Fermat point shown in the first line. Then we construct the mirror LGO where and compute its whole spectrum and symmetries. The second line shows the complex structure deformations of the dual GLSM. The LGO methods give us full control over all 4D symmetries and thus the 4D superpotential. The deformation at every step is described as a 4D matter multiplet that acquires a VEV that correspond to the Kähler moduli in world sheet theory. Thus we can Kähler correct the 4D superpotential in every geometric phase and track the breakdown of the symmetries.

4.1 The Gauged Linear Sigma Model and its Phases

In this section we introduce the basics of the GLSM that was introduced by Witten [55]. The GLSM describes a two dimensional supersymmetric field theory with a $U(1)^n$ gauge theory coupled to chiral superfields[1]. However this theory is not a SCFT by itself as the gauge kinetic term and the superpotential have a mass dimension. After taking the conformal limit i.e. taking the masses to infinity the fields get integrated out and the theory flows to a non-trivial SCFT in the infrared. There, the theory is a non-linear sigma model and all information of the target space geometry is stored in the metric of the kinetic term. However the theory still has the same symmetries as in the non conformal ultraviolet, thus the GLSM gives us a great tool to study the target space geometry of string compactifications in an easier way. In the following we give a very quick review of the main construction and constraints of GLSM's and then study the Landau-Ginzburg phase of those constructions.

4.1.1 Two dimensional supersymmetric theories

We are considering two dimensional supersymmetric field theories whose bosonic field content acts as the target space coordinates in the ground state of the theory. It can be shown that the gauged $\mathcal{N} = (1,0)$ world sheet symmetry gets enhanced to a global $(2,0)$ symmetry when the target space Calabi-Yau and a $\mathcal{N} = (2,2)$ SUSY in case of the standard embedding. Due to the high amount of supersymmetry the later theory is in particularly easy to treat although it might be less interesting for model building.
The two dimensional $\mathcal{N} = (2,2)$ theory can most easily be thought of as the compactification of a four

[1] In general a GLSM can also have non-Abelian gauge factors.

dimensional $\mathcal{N} = 1$ theory reduced on a tours. Then we stay with two bosonic coordinates σ_+ and σ_- and the fermionic ones $\theta^\pm$ and $\bar{\theta}^\pm$. Then we have the following massless representations

- **The chiral multiplet** Φ with the superfield expansion

$$\Phi = \phi + \psi^+\theta^- + \psi^-\theta^+ + \theta^2 F\,, \tag{4.1}$$

  that has a complex scalar ϕ and two complex fermions $\psi^\pm$ as well as the complex auxiliary field F. Similarly as in 4D the chiral superfield is annihilated by the supercovariant derivative $\overline{D}_\pm\Phi = 0$, with $D_\pm = \partial_{\theta_\pm} - i\bar{\theta}\partial_{\sigma_\pm}$.

- **The U(1) vector multiplet** V, that has the superfield expansion in the Wess-Zumino gauge

$$V = a_+\theta^+\overline{\theta}^+ + a_-\theta^-\overline{\theta}^- + \theta^-\overline{\theta}^+\eta + \theta^+\overline{\theta}^-\bar{\eta} + \text{ gauginos } + \theta^2\overline{\theta}^2 D\,. \tag{4.2}$$

  From a 4D perspective the $a_\pm$ are the uncompactified vector components. The complex bosonic η field comes from the two compactified directions. The D-term is the counterpart of the 4D auxiliary field.

- **Twisted Chiral multiplets** $\mathcal{F}$ have no 4D counterpart as such and are subject to the chirality condition $\overline{D}_+\mathcal{F} = D_-\mathcal{F} = 0$. We can construct twisted chiral superfields from the vector multiplets as $\mathcal{F} = \overline{D}_+ D_- V$ and thus we do not consider them as independent fields. The twisted chiral superfield can be interpreted as the superfield strength of the vector multiplet.

Action and Symmetries

In general we consider GLSM's with an $\mathrm{U}(1)^{\mathrm{n}}$ gauge symmetry but due to the supersymmetry these theories also possess a $\mathrm{U}(1)_{\mathrm{L}} \times \mathrm{U}(1)_{\mathrm{R}}$ R-symmetry. From these symmetries and field contents we can build up a an action with the following four parts

- *The kinetic term* that has the usual form

$$\mathcal{S}_{\text{kinetic}} = \int d^2\sigma d^4\theta \sum_i \Phi_i e^{2Q_i^J V^J}\overline{\Phi}_i\,. \tag{4.3}$$

  We can start with a diagonal and flat metric in the GLSM but under the RG flow to the UV theory the K$^{\prime}$ahler potential is not protected. Hence the metric will undergo substantial renormalization.

- *The gauge kinetic term*

$$\mathcal{S}_{\text{gauge}} = \int d^2\sigma d^4\theta \sum_J -\frac{1}{4e_J^2}\mathcal{F}^J\overline{\mathcal{F}}^J\,, \tag{4.4}$$

  where we have introduced the dimensionful coupling constants e^J of the $\mathrm{U}(1)_{\mathrm{J}}$. Note that this term vanishes in the conformal limit.

- *The superpotential* term given by

$$\mathcal{S}_{\text{super}} = m\int d^2\sigma d^2\theta\mathcal{W} + h.c.\,, \tag{4.5}$$

with the superpotential $\mathcal{W}$ which is a holomorphic function of the chiral superfields and constrained by $U(1)^J$ gauge invariance and to have R-charges $(1,1)$ under the $U(1)_L \times U(1)_R$ R-symmetry. Also note the mass term m in front of the superpotential.

- *The twisted superpotential* introduces the Fayet-Iliopoulos(FI) term

$$\mathcal{S}_{\text{twisted}} = \int d^2\sigma d\theta^+ d\overline{\theta^-}\, \rho_J \mathcal{F}^J + h.c.\,, \tag{4.6}$$

with the complex FI parameter $\rho_J = a_J + i\delta_I$. The world sheet Kähler parameter a_J which we can use to continuously interpolate between different phases of the GLSM, is of major interest for our discussion.

Similarly as in the four dimensional theory the scalar potential of the vacuum has to vanish in order not to break the world sheet supersymmetry. In the $\eta = 0$ patch the scalar potential is given by the usual F and D-term contributions

$$V_{\text{scalar}} = \sum_J e_J^2 (D^J)^2 + m^2 \sum_i |F_i|^2\,. \tag{4.7}$$

In order that we can take the conformal limit by setting e and m to infinity we have to make sure that both D and F-flatness is satisfied

$$D^J = \sum_i Q_i^J |\phi|^2 - a_J = 0\,, \tag{4.8}$$

$$F_j^* = \frac{\partial W}{\partial \phi_i}\,. \tag{4.9}$$

By taking the conformal limit and going to the IR we also have to check that the FI parameter and the superpotential do not undergo substantial renormalization. For the superpotential $\mathcal{W}$ this is guaranteed by non-renormalization theorems, however for the FI parameter this is only provided, when all U(1)'s satisfy the two dimensional anomaly constraints

$$\sum_i Q_i^J = 0 \quad \forall\, J = 1, \ldots, n\,. \tag{4.10}$$

The above constrained is exactly the Calabi-Yau condition and it is satisfying to note, that it follows purely from anomaly freedom of the underlying world sheet theory. In the following we take the special ansatz by splitting up the chiral superfields into two classes. First we take the chiral superfields Φ_i with *positive* $U(1)^J$ charges $Q_i^J \geq 0$ but keep them uncharged under the R-symmetries. [2] Then we have for each $U(1)_J$ a compensator field C_J with $U(1)_J$ charge $-\sum_i Q_i^J$ and R-charges $(1,1)$. In addition we allow some compensator fields to be uncharged under the R-symmetry. Compensator fields with non-trivial R-charge are associated with the overall size of the Calabi-Yau space as we will see in the following examples.
By the above charge assignment the superpotential is constrained to be of the form

$$\mathcal{W} = \sum_J C_J P(\Phi_i)_J\,, \tag{4.11}$$

[2] This sign choice guarantees compactness of the geometry.

with $P(\Phi_i)_J$ being a homogenous polynomials in the coordinates Φ_j as demanded by gauge invariance and linear in the compensator field. The D-and F-term constraints then become

$$\sum_i Q_i^J |\phi_j|^2 - \left(\sum_i Q_i^J\right)|c_J|^2 = a_J \quad \forall\, J = 1, \ldots, n\,, \tag{4.12}$$

$$c_J \partial_{\phi_i} P(\phi_i)_J = 0\,, \quad P(\phi_i)_J = 0\,. \tag{4.13}$$

Depending on the parameters a_J the above constraint fixes the target space geometry completely.

- **The smooth case**: $a_J > 0 \quad \forall J$: Here we find from the D-terms that fields have to obtain a VEV $\langle\phi_i\rangle \neq 0$ with the addition that their homogenous polynomial has to vanish, from the second F-term constraint. However generically, $\partial_{\phi_i} P_j = 0$ is only zero when the VEV of all fields is zero which we have excluded. Hence we can only satisfy the first F-term constraint by taking c_J to be zero. We note that the above system of polynomials cut out hypersurfaces within the space that is constrained by the U(1) D-term constraints. The polynomials all have the maximal charge under all U(1) actions and are transverse which precisely defines a complete intersection Calabi-Yau (CICY).

- **Partially singular case**: $a_k > 0$, $a_l < 0$: For the a_k the discussion is similar as above resulting in the VEV of the compensator fields to be $c_k = 0$ and the other fields might be unequal to zero. For the second set of parameters, a_l we find that only if the c_l acquire a VEV the D-term constraint can be satisfied. Furthermore we find that the $U(1)_l$ gets broken by the c_l field that attains the VEV. However as thess fields are maximally charged, there is a residual discrete $\mathbb{Z}_{k_l}$ subgroup with $k_l = q(c_l)$. In the following examples we find these singularities to be orbifold singularities that get resolved when we set $a_l > 0$.

- **The Landau-Ginzburg Orbifold (LGO) phase**: $a_J < 0 \qquad J$. In this case we find that the whole space has been shrunk to a singular point as the only solution of the chiral fields can be $\phi_i = 0\,\forall\, i$ and all $U(1)^n$ gaugings have been broken to a discrete subgroup. In the following sections we concentrate on this phase and its symmetries.

4.1.2 The Smooth-, $\mathbb{Z}_3$ Orbifold- and Landau-Ginzburg-phase

In this section we give two specific examples of GLSM setups that posses a $\mathbb{Z}_3$ orbifold phase and resolution phase. This section serves to make the general discussion of the last section more explicit and study the orbifold action in the given phase. Finally these two examples will be reconsidered from the Landau-Ginzburg perspective in the subsequent chapters.
We start with the *minimal resolved* $\mathbb{Z}_3$ GLSM. The reason for its name is, that it possess 27 singular points in the orbifold phase that are all resolved by setting a single FI parameter $b > 0$ and hence all singular points get replaced by the same divisor of same size [56]. Its field content is specified in Table 4.1. In the table we define the coordinates $\Phi_{\alpha,j}$ to highlight their charges under the $U(1)_a$ gaugings. The U(1)′ is the exceptional gauging with FI parameter b that resolves the orbifold singularities. For this geometry the general superpotential $\mathcal{W}$ is given by

$$\mathcal{W} = \sum_{\alpha=1}^{3} C_\alpha \underbrace{\left(\prod_{i=1}^{3} \Phi_{\alpha,i}^3 + \Phi_{\alpha,1}^3 \Phi'\right)}_{P_\alpha}, \tag{4.14}$$

	$\Phi_{1,1}$	$\Phi_{1,2}$	$\Phi_{1,3}$	$\Phi_{2,1}$	$\Phi_{2,2}$	$\Phi_{2,3}$	$\Phi_{3,1}$	$\Phi_{3,2}$	$\Phi_{3,3}$	C_1	C_2	C_3	Φ'
$U(1)_1$	1	1	1	0	0	0	0	0	0	-3	0	0	0
$U(1)_2$	0	0	0	1	1	1	0	0	0	0	-3	0	0
$U(1)_3$	0	0	0	0	0	0	1	1	1	0	0	-3	0
$U(1)'$	1	0	0	1	0	0	1	0	0	0	0	0	-3

Table 4.1: GLSM matter content and charges the minimal resolved $T^6/\mathbb{Z}_3$ orbifold [56].

which is completely fixed by gauge invariance under the four U(1)'s and the R-symmetry.

- We start by specifying the **smooth phase** where we scale all torus FI parameters $a_J > 0$ as well as the additional one $b > 0$. First we have the constraints that fix the overall size of the geometry:

$$\text{D-terms: } |\phi_{\alpha,1}|^2 + |\phi_{\alpha,2}|^2 + |\phi_{\alpha,3}|^2 - 3|c_\alpha|^2 = a_\alpha\,, \tag{4.15}$$

$$|\phi_{1,1}|^2 + |\phi_{2,1}|^2 + |\phi_{3,1}|^2 - 3|\phi'|^2 = b\,. \tag{4.16}$$

  In addition we have the F-term constraints:

$$c_\alpha \partial_{\phi_{\alpha,i}} P_\alpha = 0\,, \quad P_\alpha = 0\,, \tag{4.17}$$

$$\phi'\left(\sum_{\alpha=1}^{3}\phi_{\alpha,1}^2\right) = 0\,. \tag{4.18}$$

  By our usual argumentation we find from the F-terms that the c_α have to vanish. Hence the first D-term constraint fixes the $\phi_{\alpha,i}$ to obtain a VEV constraint by the Kähler modulus a_α which precisely defines a $\mathbb{P}^2$ space for each α. In addition the three F-term constraints $P_\alpha = 0$ cut out a degree three polynomial out of the three $\mathbb{P}^2$ spaces and hence we obtain three tori. In addition we have the $U(1)'$ action that sits diagonally in all three tori with the additional Φ' coordinate. When we go to locus $\phi' = 0$ we find from its D-term that this specifies another $\mathbb{P}^2$ with size b.

- The **orbifold phase** we take $a > 0$ and $b < 0$. Here we first observe from its D-term $\phi' \neq 0$ in order to cancel the negative b term. As ϕ' is maximally charged there is a residual $\mathbb{Z}_3$ that identifies the coordinates to $\phi_{\alpha,1} = -e^{\frac{2\pi i}{3}}\phi_{\alpha,1}$. As in the orbifold case we try to find the fixed points of that action given by $\phi_{\alpha,1} = 0$ and inserting them into the F-term constraints (4.17) and thus we find that two other coordinates are related by a cubic root:

$$\phi_{\alpha,2} = -\,e^{\frac{2k_\alpha \pi i}{3}}\phi_{\alpha,3}\,. \tag{4.19}$$

$$\tag{4.20}$$

  Our solutions are enumerated by $k_\alpha = 0, 1, 2$ and hence we find $3^3 = 27$ of those points that are precisely the fixed points we have encountered in Chapter 2.

  At this point it is also worth mentioning that the polynomials (4.17) do precisely cut out torus with a cubic in Fermat form. By mapping this elliptic curve into the Weierstrass form one can obtain its complex structure and find that it is fixed to $\tau = e^{\frac{2\pi i}{3}}$ which is that of an underlying SU(3) lattice [56]. In this way, we can identify the Φ' coordinate: For $b > 0$ it resolves all 27 singularities with the same Kähler parameter by gluing in a $\mathbb{P}^2$ into the space at the locus $\phi' = 0$. At the orbifold point this locus is absent as it is fixed by the VEV that breaks the $U(1)'$ to the

orbifold action.

- Now we turn to the **Landau-Ginzburg phase** by tuning $b < 0$ and $a_a < 0$. In this case, all c_a and ϕ' get a VEV by the D-term constraints and hence the four U(1) actions are completely broken to a $\mathbb{Z}_3^4$ discrete group. It is easy to see, that the VEV of the c_α fields leave the following charge combination invariant:

$$\widetilde{\mathrm{U}(1)}_\alpha = 3q_R + \mathrm{U}(1)_\alpha \,. \tag{4.21}$$

As the GLSM superpotential $\mathcal{W}$ had to have R-charge 1 the residual superpotential that we call $\mathcal{W}'$ at the Landau-Ginzburg point has to have R-charge 3 and all residual GLSM superfields Φ now carry R-charge 1. In order to keep our conventions we rescale all charges by a factor of 1/3 to give the superpotential R-charge 1 again. As the continuous R-symmetry is conserved the powers of the chiral fields in the superpotential $\mathcal{W}'$ of the LGO are still restricted. For the following discussion we factor out the R-charge and the other $\mathbb{Z}_3$ charges as given in Table 4.2. We can still see the torus factorization realized by the first three discrete actions whereas the

	$\Phi_{1,1}$	$\Phi_{1,2}$	$\Phi_{1,3}$	$\Phi_{2,1}$	$\Phi_{2,2}$	$\Phi_{2,3}$	$\Phi_{3,1}$	$\Phi_{3,2}$	$\Phi_{3,3}$
$\mathrm{U}(1)_\mathrm{R}$	1	1	1	1	1	1	1	1	1
$\mathbb{Z}_3^1$	1	1	1	0	0	0	0	0	0
$\mathbb{Z}_3^2$	0	0	0	1	1	1	0	0	0
$\mathbb{Z}_3^3$	0	0	0	0	0	0	1	1	1
$\mathbb{Z}_3^4$	1	0	0	1	0	0	1	0	0

Table 4.2: The discrete charge assignment for the minimal $\mathbb{Z}_3$ GLSM in its Landau-Ginzburg phase.

fourth is the orbifold action that acts in all three of them. Note that the first three $\mathbb{Z}_3$ actions are not independent and the sum of them can be rotated into the $\mathrm{U}(1)_\mathrm{R}$ R-charge. Hence we have only three independent $\mathbb{Z}_3$ actions.
The Landau-Ginzburg superpotential is simply given by a cubic polynomial in Fermat form:

$$\mathcal{W}' = \sum_{a,i=1}^{3} \Phi_{a,i}^3 \,, \tag{4.22}$$

which can be equally obtained from the GLSM after suitable scaling away the $|c|$ VEVs or by enforcing homogeneity and gauge invariance under the symmetries. Note, that the superpotential can only be of Fermat type and that no mixing term is possible[3]. Terms like these would correspond to complex structure deformations, which we do not have in the $\mathbb{Z}_3$ orbifold as the geometry is rigid.

Having motivated a possible geometric origin of the LGO phase, we go on and consider this specific phase in more detail in the following sections.

[3] Note that terms of the form $\Phi_{\alpha,i}^2 \Phi_{\alpha,j}$ that are allowed by all symmetries can nevertheless always be absorbed by a suitable redefinition of the fields.

4.2 Landau-Ginzburg Orbifolds and their symmetries

After the phase transition that we have observed in the previous section we have motivated the transition to the LGO phase from a GLSM and have obtained the defining LGO superpotential and its discrete symmetries as remnants of the geometric phase. However this was merely a motivation of how we should think of the LGO phase. Similar as in the GLSM the defining equations of the geometry are completely determined by R-symmetry and invariance under the discrete charges. In this way we can also describe many compactifications that do not have to have a geometric description in terms of a GLSM phase.
The nice fact about the LG phase is that there are methods to calculate the full massless spectrum in the four dimensional $\mathcal{N} = 1$ theory completely in terms of the WS fields using the techniques of [28].

4.2.1 The Landau-Ginzburg Spectrum

In the following we will give a short overview on how to calculate the massless spectrum of LGO theories using the techniques developed in [28]. For another review see [29].
Throughout this section a chiral superfield Φ^i has the R-charge α^i which in our cases will always be $\alpha_i = \frac{1}{3}$. It can be shown that Landau-Ginzburg models flow to minimal model CFT's [57] with central charge

$$c = 3\sum_i (1 + 2\alpha_i)\,. \tag{4.23}$$

This only specifies the internal part of the compactification, which is not enough yet to end up in a $c = (24, 12)$ compactification [58]. Hence when we choose a $c = (9, 9)$ compactification as it is on our examples with nine fields charges $1/3$ we simply have to add the following WS fields:

- Add two lightcone gauged left moving bosons and two right-moving $\mathcal{N} = (1, 0)$ multiplets that contributes $c = (2, 3)$. These coordinates provide the uncompactified 4D Minkowski target space.
- Add 10 left moving Mayorana Weyl fermions λ^I contributing c = (5,0) giving an internal SO(10) symmetry.
- Add 8 more Bosons X^I compactified on torus[4] contributing $c = (8, 0)$ leading to an E_8 gauge symmetry.

Also note here that we have made use of the *fermionic construction* of the heterotic string: Instead of having only left-moving bosons as we had in the introduction we also find fermions that we also have to distinguish independently by Ramond and Neveu-Schwartz boundary conditions. But as before, the space-time part of the modes is provided by the right moving sector.
At next we have to introduce a GSO projection in order to project onto states where left- and right-moving R-charge q_- and q_+ have an integer quantized difference which has been already noted by Gepner [59] as a necessary requirement for a consistent spectrum. The GSO projection ensures $\mathcal{N} = 1$ supersymmetry in four dimensions but also that the E_6 symmetry is manifest, although only the SO(10) symmetry is explicit at this point. The GSO action can then be written as

$$\hat{g} = e^{-\pi i J_- + F}\,, \tag{4.24}$$

[4] This torus is again fixed to be even and self dual.

with F being the left-and right fermion number. As the α^i is an R-charge bosonic and fermionic fields have different charges summarized in Table 4.3 On the other hand we can think of the GSO projection

charge	ϕ^i	ψ^i	$\bar{\phi}^i$	$\bar{\psi}^i$
q_-	α^i	$\alpha^i - 1$	$-\alpha^i$	$1 - \alpha^i$
q_+	α^i	α^i	$-\alpha^i$	$-\alpha^i$

Table 4.3: q_+ and q_- of bosonic and fermionic components of superfields.

as an orbifold and hence we have to supplemented the theory with the addition of twisted sectors. As the modes have a rational twisting by the R-symmetry α we should add additional $2k_0 - 1$ sectors with

$$\hat{g}^{2k_0} = \mathbf{1}\,. \tag{4.25}$$

Thus in our example with $\alpha^i = \frac{1}{3}$ we always have at least six sectors to consider. In addition, we can have n-discrete group actions as we have seen in the beginning that lead to additional identifications of the coordinates. Therefore we have to further orbifold the theory by each of the $\mathbb{Z}_{n_j}$ with $j = 1, \ldots, N$ factors

$$g_j = e^{\frac{2\pi i}{n_j}}\,. \tag{4.26}$$

Hence in total we get $\prod^N(n_j) - 1$ additional twisted sectors, which can easily give $\mathcal{O}(100)$ sectors that need to be considered. In the following we denote a twisted sector as $T_{(k_0;k_1,k2,\ldots k_N)}$ where we highlight the R-symmetry twist as the first entry. For each bosonic (fermionic) coordinate ϕ^i (ψ^i) we give the shift vectors ν^i ($\widetilde{\nu}^i$) that modify the oscillators in the mode expansion completely analogous to (2.46)

$$\nu^i = \frac{k_0\alpha^i}{2} + \sum_{j=1}^{N} k_j Q^i_j \qquad \text{mod } 1 \qquad \text{with } 0 \leq \nu^i \leq 1 \tag{4.27}$$

$$\widetilde{\nu}^i = \frac{k_0(\alpha^i - 1)}{2} + \sum_{j=1}^{N} k_j Q^i_j \qquad \text{mod } 1 \qquad \text{with } -1 \leq \widetilde{\nu}^i \leq 0 \tag{4.28}$$

where the super field Φ^i has charge Q^i_j under the $\mathbb{Z}^j_{n_j}$ discrete symmetry. Due to the twistings the vacuum acquires a contribution according to

$$E_{\text{vac}} = \left\{ \begin{array}{ll} -\frac{5}{8} + \frac{1}{2}\sum_i (\nu_i(1-\nu_i) + \bar{\nu}_i(1+\bar{\nu}_i)) & \text{for } k_0 \text{ odd} \\ 0 & \text{for } k_0 \text{ even} \end{array} \right\}. \tag{4.29}$$

Similarly, the vacuum is charged under the left and right moving charges:

$$q_{-,\text{vac}} = \sum_i \left((\alpha_i - 1)(\bar{\nu}_i - 1) - \alpha_i(\nu_i - \frac{1}{2}) \right), \tag{4.30}$$

$$q_{+,\text{vac}} = \sum_i \left(\alpha_i(\bar{\nu}_i + \frac{1}{2}) + (\alpha_i - 1)(-\nu_i + \frac{1}{2}) \right). \tag{4.31}$$

Analogous to the orbifold case we construct a state by acting with oszillators om the vacuum until we have an $E = 0$ state and check if it survives the orbifold projection. The q_- and q_+ quantum numbers

we find by summing up the vacuum contribution (4.30) and the ones of the oszillators (4.3). This we have to do for each twisted sector and then collect all states with the same quantum numbers into vector spaces distinguished by their left and right moving charge: $V_{(q_-,q_+)}$. However not all of them are the physical states yet.
When we construct the states we are interested in modes that are massless under the left and right moving Hamiltonian

$$2L_{\pm,0} = \{Q_\pm, \overline{Q}_\pm\} = 0\,. \tag{4.32}$$

As the supercharges are nil potent we are looking for states that are in the cohomology of the $\overline{Q}_\pm$ operator. We have already seen in the chapter before that it is the right moving part that gives rise to the space-time part and thus, this is the operator that is of main importance for us. The Q_+ operator clearly commutes with Q_- and hence does not change q_- but raises the charge of q_+ by one unit. Hence after we have computed the Vector spaces V_{q_-,q_+} in a given sector we have to find the states that are in the cohomology of the sequence

$$\ldots \xrightarrow{\overline{Q}_+} V_{(q_-,q_+)} \xrightarrow{\overline{Q}_+} V_{(q_-,q_+ +1)} \xrightarrow{\overline{Q}_+} \ldots .\,. \tag{4.33}$$

Calculating the cohomology means to find the states that are in the space

$$H = \frac{\ker(\overline{Q}_+)}{\mathrm{im}(\overline{Q}_+)}\,, \tag{4.34}$$

meaning that we should only allow for states in $V_{(q_-,q_+)}$ that get annihilated by $\overline{Q}_+$ but cannot be written as $\overline{Q}_+|\Psi\rangle$ with $|\Psi\rangle \in V_{(q_-,q_+-1)}$.
In general one should do the same for the $\overline{Q}_-$ operator but this is ensured by the GSO projection and taking the states with the correct left moving zero energy. Hence we are interested in the explicit form of the $\overline{Q}_+$ operator which can be obtained using the Noether procedure as

$$\overline{Q}_+ = \int d\sigma \overline{\psi}^i_+ \partial_+ \phi^i + i\psi^i_- \partial_{\phi^i} \mathcal{W}'\,, \tag{4.35}$$

where the first part comes from the Kähler potential and the second from the super potential. The idea is now, to consider the superpotential part as a *perturbation* of the kinetic energy part due to its scaling symmetry $\mathcal{W}' \to \epsilon \mathcal{W}'$ under which the kinetic part stays invariant. Hence we can start by considering the first term that came from the kinetic part. This part restricts us to consider states without ψ_+ and bosons that only depend holomorphically on the ϕ modes as these ones have a non-vanishing (anti-)commutator and thus cannot be in the kernel of $\overline{Q}_+$. Keeping that restriction in mind we simply have to consider the 'perturbation' of the kinetic energy given by the superpotential part

$$\overline{Q}'_+ = \psi^i_- \partial_{\phi^i} \mathcal{W}'\,. \tag{4.36}$$

The above computation can be extremely time consuming, in particular when there are $O(100)$ twisted sectors.
Having computed the left and right moving R-charge of every state that are in the $\overline{Q}$ cohomology we can identify its space-time properties: As noted in the beginning in the formalism only the SO(10) symmetry is explicit but the left moving R-symmetry on the world sheet enhances the SO(10) to an E_6 gauge symmetry in space-time. Hence we can recollect E_6 representations using the q_- according to the

following decomposition:

$$\begin{aligned}\mathbf{78} &\to \mathbf{45}_0 \oplus \mathbf{16}_{-3/2} \oplus \overline{\mathbf{16}}_{3/2} \oplus \mathbf{1}_0\,,\\ \mathbf{27} &\to \mathbf{16}_{-1/2} \oplus \mathbf{10}_1 \oplus \mathbf{1}_2\,,\\ \mathbf{1} &\to \mathbf{1}_0\,.\end{aligned}$$

Hence we find that each $SO(10) \times U(1)_-$ state can be uniquely associated to an E_6 representations. The only exception is the singlet field that also occurs in the decomposition of the adjoint. In a similar fashion we can use the right moving charge q_+ to identify the representation under the Lorentz group. This can in general be done by constructing the vertex operators corresponding to the space-time super fields and the SUSY generators [28]. The result of this computation is that fields with $q_+ = -\frac{1}{2}$ are left-chiral fermions and states with $q_+ = -\frac{3}{2}$ are gauginos in a vector multiplet. As the bosonic content of the theory is fixed by space-time supersymmetry it is sufficient to calculate the fermionic spectrum of the theory.
Now we have everything at hand to compute the full spectrum of any given Landau-Ginzburg orbifold, given that the field content and charges have been specified.

4.2.2 Classification of A_1^9 Models

We have started the chapter by taking the GLSM for the minimal resolved $\mathbb{Z}_3$ orbifold and going back to its LGO phase. Before we come back to this example, we want to present a full classification that can be done for $\mathbb{Z}_3$ models with nine fields that all have the same R-charges. This classification is independent of a possible GLSM phase and in fact we find many *non-geometric* examples that can not have a GLSM description.
We start by summarizing the defining properties of a given model:

- Fix the amount of $\mathbb{Z}_3$ moddings as well as their charge assignment for the fields. The CY-condition fixes the sum of the charges to be 0 mod 3.
- Switching on/off all superpotential couplings.

Especially the superpotential terms

$$\mathcal{W}' \ni \Phi_i \Phi_j \Phi_k\,, \tag{4.37}$$

if allowed by all symmetries can generically be identified as complex structure deformation terms.[5] For now we concentrate on potentials that are of *Fermat type* hence only super potentials that have the form

$$\mathcal{W}' \sum_{i=1}^{9} \Phi_i^3\,. \tag{4.38}$$

Potentials of that form generically have a higher symmetry as we will see in the following.

To find the maximal amount of N $\mathbb{Z}_3$ symmetries and all their charges assignments we work with the $N \times 9$ dimensional charge matrices Q_i^J. In the first step of our classification we use our freedom to

[5] Physically this can be explained that every deformation that keeps all symmetries intact must keep us at the LGO locus and hence it cannot be a Kähler deformation. However in the CFT description all those deformation correspond to (truly) marginal operators from the chiral-chiral ring that correspond the complex structure deformations.

rotate the charges in such a way that the above charge matrix has a $n \times n$ block only with unit charges. Hence N can be maximally be 8 as we have 9 fields and there must be always at least one field that has minus that charge in order to satisfy anomaly freedom of the theory: $\sum_i Q_i^J = 0 \bmod 3$. However then we can take the sum of all charges and absorb this generator into the R-charge and use that action to make one field completely neutral under all $\mathbb{Z}_3$ actions. Hence we and end up with $N = 7$ as the maximal amount of independent $\mathbb{Z}_3$ charges. As the charge assignment is completely fixed by the above argument there is one unique $\mathbb{Z}_3^Z$ orbifold model.[6] Hence when we have models with $n < 7$ discrete $\mathbb{Z}_3$ symmetries n+2 charges of the vectors are always fixed. Finally we only have to go through all possible charge assignments and check if they can be related via charge rotations to other equivalent models.

In total we have found 152 different models. All inequivalent models and their charge assignment as well as the spectra are given in Table D.1 of Appendix D. We emphasize that we calculate the whole amount of chiral and vector states that are uncharged under the E_6. We note that models like these have been often considered in the past [61, 62] but the neutral states have only been calculated when there were no additional discrete quotient factors.
Although these models do not have a geometric interpretation as the target space is just a point we describe $(2, 2)$ compactifications and we can identify the number of **27**-and $\overline{\mathbf{27}}$-plets as $h^{1,1}$ and $h^{2,1}$ Hodge numbers. In Figure 4.2 we summarize the 'geometric' data of the models by plotting the Euler number $\chi = 2(h^{1,1} - h^{2,1})$ against the sum of the Hodge numbers $h^{1,1}$ and $h^{2,1}$. We note that the whole set of

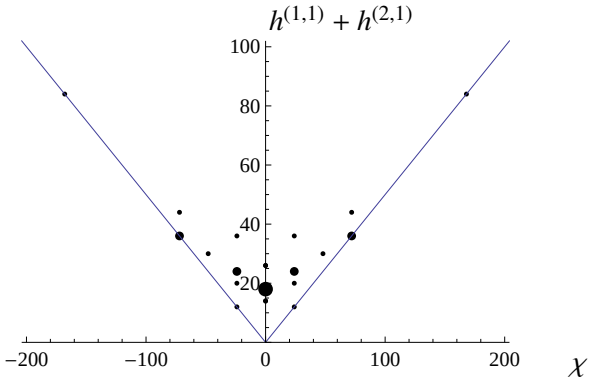

Figure 4.2: The summary of the geometric data of the A_1^9 LGO classification. We have plotted the Euler number χ against the sum of the Hodge numbers. Note that the diagram is fully mirror symmetric.

models is fully symmetric under the exchange of $h^{2,1} \leftrightarrow h^{1,1}$. This is in full agreement with the *Greene-Plesser construction* that we focus on in the next chapter. However, before we do that we remark some interesting results of our classification:

- Our list contains models with $\mathcal{N} = 1, 2$ and 4 super symmetries. This can be easily observed by the amount of additional gauginos that we have. In some $\mathcal{N} = 2$ cases we find the LGO phase of $K3 \times T^2$ compactifications which have the Hodge numbers

$$h^{2,1}(K3 \times T^2) = h^{1,1}(K3) \cdot h^{1,0}(T^2) + h^{2,0}(K3) \cdot h^{0,1}(T^2) = 21\,, \tag{4.39}$$
$$h^{1,1}(K3 \times T^2) = h^{0,0}(K3) \cdot h^{1,1}(T^2) + h^{1,1}(K3) \cdot h^{0,0}(T^2) = 21\,. \tag{4.40}$$

  We observe that the spectrum is non-chiral as expected for an $\mathcal{N} = 2$ theory.

[6] This example actually corresponds to the $T^6/\mathbb{Z}_3 \times \mathbb{Z}_3$ orbifold considered in [60].

- The boundary of the classified models in Figure 4.2 is given by the lines with $h^{2,1} = 0$ and $h^{1,1} = 0$. Models on the $h^{2,1} = 0$ line correspond to *rigid* geometries i.e. Calabi-Yaus that have no complex structure deformation. On the other side we find models that have $h^{1,1} = 0$. These are the mirror duals of those rigid geometries that have a fixed volume at the LGO locus. Those geometries cannot be obtained by the methods of toric geometry as a hypersurface (or CICY) in a given ambient space as those models necessarily have a Kähler modulus.

- At the Fermat LGO point generically all models have an enhanced gauge symmetry of at least dimension 8. But in many cases the dimension of the gauge symmetry is even higher. Geometrically this can be explained be recalling that the smallest length in string compactifications is actually not a point but the *self-dual radius*. At this point additional winding modes get massless and contribute vector-bosons. This can in fact be nicely seen in the $\mathcal{N} = 4$ compactifications. There we find models with 32 additional vector bosons. Eight of those vectors and 3 of the **27** and $\overline{\mathbf{27}}$ charged vectors enhance the E_6 to E_8 as this is a trivial T^6 compactification. The other $24 = 3 \times 8$ vectors come from the three tori with SU(3) Lie lattice structure[7] that got gauge enhanced as we are at the point of minimal compactification size which should be the self-dual radius. Another example are models with 86 additional vectors. Again 8 vectors enhance E_6 to E_8 and we are left with 78 gauge bosons. This is precisely the adjoint of the E_6 gauge group that we have used as the underlying Lie lattice of the compactification.

- Most interestingly all models satisfy the empirical formula

$$N_{\text{Add-S}} - 3N_{\text{Add-V}} = (4 - \mathcal{N}) \cdot 76\,, \tag{4.41}$$

  with $N_{\text{Add-S}}$ and $N_{\text{Add-V}}$ being the number of additional chiral singlets and vector multiplets neutral under the E_6. The astonishing fact is that this formula is satisfied by all models even with different supersymmetries. In the $\mathcal{N} = 4$ case this relation is clear as the left hand side has to vanish identically as in $\mathcal{N} = 4$ there are only vector multiplets that contain one vector and three chiral multiplets in $\mathcal{N} = 1$ language. However, the origin for $\mathcal{N} < 4$ cases is unclear, but might explained by anomaly cancellation and hint at a common moduli space for all A_1^9 models.

Note that the phenomenon of mirror symmetry in our model survey can be explained in terms of the Greene-Plesser orbifold construction that we summarize in the following.

4.2.3 The Greene-Plesser orbifold construction

In [63] B. Greene and R. Plesser explained the phenomenon of mirror symmetry in the context of minimal model CFT's. There they have found at the level of the partition function that a sign-flip of the left moving U(1) R-charge leaves the partition function invariant and is thus a symmetry of the theory. However this sign-flip interchanges changes the chiral-antichiral ring with the chiral-chiral ring which are the marginal operators that correspond to the $h^{1,1}$ and $h^{2,1}$ forms in the geometric phase.
Moreover they showed that a minimal model Z that possesses a discrete symmetry $G = \prod G_i$ can be orbifolded by a subgroup of G that we call H. The partition function then splits into two isomorphic copies that only differ by a sign of the left U(1) R-charge: One being the orbifold Z/H and the other one being the orbifold Z/F with quotient $F = G/H$.
Hence in our case the group G is $\mathbb{Z}_3^7$.[8] The orbifold action of H is specified by the set of charge vectors

[7] Remember that we consider the Fermat point that fixes the lattices to SU(3) structure.
[8] Note that this amounts to Abelian quotients only.

$Q \ni Q_i^J$ with $i = 1, \ldots, 9$ and $J = 1, \ldots, n$. The complement quotient group F we then construct by specifying the orthogonal set $Q^* \ni Q_i^{*,J}$ with $J = 1, \ldots, 7 - n$ defines as

$$Q^* := \{Q_i^{*,t} \in \mathbb{Z}_3^7 \mid \sum_i Q_i^s Q_i^{*,t} = 0 \bmod 3 \quad \forall Q_i^s \in Q\} . \tag{4.42}$$

Hence we have to construct the orthogonal subspace to H in G.

The remarkable result of Greene and Plesser was that the mirror duality keeps holding for a whole *family* of CFTs. The argument is that a mirror map Γ has to obey the following three properties

1. Γ is an isomorphism of the CFT C hence C and $\Gamma(C)$ are equivalent. Moreover the target space of both C and $\Gamma(C)$ are called *classically string equivalent*.
2. The only effect of Γ is changing the sign of the right U(1) R-charge of the CFT.
3. The map of geometrical operators of the target space Calabi-Yau is obtained from marginal operators of the CFT and is independent of Γ.

If C satisfies all those three points, then the target space Calabi-Yau's of the CFT's constitute mirror pairs.[9] The powerful statement is in fact that C belongs to a family of CFT's related by a deformation $\mathcal{U}$ then we can always define another mirror operator by the composition $\widetilde{\mathcal{U}}^{-1} \otimes \Gamma \otimes \mathcal{U}$, where $\widetilde{\mathcal{U}}^{-1}$ is precisely the inverse of the deformation $\mathcal{U}$ with the sign flip taken into account. We have depicted this statement in Figure 4.3 which shows how the mirror map extends over the whole moduli space of. This means for example when we know the CFT for a given Calabi-Yau X we can deform that CFT to

$$\begin{array}{ccc} \Gamma(C) = C_M & \longleftrightarrow & \widetilde{\mathcal{U}}(C_M) \\ \updownarrow \text{ Mirror} & & \\ \updownarrow \text{ map: } \Gamma & & \updownarrow \\ C & \longleftrightarrow & \mathcal{U}(C) \end{array}$$

Figure 4.3: Schematic graphic that shows how mirror symmetry at one point in the moduli space extends to a whole set of (marginal) deformed CFT's.

a point where we know the mirror map, for example the Landau-Ginzburg point where the mirror map Γ is given by eqn. (4.42) and then we simply have to take the mirror dual deformation and obtain the mirror Calabi-Yau $\widetilde{X}$ to the originial one. This is precisely what we will use in the following chapter where we go back to our $\mathbb{Z}_3$ orbifold example.

4.2.4 The $\mathbb{Z}_3$ mirror LGO

In this section we want to have a look at the $\mathbb{Z}_3$ orbifold from the view of its *mirror dual LGO model*.[10] We have seen that we simply have to construct the orthogonal subspace of charge vectors to the original LGO model. Observing the charge assignment of the minimal resolved LGO given in Table 4.2 we find the orthogonal subset to consist out of four independent $\mathbb{Z}_3$ actions given by the charge assignments in Table 4.4. Note that there is no torus structure as before which already hints at the non-geometric nature

[9] One can actually show, that the $h^{2,1}$ and $h^{1,1}$ forms of the target space Calabi-Yau can be constructed from marginal operators that precisely have $(-1, 1)$ and $(1, 1)$ charge under left-and right U(1)-R charge of the CFT corresponding to the antichrial-chiral and chiral-chiral ring of marginal operators.

[10] Note that this models has also been considered in [64] focusing on the WS perspective.

	$\Phi_{1,1}$	$\Phi_{1,2}$	$\Phi_{1,3}$	$\Phi_{2,1}$	$\Phi_{2,2}$	$\Phi_{2,3}$	$\Phi_{3,1}$	$\Phi_{3,2}$	$\Phi_{3,3}$
$U(1)_R$	1	1	1	1	1	1	1	1	1
$\mathbb{Z}_3^1$	0	1	-1	0	0	0	0	0	0
$\mathbb{Z}_3^2$	0	0	0	1	-1	0	0	0	0
$\mathbb{Z}_3$	0	0	0	0	0	0	0	1	-1
$\mathbb{Z}_3$	1	1	1	-1	-1	-1	0	0	0

Table 4.4: The discrete charges of the mirror to the minimal resolved $\mathbb{Z}_3$ GLSM.

of the model. In the following we want to discuss the spectrum of this LGO in more detail. However, we have already mentioned that every additional $\mathbb{Z}_3$ factor adds a factor of three new twisted sectors. Hence the above LGO requires to consider $6 \cdot 3^4 = 186$ twisted sectors which is too cumbersome at this point. Instead we are looking at the mirror of the *maximal* resolved $T^6/\mathbb{Z}_3$ GLSM constructed in [56]. The GLSM and its transition to the LGO point is given in the Appendix E. When we construct the orthogonal charge vectors, we find that the first three $\mathbb{Z}_3$ charge of the minimal mirror LGO in Table 4.4 get kicked out. The full set of charges is summarized in Table E.2.
This is a particularly nice example because we have only one $\mathbb{Z}_3$ action and thus need to consider 18 twisted sectors[11]. Before we go on, we should note that there is an $\mathbb{S}_3$ *permutation symmetry* among the coordinates $\Phi_{\alpha,\underline{i}}$ for every torus α. As we have only one $\mathbb{Z}_3$ action, it is clear that we can have

	$\Phi_{1,1}$	$\Phi_{1,2}$	$\Phi_{1,3}$	$\Phi_{2,1}$	$\Phi_{2,2}$	$\Phi_{2,3}$	$\Phi_{3,1}$	$\Phi_{3,2}$	$\Phi_{3,3}$
$U(1)_R$	1	1	1	1	1	1	1	1	1
$\mathbb{Z}_3$	1	1	1	-1	-1	-1	0	0	0

Table 4.5: The discrete charges for the minimal mirror of the $\mathbb{Z}_3$ Landau-Ginzburg phase.

superpotential terms in addition to the Fermat terms. The most general superpotential reads:

$$\mathcal{W} = \sum_{\alpha,i=1}^{3} \Phi_{\alpha,i}^3 + \sum_{\alpha=1}^{3} a_\alpha \Phi_{\alpha,1}\Phi_{\alpha,2}\Phi_{\alpha,3} + \sum_{i,j,k=1}^{3} b_{i,j,k}\Phi_{1,i}\Phi_{2,j}\Phi_{3,k}\,.$$

In total we have two types of deformations: The three a_α and the 27 deformations of type $b_{i,j,k}$. At next we want to identify these deformations with their mirror dual action. In Table 4.6 we summarize the effects of deformations on the spectrum when we switch on the respective LGO deformations. As we have specified an LGO in the above way, every deformation that we can switch on must be a 'complex structure' deformation. By the arguments of the last chapter these deformations correspond to Kähler deformation in the mirror dual model i.e. deformation that bring us back to the orbifold phase and its resolution. At next we want to identify the action of the deformation:

- Switching on an a_α term always removes two vectors. Having switched on all three a_α simultaneously leaves us precisely with the spectrum of the $T^6/\mathbb{Z}_3$ orbifold in the mirror that we have summarized in Table 2.2: There we found $27 \times 3 \cdot (1, \overline{\mathbf{3}})$-plets plus the 9 Kähler moduli give 252 E_6 singlets with the 8 residual vector states being the adjoint of the SU(3). Hence we can identify the a_α as the three Kähler deformation of the three ambient tori.

[11] The mirror of the maximal resolved LGO however has exactly the same spectrum at the Fermat point as the minimal resolved one.

Deformations	Chiral E_6 Singlets	Vector E_6 Singlets	**27**	$\overline{\mathbf{27}}$
-	270	14	36	0
a_1	264	12	36	0
a_1, a_2	258	10	36	0
a_1, a_2, a_3	252	8	36	0
$b_{\alpha,\beta,\gamma}$	214	6	36	0

Table 4.6: The in the LGO spectrum after including deformations away from the Fermat point.

- Switching on any of the 27 $b_{\alpha,\beta,\gamma}$ deformation removes exactly 8 vector states. This can be easily interpreted as the 27 blow up modes of each fixed point. From the 4D perspective these blow-up modes were precisely those fields that are charged in the fundamental of the SU(3) and hence every deformation breaks the SU(3) completely [34]. In Table E.3 we give a summary of the explicit form of the additional vector states.

After having matched the amount of the spectrum with that of the $T^6/\mathbb{Z}_3$ orbifold from the CFT computation we want to match all the symmetries as well. In the CFT point we have computed all charges of the states under continuous symmetries and had a full handle on all discrete R-and non-R symmetries. These are the symmetries we want to match in the following as well.

4.2.5 Construction of the symmetries

We start by the construction of the SU(3) gauge symmetry. For this we have to find appropriate Cartan operators and compute all the charges of the fields. First we start by the observation of how the U(1) gauginos look like. They are given by the nine states

$$\phi^{\alpha,i}_{-1/6}\bar{\phi}^{\alpha,i}_{-5/6} - 2\psi^{\alpha,i}_{-1/3}\overline{\psi}^{\alpha,i}_{-2/3}|1;0\rangle\,. \tag{4.43}$$

One of those U(1)'s must be the one that is inside the E_6 and we have seen that their U(1) charges were obtained by summing up the q_- charges of the WS fields and the vacuum acting on it. Hence we expect that this U(1) is the diagonal U(1) i.e. the sum of the above generators. Hence we propose a charge operator of a single U(1) generator simply by leaving out the sum in eq. (4.30) and that each world sheet field contributes the following charge of a state

$$\begin{aligned} q_{\alpha,i}(\phi^{\beta,j}) &= \tfrac{1}{3}\delta_{\alpha,\beta}\delta_{i,j}\,, \qquad q_{\alpha,i}(\overline{\phi}^{\beta,j}) = \tfrac{1}{3}\delta_{\alpha,\beta}\delta_{i,j}\,, \\ q_{\alpha,i}(\psi^{\beta,j}) &= -\tfrac{2}{3}\delta_{\alpha,\beta}\delta_{i,j}\,, \quad q_{\alpha,i}(\overline{\psi}^{\beta,j}) = \tfrac{2}{3}\delta_{\alpha,\beta}\delta_{i,j}\,. \end{aligned} \tag{4.44}$$

plus the charge of the corresponding twisted vacuum

$$q_{\alpha,i;\mathrm{vac}} = \left((\alpha^{\alpha,i}-1)(\bar{\nu^{\alpha,i}}-1) - \alpha^{\alpha,i}(\nu^{\alpha,i}-\frac{1}{2})\right). \tag{4.45}$$

The trace over the above U(1) generators is already familiar to us as it gives the U(1) inside E_6. But in addition we also obtain the explicit charges of the eight U(1) factors that are not inside E_6 in terms of the world sheet charges. [12]

[12] Note that the WS bosons indeed contribute different charges than the WS fermions as they come from the left moving world sheet R-symmetry.

From those residual eight U(1)'s we can construct the charge generators of all additional gauge symmetries. First we give the generators of the Cartan of the SU(3) that we call isospin and strangeness:

$$q_{\text{iso}} = \sum_{i=1}^{3} (q_{1,i} - q_{2,i}) = \hat{q}_1 - \hat{q}_2 \,, \tag{4.46}$$

$$q_{\text{str}} = \sum_{i=1}^{3} (q_{1,i} + q_{2,i} - 2q_{3,i}) = \hat{q}_1 + \hat{q}_2 - 2\hat{q}_3 \,. \tag{4.47}$$

Before we start computing the charges of actual states it is interesting to consider charges of the vacua first. From the formula (4.45) we see that the twisted vacua $|x;0\rangle$ are always uncharged. However in all the other sectors we find that the vacua form fundamental and anti-fundamental representations of the SU(3), depicted in Figure 4.4. Using the charges of the world sheet fields, we can compute the charges

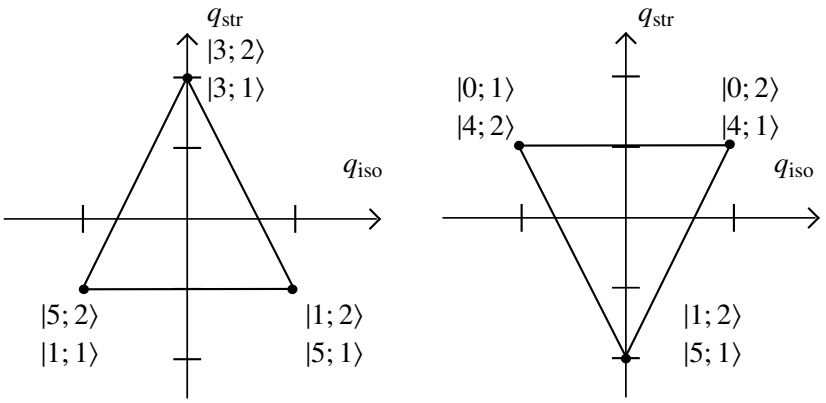

Figure 4.4: The SU(3) representation of the vacuum. Odd twisted representations form fundamental representations while even twisted ones give anti fundemantals.

of the 8 Vector multiplet states. Indeed they give exactly the octet representation of the adjoint of SU(3) whereas we find the two Cartans in the the $T_{(1;0)}$ sector whereas all the roots come from the vectors in the other sectors. The states are drawn in Figure 4.5. Note that we have introduced the shorthand notation $\overline{\Phi}_3 = \phi_{3,1}\phi_{3,2}\phi_{3,3}$. The charges under the other six additional U(1)'s are given by the combinations

$$Q_{\alpha,i} = q_{\alpha,i} - q_{\alpha,i+1} \quad \text{with } \alpha = 1,2,3\,, i = 1,2\,. \tag{4.48}$$

At this point we have to take an important fact into account: Considering the quantum numbers of all WS fields given in eq. (4.44) we see that the superfields $\Phi_{\alpha,i}$ have exactly the same quantum numbers for a fixed index choice α. Hence there are three $\mathbb{S}_3$ permutation symmetries for each α that we should take into account we constructing the target space symmetries.

At next we would like to find the representations under the additional six U(1) generators. As these six additional U(1)'s do not have an enhanced non-Abelian group structure there is actually no reason to expect some more structure here. However this is not the case as we will see in the following: For a given index choice $\alpha = 1,2,3$ there are three different kinds of representation defined by the index i. After computing the charges of all states we always find a complete structure of these representation as if they were representations of a non-Abelian group. However as there are only the Cartans one can think of the group as being the remnant of an adjoint breaking. We specify the three representations **R**

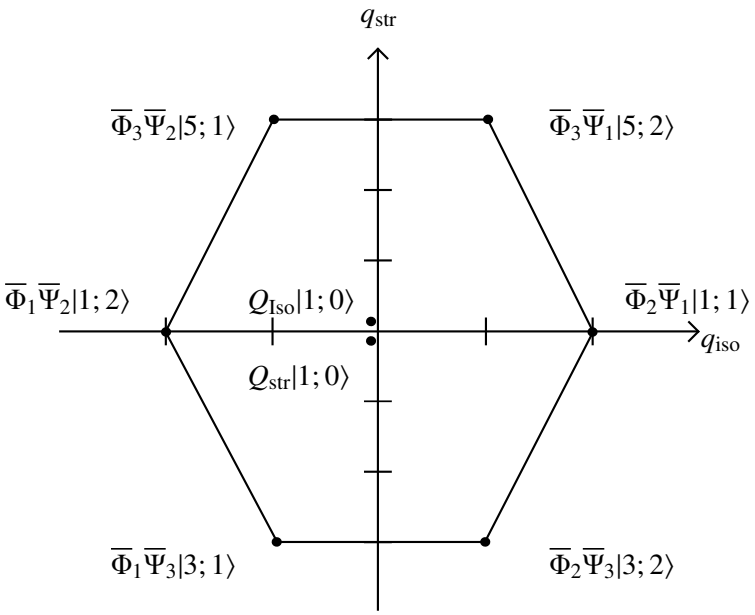

Figure 4.5: The Vector states that make up for the adjoint representation of SU(3).

as the collection of these states:

$$\mathbf{1}: \quad (0,0)\,, \tag{4.49}$$

$$\mathbf{3}^A: \quad (1,0) \to (-1,1) \to (0,-1)\,, \tag{4.50}$$

$$\mathbf{3}_a: \quad (\frac{1}{3},0) \to (-\frac{1}{3},\frac{1}{3}) \to (0,-\frac{1}{3})\,, \tag{4.51}$$

$$\mathbf{3}_b: \quad (0,\frac{2}{3}) \to (\frac{2}{3},-\frac{2}{3}) \to (-\frac{2}{3},0)\,, \tag{4.52}$$

Note that this looks very much like a highest weight construction of representations of the SU(3). However the difference is, that we are missing the roots of the adjoint representation. Moreover we find non-minimally charged states we called $\mathbf{3}^A$. As we have the very same structure for each index choice $\alpha = 1,2,3$ we collect them as direct product representations $(\mathbf{R},\mathbf{R},\mathbf{R})$ to present the states and the index structure in a more convenient way.

Similarly as in the orbifold, we demand that a coupling in four dimensions should be invariant under all quantum numbers. These include in particular the two twist quantum numbers k_0 and k_1 that we could assign to each sector.

Distler and Kachru have found in [30] that in particular the **78** gauginos are distributed over various k_0 twisted sectors. However it must be possible to find a linear combination of q_- and twisted sector charges to give them a common charge as they are in the same E_6 representation after all. For example in our case the E_6 gauginos are distributed in the sectors in the following way

State	$\mathbf{1}_0$	$\mathbf{45}_0$	$\overline{\mathbf{16}}_{-\frac{3}{2}}$	$\mathbf{16}_{\frac{3}{2}}$
Sector	$(1,0)$	$(1,0)$	$(0,0)$	$(2,0)$

$E_6 \times SU(3)$ Repres.	Flavor charges	$Q_{\mathbb{Z}_3}$	Q_R Superfield	label
$(\mathbf{27},\mathbf{3})$	$(\mathbf{1},\mathbf{1},\mathbf{1})$	0	12	$\mathbf{27}_{U1}$
$(\mathbf{27},\mathbf{3})$	$(\mathbf{1},\mathbf{1},\mathbf{1})$	1	0	$\mathbf{27}_{U2}$
$(\mathbf{27},\mathbf{3})$	$(\mathbf{1},\mathbf{1},\mathbf{1})$	2	0	$\mathbf{27}_{U3}$
$(\mathbf{27},\mathbf{1})$	$(\mathbf{3}_a,\mathbf{3}_a,\mathbf{3}_a)$	0	16	$\mathbf{27}_T$
$(\mathbf{1},\mathbf{3})$	$(\mathbf{3}_a,\mathbf{3}_a,\mathbf{3}_b)$	0	4	$\mathbf{3}_{B1}$
$(\mathbf{1},\mathbf{3})$	$(\mathbf{3}_a,\mathbf{3}_b,\mathbf{3}_a)$	1	16	$\mathbf{3}_{B2}$
$(\mathbf{1},\mathbf{3})$	$(\mathbf{3}_b,\mathbf{3}_a,\mathbf{3}_a)$	2	16	$\mathbf{3}_{B3}$
$(\mathbf{1},\mathbf{1})$	$(\mathbf{3}^A,\mathbf{1},\mathbf{1})$	0	0	$\mathbf{1}_{A,1}$
$(\mathbf{1},\mathbf{1})$	$(\mathbf{3}^A,\mathbf{1},\mathbf{1})$	1	0	$\mathbf{1}_{B,1}$
$(\mathbf{1},\mathbf{1})$	$(\mathbf{3}^A,\mathbf{1},\mathbf{1})$	2	12	$\mathbf{1}_{C,1}$
$(\mathbf{1},\mathbf{1})$	$(\mathbf{1},\mathbf{3}^A,\mathbf{1})$	0	0	$\mathbf{1}_{A,2}$
$(\mathbf{1},\mathbf{1})$	$(\mathbf{1},\mathbf{3}^A,\mathbf{1})$	1	12	$\mathbf{1}_{B,2}$
$(\mathbf{1},\mathbf{1})$	$(\mathbf{1},\mathbf{3}^A,\mathbf{1})$	2	0	$\mathbf{1}_{C,2}$
$(\mathbf{1},\mathbf{1})$	$(\mathbf{1},\mathbf{1},\mathbf{3}^A)$	0	0	$\mathbf{1}_{A,3}$
$(\mathbf{1},\mathbf{1})$	$(\mathbf{1},\mathbf{1},\mathbf{3}^A)$	1	6	$\mathbf{1}_{B,3}$
$(\mathbf{1},\mathbf{1})$	$(\mathbf{1},\mathbf{1},\mathbf{3}^A)$	2	6	$\mathbf{1}_{C,3}$

Table 4.7: All fields and their representation in the LGO mirror of the Z3 orbifold. We have explicitly given the charge under the non-Abelian like (gauged) U(1) symmetry as well as the discrete R-and non-R symmetry.

Remember that also the the other 14 additional vector states are distributed in various twisted sectors and some of them form $SU(3)$ representations adjoints that have to be incorporated in the charge operator as well. The resulting R-symmetry operator is given by

$$Q_R = 3k_0 - 2q_- + 2q_{\text{str}} \bmod 18\,, \tag{4.53}$$

which includes the SU(3) Cartan generator q_{str}. It is clear that this must be a mod 18 discrete symmetry as the sector $k_0 = 0$ is identified with $k_0 = 6$ and scalled with a factor of three. It can be easily seen that this charge operator assigns the charge 3 to all the gauginos that we have in the theory. The boson should have R-symmetry 0 which we get by subtracting 3 from the fermion charges. Hence the super potential $\mathcal{W}_{4\text{D}}$ in four dimensions should have R-charge -6. We can proceed similarly for the second twist generator $Q^1_{\mathbb{Z}_3}$ that is given by

$$Q_{\mathbb{Z}_3} = k_1 + q_{\text{iso}}\,. \tag{4.54}$$

This generator however is a pure discrete symmetry an not an R-symmetry as the gauginos are all uncharged under it. Having now found all symmetries we finally present the complete spectrum and all its charges in Table 4.7. Note that all $E_6 \times SU(3)$ singlet states are the additional LGO states and are the only states in $\mathbf{3}^A$ representations. Furthermore remember that these states were non-minimally charged under the flavor symmetries.

The four dimensional Higgs effect

We have already understood the deformation from the LGO phase to the $\mathbb{Z}_3$ orbifold phase (in the mirror) by switching on the a_α deformation terms. Now that we have all symmetries we can write down

the superpotential in 4D and understand the deformation in terms of the Higgs-mechanism in the effective field theory. First we are interested in the a_α deformations of the LGO superpotential from which we have seen that they correspond to the finite volume deformation of the α-th torus in mirror theory. But first we write down the 4D superpotential to trilinear order in the $\mathbf{1}_A$ singlet fields:

$$\mathcal{W}_{4D} = \sum_{\alpha=1}^{3} \mathbf{1}_{A,\alpha} \cdot \mathbf{1}_{B,\alpha} \cdot \mathbf{1}_{C,\alpha} \,. \tag{4.55}$$

Remember that each field such as $\mathbf{1}_{A,\alpha}$ is a quasi triplet under two flavor U(1)'s in the α-th torus with charges $Q_{\text{flav},\alpha}(\mathbf{1}^j_{A,\alpha}) = (1,0)^{j=1}, (-1,1)^{j=2}, (0,-1)^{j=3}$. The $\mathbb{S}_3$ permutation symmetry forces us to take the antisymmetric combination of the flavor group. Note that this is completely analogous to the $\mathbf{3}^3$ coupling within SU(3).
When we switch on a deformation a_α in the Landau-Ginzburg superpotential we argue that this precisely corresponds to a VEV v_α in the $\mathbf{1}_{A,\alpha}$ representation. D-and F-flatness ensure that all three components have to acquire the same VEV: Four dimensional D-term flatness of the α-th flavor symmetry reads

$$\sum_j Q_{\text{flav},\alpha} |\mathbf{1}^j_{3A,\alpha}|^2 = \begin{cases} |\langle \mathbf{1}^1_{3A,\alpha} \rangle|^2 - |\langle \mathbf{1}^2_{3A,\alpha} \rangle|^2 = 0 \,, \\ |\langle \mathbf{1}^2_{3A,\alpha} \rangle|^2 - |\langle \mathbf{1}^3_{3A,\alpha} \rangle|^2 = 0 \,. \end{cases} \tag{4.56}$$

Hence there is one VEV in the three representations

$$\langle \mathbf{1}^1_{3A,\alpha} \rangle = \langle \mathbf{1}^2_{3A,\alpha} \rangle = \langle \mathbf{1}^3_{3A,\alpha} \rangle = v_\alpha \,. \tag{4.57}$$

F-flatness is ensured by noting that $\mathbf{1}_{3A,\alpha}$ fields always appear at most linear in each Yukawa monomial. From (4.55) we find the (fermionic) mass matrix for $\mathbf{1}^j_{B,\alpha}$ and $\mathbf{1}^j_{C,\alpha}$ fields to be

$$\left(\mathbf{1}^1_{B,\alpha}\, \mathbf{1}^2_{B,\alpha}\, \mathbf{1}^3_{B,\alpha}\right) \begin{pmatrix} 0 & v_\alpha & -v_\alpha \\ -v_\alpha & 0 & v_\alpha \\ v_\alpha & -v_\alpha & 0 \end{pmatrix} \begin{pmatrix} \mathbf{1}^1_{C,\alpha} \\ \mathbf{1}^2_{C,\alpha} \\ \mathbf{1}^3_{C,\alpha} \end{pmatrix} . \tag{4.58}$$

It is easy to see that the above mass matrix has rank two and hence two complex Dirac fermions get massive and we are loosing four degrees of freedom. Then two other degrees of freedom of the $\mathbf{1}_{A,\alpha}$ are lost as Goldstone modes of the two broken U(1)'s. Hence in total we have lost two vectors and six more E_6 gauge singlets per a_α deformation. This field theory computation matches exactly the lost fields from the LGO deformations.
Furthermore note that the VEV's break the flavor group $Q_{\text{flav},\alpha}$ of one torus to two discrete subgroups[13]

$$Q_{\text{flav},\alpha} = \mathrm{U}(1)_{\alpha,1} \times \mathrm{U}(1)_{\alpha,2} \xrightarrow{v_\alpha \neq 0} \mathbb{Z}_3 \times \mathbb{Z}_3 \,. \tag{4.59}$$

Taken the semi-direct product with the $\mathbb{S}_3$ permutation factor of the world sheet coordinates we find precisely the $\Delta(54)_\alpha$ symmetry that we have found for every torus in the $\mathbb{Z}_3$ example. This calculation has also been carried out in a CFT in [38] and agrees with our result. Furthermore, we see that the singlet that obtains the VEV is neutral under the discrete R-and non-R-symmetry. Hence we have two residual symmetries that match those of the orbifold CFT.
Moreover the three D-and F-flat VEVs v_α are the three diagonal Kähler moduli of the orbifold.
Note that we can of course redo the same exercise for the blow up modes $\mathbf{3}_{B1}$ as well. It is easy to

[13] Remember that all other kind of charges were divided by three.

	$\Phi_{1,1}$	$\Phi_{1,2}$	$\Phi_{1,3}$	$\Phi_{2,1}$	$\Phi_{2,2}$	$\Phi_{2,3}$	$\Phi_{3,1}$	$\Phi_{3,2}$	$\Phi_{3,3}$
$U(1)_R$	1	1	1	1	1	1	1	1	1
$\mathbb{Z}_3^1$	1	1	1	-1	-1	-1	0	0	0
$\mathbb{Z}_3^2$	0	1	-1	0	1	-1	0	1	-1

Table 4.8: The charge assignment of the $SU(3)^4$ LGO.

see, that a VEV in such a representation breaks the R-symmetry as well as the SU(3). This is precisely what we would expect from the orbifold perspective. But we also expect that from our definition of the R-symmetry operator (4.53) which explicitly involves the strangeness Cartan operator of the SU(3) .

The nice point about this approach is that we can calculate the whole spectrum and its charges at a point in moduli space where symmetries are highly enhanced where we have no uncharged fields under any symmetry. This means that the whole structure of the super potential is completely determined by the those symmetries. Hence from this enhanced LGO Fermat point we can obtain any other point by deforming away and insert the VEVs in the 4D superpotential.

We also would like to highlight that, as this is a rigid geometry, we have an LGO formulation of the mirror dual geometry for any phase. This control gives a tool to obtain symmetries of compactifications and track them and their possible breakdown through various phases of the geometry.

4.2.6 The $SU(3)^4$ LGO example

As a final example we would like to present a model, that has very peculiar symmetries in the LGO phase and still posses a discrete (non-R) symmetry in the smooth phase. In the following we want to consider the LGO model described by the charge assignment in Table 4.8. This model corresponds to the mirror LGO to an $\mathbb{Z}_3$ orbifold on an E_6 lattice considered in [56] where another freely acting involution has been divided out which can be seen by the second $\mathbb{Z}_3^2$ action.[14] At the Fermat locus this model possesses 32 additional vector multiplets that we can collect into four SU(3)'s by the same methods as in the chapter before. We begin by the Cartan generators of the four SU(3)'s. We will call the two charge operators as $(q^I_{\text{str}}, q^i_{\text{iso}})$ with I labeling the I-th SU(3): The first SU(3) is structural exactly the same as the standard one:

$$q^A_{\text{str}} = \sum_{i=j}^{3} -2q_{3,j} + q_{1,j} + q_{2,j}\,, \tag{4.60}$$

$$q^A_{\text{iso}} = \sum_{i=1}^{3} q_{1,j} - q_{2,j}\,, \tag{4.61}$$

[14] The freely acting involution however does not identify individual fixed points among each other.

while the other ones have the following index structure:

$$q^B_{\text{str}} = \sum_{a=1}^{3} -2q_{a,1} + q_{a,2} + q_{a,3}\,, \tag{4.62}$$

$$q^B_{\text{iso}} = \sum_{a=1}^{3} q_{a,2} - q_{a,3}\,, \tag{4.63}$$

whereas the other 3 charge operators are very similar but have the shifted structure:

$$q^C_{\text{str}} = \sum_{a=1}^{3} -2q_{a,-a} + q_{a,2-a} + q_{a,1-a}\,, \tag{4.64}$$

$$q^C_{\text{iso}} = \sum_{a=1}^{3} q_{a,2-a} - q_{a,1-a}\,, \tag{4.65}$$

where we use the somehow convoluted index expression $2-a$ mod 3 meaning that the expression is to be taken mod 3 s.t. it is always positive and larger than zero. The last set is then also given as

$$q^D_{\text{str}} = \sum_{a=1}^{3} -2q_{a,1-a} + q_{a,2-a} + q_{a,a}\,, \tag{4.66}$$

$$q^D_{\text{iso}} = \sum_{a=1}^{3} q_{a,a} - q_{a,2-a}\,. \tag{4.67}$$

Note that we have again used the shifted index notation. The R-symmetry operator is constructed as

$$Q_r = 3k_0 - 2q_- + 2q^{(A)}_{\text{str}} + 2q^{(B)}_{\text{str}} + 2q^{(C)}_{\text{str}} + 2q^{(D)}_{\text{str}}\,. \tag{4.68}$$

Again we had to mix in the strangeness of the four SU(3)'s to guarantee a uniform charge for all gauginos. This time we have many more twisted sectors in which the gauginos are distributed. We proceed similarly for the other two discrete symmetries that are given as

$$Q^1_{\mathbb{Z}_3} = k_1 + q^A_{\text{iso}} + q^C_{\text{iso}} + q^D_{\text{iso}}\,, \tag{4.69}$$

$$Q^2_{\mathbb{Z}_3} = k_2 + q^B_{\text{iso}} + q^C_{\text{iso}} - q^D_{\text{iso}}\,. \tag{4.70}$$

Having all charge operators at hand, we can analyze the full spectrum and present the charges. We start with the **27**-plets in Table 4.9 These fields form tri-fundamental representations of the additional $\text{SU}(3)^4$ gauge factors. Again we summarize them and their charges in Table 4.10. It is interesting to see that the whole spectrum is completely symmetric under the permutation of the four SU(3) gauge factors. Hence at this point we cannot say which SU(3) is the one from the E_8. Similar as in the example we have presented in the section before, this permutation symmetry is inherited from the world sheet permutation symmetry. Only after applying a deformation that breaks the other SU(3)'s we can interpret the residual SU(3) factor as the one inside of E_8. So lets come to the deformations of the LGO superpotential given by

$$\mathcal{W}_{\text{Deform}} = A_a\Phi_{a,1}\Phi_{a,2}\Phi_{a,3} + B_i\Phi_{1,i}\Phi_{2,i}\Phi_{3,i} + C_i\Phi_{1,1+i}\Phi_{2,2+i}\Phi_{3,i} + D_i\Phi_{1,1-i}\Phi_{2,2-i}\Phi_{3,3-i}\,. \tag{4.71}$$

label	$E_6 \times SU(3)^4$ Repres.	$Q^1_{\mathbb{Z}_3}$	$Q^2_{\mathbb{Z}_3}$	Q_R Superfield
A^1	$(\mathbf{27},\mathbf{3},\mathbf{1},\mathbf{1},\mathbf{1})$	2	0	0
A^2	$(\mathbf{27},\mathbf{3},\mathbf{1},\mathbf{1},\mathbf{1})$	1	0	0
A^3	$(\mathbf{27},\mathbf{3},\mathbf{1},\mathbf{1},\mathbf{1})$	0	0	12
B^1	$(\mathbf{27},\mathbf{1},\mathbf{3},\mathbf{1},\mathbf{1})$	0	1	0
B^2	$(\mathbf{27},\mathbf{1},\mathbf{3},\mathbf{1},\mathbf{1})$	0	2	0
B^3	$(\mathbf{27},\mathbf{1},\mathbf{3},\mathbf{1},\mathbf{1})$	0	0	12
C^1	$(\mathbf{27},\mathbf{1},\mathbf{1},\mathbf{3},\mathbf{1})$	2	2	0
C^2	$(\mathbf{27},\mathbf{1},\mathbf{1},\mathbf{3},\mathbf{1})$	1	1	0
C^3	$(\mathbf{27},\mathbf{1},\mathbf{1},\mathbf{3},\mathbf{1})$	0	0	12
D^1	$(\mathbf{27},\mathbf{1},\mathbf{1},\mathbf{1},\mathbf{3})$	2	1	0
D^2	$(\mathbf{27},\mathbf{1},\mathbf{1},\mathbf{1},\mathbf{3})$	1	2	0
D^3	$(\mathbf{27},\mathbf{1},\mathbf{1},\mathbf{1},\mathbf{3})$	0	0	12

Table 4.9: All quantum numbers of the **27** representations of E_6

We have again used our shifted index notation to make the structure of the deformation more visible. Hence we find four kinds of deformations all with three sub deformations. Switching on any deformation, say B_i results in the following reduction of the spectra given in Table 4.11 The four SU(3)'s get broken via any *single* deformation of the type B_i to

$$SU(3)^A SU(3)^B SU(3)^C SU(3)^D \to SU(3)^B U(1)^4 \,. \tag{4.72}$$

Hence this deformation leaves exactly the $SU(3)^B$ unbroken and hence we interpret this one to have the E_8 origin. Adding additional B_i deformations will further break the four U(1) factors but keeps the $SU(3)^B$. unbroken.
We note that any other deformation in the super potential would exactly proceed in an analogous breaking, leaving the A, B, C or D SU(3) unbroken.
However switching on any additional VEV which is of a different kind, say A_I, breaks the remaining $SU(3)^B$ too. Hence this deformation must be interpreted as a blow-up mode of the orbifold singularities. The interesting point is that all deformations are completely democratic: The first deformation brings us to the orbifold phase and the second one blows up the singularities. The notation of ambient tori and the fixed points is only singled out by our choice of the deformation.
As we have again all symmetries at hand, we want to match the deformations of the LGO superpotential to the Higgs mechanism in the four dimensional effective action. In the following we claim that the three deformations correspond to VEVs inside tri-fundamentals that we called a_3, b_3, c_3 or d_3. Lets focus again on a B_i deformation that gives a VEV in the $(\mathbf{1},\overline{\mathbf{3}},\mathbf{1},\overline{\mathbf{3}},\overline{\mathbf{3}})_{b_3}$. In order to give the precise flat directions we call this state $\Phi_1^{i,j,k}$ with i, j, k being the three SU(3) indices inside $SU(3)^A, SU(3)^C$ and $SU(3)^D$. A deformation then corresponds to a VEV in the representation

$$B_1 : \langle \phi_1^{1,1,1} \rangle = \langle \phi_1^{2,2,2} \rangle = \langle \phi_1^{2,2,2} \rangle = a/2 \,, \tag{4.73}$$

$$B_2 : \langle \phi_1^{1,2,3} \rangle = \langle \phi_1^{2,3,1} \rangle = \langle \phi_1^{3,1,2} \rangle = b/2 \,, \tag{4.74}$$

$$B_3 : \langle \phi_1^{2,1,3} \rangle = \langle \phi_1^{1,3,2} \rangle = \langle \phi_1^{3,2,1} \rangle = c/2 \,, \tag{4.75}$$

label	$E_6 \times SU(3)^4$ Repres.	$Q^1_{\mathbb{Z}_3}$	$Q^2_{\mathbb{Z}_3}$	Q_R Superfield
a_1	$(\mathbf{1},\mathbf{1},\bar{\mathbf{3}},\bar{\mathbf{3}},\bar{\mathbf{3}})$	1	0	0
a_2	$(\mathbf{1},\mathbf{1},\bar{\mathbf{3}},\bar{\mathbf{3}},\bar{\mathbf{3}})$	2	0	0
a_3	$(\mathbf{1},\mathbf{1},\bar{\mathbf{3}},\bar{\mathbf{3}},\bar{\mathbf{3}})$	0	0	12
b_1	$(\mathbf{1},\bar{\mathbf{3}},\mathbf{1},\bar{\mathbf{3}},\bar{\mathbf{3}})$	0	1	0
b_2	$(\mathbf{1},\bar{\mathbf{3}},\mathbf{1},\bar{\mathbf{3}},\bar{\mathbf{3}})$	0	2	0
b_3	$(\mathbf{1},\bar{\mathbf{3}},\mathbf{1},\bar{\mathbf{3}},\bar{\mathbf{3}})$	0	0	12
c_1	$(\mathbf{1},\bar{\mathbf{3}},\bar{\mathbf{3}},\mathbf{1},\bar{\mathbf{3}})$	1	1	0
c_2	$(\mathbf{1},\bar{\mathbf{3}},\bar{\mathbf{3}},\mathbf{1},\bar{\mathbf{3}})$	2	2	0
c_3	$(\mathbf{1},\bar{\mathbf{3}},\bar{\mathbf{3}},\mathbf{1},\bar{\mathbf{3}})$	0	0	12
d_1	$(\mathbf{1},\bar{\mathbf{3}},\bar{\mathbf{3}},\bar{\mathbf{3}},\mathbf{1})$	1	2	0
d_2	$(\mathbf{1},\bar{\mathbf{3}},\bar{\mathbf{3}},\bar{\mathbf{3}},\mathbf{1})$	2	1	0
d_3	$(\mathbf{1},\bar{\mathbf{3}},\bar{\mathbf{3}},\bar{\mathbf{3}},\mathbf{1})$	0	0	12

Table 4.10: The gauge representation of the 324 E_6 singlet states and their R-charges.

Deformations	Chiral E_6 Singlets	Vector E_6 Singlets
-	324	32
B_1	264	12
B_1, B_2	258	10
B_1, B_2, B_3	252	8

Table 4.11: Spectra of the $SU(3)^4$ LGO for one B_i deformations. The structure for any other deformation such as A_i is completely analogous.

where the identifications ensure D-and F-flatness. We note, that a VEV in these representation precisely breaks not only the gauge symmetry but also the R-symmetry. Hence we expect that the orbifold phase does note have an R-symmetry but still have two discrete symmetries. Those couplings give the following super potential mass terms that we write in index notation as

$$\mathcal{W}_{4D} \in \epsilon^{a,b,c}\epsilon_{i,l,o}\epsilon_{j,m,p}\epsilon_{k,n,q}\Phi_a^{i,j,k}\Phi_b^{l,m,n}\Phi_c^{o,p,q} \,. \tag{4.76}$$

Again the *abc* indices are the flavor indices while the other ones are the gauge indices. The mass matrix can be found in the Appendix F. In the following table we list the rank of the mass matrix and the amount of Goldstone bosons that get eaten upon symmetry breaking.

Deformations	Mass matrix Rank	Goldstone Bosons	Massive Superfields
-	0	0	0
B_1	20	20	$2 \cdot 20 + 20$
B_1, B_2	22	22	$2 \cdot 22 + 22$
B_1, B_2, B_3	24	24	$2 \cdot 24 + 24$

Again we find from the field theory computation that exactly the right amount of states get massive to match the missing fields obtained from the LGO deformation given in Table 4.11. Again we can write down the whole four dimensional superpotential at the LGO point and then deform e.g. to the orbifold

phase by inserting the corresponding VEVs.
As a last remark lets consider the deformation to the smooth CY phase. The blow-up modes we have already identified by the other trifundamental representations that we called a_3, c_3 and d_3. These are indeed blow-up modes, as has been argued in [56] that always deform three fixed points simultaneously. However we have also seen, that all those deformations keep the two discrete symmetries invariant. Hence we are expecting the smooth CY to have a residual discrete symmetry.

In the above chapters we have given two examples that show the power of the LGO and mirror symmetry: We can construct a GLSM for a given geometry, go to the LGO Fermat point and then construct its mirror dual LGO. There we can compute the whole spectrum and all its symmetries. We then perform a complex structure deformation away from the Fermat point that corresponds to a Kähler deformation on the mirror side. However in the original model we stay at the LGO point where we have full control over the spectrum. As we have all symmetries at hand, we can write down the four dimensional superpotential to all orders and identify the above deformation in the four dimensional theory. We find that the gauge symmetry of the Fermat LGO point determines the amount of VEV insertions needed in the deformed superpotential similar as in the Froggat-Nielsen mechanism. The identification of the deformation as a VEV in certain representations allows in particular to track the breakdown of symmetries in different phases of the theory. This allows to compute R-symmetries in non-factorizable orbifold lattices where CFT methods are very hard to apply. Furthermore we have the hope to find a particular example where the blow-up (in the geometric dual) respects an R-symmetry, which will be the topic of future research.

CHAPTER 5

F-theory: Particle Physics from singular fibers

In this chapter we switch to Type IIB string theory and its low energy generalization called F-theory. This chapter serves as an introduction to the general concepts of F-theory compactification and pave the ground for Chapter 6 and 7. We start in Section 5.1 by observing the $SL(2,\mathbb{Z})$ symmetry of the axio-dilaton in Type IIB string theory and motivate its non-perturbative reformulation which is F-theory. In Section 5.2 we construct F-theory from M-theory and give the SL(2,$\mathbb{Z}$) symmetry a clear geometric interpretation as the modular properties of an auxiliary torus that is fibered over the physical compactification. Having clarified the role of the torus or more in general genus-one curves in F-theory compactifications we consider the construction of elliptic curves as toric hypersurfaces in more detail in Section 5.3. There we promote the elliptic curve to a fibration and consider the relevance of additional global sections for the derived physics. In Section 5.4 we analyze how to obtain gauge and matter spectrum by considering the codimension one and two singularities of the fiber as well as the neutral matter in the specific six dimensional case and its anomaly cancellation constraints. In the final Section 5.5 we present possibilities to engineer additional SU(5) gauge symmetries in two ways: First we consider a local approach, called the spectral cover where the SU(5) descents as a subgroup of an underlying E_8 and second we engineer SU(5) gauge groups onto the hypersurfaces we have considered before, called a *top*. In both approaches we obtain the gauge and matter spectrum that we reconsider in Chapter 7 in order to persue phenomenologically motivated model building.

5.1 The Type IIB string and SL(2,$\mathbb{Z}$) invariance

We get the first motivation for F-theory by considering the Type IIB string action[1]. In the following we consider the bosonic field content of the theory with the antisymmetric p-form potentials C_0, C_2, C_4, B_2 as well as the dilaton ϕ and the 10D Einstein frame metric $g_E^{M,N}$. We write the fields conveniently as

$$\begin{aligned} &F_1 = dC_0 \ , \qquad F_3 = dC_2 \ , \quad F_5 = dC_4 \ , \\ &\tau = C_0 + ie^{-\phi} \ , \quad H_3 = dB_2 \ , \quad G_3 = F_3 - \tau H_3 \ , \\ &\hat{F}_5 = F_5 - \tfrac{1}{2} C_2 \wedge H_3 + \tfrac{1}{2} B_2 \wedge F_3 \ , \end{aligned}$$

[1] for more information see i.e. [65]

where we are mainly interested in the following part of the action

$$\mathcal{S}_{IIB} = \frac{2\pi}{l_s^8}\int d^{10}x\,\sqrt{-g}R - \frac{1}{2}\left(\frac{|d\tau|^2}{(Im(\tau))^2} + \frac{|G_3|^2}{Im(\tau)} + \frac{1}{2}|\hat{F}_5|^2...\right), \tag{5.1}$$

and keeping in mind the geometrical duality relations $F_9 = *F_1\,, F_7 = -*F_3\,, F_5 = *\hat{F}_5 = -\hat{F}_5$ at the level of the equations of motion. Note that we have combined the axion C_0 and the dilaton ϕ into one object τ. In particular the dilaton part

$$e^{-\phi} = \frac{1}{g_{\text{IIB}}} \tag{5.2}$$

can be identify with the Type IIB coupling constant. The property of τ is that its kinetic term is invariant under $\text{SL}(2,\mathbb{Z})$ transformations[2]

$$\tau \to \frac{a\tau + b}{c\tau + d} \quad \text{with} \quad M = \begin{pmatrix} a & b \\ c & d \end{pmatrix} \in \text{SL}(2,\mathbb{Z})\,. \tag{5.3}$$

However, the τ term also appears in the G_3 kinetic term and hence we can only make this term invariant if B_2 and C_2 transform as $\text{SL}(2,\mathbb{Z})$ doublet according to

$$\begin{pmatrix} C_2 \\ B_2 \end{pmatrix} \to M\begin{pmatrix} C_2 \\ B_2 \end{pmatrix} = \begin{pmatrix} aC_2 + bB_2 \\ cC_2 + dB_2 \end{pmatrix}, \tag{5.4}$$

and all other fields stay invariant under the action. Of particular interest are transformations of the type

$$S = \begin{pmatrix} 0 & 1 \\ -1 & 0 \end{pmatrix}, \tag{5.5}$$

that map the type IIB coupling constant g_{IIB} to its inverse. This tells us that the strong coupling regime of type IIB strings does not map under strong-weak duality to different string theory but also to a IIB theory. In the following we consider the action of a D7/O7 brane system and see that these objects induce transformations like the ones we have just seen above.

Now we consider a single D7 brane that fills out eight dimensions and is a point in the other two spatial directions. We complexify these transversal coordinates to the brane as $z = x^8 + ix^9$ where the D7 brane is located at z_0. The RR-form field C_8 with Poincaré dual C_0 sources the D7 brane. Hence the Poisson equation for C_8 can be written as

$$d * F_9 = \delta^{(2)}(z - z_0)\,. \tag{5.6}$$

The total charge of the source is obtained by integration of the above equation to

$$1 = \int_{\mathbb{C}} d * F_9 = \oint_{S^1} *F_9 = \oint_{S^1} dC_0\,, \tag{5.7}$$

[2] The actual transformation is in $\text{SL}(2,\mathbb{R})$, however one can show [66] that D(-1) brane instantons break the group down to $\text{SL}(2,\mathbb{Z})$.

where we take the S^1 encircling the brane at z_0. To give dC_0 the right residual behavior at $z = z_0$ we get the solution

$$C_0 = \mathrm{Re}\left(\frac{1}{2\pi \mathrm{i}} \ln(\mathrm{z} - \mathrm{z}_0) + \mathrm{regular}\right), \tag{5.8}$$

such that we get by holomorphicity of τ:

$$\tau(z) = \tau_0 + \frac{1}{2\pi i} \ln(z - z_0)\,. \tag{5.9}$$

This solution has the shift behavior $\tau(e^{2i\pi} z) = \tau(z) + 1$ when we encircle the brane at z_0. But we also observe that τ goes to i∞ at $z = z_0$ and hence the string coupling vanishes at this point. Now we rewrite τ to to

$$\tau(z) = \frac{1}{2\pi i} \ln(\frac{z - z_0}{\lambda})\,, \tag{5.10}$$

to find that at $z - z_0 = \lambda$ the string coupling becomes infinity. If we want to deal with these D7 branes in a perturbative manner we have to confine us to distances with $|z - z_0| \ll \lambda$. Strictly speaking the perturbative calculations are only valid in the regions where g_{IIB} is small in a sufficiently large area i.e. $\lambda \to \infty$. But in any case, the fact that g_{IIB} develops a varying profile shows that the presence of the D7 branes strongly back-reacts on the geometry.

But lets go back to the monodromy shift $\tau \to \tau + 1$ we have encountered before. This action is simply generated by the T-duality subgroup

$$M_{1,0} = \begin{pmatrix} 1 & 1 \\ 0 & 1 \end{pmatrix} \in \mathrm{SL}(2, \mathbb{Z})\,, \tag{5.11}$$

which is not the most general transformation. In particular the fields C_2 and B_2 are a doublet under the whole $SL(2, \mathbb{Z})$ symmetry as we have seen before and hence it is natural to expect the existence of objects that are charged under both fields simultaneously. These objects are [p,q] branes with $(p, q)^T$ strings that can end on them.
The fundamental object of perturbative Type IIB strings is the $F1$ string, a B_2 sourced object with charge $(1, 0)^T$ whereas its dual is the C_2 charged counterpart, a D_1 string with the charge $(0, 1)^T$. However in the same theory, a D1 string is a non-perturbative solitonic object. The most general string however, that the symmetry of the theory suggests, is a $(p, q)^T$ string which is a linear combination of both objects. This $(p, q)^T$ string, with p and q being relatively prime end on a [p,q] brane that generates a $M_{[p,q]}$ monodromy when encircled. The monodromy action can be shown to be generated by

$$M_{[p,q]} = \begin{pmatrix} 1 - pq & p^2 \\ -q^2 & 1 + pq \end{pmatrix}, \tag{5.12}$$

that has only a $(p, q)^T$ string as an eigenvector. The above monodromy can always *locally*be brought into the diagonalized form of an $M_{[1,0]}$ brane action which is that of a D7 brane. However, in the presence of multiple $M_{p,q}$ branes with mutually different p and q this is not possible globally hence these systems are called *mutually non-local*. However in a consistent IIB compactification, the RR-Tadpoles have to cancel globally which demands the simultaneous presence of different [p,q] branes.
There is a particularly nice example in which Sen [67] considers a D7/O7 brane stack system and

decomposes it into a system of [p,q] branes which we review in the following.
Consider a [p,q] brane system $B = M_{[3,-1]}$ and $C = M_{[1,-1]}$ that is combined to

$$BC = \begin{pmatrix} -1 & 4 \\ 0 & -1 \end{pmatrix}, \tag{5.13}$$

that precisely acts as an orientation reversal on a fundamental string $BC(1,0)^T = (-1,0)^T$ and hence describes an orientifold $O7$ plane in IIB language. On τ on the other hand it acts as

$$BC(\tau) = \tau - 4\,, \tag{5.14}$$

and hence, the orientifold plane has -4 units of B_2 charge. Note that we can solve again for τ as we did before, and find that the coupling g_{IIB} becomes negative in an area close to the O7 plane. However a stack of four D7 branes has four times B_2 charge given by the monodromy matrix A

$$A = \begin{pmatrix} 1 & 4 \\ 0 & 1 \end{pmatrix}, \text{ such that } \quad ABC = \begin{pmatrix} -1 & 0 \\ 0 & -1 \end{pmatrix}. \tag{5.15}$$

Acting with the ABC matrices on the axio-dilaton generates a constant action. Hence we can choose the value of the axio-dilaton to be small and constant such that we are indeed dealing with a perturbative IIB model. Furthermore the RR-charge is zero not only locally but even globally. This brane configuration is known to give an SO(8) gauge symmetry in Type IIB.
The above example is in particular nice, as it shows how the $[p,q]$ brane system is decomposed purely into perturbative Type IIB objects. However this is only applicable when all the tadpoles cancel already locally. Compactifications with mutually non-local brane systems on the other hand need of a tool that keeps track of the global $\mathrm{SL}(2,\mathbb{Z})$ monodromy which can be done within F-theory.

5.2 From M- to F-theory

The main observation to treat the previously shown strong variation of the axio-dilaton system consistently lies in the interpretation of the $\mathrm{SL}(2,\mathbb{Z})$ symmetry as the modular transformation properties of a torus with complex structure τ . The similar behavior of the B_2 and C_2 two-form fields even suggest a torus compactification of a twelve dimensional theory. However there are two obvious problems with that interpretation:

- Where is the Kähler modulus of the torus?
- There is no twelve dimensional supersymmetric theory with signature (11,1).[3]

However the maximal supergravity that we know is 11D supergravity or M-theory. From M-theory on the other hand we know how to obtain a Type IIB string theory which we have summarized in Figure 5.1. The strategy in order to see the torus within M-theory is based on the following steps: Type IIB strings compactified on a circle and then T-dualized along that circle gives Type IIA in 9D. Finally Type IIA string theory is obtained by another circle reduction from M-theory. Hence there are two circle reductions of M-theory to be considered which is exactly the torus we were looking for. However, the actual limit is a more delicate as we have to perform T-duality and perform the limit to shrink the circle

[3] In [23] Vafa argued F-theory can also be obtained from a twelve dimensional theory of signature (10,2) compactified on a (1,1) Minkowski torus.

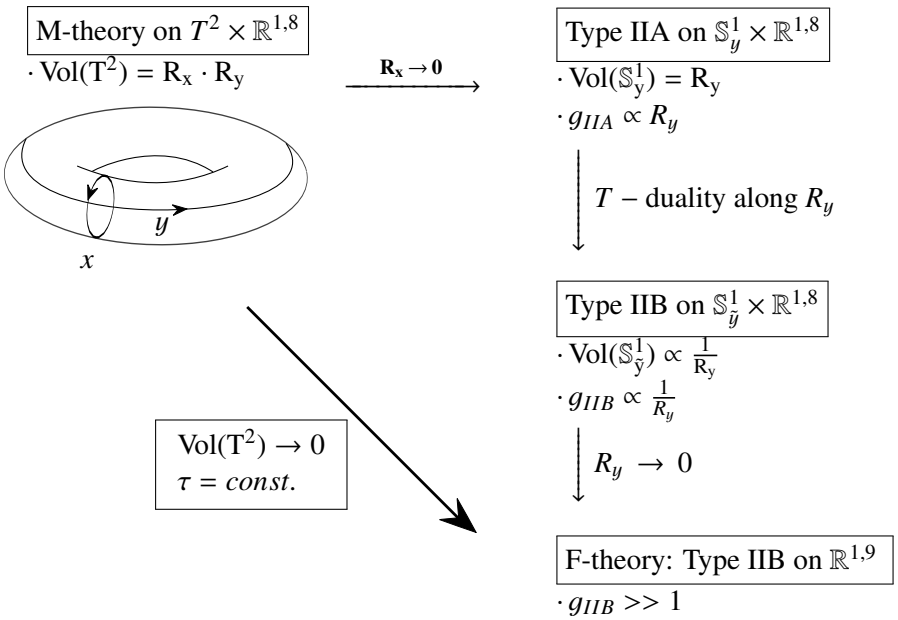

Figure 5.1: A Diagram of how to obtain F- from M-theory: The vanishing torus volume in M-theory while keeping τ constant corresponds to a chain of 1. dimensional reduction 2. T-dualization 3. dimensional oxidation towards Type IIB strings in ten dimensions.

radius. Hence first we consider 11D supergravity. The exceptional simple field content of M-theory is just the metric $g^{M,N}$ and the three form field strength C_3 that couples electrically and magnetically to M2 and M5 branes respectively together with their fermionic superpartners. The bosonic supergravity action then reads

$$\mathcal{S}_M = \int d^{11}x\sqrt{-g}R - \frac{1}{2}\int dC_3 \wedge *dC_3 - \frac{1}{6}C_3 \wedge dC_4 \wedge dC_4 + l_m^6 C_3 \wedge I_4(R)... \tag{5.16}$$

with $I_4(R)$ being a polynomial of degree four in the curvature and $C_6 = *dC_3$. The first step is to compactify this theory on a two torus to an $R^{8,1} \times T^2$ theory with the Ansatz for the metric:

$$ds_M^2 = \frac{v}{\tau_2}\left((dx + \tau_1 dy)^2 + \tau_2^2 dy^2\right) + ds_9^2\,. \tag{5.17}$$

x and y are the periodic circle coordinates on the torus with complex structure $\tau = \tau_1 + i\tau_2$ and volume v. One key point is, that we can allow the torus to vary depending on the ds_9^2 coordinates i.e. allow for a non-trivial fibration. The x directional circle we interpret as the Type IIA one. We identify the resulting Type IIA metric as

$$ds^2 = R_y^2 e^{\frac{4}{3}\phi}(dx + C_1)^2 + e^{-\frac{2}{3}\phi}ds_{\mathrm{IIA}}^2\,, \tag{5.18}$$

matching to M-theory $C_1 = \tau_1 dy$ with the type IIA dilaton: $e^{-\frac{4}{3}\phi} = \frac{v}{R_y^2\tau_2}$ and metric

$$ds_{\mathrm{IIA}}^2 = \frac{\sqrt{v}}{R_y\sqrt{\tau_2}}(v\tau_2 dy^2 + ds_9^2)\,. \tag{5.19}$$

R_y is the length modulus of the M-theory circle. The next step is to perform the T-duality transformation along the y-direction. Hence the y-circle length is mapped to $\hat{R} = l_s^2/R_y$, the axion C_0 becomes the y-component of C_1 i.e. $C_0 = \tau_1$. Furthermore, the coupling constant is mapped to that of type IIB $g_{\text{IIB}} = \frac{l_s}{\hat{L}} g_{\text{IIA}}$. Hence we can recollect the axio-dilaton system to

$$\tau = C_0 + \frac{i}{g_{\text{IIB}}} \tag{5.20}$$

which is the complex structure of the M-theory torus. However, we should have a look to the residual 9 dimensional theory in the vanishing circle limit in Einstein frame given as

$$ds^2_{\text{IIB}} = \frac{\sqrt{v}}{R_y}\left(\frac{L^2 ls^4}{v^2} dy^2 + ds^2_9\right). \tag{5.21}$$

The overall volume scales with the length modulus as $v = \sqrt{L_y}$. As we had to sent $L_y \to 0$ in the IIA reduction, we see how the length measure of the circle in x direction in the metric diverges and we obtain the decompactification limit to 10D type IIB with full Lorentz symmetry. This procedure can be employed also, when the theory is further compactified on a complex base[4] space B_n, however the whole space of the fibration must be an elliptically fibered Calabi-Yau Y_{n+1} fold in order to preserve the right amount of SUSY generators. The M-theory three-form potential can then be expanded upon the two shrinking cycles dx and dy as

$$C_3 = \hat{C}_3 + C_2 \wedge dx + B_2 \wedge dy + B_1 \wedge dx \wedge dy\,. \tag{5.22}$$

Here, the type IIB four-form is identified with $C_4 = \hat{C}_3 \wedge dy$ and B_1 will be part of the Minkowski metric in the F-theory limit. Furthermore we see, that the Type IIB NSNS and RR two forms come from a reduction of the two torus cycles which explains their transformation properties under $SL(2,\mathbb{Z})$. For more details how to obtain F-theory from M-theory see i.e. [68]. Finally we want to summarize the above procedure to give a *definition of F-theory*: F-theory on an elliptically fibered Calabi-Yau $n+1$ fold Y_{n+1}

$$\begin{array}{ccc} T^2 & \to & Y_{n+1} \\ & & \downarrow \\ & & B_n \end{array} \tag{5.23}$$

means to consider M-theory on the same $n+1$ fold in the vanishing fiber limit, that gives the Type IIB geometry B_n with the complex structure identified as the axio-dilaton of the fibration. Before we go to the next section we want to note that F-theory can also be motivated from the $E_8 \times E_8$ heterotic string [23] compactified on an elliptically fibered K3 manifold.

5.3 Elliptic curves as toric hypersurfaces

The above mentioned geometrization of the axio-dilaton as complex structure of the elliptic fiber is the greatest power of F-theory as we can use the techniques of algebraic and toric geometry to describe the gauge data of an F-theory compactification.
In the following sections we will use many different representations of the elliptic or more general the genus-one curve C. Hence this section is devoted to study various representations of genus-one curves

[4] The base must be complex such that τ can depend holomorphically on it as demanded by supersymmetry.

and their construction in more detail.
For analyzing the singularity structure it is particularly convenient to birationally map $\mathcal{E}$ into the Weierstrass form. The Weierstrass form is described as a hypersurface in the complex two dimensional space $\mathbb{P}^{(1,2,3)}$. The three complex coordinates admit a $\lambda \in C^*$ scaling that identifies coordinates as $(z, x, y) \sim (\lambda z, \lambda^2 x, \lambda^3 y)$. By the adjunction formula 2.27 the hypersurface constraint has to scale with the sum of all charges under a given scaling relation, i.e. a degree six polynomial in the $\mathbb{C}^*$ action. the Weierstrass equation is the vanishing of the polynomial

$$P_w = y^2 - x^3 - fxz^4 - gz^6 = 0\,, \tag{5.24}$$

with f and g being free complex coefficients. Of particular importance is the point P_0: $(z, x, y) = (0, \eta^3, \eta^2)$ that solves (5.24) independently of f and g. This point P_0 can be used to define the zero point on the elliptic curve.
In the following we are interested in cases when the elliptic fiber becomes singular i.e. Eq. (5.24) admits solutions with

$$dP_w = 0\,. \tag{5.25}$$

This behavior is encoded in the vanishing of the discriminant that can be expressed as

$$\Delta = 4f^3 + 27g^2\,. \tag{5.26}$$

A useful object we introduce is the $\mathrm{SL}(2,\mathbb{Z})$ invariant *Jacobi j-function* that can be expressed in the large complex structure limit as:

$$j(\tau) = \frac{4(24f)^3}{\Delta} = e^{-2\pi i\tau} + 744 + 196884e^{2\pi i\tau} + ... \tag{5.27}$$

As the torus is the unique Calabi-Yau in one dimension all descriptions of the elliptic curve are actually equivalent and we will see that they can always be birationally mapped into the Weierstrass form (5.24). But often it is convenient to start from higher dimensional spaces that contain the elliptic curve as a sub manifold that we can restrict on using a polynomial constraint just as we did for the Weierstrass equation. However we could have also started from a different or higher dimensional ambient space and describe the elliptic curve as a complete intersection Calabi-Yau (CICY) or a determinantal variety. In the following we will stick to the simpler cases, where there is only one defining polynomial for the elliptic curve and hence the ambient space is a two dimensional complex variety. This has two advantages: First these spaces have been classified completely in [69] and there are only 16 cases to choose from. Secondly the construction of *tops* [70] allows to engineer additional non-Abelian groups on top of those 16 varieties very easily.

The 16 toric varieties we are considering are generalizations of weighted projective spaces. Their structure is completely determined by the combinatorics of a two dimensional polyhedron F_i with edges v_i in a two dimensional lattice $N = \mathbb{Z}^2$. The sixteen possibilities are depicted in Figure 5.2. The variety P_F is constructed by associating a coordinate $x_i \in \mathbb{C}$ to every vertex v_i with $i = 1, \ldots, 2 + m$. As there are more than two vertices, there are m linear relations among them

$$\sum_{i=1}^{2+m} Q_i^a v_i = 0\,, \tag{5.28}$$

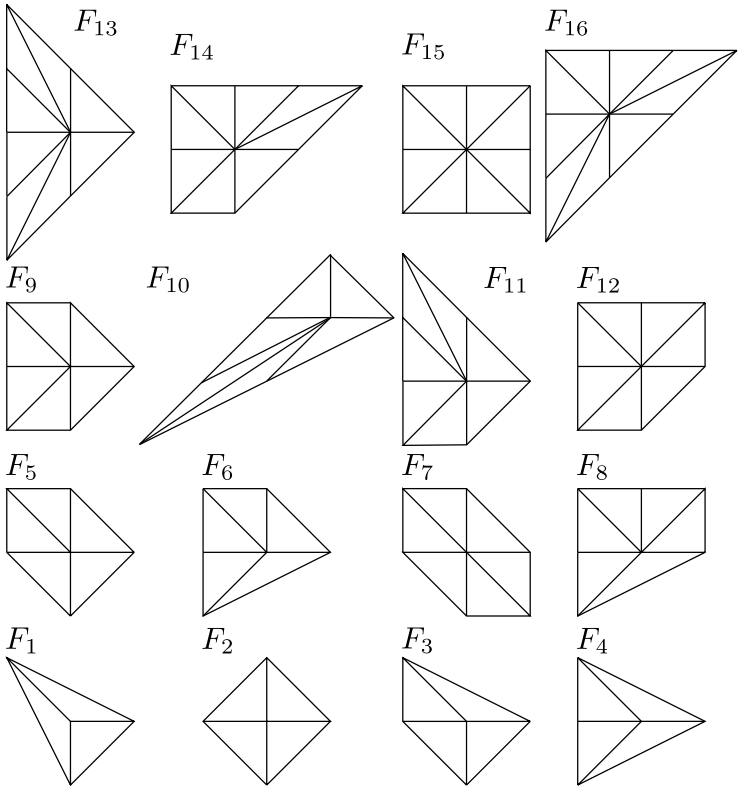

Figure 5.2: The 16 polyhedra that describe the all 2D toric varieties. Polyhedra F_i are dual to F_{17-i} for $i = 1, \ldots, 6$ and self-dual for $i = 7, \ldots, 10$.

with the scaling Q_i^a in order to constrain the dimensionality of the variety. These scalings Q_i^a can be viewed as the charges of the coordinates x_i transforming under a $\mathbb{C}^*$ action[5]. The variety is then specified by $m + 2$ copies of $\mathbb{C}$ **minus** the Stanley-Reisner ideal (SR) divided by the m $\mathbb{C}^*$ actions:

$$P_{F_i} = \frac{\mathbb{C}^{m+2} - \mathrm{SR}}{(\mathbb{C}^*)^m} = \left\{ x_i \sim \prod_{a=1}^{m} \lambda^{Q_i^a} x_i | \hat{x} \notin \mathrm{SR}, \lambda \in \mathbb{C}^* \right\}, \tag{5.29}$$

whereas $\hat{x}$ is a point not allowed to lie in the SR-ideal. The Stanley-Reisner ideal defines a set of coordinate monomials that we have to remove in order to keep the variety non-singular. The polyhedron F_i includes also intersections of the coordinates x_i geometrically: Two coordinates are defined to have a common solution if their associated vectors v_i span a cone $\sigma_k \in F$ i.e. when the two vectors are neighboring. When we consider divisors defined by the locus

$$D_i : \quad \{x_i = 0\}, \tag{5.30}$$

then they are defined to have intersection number one, when their associated coordinates lie in a cone. Hence all the other coordinates lie in the SR ideal and cannot have a common solution and their divisors have intersection number zero. The set of non-intersecting divisors or monomials of coordinates that cannot vanish simultaneously is then given exactly by the Stanley-Reisner ideal.

[5] Note that this charge is actually the same charge as in the GLSM of a torus Chapter 4

Self intersections of divisors can then be calculated by the following linear relations of the divisors

$$\sum_k v_k^i D_k = 0\,, \tag{5.31}$$

Now we define how to cut out the elliptic or genus-one curve (the difference is explained in Section 5.3.1) from a given variety P_F. For this it is convenient to introduce the *dual polyhedron* F^* defined on the dual lattice $M = \mathbb{Z}^2$, generated by the dual vectors $\hat{v}_k$:

$$F^* = \{\hat{v} \in M | \langle v_i, \hat{v}\rangle \geq -1, \forall v_i \in F\}\,, \tag{5.32}$$

with the pairing $\langle , \rangle$ given as the standard scalar product of the two vectors. Note that the whole set of all 16 toric varieties is closed under this duality i.e. F_i is dual to F_{17-i} for $i = 1, \ldots, 6$ and the polyhedra with $i = 7, \ldots, 10$ are selfdual.[6] Each point $\hat{v}_t$ in the dual polyhedron defines a monomial m_t in the coordinates given as

$$m_t = s_t \prod_{v_i \in F} x_i^{\langle \hat{v}_t, v_i\rangle + 1}\,, \tag{5.33}$$

with coefficient s_t in the field $\mathbb{C}$. Note that the dual polyhedron is defined in such a way, that every coordinate x_i appears with positive powers in the monomial. The hypersurface constraint is defined as the vanishing of the sum of those monomials m_t:

$$P_F = \sum_{t=1} m_t = 0\,. \tag{5.34}$$

We remark that the hypersurface constraint transforms *homogeneously* under the $\mathbb{C}^*$ scaling relations whereas its charge is the sum of charges of all coordinates. The dual polyhedron encodes all combinations of monomials that have exactly that charge under those scalings. Hence the more coordinates there are the more scalings we have and hence there are less points in the dual polyhedron that are possible. This property is also encoded in the first Chern class c_1 of the bundle: Every C^* action corresponds a divisor class and when we add up all divisors weighted with their respective charge under all scalings we exactly obtain the canonical bundle of the variety. Hence if we want to cut out a Calabi-Yau, we have to do this by an equation that exactly transforms in the anti-canonical bundle such that $c_1 = 0$.

In summary, when we describe a given genus-one curve then we always deal with a pair of polyhedra (F_i, F_i^*) whereas the first gives the coordinates, and the second one the monomials in the hypersurface constraint. In the following we will mainly deal with *specializations* of a given hypersurface, i.e. cases where certain coefficients s_t in front of the monomials are set to zero. Those specializations correspond to edges that are missing in the dual polyhedron and hence, when we dualize back to the original polyhedron gives rise to the introduction of additional coordinates. By this method, we only have to consider a set of three base polyhedra, because all the other ones are specializations of those. These are the polyhedra F_1, F_2 and F_4 that correspond to the spaces $\mathbb{P}^2, \mathbb{P}^1 \times \mathbb{P}^1$ and $P^{(1,1,2)}$, respectively.

[6] Also note, that $(F^*)^* = F$.

5.3.1 Points on genus-one curves

In the following we are particularly interested in points on the elliptic curve i.e. a point of the ambient space that solves the given hypersurface constraint (5.34). Two kinds of points will be of main interest:

- A rational point, that solves the hypersurface constraint with rational coefficients. These give rise to well defined divisors in the ambient space that intersects the elliptic curve exactly once.
- A multi-point, that is a multi valued solution of the hypersurface constraint. Hence its divisors intersects the elliptic fiber multiple times.

When a given genus-one curve admits at least one rational point, this point can be used to define a zero-point on the curve and in this case we will call it an elliptic curve. However in the following we also encounter curves that do not have rational points and are thus not an elliptic curve. However these curves can be mapped to its *Jacobian* that have the same complex structure modulus τ and have a zero-section and are thus elliptic curves. The set of rational points together with the zero-point, form a group under addition[7]. It can be shown that this group is finitely generated [72] and can therefore be decomposed into r-free and n-discrete parts: $\mathbb{Z}^r \oplus \mathbb{Z}_{k_1}, \ldots, \mathbb{Z}_{k_n}$. When we promote the elliptic curve to a fibration, the rational points become sections that generate $\mathrm{U}(1)^{\mathrm{r}}$ gauge symmetries in the field theory, whereas the n torsion parts give quotient factors of the total gauge group [73]. We summarize these concepts in a convenient example, that will be also of use later on: The ambient space we consider is given by F_{11} with the polyhedron depicted in Figure 5.3. The Stanley-Reisner ideal is read off to be

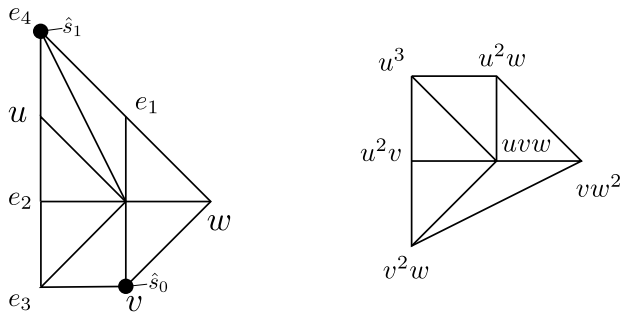

Figure 5.3: Polyhedron F_{11} and the corresponding coordinates. Edges in the dual polyhedron correspond to coordinate monomials, where we have set $e_i = 1$ for convenience. The choices for the inequivalent rational points are denoted with a dot.

$$SR = \{ue_1, uw, uv, ue_3, e_4w, e_4v, e_4e_3, e_4e_2, e_1v, e_1e_3, e_1e_2, we_3, we_2, ve_2\}\,. \tag{5.35}$$

The elliptic curve is specified by the vanishing of the hypersurface

$$p_{F_{11}} = s_1e_1^2e_2^2e_3e_4^4u^3 + s_2e_1e_2^2e_3^2e_4^2u^2v + s_3e_2^2e_3^2uv^2 + s_5e_1^2e_2e_4^3u^2w + s_6e_1e_2e_3e_4uvw + s_9e_1vw^2\,. \tag{5.36}$$

Indeed we find that the hyperplane Equation (5.36) is charged as the sum under each scaling or put differently transforms in the anti-canonical bundle

$$K_{F_{11}}^{-1} = \mathcal{O}(3H - E_1 - E_2 - E_3 - E_4)\,. \tag{5.37}$$

[7] For an example of the geometric group law, see appendix A of [71].

At next we can find the rational points on the curve by considering the coordinates of F_{11}, $[u : v : w : e_1 : e_2 : e_3 : e_4]$ that admit five $\mathbb{C}^*$ scalings summed up in the Table 5.1. We can then find the points on the curve, by

Coord.	H	E_1	E_2	E_3	E_4
u	1	-1	-1	0	-1
v	1	0	-1	-1	0
w	1	-1	0	0	0
e_1	0	1	0	0	-1
e_2	0	0	1	-1	0
e_3	0	0	0	1	0
e_4	0	0	0	0	1

Table 5.1: Summary of the scalings of the coordinates obtained from linear equivalences and the five divisor classes H, E_1, E_2, E_3, E_4.

setting one coordinate to zero and use the $\mathbb{C}^*$ scalings to set as many other coordinates to 1 as possible and then solve for the other coordinates[8]. In the following we give the rational points obtained by that procedure when we use the scalings to set all remaining coordinates that appear with powers greater than one in (5.36).

$$\hat{s}_0 : [1 : 0 : s_1 : 1 : 1 : -s_5 : 1] \,, \tag{5.38}$$

$$\hat{s}_1 : [1 : s_5 : 1 : 1 : -s_9 : 0 : 1] \,, \tag{5.39}$$

$$\hat{s}_2 : [s_9 : 1 : 1 : -s_3 : 1 : 1 : 0] \,. \tag{5.40}$$

Using the group law it can be shown that there is a linear relation among the sections and hence there are only two independent rational points. Hence the Mordell-Weil group has rank one [74, 71]. Note that we can also find non-rational points by setting $w = 0$ and use the scalings to set $v = e_1 = e_2 = e_3 = 1$. The hypersurface (5.36) then becomes

$$s_1 e_4^4 + s_2 e_4^2 u^2 + s_3 u = 0 \,, \tag{5.41}$$

that has the solutions $e_4^2 = \frac{-s_3 \pm \sqrt{s_3^2 - 4 s_1 s_2 u^6}}{2 s_2 u^2}$ that is clearly not a rational expression in the coefficients.

5.3.2 From elliptic curves to Elliptic fibrations

In the next step we have to promote the elliptic curve to an elliptic fibration of an n+1 fold

$$Y_{n+1} \xrightarrow{\pi} B_n \,. \tag{5.42}$$

We consider first the Weierstrass form of the elliptic curve, given in Equation (5.24). It is crucial that now the coordinates transform as functions of the base coordinates. More mathematically put they transform in powers of the bundle classes $\mathcal{L}_B$ of the base, that is the anti-canonical bundle K_B^{-1} of B_n. As there is one scaling relation among the coordinates, we choose the coordinates (z, x, y) to transform in $(\mathcal{L}^0, \mathcal{L}^2, \mathcal{L}^3)$. But the Weierstrass equation has to transform in a well defined way and hence the coefficients f and g have to transform in the powers $\mathcal{L}_B^4$ and $\mathcal{L}_B^6$.

[8] Note that this procedure only guarantees to find the *toric points* and do not have to be all rational points.

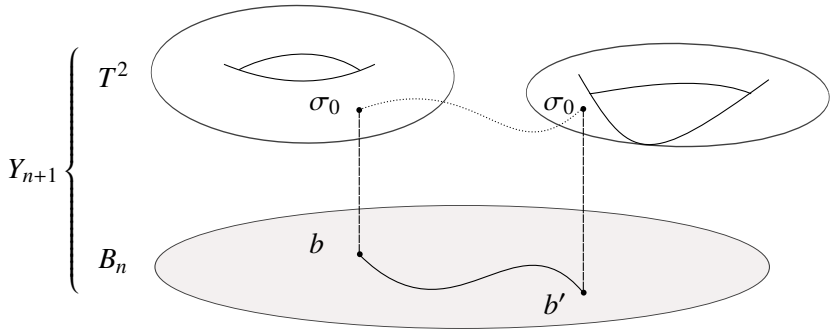

Figure 5.4: Picture of an elliptically fibered Calabi-Yau n+1-fold. The zero-section σ_0 identifies a point on the elliptic fiber over every point in the base B_n.

Another important fact is that a fibration needs at least one exceptional point O on the fiber, that distinguishes the fiber part from the base part. This point is usually referred to as the zero point, that gets promoted to the *zero section* σ_0 of the elliptic curve.
The zero section σ_0 gives an embedding of the base into the fibration $B_n \hookrightarrow Y_{n+1}$ that acts trivial on the base when composed with the projection: $\pi \circ \sigma_0 = \mathbf{1}_B$. σ_0 can then be used to globally keep track of the torus over a generic point in the base, see Figure 5.4. We have seen, that this point in the Weierstrass form given as $(z, x, y) = (0, \lambda^2, \lambda^3)$ is independent of f and g and is well defined everywhere over the base. In this case, the zero-section is holomorphic however it happens that even the zero section might not be well defined over certain codimension two loci, where it can wrap whole fiber components and is not just a point [75]. In this case, the zero-section is only rational but it is still sufficient for an F-theory compactification. In the following we generalize this procedure to all the other 16 polyhedra that we have discussed before. When we have at least one rational point, we will use this as the zero-section and if not, we will use the Jacobian fibration that possess one.
As the first step we promote the coordinates x_i to be sections of the base bundles $\mathcal{L}_B$. As we have m scaling relations for $m + 2$ coordinates we can use them to let only two coordinates transform non-trivially under the base bundles $\mathcal{L}_B$. In general the coordinates transform only in two different base bundles that we will take to be $\mathcal{S}_7$ and $\mathcal{S}_9$. When we choose the transformation of the coordinates properly then the monomial coefficients s_7 and s_9 in the hyperplane equation transforms exactly in the two bundles base bundles $\mathcal{S}_7$ and $\mathcal{S}_9$ motivating their names. We can then use adjunction again to fix the anti-canonical class of the base space in order to make the whole fibration a Calabi-Yau n+1 fold.

Lets get concrete by going on with the example of F_{11} and turn it to a whole fibration over a general base. We now choose the coordinates $u \in O(H-E_1-E_2-E_4+\mathcal{S}_9+[K_b])$ and $v \in O(H-E_2-E_3+\mathcal{S}_9-\mathcal{S}_7)$ whereas all the other ones have not changed compared to Table 5.1. Again the adjunction formula tells us that the sum of all divisors has to be trivial, which on the other hand fixes the anti-canonical class of the fiber in i.e.

$$3H - E_1 - E_2 - E_3 - E_4 + 2\mathcal{S}_9 - \mathcal{S}_7 + [K_B] = 0\,, \tag{5.43}$$

$$\rightarrow [K_B]^{-1} = 3H - E_1 - E_2 - E_3 - E_4 + 2\mathcal{S}_9 - \mathcal{S}_7\,. \tag{5.44}$$

Remember that the hypersurface constraint has to transform in the anti-canonical bundle given above. This we can use to read off the appropriate transformations for the s_i coefficients summed up in Table 5.2. Note that especially the coefficient of the middle point in the dual polyhedron has to scale with the

section	divisor class
s_1	$3[K_B^{-1}] - \mathcal{S}_7 - \mathcal{S}_9$
s_2	$2[K_B^{-1}] - \mathcal{S}_9$
s_3	$[K_B^{-1}] + \mathcal{S}_7 - \mathcal{S}_9$
s_5	$2[K_B^{-1}] - \mathcal{S}_7$
s_6	$[K_B^{-1}]$
s_9	$\mathcal{S}_9$

Table 5.2: Line bundle assignments of the monomial coefficients for the whole space to become a Calabi-Yau n+1-fold.

anti-canonical class. These assignments will be of particular interest, as they will give the multiplicity of the matter curves that are found at loci such as $s_i = s_j = 0$.

5.3.3 Jacobian Fibrations

In the very beginning we have stressed the point that an F-theory compactification needs a zero-section in order to identify the elliptic fibration. As it was first believed that this section should be holomorphic, this paradigm was relaxed to only allow for rational sections. However we can relax this condition even more i.e. the fibration does not need to have a section at all [76, 77]. In that case, we call the fibration a *genus-one* fibration as opposed to an *elliptic* fibration that always possesses a zero section. However we can use the mathematical fact that we can use for every genus-one curve C its *Jacobian* $\mathcal{J}(C)$ constructed by

$$\mathcal{J}(C) = \mathbb{C}/\left(\mathbb{Z} + \tau\mathbb{Z}\right) , \tag{5.45}$$

with the same τ as the genus-one curve C. Furthermore, the invariant Jacobi function J, see (5.27) coincide. The main point is that the Jacobian always has a Weierstrass [78] and in particular a zero point that becomes the zero-section.
It is naturally to expect that F-theory on the genus-one fibration C as well as its Jacobian $\mathcal{J}(C)$ should give the same compactification given that τ and J are the same. The group of curves with the isomorphic Jacobians is defined to be the *Tate-Shafarevich group* of a curve and in general is a subgroup of $\mathbb{Z}/\mathbb{Z}_k$ where k is the smallest k-section of the curve C. Hence when there exists a section on C, $k = 1$ and the Tate-Shafarevich group is trivial. In [79, 80] it was shown that in that the five dimensional M-theory compactification of genus-one curves differ from each other and correspond to different elements of the Tate-Shafarevich group. However, in the F-theory limit all compactifications coincide. In Chapter 6 we also encounter non-trivial examples of genus-one curves.

5.3.4 Singularities

With the fibration structure it can happen that the coefficients vary in such a way, that the elliptic fiber develops singularities over certain loci in the base. These singularities make the whole Y_{n+1} Calabi-Yau

singular and hence need a resolution in the fiber. This resolution can be done with the standard methods of algebraic geometry by blowing up and resolve fiber singularities. This means that we glue in additional $\mathbb{P}^1$'s into the spot of the original point until the space is smooth.
This resolution process is most easily depicted in the Weierstrass form of the elliptic curve, as there we have a criterion when we have hit a singularity. This is described by the vanishing of the discriminant Δ in (5.26) and it could be shown the resolution process depends only on the vanishing orders of f, g and Δ. Kodaira [81] has classified these resolutions in the case of K3 and shown that the classification is a reformulation of Dynkin's classification of semi-simple Lie Algebras: the A-D-E classification. By an A-D-E singularity we mean, that the additional $\mathbb{P}^1$'s intersect like the affine Dynkin diagram of an A-D-E group. Moreover if the singularity is too bad, i.e. ord$(\Delta) \geq 12$ it is a *terminal* singularity meaning the fiber cannot be resolved while preserving the whole space to be a Calabi-Yau. Hence there is an upper limit of gauge structures that can be expected in an F-theory description. We note that we have a way to engineer exceptional group structures which is not possible in the perturbative Type II theories. However we should be carefull as the above classification has been made for elliptically fibered K3 folds. On the other hand this does not mean, that the results are not applicable to three-or fourfolds, but in those cases we can expect additional features. For example there can be monodromies in the base space, that identify the three outer roots of an SO(8) gauge group which results in a G_2 group[9]. There are also certain cases (at higher codimension in the base) when the singularity cannot be resolved in a way such as given in Table [82] leading to non A-D-E singularities.
However it was shown, at least in the case of threefolds [83, 84] that this does not post problems on the low energy physics obtained by those fibrations.

ord(f)	ord(g)	ord(Δ)	Fiber Type	Singularity Type	group
≥ 0	≥ 0	0	smooth	none	-
0	0	n	I_n	A_{n-1}	SU(n)
≥ 1	1	2	II	none	-
1	≥ 2	3	III	A_1	SU(2)
≥ 2	2	4	IV	A_2	SU(3)
2	≥ 3	$n+6$	I_n^*	$D_n + 4$	SU(2n + 8)
≥ 2	3	$n+6$	I_n^*	$D_n + 4$	SU(2n + 8)
≥ 3	4	8	IV^*	E_6	E_6
3	≥ 5	9	III^*	E_7	E_7
≥ 4	5	10	II^*	E_8	E_8

Table 5.3: The Kodaira classification of singular fibers of an elliptically fibered K3[81].

5.4 The F-theory Spectrum

In the following sections we will workout, how to obtain the whole gauge and matter content in F-theory using the intersection properties and singularity structure of the fiber. We will again go through the example of F_{11} to be as concrete and instructive as possible.

[9] F_4 is another example but there are also other non-simply laced possibilities.

5.4.1 Non-Abelian Gauge symmetry: Singularities at Codimension 1

We consider an elliptically fibered CY that develops a singularity at codimension one over a given base divisor S defined by the locus[10]

$$S : \Delta = 0 \,. \tag{5.46}$$

We replace the singularity in the fiber by a tree of $\mathbb{P}^1$'s giving rise to new two-cycles Γ_i. These cycles give new divisors in the full Calabi-Yau D_i that are the fibrations over the base divisor S that supports the gauge group

$$D_i : \Gamma^i \to S \,. \tag{5.47}$$

Reducing the M-theory C_3 form along the new fiber divisor Γ^i gives a one-form in the uncompactified space:

$$\int_{\Gamma^i} C_3 = A_1^i \,. \tag{5.48}$$

The fiber component that is intersected with the zero-section is identified as the affine node Γ^0 and we can build up the divisor $D_0 = S - \sum_i a_i D_i$, with Dynkin labels a_i of the Lie algebra G obtained from the intersections of the divisors. The divisors intersect in the following way

$$\Gamma_i^{G_I} D_j^{G_J} = -C_{i,j}\delta_{I,J} \int_S \omega \, i, j = 0, \ldots, \mathrm{rank(G_I)} \,, \tag{5.49}$$

with $C_{i,j}$ being the Cartan matrix of the Affine Lie group (G_I) and $\omega \in H^{3-n}(B_n)$. The physical interpretation comes from M-theory: There are M2 branes that wrap the above $\mathbb{P}^1$'s that become massless when the fiber volume is shrunk zero size and will contribute massless vectors. Additionally there are M2 branes that wrap intersections of $\mathbb{P}^1$'s that give rise to the roots of the non-Abelian group.
The appearance of singularities and the connection of the Cartan matrix to the intersection of the resolution $\mathbb{P}^1$'s gives a straight forward description of non-Abelian groups in F-theory.
Lets check this again in the example of F_{11}. After mapping the cubic curve into the Weierstrass[11] form Δ is given as

$$\begin{aligned} \Delta =& 265 s_3^2 s_9^3 (27 s_3^2 s_5^4 s_9 + (s_6^2 - 4 s_2 s_9)^2 (-s_2 s_5^2 + s_1 (s_5 s_6 - s_1 s_9)) & (5.50) \\ &+ s_3 (s_5 s_6 - 2 s_1 s_9)(32 s_1 s_5 s_6 s_9 - 32 s_1^2 s_9^2 + s_5^2 (s_6^2 - 36 s_2 s_9))) \,. & (5.51) \end{aligned}$$

By setting $s_9 = 0$ or $s_3 = 0$ the discriminant develops a zero of order two and three respectively whereas f and g do not. From Table 5.3 it becomes clear that we have hit an SU(2) and an SU(3) singularity. To make this clear, lets inspect the elliptic curve in its original form that becomes:

$$\begin{aligned} P_{F_{11}}|_{s_3=0} =& e_1 \cdot q_2 \,, & (5.52) \\ P_{F_{11}}|_{s_9=0} =& e_2 \cdot u \cdot q_2 \,. & (5.53) \end{aligned}$$

[10] In the case of K3 this S would be just a point.
[11] We are leaving out the expressions of f and g for convenience as they are lengthy expressions but can be obtained from the general expressions found in the Appendix G after setting $s_4 = s_7 = s8 = s_{10} = 0$

We find, that in both cases the elliptic curve *factorizes* into two and three polynomials that describe $\mathbb{P}^1$ factors respectively. The three divisors give us the roots of the SU(2) and SU(3) gauge factors:

$$[e_1] = D_1^{\mathrm{SU}(2)}, \quad [e_2] = D_1^{\mathrm{SU}(3)}, \quad [u] = D_2^{\mathrm{SU}(3)}. \tag{5.54}$$

It can readily be checked, using the linear equivalences (5.31) that these divisors intersect like the roots of the corresponding gauge groups depicted in Figure 5.5.

We have also depicted the intersection of the zero-section σ_0 and the second section σ_1 with the fiber

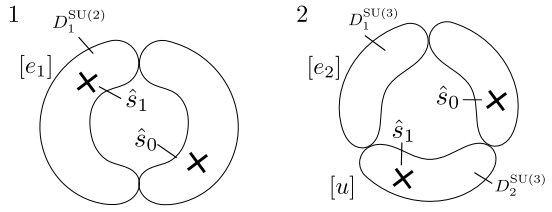

Figure 5.5: Codimension one fibers of $X_{F_{11}}$. The crosses denote the intersections with the two sections.

components.

Note there is a general lesson to learn from here that helps us to read off the non-Abelian gauge factors directly from the toric polyhedron: Whenever there N points lying on a line connecting two vertices this results in an SU(N) singularity by linear equivalence.

5.4.2 Abelian groups and rational sections

Non-Abelian gauge symmetries are much better understood than their Abelian counterparts because they allow for a local treatment of the singular behavior of the elliptic fiber. However, in the Abelian case the general fiber stays smooth i.e. we have an I_1 fiber. We have to find a new divisor $\hat{\omega} \in H^2(Y_{n+1})$ to expand the M-theory three-form $C_3 = \hat{\omega}^i A_i$ that is wrapped by the M2 brane but forbid the higher gauge enhancement.

These additional divisors are exactly supported by the additional rational points that we have discussed before. In the promotion to an elliptic fibration, the rational points become rational sections and the rank r of the free part of the Mordell-Weil group gives the amount of independent U(1) gauge factors, whereas the n torsion parts will be promoted to quotient factors of the total gauge group [73]. A rational section σ_Q gives another embedding of the base space into the CY: $B_n' \hookrightarrow Y_{n+1}$. When we track this embedding over various points in the base and take the difference to the zero-section this gives the desired new divisor whose Poincaré dual supports the desired U(1) gauge group, see Figure 5.6

One main feature of a rational section is that it does not need to stay holomorphic over the whole base space, i.e. it can wrap whole $\mathbb{P}^1$ fiber components at codimension higher one in the base and thus is not well defined: If we approach a given point in the base from all possible directions then the rational section maps to various points in the fiber whereas the collection of all paths gives the whole fiber $\mathbb{P}^1$. In the case when we have multiple sections, fixing the zero-section is a choice we are free to make. Hence the zero-section is no exception and does not need to stay holomorphic as well.

The mentioned divisor which we get in the full geometry is given by the Shioda map σ i.e. see [85]

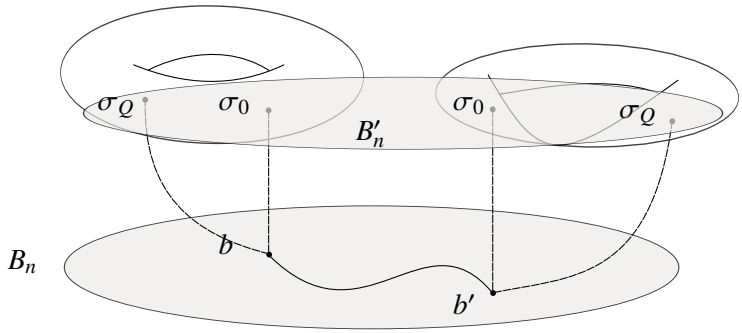

Figure 5.6: A illustrative picture of how a ration point induces another divisor.

that we can associate to a rational section S_m as

$$\sigma(S_m) := S_m - S_0 + [K_B] - \pi(S_m \cdot S_0) + \sum_{I=1}^{N} (S_m c_i^{G_I})(C_{G_I}^{-1})^{ij} D_j^{G_I} \,. \tag{5.55}$$

Note the appearance of the canonical class of the base $[K_B]$ as well as the projection onto the base part of the divisors S_m. The last term in the Shioda map gives a contribution when a section S_m intersects additional non-Abelian group factors hence the appearance of the inverse Cartan matrix $C_{G_I}^{-1}$. This contribution ensures orthogonalization of the U(1) and non-Abelian gauge factors. The charge of a given field under an $\mathrm{U}(1)_{\mathrm{M}}$ gauge factor is calculated by intersecting the corresponding Shioda map $\sigma_{(s_m)}$ with the divisors of the matter curves.
Before we continue with our example, we note that the intersection of the Shioda map allows to define the *Néron-Tate height pairing*

$$\pi(\sigma(\hat{s}_m) \cdot \sigma(\hat{s}_n)) = \pi(S_m \cdot S_n) + [K_B] - \pi(S_m \cdot S_0) - \pi(S_n \cdot S_0) + \sum_I (C_{G_I}^{-1})^{ij} (S_m \cdot c_{-\alpha_i}^{G_I})(S_n \cdot c_{-\alpha_j}^{G_I}) \mathcal{S}_{G_I}^{\mathrm{b}} \,, \tag{5.56}$$

that resembles the intersection of two rational sections projected to a divisor of the base. This intersection matrix supports Green-Schwartz counterterms that are needed for anomaly cancellation, for more details see [85].
To be concrete, the Shioda map in the F_{11} example is given by

$$\sigma(\hat{s}_1) = S_1 - S_0 + [K_B] + \frac{1}{2} D_1^{\mathrm{SU}(2)} + \frac{1}{3}(D_1^{\mathrm{SU}(3)} + 2D_2^{\mathrm{SU}(3)}) \,. \tag{5.57}$$

Intersecting the curve with $D_1^{\mathrm{SU}(2)}$, $D_1^{\mathrm{SU}(3)}$ and $D_2^{\mathrm{SU}(3)}$, where we have used that $S_1 \cdot D_1^{\mathrm{SU}(2)} = 1$ and $S_1 \cdot D_2^{\mathrm{SU}(3)} = 1$ as depicted in Figure 5.5, we can indeed confirm that the roots of the non-Abelian factors are uncharged[12] under the U(1). Hence (5.57) is a good definition of the U(1) charge generator.

5.4.3 Matter

Having outlined the procedure to obtain the gauge group and its generators we can compute the matter content. The charged matter content is generically given by fiber singularities of codimension two in the base, as opposed to the uncharged part.

[12] Note that the divisors do not intersect the $[K_B]$.

Charged matter: Codimension 2 singularities

In a similar spirit as the gauge groups, we can identify loci of charged matter in F-theory as a singularity of codimension two. These loci are generically obtained when we intersect multiple divisors in the base B_n that already give codimension one singularities and see how the vanishing order of the discriminant Δ increases. Similarly to the codimension one case, the elliptic curve factorizes at codimension two and contributes additional fiber components c_i. These curves corresponds to the *weights* of a given representation and we can compute their *Dynkin labels* λ_i by intersecting with the Cartan divisors D_i

$$\lambda_i = c \cdot D_i \,, \tag{5.58}$$

and obtain their U(1) charge completely analogous by intersecting with the Shioda map:

$$q_n = c \cdot S_n - c \cdot S_0 + \sum_{I=1}^{N} (S_m c_i^{G_I})(C_{G_I}^{-1})^{ij}(D_j^{G_I} \cdot c) \,. \tag{5.59}$$

Note that the charges are generically quantized but the sum that involves the inverse Cartan matrix contributes factors of $1/\text{rank}(G_I)$.

The matter loci of purely U(1) charged matter are a bit harder to find than their non-Abelian counter parts because there is no codimension one locus to begin with where we could start from and observe where the singularity enhances further. However the existence of a rational point s_l that has coordinates $(1, A, B)$ in the Weierstrass form implies its factorization [86]

$$0 = -(y - B)(y + B) + (x - A)(x^2 + Ax + C) \,, \tag{5.60}$$

which then gives a relation for f, g and Δ by expanding and comparing coefficients in (5.24)

$$f = C - A^2 \,, \tag{5.61}$$

$$g = B^2 - AC \,, \tag{5.62}$$

$$\Delta = 16 \cdot \left(B^2 \left(27B^2 - 54AC \right) + (C + 2A^2)^2 (4C - A^2) \right) . \tag{5.63}$$

We find for the Weierstrass equation to be singular, the constraints

$$B = (C + 2A^2) = 0 \,, \tag{5.64}$$

have to hold with vanishing order of Δ to be two. This corresponds to an A_1 singularity (compare with Table 5.3) and is indeed codimension two in the base.
The complete intersection (5.64) is in general a reducible variety in the base. The main complication is that certain non-generic loci that fulfill these constraints are also included in other more complicated ones. Mathematically we have to decompose these loci by making a *prime ideal decomposition*. A given component we denote by $I_{(k)}$ and the vanishing locus as $V(I_{(k)})$. After having found all loci by using algebra programs such as `Singular`, we analyze the fiber for all components $I_{(k)}$ and compute the charges of the associated matter curves.
To obtain the multiplicities of the states we have to distinguish the cases of a six and to four dimensional compactification. The four dimensional case we discuss in Chapter 7. Six dimensions are special as there the chirality is fixed [33] and a codimension two locus in the base is simply a point. Hence in order to find the multiplicities of a matter curve defined by the vanishing of a polynomial, or more in

general the ideal $I_{(k)}$, we have to count the amount of solutions to that constraint.
Lets for example consider a matter locus that is defined by the intersection of the two ideals $V(I_{(1)} \cap I_{(2)})$. If this variety contains simpler constraints, such as $s_1 = s_2 = 0$ which however are different matter curves, we have to subtract those solutions as they correspond to matter multiplicities of other states. In general it can happen that the simpler solutions $s_1 = s_2 = 0$ are included n-times in the variety $V(I_{(1)} \cap I_{(2)})$. In such a case we have to be subtract exactly n-times the corresponding points. The factor n can be easily computed using the *resultant* of the polynomial system $I_{(1)} = 0$ and $I_{(2)} = 0$ when s_1 and s_2 are viewed as variables in those polynomials. More details concerning the resultant techniques can be found in [75].

Lets apply those computations again concretely in the F_{11} example: By specifying $s_9 = 0$ we first go to the SU(3) locus and then we also set $s_5 = 0$ and go to codimension two. By inspecting (5.50) and comparing with (5.3) we see that the singularity enhances to an SU(4) factor and we expect to find triplet states. This can be explicitly seen by confirming the factorization of the elliptic curve in its cubic form on that locus to

$$p_{F_{11}}|_{s_9=s_5=0} = u \cdot e_2 \cdot e_3 \cdot p_2 \,, \tag{5.65}$$

with p_2 a quadratic polynomial. The situation of how the elliptic curve enhances further is depicted in Figure 5.7. Now we can see, how the polynomial q_2 splits up into the curves p_2 and e_3. We choose

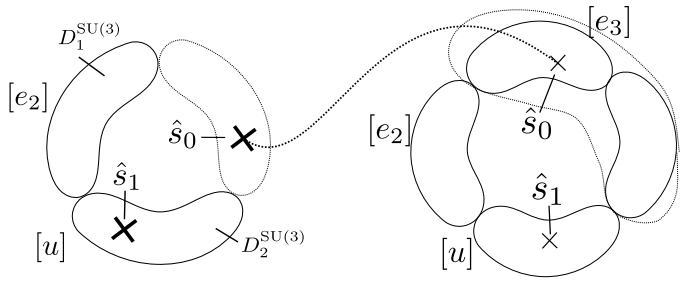

Figure 5.7: The enhancement of the SU(3) gauge locus at $s_9 = 0$ to the SU(4) matter point at $s_5 = 0$. Note how we can use the zero section to track the affine node that splits up over the enhanced locus.

$p_2 = c_1$ as the matter curve and by subsequently adding roots of the non-Abelian group we can complete the full representation. The Dynkin labels $\lambda_i(c_j) = c_j \cdot D_i$ can be readily obtain from Fig. 5.7 where we can read off the intersection properties.

Curve	Dynkin label
c_1	$(0, 1)$
$c_1 + D_2$	$(1, -1)$
$c_1 + D_1 + D_2$	$(-1, 0)$

The U(1) charges we obtain similarly by intersecting the curve with the Shioda map 5.55:

$$q_{c_1} = c_1 \cdot \sigma_1 = \underbrace{c_1 \cdot S_1}_{=0} - \underbrace{c_1 \cdot S_0}_{=0} + \frac{1}{3}\left(\underbrace{c_1 \cdot D_1}_{=0} + 2\,\underbrace{c_1 \cdot D_2}_{=1}\right) = \frac{2}{3}\,. \tag{5.66}$$

To summarize we got a $(\overline{\mathbf{3}}, \mathbf{1})_{2/3}$ representation, with the multiplicity simply given as the product of the two bundle classes of the base in which the sections s_9 and s_5 have transformed obtained from Table 5.2: $\#\left((\overline{\mathbf{3}}, \mathbf{1})_{2/3}\right) = \mathcal{S}_9 \cdot (2[K_B^{-1}] - \mathcal{S}_7)$. Equivalently we could have chosen the curve e_3 as the matter curve resulting in the conjugated representation which still gives the the state in the 6D theory.

Uncharged matter: Adjoints and moduli

The last two kinds of states do not come from codimension two singularities. The first ones are multiplets in the adjoint representation. In [87] it was shown that over a divisor $\mathcal{S}_I$ in a two dimensional base B_2 that supports a non-Abelian group G_I the quantization of the M2-brane moduli space gives additional g_I hyper multiplets charged in the adjoint representation. Here g_I denotes the *genus* of the divisor $\mathcal{S}_I$ given by

$$g_I = 1 + \frac{1}{2}\mathcal{S}_{G_I} \cdot (\mathcal{S}_{G_I} + [K_B]) \,, \tag{5.67}$$

where we took $\mathcal{S}_{G_I}$ as the divisor classes in the base and $\cdot$ denotes their intersection. These adjoint hypermultiplets come along with the vector multiplets of the gauge symmetry which makes them a codimension one phenomenon.

The last type of matter we want to discuss are the geometric moduli of the compactification and are neutral singlets. We start by noting that the rank of the **total** gauge group of the fibration Y_{n+1} is given by the Hodge numbers

$$\text{Rank}(G_Y) = h^{(1,1)}(Y) - h^{(1,1)}(B) - 1 \,. \tag{5.68}$$

This formula simply counts the amount of $h^{(1,1)}$ forms that come from the fiber minus its overall volume that is not physical in the F-theory limit. The Euler number of a threefold is given by

$$\chi = 2\left(h^{(1,1)} - h^{(2,1)}\right) . \tag{5.69}$$

The neutral singlets are then essentially given by the complex structure moduli that can be related to the geometric properties as

$$H_{\text{neutral}} = h^{(2,1)}(Y) + 1 = h^{(1,1)}(B) + 2 + \text{rank}(G_Y) - \frac{1}{2}\chi(Y) \,. \tag{5.70}$$

Finally we also have T tensor multiplets in our construction. The tensor multiplets are supported along cycles that are only in the base B and hence their multiplicity is given by

$$T = h^{(1,1)}(B) - 1 \,, \tag{5.71}$$

whereas we have to subtract the overall volume of the base, as it is supported by an uncharged hypermultiplet. The knowledge of all the matter and their multiplicities is essential in the cancellation of the anomalies by the Green-Schwarz mechanism that we review in the next section.

5.4.4 Anomalies in six dimensions

In this section we focus on the anomaly cancellation mechanism in F-theory in a six dimensional $\mathcal{N} = 1$ compactification. In Chapter 7 we discuss four dimensional compactifications but impose anomaly and

flux constraints from a bottom up-perspective.
In a six dimensional $\mathcal{N} = 1$ compactification the SUSY generators are automatically [33] chiral and hence there are non-trivial constraints on the spectrum that have to be fulfilled to give a consistent SUGRA theory. Those constraints are given by the cancellation of one-loop diagrams involving four external currents by diagrams where the same currents are coupled to the two form B-field at tree-level depicted in Figure 5.8. Cancellation is guaranteed when all the following conditions are satisfied

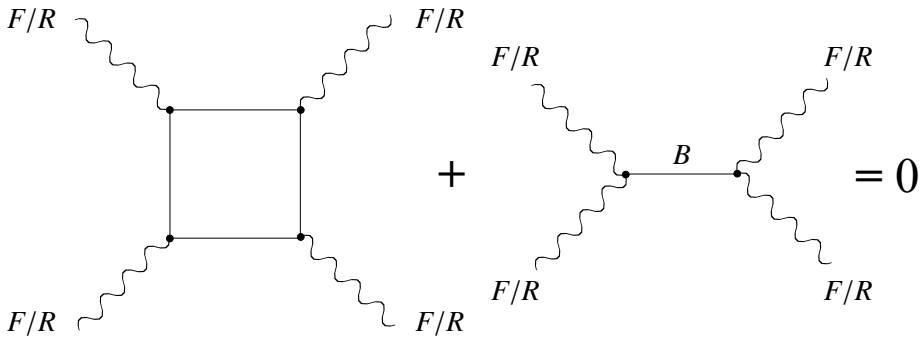

Figure 5.8: The one-loop gauge and gravity anomaly graph and the Green-Schwartz counter terms that have to cancel each other. In the above one-loop graph we can have external gauge or gravity currents as external currents denoted by F and R.

$$
\begin{array}{lcll}
\mathrm{tr}R^4 & : & H - V + 29T = 273\,, \quad (\mathrm{tr}R^2)^2 : \; 9 - T = a \cdot a & \text{(Pure gravitational)} \\
\mathrm{tr}F_\kappa^2 \mathrm{tr}R^2 & : & -\frac{1}{6}\left(A_{adj_\kappa} - \sum_{\mathbf{R}} x_{\mathbf{R}} A_{\mathbf{R}}\right) = a \cdot \left(\frac{b_\kappa}{\lambda_\kappa}\right) & \text{(Non-Abelian-gravitational)} \\
F_m F_n \mathrm{tr}R^2 & : & -\frac{1}{6}\sum_{\underline{q}} x_{q_m,q_n} q_m q_n = a \cdot b_{mn} & \text{(Abelian-gravitational)} \\
\mathrm{tr}F_\kappa^4 & : & B_{adj_\kappa} - \sum_{\mathbf{R}} x_{\mathbf{R}} B_{\mathbf{R}} = 0\,, & \text{(Pure non-Abelian)} \\
\mathrm{tr}F_\kappa^2 \mathrm{tr}F_\kappa^2 & : & \frac{1}{3}\left(\sum_{\mathbf{R}} x_{\mathbf{R}} C_{\mathbf{R}} - C_{adj_\kappa}\right) = \left(\frac{b_\kappa}{\lambda_\kappa}\right)^2 & \\
F_m F_n F_k F_l & : & \sum_{\underline{q}} x_{q_m,q_n,q_k,q_l} q_m q_n q_k q_l = b_{(mn} \cdot b_{kl)} & \text{(Pure Abelian)} \\
F_m F_n \mathrm{tr}F_\kappa^2 & : & \sum_{\mathbf{R},q_m,q_n} x_{\mathbf{R},q_m,q_n} q_m q_n A_{\mathbf{R}} = \left(\frac{b_\kappa}{\lambda_\kappa}\right) \cdot b_{mn} & \text{(Non-Abelian-Abelian)} \\
F_m \mathrm{tr}F_\kappa^3 & : & \sum_{\mathbf{R},q_m} x_{\mathbf{R},q_m} q_i E_{\mathbf{R}} = 0\,, &
\end{array}
$$

where the corresponding anomaly is highlighted. The numbers H,T and V denote the total amount of Hyper, Tensor and Vector multiplets. The $x_{\mathbf{R},q_m}$ denotes the multiplicity of a field of representation $\mathbf{R}$ and charge q_m. Moreover the $A_{\mathbf{R}}$ are quadratic Casimir operators representation $\mathbf{R}$ whose values are given as

$$
\mathrm{tr}_{\mathbf{R}} F_\kappa^2 = A_{\mathbf{R}} \mathrm{tr}F_\kappa^2\,, \qquad \mathrm{tr}_{\mathbf{R}} F_\kappa^3 = E_{\mathbf{R}} \mathrm{tr}F_\kappa^3\,, \qquad \mathrm{tr}_{\mathbf{R}} F_\kappa^4 = B_{\mathbf{R}} \mathrm{tr}F_\kappa^4 + C_{\mathbf{R}} (\mathrm{tr}F_\kappa^2)^2\,. \tag{5.72}
$$

Finally we have the coefficients $\lambda_\kappa = 2c_\kappa / E_{\mathbf{adj}_\kappa}$ with the dual Coxeter number c_κ. For $G_\kappa = \mathrm{SU(N)}$ we have $\lambda_\kappa = 1$. SU(2) and SU(3) are special cases. For both cases the coefficients in Table 5.72 get modified to $B_{\mathbf{R}} = E_{\mathbf{R}} = 0$ and $C_{\mathbf{R}}$ gets shifted to $\tilde{C}_{\mathbf{R}} = C_{\mathbf{R}} + \frac{1}{2} B_{\mathbf{R}}$. With that we have specified the field theoretic content i.e. the left hand sides of the anomalies. The Green-Schwarz counter-terms on the right hand side are specified by the anomaly coefficients a, b_κ and $b_{m,n}$. These transform as vectors of $\mathrm{SO}(1,T)$ determined by the microscopic structure of the theory. For more details on anomaly cancellation in six dimensions see [88].

In the F-theory cases these vectors can be matched to divisor classes of the three-fold geoemtry

$$a = [K_B]\,, \qquad b_\kappa = \mathcal{S}^b_{G_\kappa}\,, \qquad b_{mn} = -\pi(\sigma(\hat{s}_n)\cdot\sigma(\hat{s}_m))\,, \tag{5.73}$$

with canonical class $[K_B]$, the divisor class of non-Abelian groups and the Néron-Tate height pairing defined in (5.56). Note that the contractions $\cdot$ in the anomalies denote intersection relations among the divisors. All the above formulas are completely general and base independent.

We exemplify the cancellation of gravitation anomalies in the example of the F_{11} fibration with a general base. We note that the number of tensors Eq. (5.71) and the gravitational anomaly puts non-trivial constraints on the base space B to satisfy

$$[K_B^{-1}]^2 + h^{(1,1)}(B) = 10\,. \tag{5.74}$$

Actually it can be shown that a valid base spaces (e.g. see [88]) can only be Enrique surfaces, $\mathbb{P}^2$ and the Hirtzebruch surfaces F_m as well as blow-ups thereof[13]. Lets make the above statements more clear by checking the gravitational R^4 anomaly with general base for the F_{11} fiber in a bit more detail. For the charged hypermultiplets we find from Table H.1:

$$\begin{aligned} N_{\text{charged}} =& 6N_{(\mathbf{3},\mathbf{2})_{-1/6}} + 2N_{(\mathbf{1},\mathbf{2})_{1/2}} + 3N_{(\mathbf{3},\mathbf{1})_{-2/3}} + N_{(\mathbf{3},\mathbf{1})_{1/3}} + N_{(\mathbf{1},\mathbf{1})_{-1}} + 6N_{(\mathbf{8},\mathbf{1})_0} + 2N_{(\mathbf{1},\mathbf{3})_0}\,, && (5.75)\\ =& 8 + 18[K_B^{-1}] + 4[K_B^{-1}]\mathcal{S}_7 - 2\mathcal{S}_7^2 + 7[K_B^{-1}]\mathcal{S}_9 + \mathcal{S}_9\mathcal{S}_7 - 3\mathcal{S}_9^2\,. && (5.76)\end{aligned}$$

Note that we have included the adjoint matter representations but neglected the two 'Cartan' generators within the **8** and **3** representations as they are accounted for in the neutral matter part. The neutral part is given by

$$\begin{aligned} N_{\text{neutral}} =& 2 + \text{rank}(F_{11}) + h^{(1,1)}(B) - \frac{1}{2}\chi(Y_{F_{11}}) && (5.77)\\ =& 16 + 11[K_B^{-1}] - 4[K_B^{-1}]\mathcal{S}_7 + 2\mathcal{S}_7^2 - 7[K_B^{-1}]\mathcal{S}_9 - \mathcal{S}_9\mathcal{S}_7 + 3\mathcal{S}_9^2\,, && (5.78)\end{aligned}$$

using the rank of the gauge group to be four and the Euler number $\chi_{F_{11}}$ from Table J.1 in Appendix J for a general F_{11} fibration. Including the $8+3+1$ vector multiplets one confirms the cancellation of the $\mathbf{R}^4$ gravitational anomaly

$$\underbrace{N_{\text{charged}} + N_{\text{neutral}}}_{24+29[K_B^{-1}]^2} - \underbrace{V}_{12} + 29\ \underbrace{T}_{-[K_B^{-1}]^2+9} = 273\,. \tag{5.79}$$

All other gauge anomalies can be readily checked to be canceled as well. Note that we have not specified the overall base space but only used the constraints given by the $(\text{tr}\mathbf{R}^2)^2$ anomaly.

5.5 Enhanced singularities in the fiber

In the section above we have analyzed particular classes of elliptic fibrations and their *generic* singularity structure that is inherrited from the ambient space we start from. However for phenomenological applications additional gauge factors are very desirable such as SU(5) factors in order to build grand

[13] Note that the heterotic duality can only work in fibrations with $h^{(1,1)}(B) \geq 2$ where we have one more Tensor multiplet that can play the role of the heterotic axio-dilaton. [88]

unified models of particle physics. In principle it is possible to engineer such gauge groups by a further *specialization* of the generic fiber coefficients we have in order to precisely obtain additional codimension one singularities. In the following we present two ways to do that, one is the *spectral cover* [89] that starts from a local E_8 symmetry that gets broken to a subgroup and secondly we have the *top* [70] construction that can be used to engineer an additional gauge group on top of an existing fiber polyhedron that does not need for a common gauge factor such as E_8.

5.5.1 Local gauge enhancement: The spectral cover

Before we consider a full global fibration we introduce a first attempt to engineer interesting SU(5) GUT theories within F-theory. For this we use a local approach that became relevant in the literature [89, 90, 91]. This approach focuses mainly on the singularity structure directly on the SU(5) GUT divisor where additional semi-global information can be manually introduced. The phenomenological implications of these models will be worked out in Chapter 7 but first we focus on the more technical details on how the spectrum is obtained.
We begin by considering a Tate model that can be obtained by a local coordinate transformation of the Weierstrass form. By this treatment we can make the SU(5) singularity more explicit. The Tate form is given as

$$y^2 = x^3 - \alpha_1 xy + \alpha_2 x^2 - \alpha_3 y + \alpha_4 x + \alpha_6 \,, \tag{5.80}$$

with the base dependent sections α_i. This equation can be brought in the familiar Weierstrass form using Tates algorithm by first applying the coordinate shift back and then identify

$$f = -\frac{1}{48}\left(\beta_2^2 - 24\beta_4\right) , \tag{5.81}$$

$$g = -\frac{1}{864}\left(-\beta_2^3 + 36\beta_2\beta_4 - 216\beta_6\right) , \tag{5.82}$$

$$\Delta = -\frac{1}{4}\beta_2^2\left(\beta_2\beta_6 - \beta_4^2\right) - 8\beta_4^3 - 27\beta_6^2 + 9\beta_2\beta_4\beta_6 \,, \tag{5.83}$$

where we have employed abbreviations:

$$\beta_2 = \alpha_1^2 + 4\alpha_2 \,, \quad \beta_4 = \alpha_1\alpha_3 + 2\alpha_4 \,, \quad \beta_6 = \alpha_3^2 + 4\alpha_6 \,. \tag{5.84}$$

We are interested in engineering an SU(5) group, which we can do by specifying the α_i to attain the following form:

$$\alpha_1 = b_5 \,, \alpha_2 = b_4\omega \,, \alpha_3 = b_3\omega^2 \,, \alpha_4 = b_2\omega^3 \,, \alpha_6 = b_0\omega^5 \,. \tag{5.85}$$

Plugging in the definitions back yields the following discriminant

$$\Delta = -\omega^5\left(P_{10}^4 P_5 + \omega P_{10}^2(8b_4P_5 + b_5R) + O(\omega^2)\right) \tag{5.86}$$

$$P_{10} = b_5 \,, \tag{5.87}$$

$$P_5 = b_3^2 b_4 - b_2 b_3 b_5 + b_0 b_5^2 \,. \tag{5.88}$$

We omit the full expressions for f and g as a full classification of singularities in the Tate form only depending on the vanishing orders of the α_i has been carried out in [65]. However from Kodairas Table

5.3 we find that we have engineered an SU(5) singularity over the divisor

$$S: \quad \omega = 0\,, \tag{5.89}$$

as there the discriminant vanishes to order five and f and g are non vanishing. Additionally there are codimension two loci on S where the fiber can degenerate further. This happens when the polynomials P_{10} or P_5 vanishes and corresponds to an SO(10) and SU(6) singularity. Additionally we give the following codimension three points and their gauge enhancement

$$\begin{array}{rcc} \omega = P_{10} = b_4 = 0: & \mathrm{E}_6 & \mathbf{10\,10\,5} \\ \omega = P_{10} = b_3 = 0: & SO(12) & \bar{\mathbf{5}}\,\bar{\mathbf{5}}\,\mathbf{10} \\ \omega = P_5 = R = 0: & \mathrm{SU}(7) & \bar{\mathbf{5}}\,\mathbf{5}\,\mathbf{1} \end{array} \tag{5.90}$$

In particular the E_6 point induces the Top-quark Yukawa coupling which is only induced via instantons in Type IIB string theory [92] and makes F-theory a valuable alternative for unified model building.
In fact we note, that there is even an E_8 singularity, when all b_i but b_0 vanish. In general we have to determine the b_i as the sections of the fibration. However this might be very hard in general as there can be monodromies in the geometry that identify certain b_i's when we move around the base space. Here we take the approach to focus on the b_i only locally on the GUT divisor and invoke the effects of these monodromies per hand. For this we consider an E_8 divisor that is broken as $\mathrm{E}_8 \to \mathrm{SU}(5)_{\mathrm{GUT}} \times \mathrm{SU}(5)_\perp$. We consider the b_i take values in $\mathrm{SU}(5)_\perp$. The Cartan generators within $\mathrm{SU}(5)_\perp$ we call t^a $a = 1, \ldots, 5$ that are subject to the trace condition $\sum_a t_a = 0$. By decomposing the adjoint of E_8 we can directly see the **5** and **10**-plets together with their $\mathrm{SU}(5)_\perp$ weights arising as

$$\mathbf{248} \to (\mathbf{24},\mathbf{1}) \oplus (\mathbf{1},\mathbf{24}) \oplus (\mathbf{10},\bar{\mathbf{5}}) \oplus (\overline{\mathbf{10}},\mathbf{5}) \oplus (\mathbf{5},\overline{\mathbf{10}}) \oplus (\bar{\mathbf{5}},\mathbf{10})\,. \tag{5.91}$$

We see that there are at most five **10** curves and ten **5**-curves and 24 singlet states. We use the weights t_i of the matter curves under the $\mathrm{SU}(5)_\perp$ to parametrize these loci by rewriting the b_i in terms of *symmetrical elementary polynomials* of degree i in the t_i over the GUT divisor. A simple example is given by

$$b_5 = t_1 t_2 t_3 t_4 t_5\,. \tag{5.92}$$

Hence we find for the vanishing of each of the t_i one **10** matter locus. We summarize all loci by

$$\begin{array}{rcrl} C_{10_i} & : & t_i & = 0\ , \\ C_{5_{i,j}} & : & -t_i - t_j & = 0 \text{ with } i \neq j\ , \\ C_{1_{i,j}} & : & \pm(t_i - t_j) & = 0 \text{ with } i \neq j\ . \end{array} \tag{5.93}$$

The charge of a curve under a $\mathrm{SU}(5)_\perp$ Cartan $\mathrm{U}(1)^{\mathrm{a}}$ can be calculated by simply contracting the weight with the generator $t^a t_b = \delta^a_b$. However here we have restricted only to the $\mathrm{SU}(5)_{\mathrm{GUT}}$ divsor S and we do not now what happens away from it i.e. if there are some monodromies in the full geometry that identify certain Cartan generators that look distinct only over S_{GUT}. To account for that effect we introduce the *spectral line* C which is a five-sheeted $\mathbb{P}^1$ fiber over S_{GUT} with the $\mathbb{P}^1$ coordinate s

$$C: \quad b_0 s^5 + b_2 s^3 + b_3 s^2 + b_4 s + b_5 = 0\,. \tag{5.94}$$

Curve	q
$\mathbf{10}_1$	1
$\mathbf{10}_5$	-4
$\overline{\mathbf{5}}_{11}$	2
$\overline{\mathbf{5}}_{15}$	-3

(a) 4+1 factorization

Curve	q
$\mathbf{10}_1$	2
$\mathbf{10}_4$	-3
$\overline{\mathbf{5}}_{11}$	4
$\overline{\mathbf{5}}_{14}$	-1
$\overline{\mathbf{5}}_{44}$	-6

(b) 3+2 factorization

Curve	q_1	q_2
$\mathbf{10}_1$	1	5
$\mathbf{10}_3$	1	-5
$\mathbf{10}_5$	-4	0
$\overline{\mathbf{5}}_{11}$	2	10
$\overline{\mathbf{5}}_{13}$	2	0
$\overline{\mathbf{5}}_{33}$	2	-10
$\overline{\mathbf{5}}_{15}$	-3	5
$\overline{\mathbf{5}}_{35}$	-3	-5

(c) 2+2+1 factorization

Curve	q_1	q_2
$\mathbf{10}_1$	2	0
$\mathbf{10}_4$	-3	5
$\mathbf{10}_5$	-3	-5
$\overline{\mathbf{5}}_{11}$	4	0
$\overline{\mathbf{5}}_{14}$	-1	5
$\overline{\mathbf{5}}_{15}$	-1	-5
$\overline{\mathbf{5}}_{45}$	-6	0

(d) 3+1+1 factorization

Table 5.4: U(1) charges of $SU(5)_{GUT}$ representations for different factorizations with up to two U(1) factors. The indices specify the $SU(5)_\perp$ Cartan weights.

s takes values in the canonical bundle $K_{S_{GUT}}$ of S_{GUT}. We can account for effects of the global geometry by imposing a factorization of the spectral line into different splittings into polynomials that have total degree of five. These splittings lead to an identification of the different t^i's. By fixing a certain split it is possible to obtain the divisor classes for the matter curves that can be used to deduce the flux constraints for the curves [90]. In Chapter 7 we are interested in models with up to two U(1) gauge factors. In general there are four splittings that allow for such models: For example the 4 + 1 split results in an identification of the U(1) generators $t^1 = t^2 = t^3 = t^4$ and together with the tracelessness condition this results in only one U(1) gauge factor. Hence the resulting U(1) charge generator is given by $U(1) = \text{diag}(1, 1, 1, 1, -4)$. This identification also gives identifications of the matter curves that are only distinguished by their corresponding weights. Hence we find only two different **5** and **10** matter curves. The matter curves for the four different splittings are specified in Table 5.4

5.5.2 Enhancing the fiber: The TOP construction

Some of the 16 2D polyhedra in Table 5.2 do not all provide non-Abelian gauge groups and thus seem not to be of any phenomenological relevance. However, by specifying the coefficients s_i of a given hypersurface we can engineer new non-Abelian gauge factors over a given new divisor

$$S: \quad z = 0\,, \tag{5.95}$$

in the base B similar as we did with the b_i in the spectral cover. A systematic way of engineering those additional factors has been introduced in [93] and systematically classified by [70]. The idea is to have a two dimensional base polyhedron that is enlarged to a three dimensional polyhedron. Hence there is a new lattice $N = \mathbb{Z}^3$ with coordinates (x, y, z) and dual one $M = \mathbb{Z}^3$ with coordinates $(\bar{x}, \bar{y}, \bar{z})$. The polyhedron is again specified by

$$F_t = \{v_i \in N | \langle v_i, u_i\rangle \geq -1 \wedge \langle v_i, u_0\rangle \geq 0 \quad \forall u_i \in M\} \tag{5.96}$$

Due to the $GL(3, \mathbb{Z})$ transformation we can always choose $u_0 = (0, 0, 1)$. We note that we find the reflexive polyhedron F_i at $z = 0$. The dual constraint gives only constraints in the $\bar{x}$ and $\bar{y}$ coordinates of the dual polyhedron which gives us exactly the two dimensional polyhedron F_i^* at some coordinate

$\bar{z}$. The remaining vertices in F_t constrain the $\bar{z}$ coordinate to be

$$z_i\bar{z} \geq -1 - x_i\bar{x} - y_i\bar{y}\,. \tag{5.97}$$

Hence we find, that for a fixed vertex in F_t the $\bar{z}$ coordinates are only restricted from below as $z \geq 0$. This means that F_t^* is an infinitely high tower in positive $\bar{z}$-direction that has F_i^* as a cross section. There is a set of *minimal* $\bar{z}_i$ coordinates and [70] have shown that a choice of them uniquely specifies the *top* and can be found in the Appendix of [70] for each of the 16 polyhedra as a base. The connection of the top is given by the usual hypersurface constraint

$$P_{\text{top}} = \sum_{u_i \in F_t^*} a_i \prod_{v_j \in F_t} x_j^{\langle u_i, v_j\rangle + 1} = \sum_{u_i \in F_t^*} a_i \left(\prod_{v_k \in F_t, z>0} x_k^{\langle u_i, v_k\rangle + 1} \right) \left(\prod_{v_s \in F_i} x_k^{\langle u_i, v_s\rangle + 1} \right), \tag{5.98}$$

where we have factored the product into the contribution at $z > 0$ and $z = 0$ that gives exactly the vectors of the lowest laying polyhedron F_i. Comparing this equation with (5.34) we still find the contribution of the original base polyhedron F_i but with specialized coefficients depending on the $z > 0$ part of the polyhedron. Note however that these prefactors, due to the infinite sum, are power series in the coordinates. As the coordinates are divisors and we are interested in their vanishing we are interested only in the lowest contribution of those power series that are specified by the smallest F_i's.
The coefficients exactly correspond to additional divisors that resolve the new singularities. Furthermore we can read off from the polyhedron which gauge group is added to the base polyhedron F_i by the additional piece at higher z: As these divisors lie in a common plane, there is a linear equivalence among them. If the coordinates are neighbouring they intersect each other exactly ones which makes it easy to read of the corresponding Dynkin structure.
The definition above also gives us the projection to the new base divisor of the elliptic fibration i.e

$$\pi : (x_1, x_2, , , x_n) \to \omega = \prod_{v_i \in F_t} x_i^{\langle u_0, v_i\rangle - 1} = \prod_{v_i \in F_t | z>0} x_i^z\,, \tag{5.99}$$

with the new base divisor ω. In the Chapter 7 we are interested in SU(5) tops over the base F_5 that gives an additional $\text{U}(1)^2$ gauge group which is why we give an example of such a *top*. We will construct the *top* by taking the minimal points in the dual polyhedron F_t^* and then dualize back. In the following we choose the minimal coordinates as found in Table 3 of [70] as well as in [94]. They are given as $\bar{z}_{\text{min},i} = \{-1,-1,-1,-1,0,1,1,1\}$ that are the $\bar{z}$-coordinates of the 2D polyhedron F_{12} the dual of F_5. The $i = 0$ point denotes the origin specified with the uvw monomial and then we enumerating clockwise with $i = 7$ being the corner at the upper left that has the u^3 polynomial in F_5 coordinates. Both F_t^* and F_t for this choice are depicted in Figure 5.9 as well as the corresponding monomials in the F_5 coordinates. In Figure 5.9 we have depicted the vertices and marked the three rational points that intersect them. Note that those sections also intersect the additional nodes at height $z = 1$. Those divisors give the nodes of the additional SU(5), and the choice of the zero section fixes the affine node. We consider this by having a look at the hypersurface constraint and start first solely with the one of the 2D polygon of F_5 that without the top:

$$p_{F_5} = s_1 e_2^2 e_1^2 u^3 + s_2 e_2^2 e_1 u^2 v + s_3 e_2^2 u w^2 + s_5 e_2 e_1^2 u^2 w + s_6 e_2 e_1 u v w + s_7 e_2 v^2 w + s_8 e_1^2 u w^2 + s_9 e_1 v w^2\,, \tag{5.100}$$

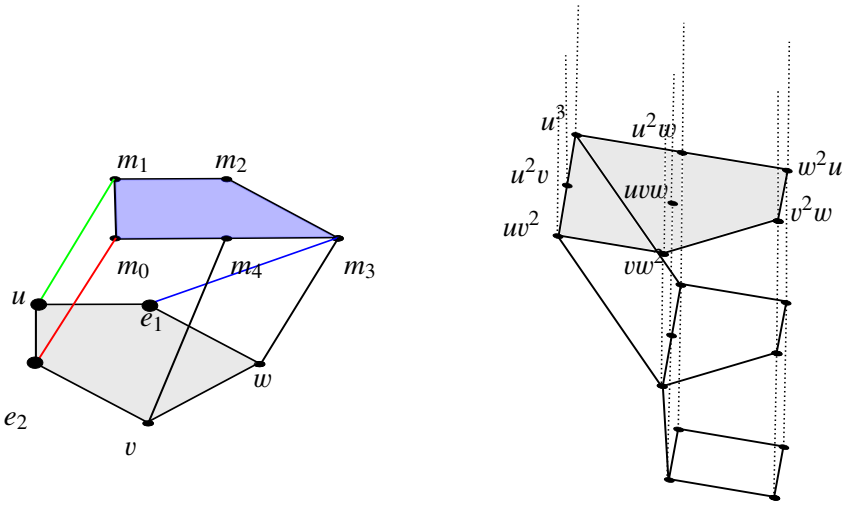

Figure 5.9: One SU(5) *top* over F_5 and its dual polyhedron. Note that the dual polyhedron is only bounded from below in the $\bar{z}$-direction.

that has three rational sections at

$$\begin{aligned} \hat{s}_0 = X_{F_5} \cap \{e_2 = 0\}: &\quad [s_9 : -s_8 : 1 : 1 : 0]\,, \\ \hat{s}_1 = X_{F_5} \cap \{e_1 = 0\}: &\quad [s_7 : 1 : -s_3 : 0 : 1]\,, \\ \hat{s}_2 = X_{F_5} \cap \{u = 0\}: &\quad [0 : 1 : 1 : s_7 : -s_9]\,. \end{aligned} \tag{5.101}$$

Choosing s_0 as the zero-section we get at $\mathrm{U}(1)^2$ gauge group generated by $\hat{s_1}$ and $\hat{s_2}$. Moreover we can compute its spectrum which can be found in [94] and is summarized in table 5.6e together with their six dimensional multiplicities. Now we take the SU(5) *top* at $z = 1$ in consideration with the five additional coordinates m_i. Taking the additional products of (5.98) into account this amounts to the following specialization of coefficients in (5.100) where we have omitted higher order terms:

$$\begin{aligned} s_1 &\to \tilde{s}_1 m_0^2 m_1^3 m_2^2 m_4^1\,, & s_2 &\to \tilde{s}_2 m_0^2 m_1^2 m_2^1 m_4^1\,, & s_3 &\to \tilde{s}_3 m_0^2 m_1^1 m_4^1\,, \\ s_5 &\to \tilde{s}_5 m_1^1 m_2^2\,, & s_6 &\to \tilde{s}_6\,, & s_7 &\to \tilde{s}_7 m_0^1 m_3^1 m_4^1\,, \\ s_8 &\to \tilde{s}_8 m_1^1 m_2^2 m_3^2 m_4^1\,, & s_9 &\to \tilde{s}_9 m_2^1 m_3^2 m_4^1\,. \end{aligned}$$

From equation (5.99) we that the new base divisor ω is simply given by the product of the new coordinates

$$\omega := m_0 \cdot m_1 \cdot m_2 \cdot m_3 \cdot m_4\,. \tag{5.102}$$

Mapping the cubic curve into the Weierstrass form we can again see the factorization of the discriminant Δ to be

$$\Delta = \omega^5 \left(c + \omega P + ...\right)\,. \tag{5.103}$$

Hence the vanishing of ω does precisely give us the SU(5) locus we wanted to engineer. Finding codimension two loci where the polynomial c vanishes at order one on S gives the loci of SU(6) i.e. loci with **5**-plet matter. Generically there are also curves, where the fiber enhances to SO(10) singularities,

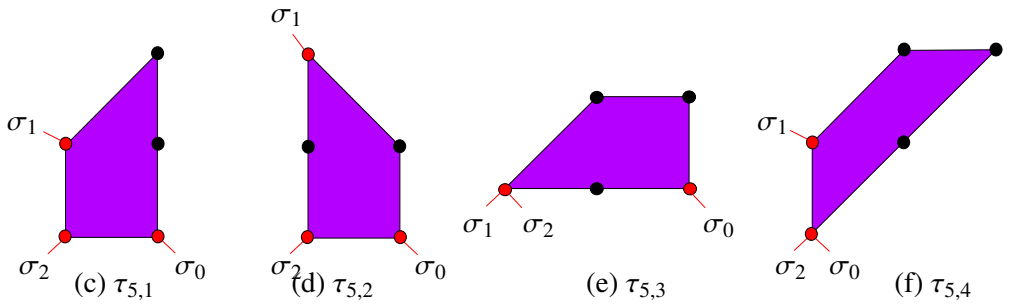

Figure 5.10: The allowed *top* polyhedra at height $z = 1$ that can lead to an $SU(5) \times U(1)^2$ gauge group over F_5 and their intersections with the rational sections.

hence these are the loci where **10** matter can be found.
We note that in the analysis of [94] some of the *tops* had loci where the fibration becomes non-flat. This means, that the dimensionality of the fibration jumps over those loci. In [95] it was found, that these non-flat fibers can be wrapped my M5 branes that support an infinite tower of massless strings. This situation is phenomenologically unacceptable and hence we have to avoid these situations in the following by either forbidding divisors that are involved in the intersection or by tuning the complex structure of the manifold such that these points disappear. Generically the matter curves are also charged under the the two U(1)'s which can be calculated by the intersection of the curves with the Shioda maps. There is a generic charge pattern for the matter curves that we can observe already from the geometry. This charge pattern is fixed by the way how the SU(5) nodes are intersected by the zero-and and the other rational section. To see this we observe again the Shioda map (5.55) for a rational section s_m. To calculate the U(1) charge of a matter curve the we call $\hat{c}$ we have to intersect the Shioda map with the curve given by:

$$\sigma(S_m) \cdot \hat{c} := 5(S_m \cdot \hat{c}) - 5(S_0 c) + (S_m \cdot \hat{c}_i) \begin{pmatrix} 4 & 3 & 2 & 1 \\ 3 & 6 & 4 & 2 \\ 2 & 4 & 6 & 3 \\ 1 & 2 & 3 & 4 \end{pmatrix}_{ij} (D_j \cdot \hat{c}), \tag{5.104}$$

where we have plugged in the inverse Cartan matrix of SU(5) and scaled by a factor of 5 to get integral charges. The intersections of the matter curve $\hat{c}$ with the section S_m give integer numbers that we have to find geometrically and depends on how the matter fiber splits. However the intersection of the curve with the nodes $S_m \cdot c_i$ can be read of from the picture by simply observing which ration section hits which node. . The $D_j \cdot \hat{c}$ intersections give the Dynkin label of the SU(5) representation of the matter curve $\hat{c}$ as usual. In the case given in Figure 5.9 we can read of the intersections to be

$$S_1 \cdot c_i = \begin{pmatrix} 0 & 0 & 1 & 0 \end{pmatrix}, \tag{5.105}$$

$$S_2 \cdot c_i = \begin{pmatrix} 1 & 0 & 0 & 0 \end{pmatrix}. \tag{5.106}$$

Hence for a **5** or a **10** curve with Dynkin label $\begin{pmatrix} 1 & 0 & 0 & 0 \end{pmatrix}$ and $\begin{pmatrix} 0 & 1 & 0 & 0 \end{pmatrix}$, respectively the charges are given as

$$Q_1(\mathbf{5}) = 2 \bmod 5\,, \quad Q_1(\mathbf{10}) = 4 \bmod 5\,, \tag{5.107}$$
$$Q_2(\mathbf{5}) = 4 \bmod 5\,, \quad Q_2(\mathbf{10}) = 3 \bmod 5\,. \tag{5.108}$$

Where the mod 5 factor is fixed by the intersection number of the rational section with the curve. In general there can be five cases of how the rational sections intersect another SU(5) node c_i. The resulting charge pattern is summarized in Table 5.5. In [71] all possible SU(5) *tops* have been listed as well as

node i	0	1	2	3	4
$Q_{\mathbf{5}}$	0	4	3	2	1
$Q_{\mathbf{10}}$	0	3	1	4	2

Table 5.5: Charge assignments for **5**- and **10**-curves for all possible splittings.

their intersections with the rational sections. The four different choices for polyhedra at height $z = 1$ that permit us to engineer an SU(5) divisor[14] as well as their intersections are drawn in Figure 5.10

The matter spectra for the four cases are summarized in Table 5.6. We have added the universal singlet spectrum and give more detail about their loci and classes of the curves as this will be of interest in the following chapters. We note, that all *tops* develop only one $SO(10)$ singularity because these singularities are uniquely fixed by the triangulation of the polyhedron as opposed to the SU(6) case. Hence there is only one **10** matter curve with a fixes U(1) charge. However, in [97, 98] it was observed that fibrations realized as complete intersections can have multiple **10** curves with different U(1) charges. It is actually interesting to note that upon that all operators of SU(5) that we can build have always U(1) charges mod 5 which we can easily see from the charge patterns of the five and the ten curves given in table 5.5. Hence after the full breakdown of the additional U(1) factors all operators are only restricted by their residual SU(5) symmetry as expected.

[14] There is a fifth polyhedron that is not listed as it leads to a non-flat fibration at codimension one.

Curve	q_1	q_2
$\mathbf{10}_1$	-1	2
$\overline{\mathbf{5}}_1$	3	-1
$\overline{\mathbf{5}}_2$	-2	4
$\overline{\mathbf{5}}_3$	-2	-6
$\overline{\mathbf{5}}_4$	3	4
$\overline{\mathbf{5}}_5$	-2	-1

(a) Top $\tau_{5,1}$.

Curve	q_1	q_2
$\mathbf{10}_1$	1	2
$\overline{\mathbf{5}}_1$	-3	4
$\overline{\mathbf{5}}_2$	-3	-6
$\overline{\mathbf{5}}_3$	-3	-1
$\overline{\mathbf{5}}_4$	2	4
$\overline{\mathbf{5}}_5$	2	-1

(b) Top $\tau_{5,2}$.

Curve	q_1	q_2
$\mathbf{10}_1$	-1	-1
$\overline{\mathbf{5}}_1$	3	-2
$\overline{\mathbf{5}}_2$	-2	-7
$\overline{\mathbf{5}}_3$	-2	3
$\overline{\mathbf{5}}_4$	3	3
$\overline{\mathbf{5}}_5$	-2	-2

(c) Top $\tau_{5,3}$.

Curve	q_1	q_2
$\mathbf{10}_1$	2	0
$\overline{\mathbf{5}}_1$	4	5
$\overline{\mathbf{5}}_2$	4	0
$\overline{\mathbf{5}}_3$	-1	5
$\overline{\mathbf{5}}_4$	-1	-5
$\overline{\mathbf{5}}_5$	-1	0

(d) Top $\tau_{5,4}$.

Curve	q_1	q_2	Locus	Class/Multiplicity
$\mathbf{1}_1$	5	-5	$s_3 = s_7 = 0$	$\mathcal{S}_7([K_B^{-1}] + \mathcal{S}_7 - \mathcal{S}_9)$
$\mathbf{1}_2$	5	0	$s_2 s_7^2 + s_3^2 s_9 = 0$ $s_5 s_3 s_7 - s_3^2 s_8 - s_7^2 s_1 = 0$	$6[K_B^{-1}]^2 + [K_B^{-1}](4\mathcal{S}_7 - 5\mathcal{S}_9)$ $-2\mathcal{S}_7^2 + \mathcal{S}_7\mathcal{S}_9 + \mathcal{S}_9^2$
$\mathbf{1}_3$	-5	-10	$s_8 = s_9 = 0$	$\mathcal{S}_9([K_B^{-1}] - \mathcal{S}_7 + \mathcal{S}_9)$
$\mathbf{1}_4$	-5	-5	$s_2 s_8 s_9 - s_3 s_8^2 - s_9^2 s_1 = 0$ $s_5 s_9^2 - s_6 s_8 s_9 - s_8^2 s_7 = 0$	$6[K_B^{-1}]^2 + [K_B^{-1}](-5\mathcal{S}_7 + 4\mathcal{S}_9)$ $+\mathcal{S}_7^2 + \mathcal{S}_7\mathcal{S}_9 - 2\mathcal{S}_9^2$
$\mathbf{1}_5$	0	10	$s_9 = s_7 = 0$	$\mathcal{S}_7\mathcal{S}_9$
$\mathbf{1}_6$	0	5	non-trivial ideal	$6[K_B^{-1}]^2 + [K_B^{-1}](4\mathcal{S}_7 + 4\mathcal{S}_9)$ $-2\mathcal{S}_7^2 - 2\mathcal{S}_9^2$

(e) Singlet spectrum and charges.

Table 5.6: U(1) charges of the four inequivalent tops based on the fiber polygon F_5. The singlet charges are the same for all tops. We have also listed their loci and classes of the curves, that give the multiplicity in 6D. The ideal of $\mathbf{1}_6$ it too long to fit into the table but can be found in [96].

CHAPTER 6

A Network in F-theory

In the last chapter we have seen that the 16 2D polyhedra are a very interesting starting point to study U(1) symmetries and deliver interesting building blocks to engineer more realistic theories using *tops*. Hence it is desirable to analyze all 16 cases over a generic base space as well as their effective theories. This is in particular useful as those spectra are invariant upon a *top* completion as we have seen in the Section 5.5.2. In general the 16 2D polyhedra are connected in a network of geometrical transitions such as blow ups and we find that also the F-theory effective actions are connected by a physical process namely the Higgs-mechanism. This whole chapter is structured in order to describe a sub branch of this network in which we give particular emphasis to fibers with novel features. In section 6.1 we start by describing the general properties of the toric Higgs effect and establishing which quantities can be matched. In the same chapter we perform an example of the toric Higgsing on a general base manifold as well as for a $\mathbb{P}^2$ base choice. In section 6.3 we descend further down to models that exhibit peculiar fiber structures such as a *non-toric* rational section as well as discrete symmetries. In section 6.4 we then finally give a look to the full network and appreciate its symmetries and motivate various conjectures.

6.1 The toric Higgs effect

In this section we introduce the *toric Higgs effect* that is depicted in Figure 6.1. This correspondence between the physical effect and the geometry of the underlying fibrations is very helpful in both directions of the correspondence

- Use a Higgsed field theory to infer the mathematical structure of an elliptic fibration.
- Use symmetries of the elliptic fiber to conclude equivalent Higgs transitions.

In the following we want to relate six dimensional $\mathcal{N} = 1$ SUGRA theories connected by the Higgs mechanism. These theories are obtained from F-theory on elliptically fibered CY threefolds Y_A and Y_B with the same base space B_2 and the fiber realized as F_A and F_B respectively.

The match works in the following way: We have to assign a VEV to a Higgs field in a D-flat direction of the field theory corresponding to F-theory with fiber F_A. Generically we have seen that non-trivial representations are specified by the vanishing of two coefficients $s_i = s_j = 0$ with $i \neq j$. We have seen that the s_i are the prefactors of monomials in the hypersurface constraint that appear as (mostly) neighboring nodes in the dual polyhedron of F_A^* connected by an edge.

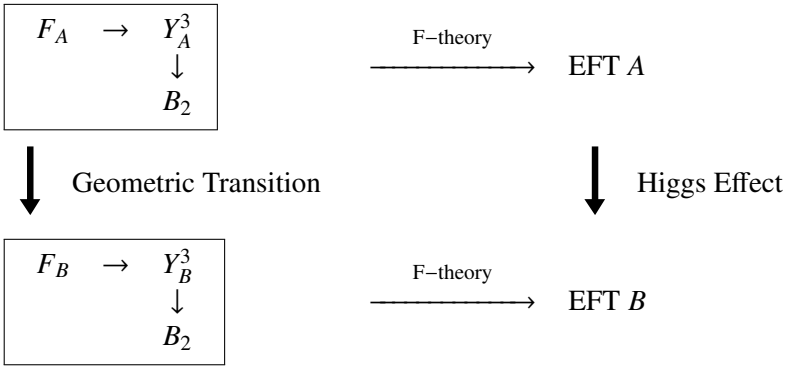

Figure 6.1: The toric Higgs effect: Geometrical transitions in the elliptic fiber correspond to the Higgs effect in the effective field theories.

6.2 Higgsing F_9 to F_5

We start by considering the polyhedron of F_9 and its dual given in Figure 6.3. Giving a VEV to this representation corresponds geometrically to deleting the edge between s_i and s_j by *adding* another integral point in the dual polyhedron[1]. As we argued in chapter 5 adding another monomial in the dual polyhedron F_A^* corresponds to deleting a coordinate in the original polyhedron F_A i.e. a blow-down to F_B. Up to a $GL(2,\mathbb{Z})$ transformation the geometric match is obvious. In the effective field theory we then match multiplicities of the matter fields after the breakdown of the symmetry to the computations of F-theory on F_B if available. In the M-theory the Higgsing means that we go to a locus where the resolution divisor that corresponds to the vanishing locus of the coordinate that got blown down is frozen and hence not M2 branes can wrap the divisor to support the gauge group in the F-theory limit. As first example we consider the Higgsing from F_9 to F_5 in some details that will pave the grounds for the upcoming sections. In the following section we consider a sub-branch of the total Higgs network which we consider in section 6.4. We choose F_9 as a particularly simple starting point to introduce

[1] The adjoint representation always fails that definition and thus can never be used as a *toric* Higgs. Hence all transitions we consider are not gauge group rank preserving.

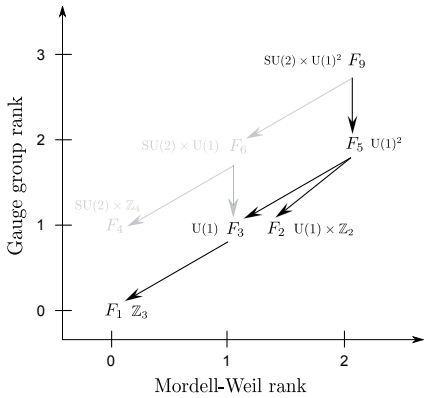

Figure 6.2: A subbranch of the Higgs chain starting from fibrations over F_9. We are not considering the gray sub branch.

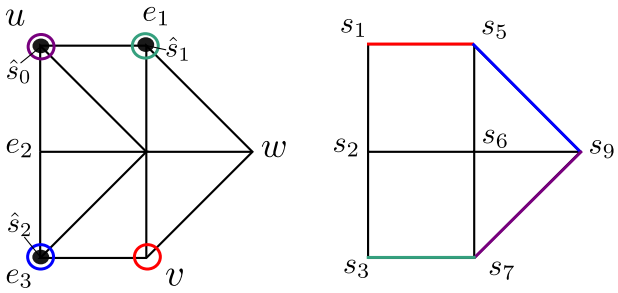

Figure 6.3: The polyhedron of F_9 and its dual specified by the coefficients s_i in front of the coordinate monomials.

the generic features and then go down from F_5 to the Jacobian fibrations of F_3, F_2 and F_1 that exhibit discrete symmetries[2]. The picture of the Higgsing chain is depicted in Figure 6.2. In for the dual polyhedron we have written the coefficients s_i in front of the coordinate monomials that appear in the hypersurface constraint:

$$p_{F_9} = s_1 e_1^2 e_2^2 e_3 u^3 + s_2 e_1 e_2^2 e_3^2 u^2 v + s_3 e_2^2 e_3^3 u v^2 + s_5 e_1^2 e_2 u^2 w + s_6 e_1 e_2 e_3 u v w + s_7 e_2 e_3^2 v^2 w + s_9 e_1 v w^2 \,. \quad (6.1)$$

Note that the general base divisor classes of the sections s_i can be found in the appendix I and the divisor classes of the fiber coordinates are given in table 6.2.

Section	Divisor class
u	$H - E_1 - E_2 + \mathcal{S}_9 + [K_B]$
v	$H - E_2 - E_3 + \mathcal{S}_9 - \mathcal{S}_7$
w	$H - E_1$
e_1	E_1
e_2	$E_2 - E_3$
e_3	E_3

(6.2)

At $s_9 = 0$ we find an SU(2) singularity given by the factorization of (6.1) to $P_{F_9}|_{s_9=0} = e_2 q_3$ with q_3 the residual polynomial. Furthermore we have depicted our choices for the three independent rational points

$$\begin{aligned} \hat{s}_0 = X_{F_9} \cap \{u = 0\} : &\quad [0 : 1 : 1 : s_7 : -s_9 : 1] \,, \\ \hat{s}_1 = X_{F_9} \cap \{e_1 = 0\} : &\quad [s_7 : 1 : -s_3 : 0 : 1 : 1] \\ \hat{s}_2 = X_{F_9} \cap \{e_3 = 0\} : &\quad [1 : s_5 : 1 : 1 : -s_9 : 0] \,, \end{aligned} \quad (6.3)$$

that are also indicated in Figure 6.3. These facts already tell us that we have an $\mathrm{SU}(2) \times \mathrm{U}(1)^2$ gauge group. From the toric diagram 6.3 we see that the curve in the class of $[e_2]$ must be the affine node as it is intersected by the zero section s_0 and hence the vanishing of q_3 is the Cartan divisor D_1 of the SU(2) that is intersected by $\hat{s}_1$. We can then write down the Shioda maps of the two U(1) gauge factors

$$\sigma(\hat{s}_m) = S_m - S_0 + [K_B] - \delta_{m,1}\mathcal{S}_7 + \frac{1}{2}\delta_{m,1} D_1 \,. \quad (6.4)$$

[2] The subbranch including F_4 has been considered in the literature as well [99, 100].

Using the aforementioned methods we can calculate the codimension two matter loci, their corresponding charges by intersecting the curves with the Shioda maps and their multiplicities. The spectrum together with the loci and the multiplicities are given in Table 6.1. For completeness we give the non-

Repr.	$\mathbf{1}_{(1,2)}$	$\mathbf{1}_{(1,0)}$	$\mathbf{1}_{(0,1)}$	$\mathbf{1}_{(1,1)}$	$\mathbf{2}_{(-1,-1/2)}$	$\mathbf{2}_{(1,3/2)}$	$\mathbf{2}_{(0,-1/2)}$	$\mathbf{3}_{(0,0)}$
Locus	$s_7 = s_3 = 0$	$s_5 = s_1 = 0$	$V(I_{(3)})$	$V(I_{(4)})$	$s_9 = s_5 = 0$	$s_9 = s_7 = 0$	$V(I_{(7)})$	$s_9 = 0$
Multi	$\mathcal{S}_7([K_B^{-1}] + \mathcal{S}_7 - \mathcal{S}_9)$	$(2[K_B^{-1}] - \mathcal{S}_7)$ $(3[K_B^{-1}] - \mathcal{S}_7 - \mathcal{S}_9)$	$(3[K_B^{-1}] - \mathcal{S}_9)$ $\times(2[K_B^{-1}] + 2\mathcal{S}_7 - \mathcal{S}_9)$ $-2\mathcal{S}_7([K_B^{-1}] + \mathcal{S}_7 - \mathcal{S}_9)$	$6[K_B^{-1}]^2 + [K_B^{-1}]$ $\times(4\mathcal{S}_7 - 2\mathcal{S}_9) - 2\mathcal{S}_7^2$	$\mathcal{S}_9(2[K_B^{-1}] - \mathcal{S}_7)$	$\mathcal{S}_7\mathcal{S}_9$	$2\mathcal{S}_9(3[K_B^{-1}] - \mathcal{S}_9)$	$1 + \mathcal{S}_9 \frac{(\mathcal{S}_9 - [K_B^{-1}])}{2}$

Table 6.1: Summary of the matter representations, loci and multiplicities of the charged matter states in F_9 fibrations.

toric matter loci given by the following ideals

$$V(I_{(3)}) := s_2 s_7^2 + s_3^2 s_9 - s_3 s_6 s_7 = 0\,, \quad s_5 s_3 - s_7 s_1 = 0 \quad \text{w/0 } s_7 = s_3 = 0\,, \tag{6.5}$$

$$V(I_{(4)}) := s_2 s_9 s_7^2 + s_3^2 s_9^2 - s_3 s_6 s_9 s_7 - s_7^3 s_5 = 0\,, \tag{6.6}$$

$$s_1 s_9 s_7 + s_5(s_3 s_9 - s_7 s_6) = 0 \quad \text{w/0 } s_9 = s_7 = s_5 = s_3 = 0\,, \tag{6.7}$$

$$V(I_{(7)}) := s_9 = 0\,, \quad s_3^2 s_5^2 + s_3(-s_6 s_2 s_5 + s_6^2 s_1 - 2 s_7 s_5 s_1) + s_7(s_2^2 s_5 - s_6 s_2 s_1 + s_7 s_1^2) = 0\,. \tag{6.8}$$

Note that the above ideals are particularly specified by not allowing the simpler constraints to vanish. Apart from the vanishing loci of the above shown ideals the constraints of the other representations are much simpler and match our definition of a *toric* Higgs candidate that we can use to break to a fibration over one of the 16 polyhedra. In Figure 6.3 we have drawn in F_9^* the corresponding edges that connect two s_i that define the *toric* Higgs matter in the same color as the coordinates that get blown down by their Higgsing in the original polyhedron F_9^*.
Hence if we want to Higgs down to F_5 that exhibits the gauge group $\mathrm{U}(1)^2$ we have to break the SU(2) and blow down the blue or the violet point such that e_2 is not an SU(2) divisor anymore. This choice exactly matches the Higgsing with the two doublets $\mathbf{2}_{(-1,-1/2)}$ or $\mathbf{2}_{(1,3/2)}$ in the EFT. The two other choices would break to F_6 whose path we will not follow here.
The two deformations have been depicted in Figure 6.4. From the geometry point of view we have

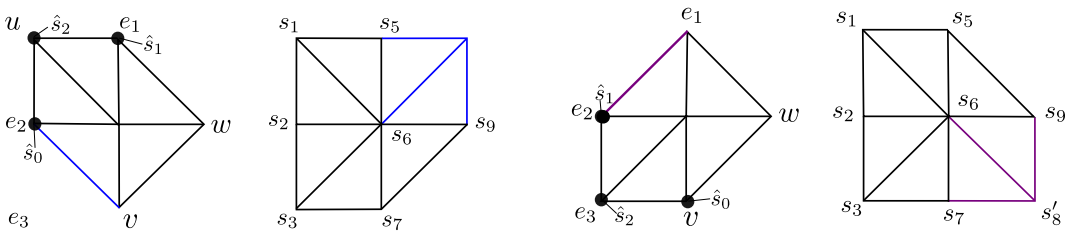

Figure 6.4: The two resulting toric deformations correspond to a Higgsing from F_9 to F_5.

clearly obtained a deformation to F_5. It is nice to see that, although we have Higgsed in both cases by two different representations, we have obtained the same theory up to a redefinition of the bundle classes and charge operators which is nicely encoded in the symmetry of the polyhedron but maybe not visible in the field theory for a given (unlucky) choice of charge generators.

We start by choosing the *canonical* Higgsing with the $\mathbf{2}_{(-1,-1/2)}$ representation because the F_5 is already in the canonical rotated form. Lets first compare the Shioda maps that are given for F_5 in terms of the

classes of the coordinates as:

$$\sigma_{F_5}(\hat{s}_1) = [e_1] - [e_2] - [K_B^{-1}]\,, \qquad \sigma_{F_5}(\hat{s}'_2) = [u] - [e_2] - [K_B^{-1}] - \mathcal{S}_9\,. \tag{6.9}$$

As the Higgsing corresponds to a blow-down of e_3 in F_9 we can set its divisor class in (6.4) to zero. Using this, we can represent (6.9) as linear combinations of the F_9 Shioda maps, up to base divisors that do not contribute to the U(1) charge:

$$\sigma_{F_9}(\hat{s}'_1) = \sigma_{F_5}(\hat{s}_2) - \sigma_{F_5}(\hat{s}_1) + \frac{1}{2}D_1 - [K_B^{-1}] + \mathcal{S}_7 - \mathcal{S}_9\,, \qquad \sigma_{F_9}(\hat{s}'_2) = -\sigma_{F_5}(\hat{s}_1) + D_1 - 2([K_B^{-1}] + \mathcal{S}_9)\,. \tag{6.10}$$

Rewriting the above expression into the more familiar form of a charge generator of Q'_1 and Q'_2 in F_5 in terms of the charges in Q_1 and Q_2 and the Cartan generator $\frac{1}{2}D_1 = T^3$ of F_9 we obtain:

$$Q'_1 = Q_2 - Q_1 + T^3\,, \quad Q'_2 = -Q_1 + 2T^3\,. \tag{6.11}$$

For the second Higgsing, we Higgs with the $\mathbf{2}_{(1,3/2)}$ representation corresponding to a blow-down of the u coordinate in F_9. In the second picture of Figure 6.4 we see that we have to reflect the deformed polyhedron to match exactly with the one of F_5. Hence after setting $[u] = 0$ in (6.4) we have to redefine the bundle classes in F_9 to those of F_5 by setting

$$[e_3] \to [u]\,, \qquad [v] \to [e_1]\,, \tag{6.12}$$

$$[e_1] \to [v]\,, \quad \mathcal{S}_7 \to 2[K^- - 1_B] - \mathcal{S}_7 \tag{6.13}$$

After that identification we can again express the F_5 Shioda maps as

$$\sigma_{F_5}(\hat{s}'_1) = \sigma_{F_9}(\hat{s}_2) - \sigma_{F_9}(\hat{s}_1) + \tfrac{1}{2}D_1 - \mathcal{S}_9\,, \qquad \sigma_{F_5}(\hat{s}'_2) = \sigma_{F_9}(\hat{s}_1) + D_1 - 2\mathcal{S}_9\,. \tag{6.14}$$

Again, the base divisors do not change the charges of the fields and we see, that these identifications correspond to the field theory expectations

$$Q'_1 = Q_2 - Q_1 + T^3\,, \quad Q'_2 = Q_1 + 2T^3\,. \tag{6.15}$$

The multiplet decomposition of the states is summarized in Table 6.2. There we indeed find that for both Higgsings there is a total gauge singlet under the residual group in the decomposed Higgs multiplet, which verifies our charge formulas for the unbroken group. We see that at this point we have successfully matched the charges of F_5. In the next step we have to match the resulting multiplicities of the states as well. Luckily there is no superpotential in six dimensions and hence also no F-term constrain -term in 6D and we do not have to worry about Yukawa coupling induced mass terms [33]. But in order to achieve a supersymmetric vacuum we have to assign a D-flat VEV to the Higgs multiplet. In [101] it was observed that to guarantee D-term constraints it is necessary that at least two hyper multiplets of the same charge acquire a VEV. Hence in total three hypermultiplets support the longitudinal components of the three vectors that get massive. Hence we have to simultaneously remove the three vectors and three hypers as expected from Goldstone's theorem. This amount is also in agreement with the pure gravitational anomaly in 6D given in section 5.4.4 that enforces the simultaneous removal of one hypermultiplet per vectormultiplet. In the next section we will have a precise example where we chose a $\mathbb{P}^2$ base and we will see, that the D-term constraints are encoded in the geometry as well.
Finally if we want to match the other states we have to recall the structure of a hypermultiplet, that is an SU(2)-R symmetry doublet of two conjugate chiral $\mathcal{N} = 1$ multiplets. We have to take this into account

	VEV: $\mathbf{2}_{(-1,-1/2)}$ $Q_1' = (Q_2 - Q_1 + T^3)$ $Q_2' = (-Q_1 + 2T^3)$	VEV: $\mathbf{2}_{(1,3/2)}$ $Q_1' = (Q_2 - Q_1 + T^3)$ $Q_2' = (Q_1 + 2T^3)$
$\mathbf{1}_{(1,2)}$	$\mathbf{1}_{(1,-1)}$	$\mathbf{1}_{(1,1)}$
$\mathbf{1}_{(1,0)}$	$\mathbf{1}_{(-1,-1)}$	$\mathbf{1}_{(-1,1)}$
$\mathbf{1}_{(0,1)}$	$\mathbf{1}_{(1,0)}$	$\mathbf{1}_{(1,0)}$
$\mathbf{1}_{(1,1)}$	$\mathbf{1}_{(0,-1)}$	$\mathbf{1}_{(0,1)}$
$\mathbf{2}_{(-1,-1/2)}$	$\mathbf{1}_{(0,0)} + \mathbf{1}_{(1,2)}$	$\mathbf{1}_{(1,0)} + \mathbf{1}_{(0,-2)}$
$\mathbf{2}_{(1,3/2)}$	$\mathbf{1}_{(0,-2)} + \mathbf{1}_{(1,0)}$	$\mathbf{1}_{(1,2)} + \mathbf{1}_{(0,0)}$
$\mathbf{2}_{(0,-1/2)}$	$\mathbf{1}_{(-1,-1)} + \mathbf{1}_{(0,1)}$	$\mathbf{1}_{(0,1)} + \mathbf{1}_{(-1,-1)}$
$\mathbf{3}_{(0,0)}$	$\mathbf{1}_{(-1,-2)} + \mathbf{1}_{(1,2)} + \mathbf{1}_{(0,0)}$	$\mathbf{1}_{(1,2)} + \mathbf{1}_{(-1,-2)} + \mathbf{1}_{(0,0)}$

Table 6.2: Possible state decompositions from F_9 to those of F_5 for different Higgses.

when we calculate the multiplicity of the decomposed states because we have to add the multiplicity of states that are identified up to charge conjugation. The multiplicities of the broken states of F_9 perfectly agree with the ones geometrically calculated in F_5.

Finally we have to match the multiplicity of the uncharged matter as well. Using (5.70) the change of the complex structure moduli can be expressed as

$$h^{(2,1)}(X_{F_j}) - h^{(2,1)}(X_{F_i}) = \mathrm{rk}(G_{F_j}) - \mathrm{rk}(G_{F_i}) + \frac{\chi(X_{F_i}) - \chi(X_{F_j})}{2} \,. \tag{6.16}$$

Using the Euler numbers for F_9 and F_5 given in Table J.1 of appendix J we find in our case precisely

$$h^{(2,1)}(X_{F_5}) - h^{(2,1)}(X_{F_9}) = \mathcal{S}_9(2[K_B^{-1}] - \mathcal{S}_7) - 1 \,. \tag{6.17}$$

This is exactly the multiplicity of the $\mathbf{2}_{(-1,-1/2)}$ representation in F_9 that we have used for Higgsing and that are now neutral singlets under the unbroken group. The one missing representation is the massive direction in the adjoint representation.

In case of the non-toric Higgsing we have to apply the bundle redefinitions

$$\mathcal{S}_7 \to 2[K_B^{-1}] - \mathcal{S}_7 \,, \tag{6.18}$$

that gives

$$h^{(2,1)}(X_{F_5}) - h^{(2,1)}(X_{F_9}) = \mathcal{S}_9\mathcal{S}_7 - 1 \,, \tag{6.19}$$

which is the multiplicity of the non-canonical Higgs representation $\mathbf{2}_{(1,3/2)}$ that we gave a VEV to.

6.2.1 A $\mathbb{P}^2$ example

We want to emphasis again that all considerations above are completely base independent and fully general. In this section we want to be completely explicit and choose $\mathbb{P}^2$ as a base space and consider

the Higgsing again. In that case the divisors classes are all powers of the hyperplane class H_B of $\mathbb{P}^2$ that are given as

$$\mathcal{S}_7 = n_7 H_B\,, \quad \mathcal{S}_9 = n_9 H_B\,, \quad [K_B^{-1}] = -3H_B\,, \tag{6.20}$$

with $H_B^2 = 1$ with n_7 and n_9 being the integer values that specify the power of the corresponding bundles. The consistency conditions imposed by an elliptic fibration Y_{F_i} on the points n_7 and n_9 are such that all matter divisors are *effective* to give a non-negative amount of matter. From a physical perspective this guarantees, that all matter multiplicities are positive. depicted all allowed regions both for all Y_{F_9} and

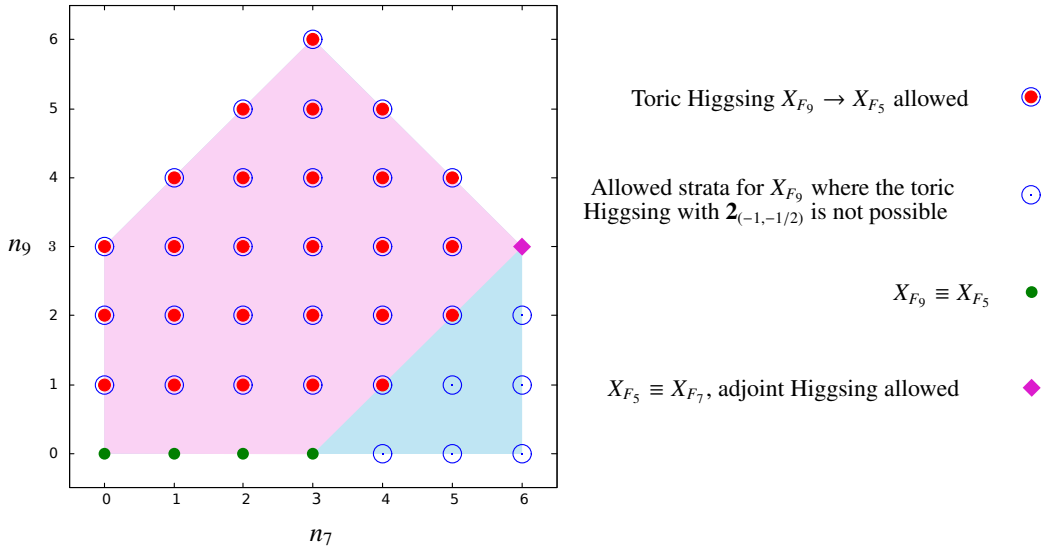

Figure 6.5: Allowed regions of $\mathcal{S}_7$ and $\mathcal{S}_9$ for X_{F_9} (blue) and X_{F_5} (purple region) with base $B = \mathbb{P}^2$. The Higgsing is only possible at the overlap.

Y_{F_5} both fibered over $\mathbb{P}^2$. Every point inside the allowed regions is a valid F-theory background where the matter spectrum is fully determined.
In the picture we note that X_{F_5} is fully contained in X_{F_9}. Considering the Higgsing of Y_{F_9} to Y_{F_5} we can distinguish three scenarios highlighted with the different colored dots

- In case of the red dots there exists a *canonical* Higgsing the way it was discussed in the section before.
- For the blue dots there does not exist a canonical Higgsing as it is not in the allowed region of Y_{F_5}.
- Green dots and the pink shade on the boundary of the allowed regions.

Here we see, that the choice of a certain stratum in the allowed region fixes whether Y_{F_9} is Higgsable to Y_{F_5} or not[3]. Physically such a choice corresponds to a situation where D-flatness of the VEV cannot be guaranteed: The multiplicity for the Higgs in this case $\mathbf{2}_{(-1,-\frac{1}{2})}$ is given by

$$\mathcal{S}_9\left(2[K_B^{-1}] - \mathcal{S}_7\right) = n_9\,(6 - n_7)\,, \tag{6.21}$$

[3] Note that we constraint ourselves to the canonical Higgsing for. The non-canonical Higgsing might still be possible, as it comes with a divisor mapping that reflects the allowed regions of F_5 along the line $(3, x)$

and is always smaller than two in the blue region. Remember that D-flatness requires at least two Higgs field in the same representation to acquire a VEV and hence this cannot be assured here.
Finally we want to look at some special points at the boundary of the valid region. There are first the strata with $n_9 = 0$ that are depicted with green dots. In Y_{F_9} the SU(2) locus is at the locus $s_9 = 0$ which at this stratum becomes a trivial divisor and hence, the gauge symmetry and matter multiplets charged under it are absent[4]. On the other hand, in X_{F_5} matter states are missing too and when we compare the states we see that the two spectra actually coincide and hence the two fibrations are the same at this stratum.
The last point is even more delicate. It is specified at the stratum $(n_7, n_9) = (6, 3)$. Here we find that states in the $\mathbf{2}_{(-1,1/2)}$ are again absent and a Higgsing is not possible. But we also find that the SU(2) that lives at the $s_9 = 0$ divisor is present. However, in F_5 we find that at this specific locus s_1, s_5 and s_8 do transform in the trivial bundle (see table I and eq. 5.100 for the hypersurface equation of F_5) and hence are simply constants. As these are only constants we can shift the coordinates u, v and w to globally set $e_1 = 0$. In [75] it was shown that this results in a *non-toric* U(1) at this point. Hence at this point we have actually three U(1)'s in F_5 and the spectrum agrees precisely with that of F_7 (see Figure 6.13). Hence again we find a point the strata of two different fibrations coincide as we have already observed above. As the rank of F_9 and F_7 are the same can only connect the two theories by a rank preserving Higgsing i.g. induced by a VEV in the adjoint representation. Indeed one can show that this is what is happening here and the the field theory charges and multiplicities fully agree. Moreover we can see that the Euler numbers of F_7 and F_9 coincide at this specific stratum by consulting table J.1 in appendix J and plugging in the above definitions four the base.

6.3 Fibers with discrete symmetries

After having clarified the general mechanism of a Higgs transition we use that knowledge to descend, starting form F_5 with gauge group $\mathrm{U}(1)^2$ down to lower symmetries. The Higgs transition will help us to describe novel features of the elliptic fiber namely a *non-toric* section in F_3 and discrete symmetries that have not been observed before in F_2 and F_1.

6.3.1 Higgsing F_5 to F_3

The last section served as an introduction for the tools and the methods of the toric Higgs effect. In the following we will further descend the chain and go on to Higgs the theory. Here our Field theory expectations will help us to deduce some of the geometrical properties of more complicated fibers, i.e. F_3, F_2 and F_1. and the toric Higgs effect and the field theory expectations will help us to deduce the geometrical properties of the more complicated polyhedra F_3, F_2 and F_1.
We consider the transition from F_5 to F_3. First we start with the field theory expectations: We perform the canonical Higgsing using the $\mathbf{1}_{(-1,1)}$ representation[5]. From Table 5.6e and Figure 5.10 we see that this precisely corresponds to the Higgsing to F_3 in the canonical way. The unbroken charge operator is simply given by

$$Q' = Q_1 + Q_2\,, \tag{6.22}$$

and the decomposition of the states is summarized in Table 6.3. Here we note first, that we find a state that has charge three. This is very unusual and it is the first time that such a state appears in F-theory.

[4] The multiplicity of adjoint matter given by (5.67) when the divisor transforms in the trivial class.
[5] Note that we have divided the charges by 5 again.

F_5 origin	F_3 state	combined multiplicity
$\mathbf{1}_{(1,0)} + \mathbf{1}_{(0,1)}$	$\mathbf{1}_1$	$12[K_B^{-1}]^2 + [K_B^{-1}](8\mathcal{S}_7 - \mathcal{S}_9)$ $-4\mathcal{S}_7^2 + \mathcal{S}_7\mathcal{S}_9 - \mathcal{S}_9^2$
$\mathbf{1}_{(-1,-1)} + \mathbf{1}_{(0,2)}$	$\mathbf{1}_2$	$6[K_B^{-1}]^2 + [K_B^{-1}](4\mathcal{S}_9 - 5\mathcal{S}_7)$ $+\mathcal{S}_7^2 + 2\mathcal{S}_7\mathcal{S}_9 - 2\mathcal{S}_9^2$
$\mathbf{1}_{-1,-2}$	$\mathbf{1}_3$	$\mathcal{S}_9([K_B^{-1}] + \mathcal{S}_9 - \mathcal{S}_7)$

Table 6.3: The Higgsing from F_5 to F_3 induced by a VEV in $\mathbf{1}_{(1,-1)}$ and the resulting multiplicities.

The puzzle is, the U(1) charges are related to intersection properties of the matter curve with the fiber and in order to observe such a charge we have to have a matter curve that is intersected more than once by the rational sections, which can be realized when the rational section is a multi cover over the given codimension two locus.
Lets consider next the geometry of F_3 directly and compare it to the Higgsing. F_3 and its dual are given it Figure 6.6. We read of the Stanley-Reisner ideal to be

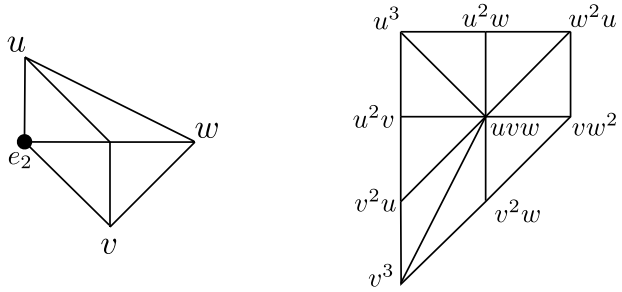

Figure 6.6: Polyhedron F_3 with a choice of projective coordinates and its dual F_{14} with the corresponding monomials. We have set $e_2 = 1$ for brevity of our notation. The zero section is indicated by the dot.

$$SR_{F_3} = \{uv, we_2\}\,, \tag{6.23}$$

and construct the elliptic curve from the dual polyhedron as the vanishing hypersurface:

$$p_{F_3} = s_1u^3e_2^2 + s_2u^2ve_2^2 + s_3uv^2e_2^2 + s_4v^3e_2^2 + s_5u^2we_2 + s_6uvwe_2 + s_7v^2we_2 + s_8uw^2 + s_9vw^2\,. \tag{6.24}$$

The zero section is given at the vanishing locus of e_2:

$$\hat{s}_0 = X_{F_3} \cap \{e_2 = 0\}: \quad [s_9 : -s_8 : 1 : 0]\,. \tag{6.25}$$

This section is the only *toric* independent section that we can find. However, from the Higgsing we know that there has to exist a second section that is not visible directly. Indeed one can show that there exists a second section constructed in the following way:
Setting $e_2 = 1$ we are constructing a line, that is *tangent* to the cubic curve at the point $P_0 : [u, v, w] = [0, 0, 1]$

$$t_p = s_8u + s_9v\,. \tag{6.26}$$

We can confirm that P_{F_3} and $dP_{F_3} = 0$ vanish at P_0 and that this point also lies on t_p. Then we can use that a line intersects a cubic curve always three times. Hence we can compute the third intersection of $t_p = 0$ with P_{F_3} that is given by

$$\hat{s}_1 = X_{F_3} \cap \{t_P = 0\} : \; [-s_9 : s_8 : s_1 s_9^3 - s_4 s_8^3 + s_3 s_9 s_8^2 - s_2 s_9^2 s_8 : s_7 s_8^2 - s_6 s_9 s_8 + s_5 s_9^2] \,. \tag{6.27}$$

This is exactly the rational point that we were looking for. Its Shioda map is given by

$$\sigma(\hat{s}_1) = S_1 - S_0 + 3[K_B] + \mathcal{S}_7 - 2\mathcal{S}_9 \,. \tag{6.28}$$

Now we can turn to calculate the matter curves. As outlined before it is necessary to map the cubic into the Weierstrass form and find all codimension two singularities. The most interesting of these loci is easy to find, as it is the *toric* one given by the vanishing of the simple constraints $s_8 = s_9 = 0$ where the hypersurface constraint (6.24) factorizes to

$$p_{F_3}\big|_{s_8=s_9=0} = e_2 \underbrace{(s_1 u^3 e_1 + s_2 u^2 v e_2 + s_3 u v^2 e_2 + s_4 v^3 e_2 + s_5 u^2 w + s_6 u v w + s_7 v^2 w)}_{q_3} \,. \tag{6.29}$$

As expected this is an I_2 fiber. As the zero section is at $e_2 = 0$ it wraps the first component of the curve. For the intersection with the non-toric section we have to recall that it was constructed as the second intersection line through the tangent and $[u, v, w, e_2] = [0, 0, 1, 1]$. However at $s_8 = s_9$ the whole curve is singular at this point as well and hence every curve through P_0 is also a tangent to P_0. Hence all points that go through the second component q_2 are tangent to P_0 and thus the whole rational section $\hat{s}_1$ wraps the q_3 component.
The whole intersection pattern is summarized in Fig. 6.7. We note the peculiar behavior that both

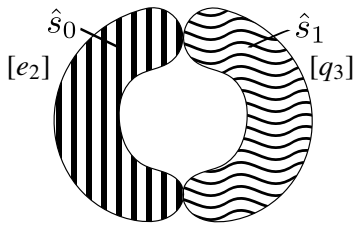

Figure 6.7: The F_3 fiber at codimension two and its fiber components $[e_2]$ and $[q_3]$. The components are wrapped by the rational sections $\hat{s}_0$ and $\hat{s}_1$ respectively.

sections wrap whole fiber components at the same time. Taking $[e_2]$ as the affine node, we intersect the Shioda map with the $[q_3]$ component:

$$\sigma(\hat{s}_1) \cdot q_3 = \underbrace{\hat{s}_1 \cdot q_3}_{=1} - \underbrace{\hat{s}_0 \cdot q_3}_{=-2} = 3 \,, \tag{6.30}$$

hence we have found the charge three representation $\mathbf{1}_3$. The multiplicity is given by the divisor classes $[s_8] \cdot [s_9] = \mathcal{S}_9([K_B^{-1}] + \mathcal{S}_9 - \mathcal{S}_7)$ that can be found Table I in the appendix I. Comparing with the expected result from the Higgsing in Table 6.3 we find indeed a match. All other loci are not toric and hence we have to work much harder to find them as described in chapter 5. We first have to map the rational points into Weierstrass coordinates, using Nagel's algorithm and then find the sub varieties in

(5.64). The charge two matter locus is present when the following simpler constrains vanish:

$$V(I_{(2)}) := \{s_4 s_8^3 - s_3 s_8^2 s_9 + s_2 s_8 s_9^2 - s_1 s_9^3 \tag{6.31}$$

$$= s_7 s_8^2 + s_5 s_9^2 - s_6 s_8 s_9 = 0 \text{ with } (s_8, s_9) \neq (0,0)\}\,, \tag{6.32}$$

where the hypersurface (6.27) splits as

$$P_{F_3}|_{V(I_2)} \to \underbrace{(s_8 u + s_9 v)}_{t_p} q_2\,, \tag{6.33}$$

With the order two polynomial q_2. The I_2 locus corresponds to the $\mathbf{1}_2$ representation as it can be seen that the first component is precisely the tangent line t_p at P_0 which is intersected by the zero section. The non-toric section on the other hand is precisely defined by the intersection with t_p and the elliptic curve and again the section wraps the entire fiber component. The picture of the fiber is summarized in Fig. 6.8Finally the last locus gives a factorization, after setting $e_2 = 1$ to

$$P_{F_3}|_{V(I_3)} \to \underbrace{(d_1 u + d_2 v + d_3 w)}_{d} q_2'\,, \tag{6.34}$$

with non vanishing coefficients d_i and a generic quadric q_2 without the w^2 term because there is no cubic w term in F_3. The zero section $\hat{s}_0$ with coordinates $[0,0,1]$ does not intersect the polynomial d but the quadric one q_2'. The section $\hat{s}_1$ defined by $Y_{F_3} \cup t_p = 0$ intersects the first term d in a point as one can easily see. Again the intersection properties of the codimension two fiber is summarized in Figure 6.8 and we readily compute the charge of the I_1 matter to be $\mathbf{1}_1$ from the pictures. The locus $V(I_3)$ is then

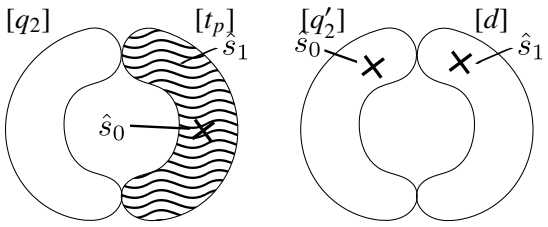

(a) I_2 fiber (b) I_3 fiber

Figure 6.8: The singular F_3 fiber for two singular codimension two loci I_2 and I_3 including the intersections with the rational sections and the irreducible fiber components.

given by the whole vanishing of (5.64) and using the *elimination ideal* techniques one can confirm that it is indeed a prime ideal when the I_2 and I_3 ideals are subtracted and that I_1 lies in (5.64) . Calculating the number of solutions of $V(I_2)$ and $V(I_3)$ we can indeed confirm the multiplicities we find from the Higgsing in given in Table 6.3.
We note that the $\mathbf{1}_3$ matter locus is again *toric* and hence this representation can be used for Higgsing down to F_1 .

6.3.2 Hissing F_5 to F_2

The next part we want to discuss is the Higgsing from F_5 to F_2. The only way to achieve that is by taking the Higgs to be in the $\mathbf{1}_{(0,2)}$ representation. This representation has a non-minimal charge

under the second U(1) but is uncharged under the first. Hence from our field theory expectations we can guess that the resulting theory will exhibit a $\mathrm{U}(1) \times \mathbb{Z}_2$ symmetry generated by the F_5 charges $Q_{F_2} = Q_{F_{5,1}}, Q_{\mathbb{Z}_2} = Q_{F_{5,2}} \bmod 2$ whereas we call the $\mathbb{Z}_2$ charge $\pm$ according to their two eigenvalues. We again summarize the states from the Higgsing and their F_5 origin in Table 6.4 Again we know what

F_5 origin	F_2 state	combined multiplicity
$\mathbf{1}_{(1,0)} + \mathbf{1}_{-1,-2}$	$\mathbf{1}_{(1,+)}$	$6[K_B^{-1}]^2 + 4[K_B^{-1}](\mathcal{S}_7 - \mathcal{S}_9) - 2\mathcal{S}_7^2 + 2\mathcal{S}_9^2$
$\mathbf{1}_{(-1,-1)}+$	$\mathbf{1}_{(1,-)}$	$6[K_B^{-1}]^2 + 4[K_B^{-1}](\mathcal{S}_9 - \mathcal{S}_7) + 2\mathcal{S}_7^2 - 2\mathcal{S}_9^2$
$\mathbf{1}_{(0,1)}+$	$\mathbf{1}_{(0,-)}$	$6[K_B^{-1}]^2 + 4[K_B^{-1}](\mathcal{S}_7 + \mathcal{S}_9) - 2\mathcal{S}_7^2 - 2\mathcal{S}_9^2$

Table 6.4: The Higgsing from F_5 to F_2 induced by a VEV in $\mathbf{1}_{(0,2)}$ and the resulting matter multiplicities.

we should expect in F_2: one U(1) generated by two rational sections as well as a discrete symmetry generator. Lets see how we can match these properties from the geometry side. The toric diagram of F_2 is that of $\mathbb{P}^1 \times \mathbb{P}^1$ and depicted in Figure 6.9. The SR-ideal is simply again given by

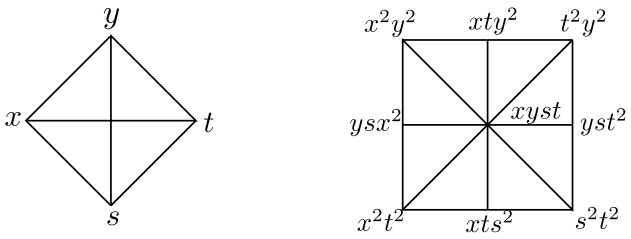

Figure 6.9: Polyhedron F_2 with a choice of projective coordinates and its dual F_{15} with the corresponding monomials.

$$SR_{F_3} = \{ys, xt\}\,, \tag{6.35}$$

and the hypersurface equation is given by the vanishing of

$$p_{F_2} = (b_1 y^2 + b_2 sy + b_3 s^2)x^2 + (b_5 y^2 + b_6 sy + b_7 s^2)xt + (b_8 y^2 + b_9 sy + b_{10} s^2)t^2\,, \tag{6.36}$$

Note this genus-one curve is not a cubic as we have seen before but a bi-quadric. Hence the coordinates have different names and we have a different set of coefficients b_i. All divisor classes[6] can be read of from Table I.

The hypersurface in F_2 is a genus-one curve and does not have a rational section but only two two-sections. These are given by

$$\begin{aligned} \hat{s}_0^{(2)} &= X_{F_2} \cap \{x = 0\}: \quad b_8 y^2 + b_9 sy + b_{10} s^2 = 0\,, \\ \hat{s}_1^{(2)} &= X_{F_2} \cap \{y = 0\}: \quad b_3 x^2 + b_7 xt + b_{10} t^2 = 0\,, \end{aligned} \tag{6.37}$$

that are still quadratic in the residual coordinates and thus multivalued. Hence in the following we have to consider the *Jacobian* of the curve to map the bi-quadric to curve that has at least a zero-section. However instead of taking the Jacobian directly in the Weierstrass form we want to map it into the cubic form of F_5. We do this by a shift of the coordinates of the form $x \to x + \alpha t$. This shift involves square

[6] Note that the F_2 has two hyperplane classes associated to the two $\mathbb{P}^1$'s.

roots of the b_i in α. The new elliptic curve we obtain has the form

$$\tilde{p} = (\tilde{s}_1 y^2 + \tilde{s}_2 sy + \tilde{s}_3 s^2)x^2 + (\tilde{s}_5 y^2 + \tilde{s}_6 sy + \tilde{s}_7 s^2)xt + (\tilde{s}_8 y^2 + \tilde{s}_9 sy)t^2\,, \tag{6.38}$$

with the $\tilde{s}_i$ being the redefined coefficients depending (possibly on square roots of) the b_i's and are given in appendix K. The structure of this equation is the same as for the cubic, provided the coordinate match

$$t \to w\,, \quad s \to v\,, \quad x \to e_2\,, \quad y \to e_1\,, \quad u = 1\,. \tag{6.39}$$

Hence now we are dealing with the F_5 cubic again when identifying the sections $\tilde{s}_i$ with the untilded s_i. By this map we can simply plug in the values for the s_i in terms of the b_i's and track the behavior of the rational sections we found in F_5 given by (5.101). First obtain a zero-point $\hat{s}_0$ for free at $x \to e_2 = 0$ that was not present in the original genus-one curve. Next we look at the two-sections and how these behave, when they are mapped into the cubic form. The two section $\hat{s}_1^2$ with $y = 0$ maps to a rational point of the cubic 6.38 of the form $[t, s, x, y] \to [-\hat{s}_3/\hat{s}_7, 1, 1, 0]$. Note that this is precisely a point on F_5 that gave us a rational section as well at $e_1 = 0$ At last we have to confirm, that the section $\hat{s}_1^2$ in the Weierstrass coordinates is indeed a rational expression in the sections b_i. By transforming the cubic of F_5 into WSF using Nagel's algorithm and we find for the first rational point the coordinates

$$\begin{aligned} x_1 &= \tfrac{1}{12}(\tilde{s}_6^2 - 4\tilde{s}_5\tilde{s}_7 + 8\tilde{s}_3\tilde{s}_8 - 4\tilde{s}_2\tilde{s}_9)\,, \\ y_1 &= \tfrac{1}{2}(\tilde{s}_3\tilde{s}_6\tilde{s}_8 - \tilde{s}_2\tilde{s}_7\tilde{s}_8 - \tilde{s}_3\tilde{s}_5\tilde{s}_9 + \tilde{s}_1\tilde{s}_7\tilde{s}_9)\,, \\ z_1 &= 1\,. \end{aligned} \tag{6.40}$$

Note that some of the $\tilde{s}_i$ involve square roots of the b_i however after inserting them we stay with the purely rational expressions

$$\begin{aligned} x_1 =& \tfrac{1}{12}(8b_1b_{10} + b_6^2 - 4b_5b_7 + 8b_3b_8 - 4b_2b_9)\,, \\ y_1 =& \tfrac{1}{2}(b_{10}b_2b_5 - b_1b_{10}b_6 + b_3b_6b_8 - b_2b_7b_8 - b_3b_5b_9 + b_1b_7b_9)\,, \\ z_1 =& 1\,. \end{aligned} \tag{6.41}$$

Hence we have found that the two-section $\hat{s}_1^2$ indeed maps to the rational section $\hat{s}_1$ of F_5 which we can consider as the Jacobian fibration of F_2. This result is indeed expected from the field theory point of view as the Higgs field $\mathbf{1}_{0,2}$ is not intersected i.e. uncharged under the $\tilde{s}_1$and thus it should stay unbroken. We employ exactly the same logic to the section s_2 defined at the point $[t, s, x, y] \to [1, -\hat{s}_8/\hat{s}_9, 0, 1]$, that precisely maps to the rational section in F_5 that is $\hat{s}_2^2$. Also this time we have to check whether this section stays rational when we map its coordinate into the WSF in terms of the original b_i coordinates. The Weierstrass coordinates of s_2 of the cubic are given by

$$\begin{aligned} x_2 &= \tfrac{1}{12}(12\tilde{s}_7^2\tilde{s}_8^2 + \tilde{s}_9^2(\tilde{s}_6^2 + 8\tilde{s}_3\tilde{s}_8 - 4\tilde{s}_2\tilde{s}_9) + 4\tilde{s}_7\tilde{s}_9(-3\tilde{s}_6\tilde{s}_8 + 2\tilde{s}_5\tilde{s}_9))\,, \\ y_2 &= \tfrac{1}{2}(2\tilde{s}_7^3\tilde{s}_8^3 + \tilde{s}_3\tilde{s}_9^3(-\tilde{s}_6\tilde{s}_8 + \tilde{s}_5\tilde{s}_9) + \tilde{s}_7^2\tilde{s}_8\tilde{s}_9(-3\tilde{s}_6\tilde{s}_8 + 2\tilde{s}_5\tilde{s}_9) \\ &\quad + \tilde{s}_7\tilde{s}_9^2(\tilde{s}_6^2\tilde{s}_8 + 2\tilde{s}_3\tilde{s}_8^2 - \tilde{s}_5\tilde{s}_6\tilde{s}_9 - \tilde{s}_2\tilde{s}_8\tilde{s}_9 + \tilde{s}_1\tilde{s}_9^2)\,, \\ z_2 &= \tilde{s}_9\,. \end{aligned} \tag{6.42}$$

Inserting the identifications the b_i we get long expressions mostly involving square root factors in the b_i. However this can be seen simply by noting that the z_2 coordinate becomes $\tilde{s}_9 = -\sqrt{-4b_{10}b_8 + b_9^2}$. We conclude that the two section $\hat{s}_s^2$ of F_2 does not become rational in the associated Jacobian and thus does

not provide another U(1) factor but to a discrete charge. The charge of the MW-generator is generated by the Shioda map:

$$\sigma(\hat{s}_1^{(2)}) = S_1^{(2)} - S_0^{(2)} + \tfrac{1}{2}([K_B] - \mathcal{S}_7 + \mathcal{S}_9)\,, \tag{6.43}$$

where we had to modify the base part as this comes from a two section. For the $\mathbb{Z}_2$ charge we *propose* the following discrete Shioda map:

$$\sigma_{\mathbb{Z}_2}(\hat{s}_2^{(2)}) = S_2^{(2)} + [K_B^{-1}] - \mathcal{S}_9\,. \tag{6.44}$$

Note the we have not subtracted the zero-section in the above form, which fundamentally differentiates it from the traditional Shioda map. By matching the charges generated by (6.44) we indeed argue that the above generator is correct.

At next we have to find the matter loci. Here we work again with the genus-one curve in the bi-quadric form. As we have seen before, hitting a matter locus imposes an I_2 factorization of the bi-quadric curve into two components. These splittings are with respect to the two hyperplane classes of the two underlying $\mathbb{P}^1$'s that have the coordinates $[x, y]$ and $[s, t]$. Remember that we can easily read of the transformation properties of the coordinates by observing the linear dependencies within the toric diagram of F_2 given in Figure 6.9. Hence the $(2, 2)$ charged curve can be expanded the ways $(1, 1) + (1, 1)$, $(1, 2) + (1, 0)$ and $(2, 1) + (0, 1)$ corresponding to the three matter[7] loci.We give only the first factorization explicitly as

$$p_{F_2} \overset{!}{=} b_1 \underbrace{[(y + \alpha_1 s)x + (\alpha_2 y + \alpha_3 s)t]}_{q^1_{(1,1)}} \underbrace{[(y + \beta_1 s)x + (\beta_2 y + \beta_3 s)t]}_{q^1_{(1,1)}}\,. \tag{6.45}$$

We can already factor out b_1 however it must not vanish in order not to give a codimension one singularity. Hence by imposing that splitting, we find for the six α_i and β_i eight constraints on the b_i. This gives a codimension two constraint as it is needed for a matter locus. We represent the above curve as well as their intersection with the two-sections in Figure 6.10 Intersecting one of the fiber components

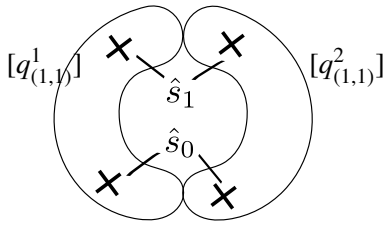

Figure 6.10: The F_2 fiber at codimension two and its fiber components $[q^1_{(1,1)}]$ and $[q^2_{(1,1)}]$ and their intersections.

with (6.43) reveals that the matter is uncharged under the U(1). This means we find matter that is neutral under the U(1) but it cannot be a modulus either as it leads to a degeneration of the fiber. Hence it has to have a charge. Indeed we find that each component of the polynomials is intersected by a two-section and we can assign the value 1 to the curve $[q^1_{(1,1)}]$. However we also know that the other curve has to be

[7] Note that a $(2, 0) + (0, 2)$ split corresponds not to a two split and hence does not give a matter curve.

oppositely charged under the same symmetry. But for the curve $[q^2_{(1,1)}]$ is intersected in the very same way and hence we also have to assign the charge 1 to the same curve. Hence This can only be valid when $1 + 1 = 0$ which implies a $\mathbb{Z}_2$ symmetry.
This procedure works completely analogously for the other two splits and we can indeed confirm, that the $\mathbf{1}_{(1,+)}$ and $\mathbf{1}_{(1,-)}$ loci are produced. To calculate the multiplicities we use again the *elimination* ideal techniques which confirm the multiplicities we expected from the Higgsing, summarized in Table 6.4.

6.3.3 Higgsing F_3 to F_1

Finally, we Higgs F_3 down to F_1 corresponding to a symmetry breaking in the field theory of the form

$$\mathrm{U}(1) \xrightarrow{\langle \mathbf{1} \rangle} \mathbb{Z}_3 \,. \tag{6.46}$$

We find that in F_1 there is only one state coming from the decomposition of the states summarized in Table 6.5 We note here that there is indeed only one discrete charged state in the spectrum. This comes

F_3 Origin	F_1 State	Combined multiplicity
$\mathbf{1}_1 + \mathbf{1}_2$	$\mathbf{1}_1$	$3\left(6[K_B^{-1}]^2 - \mathcal{S}_7^2 + \mathcal{S}_7\mathcal{S}_9 - \mathcal{S}_9^2 + [K_B^{-1}](\mathcal{S}_7 + \mathcal{S}_9)\right)$

Table 6.5: The Higgsing from F_3 to F_1 induced by a VEV in the $\mathbf{1}_3$ and the resulting from the Higgsing.

from the fact that a 6D hypermultiplet of the state $\mathbf{1}_1$ always includes the conjugate state $\mathbf{1}_{-1}$ as well. However this time $-1 = 2$ mod 3 and hence the states are identified to be in the same multiplet. Thus we we have to add the individual multiplicities. We encounter the same phenomenon when we have a look at the geometry side that we consider in the following:

The toric diagram is depicted in Figure 6.11 and can be identified with the ambient space of an $\mathbb{P}^2$. The SR-ideal is only generated by the vanishing of all three coordinates $SR = \{uvw\}$. The hypersurface

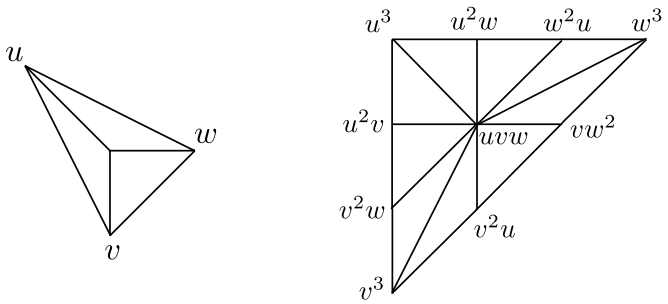

Figure 6.11: Polyhedron F_1 with choice of projective coordinates and its dual with corresponding monomials.

constraint is generated by the most general cubic curve

$$p_{F_1} = s_1u^3 + s_2u^2v + s_3uw^2 + s_4v^3 + s_5u^2w + s_6uvw + s_7v^2w + s_8uw^2 + s_9vw^2 + s_{10}w^3 \,, \tag{6.47}$$

whereas the divisor classes of the coordinates and base sections are again depicted in the appendix I in Table I. The cubic curve does not possess a rational section but only a three-section at $u = 0$:

$$\hat{s}^{(3)} = X_{F_1} \cap \{u = 0\} : \quad s_4 v^3 + s_7 v^2 w + s_9 v w^2 + s_{10} w^3 = 0\,. \tag{6.48}$$

Hence again we employ the *Jacobian* map to the Weierstrass form. We note that the three-section $\hat{s}^{(3)}$ maps to the zero point $[0, 0, 1]$ of the Weierstrass form. Again, we propose the discrete Shioda map to be

$$\sigma_{\mathbb{Z}_3}(\hat{s}^{(3)}) = S^{(3)} + [K_B] + \tfrac{4}{3}\mathcal{S}_9 - \tfrac{2}{3}\mathcal{S}_7\,, \tag{6.49}$$

that we infer to calculate the corresponding discrete charge of the matter curve. To find that matter curve we impose the splitting condition of the cubic curve to a degree one line and a quadric polynomial in a similar spirit as in F_2:

$$p_{F_1} \overset{!}{=} s_1 \underbrace{(u + \alpha_1 v + \alpha_2 w)}_{q^1} \underbrace{(u^2 + \beta_1 v^2 + \beta_2 w^2 + \beta_3 uv + \beta_4 vw + \beta_5 uw)}_{q^2}\,. \tag{6.50}$$

where again the seven α_i and β_i coefficients are subject to be polynomial constraints in the s_i determined by the comparison with Eq. (6.47). Indeed the nine s_i coefficients give an over constrained system for the seven polynomials and are thus subject to a codimension two constraints as expected for a matter locus. The intersection of the three-section with the irreducible fiber components is depicted in Figure 6.12 Again we find that the $[q^1]$ component has charge one while the $[q^2]$ piece is intersected twice and

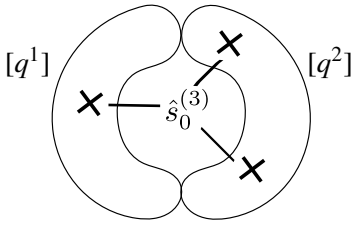

Figure 6.12: The F_1 fiber at codimension two and its fiber components $[q^1]$ and $[q^2]$ and their intersections with the three-section.

hence has charge two. However the two components should have opposite charges. Hence we have to identify the charge two with minus one which only makes sense in a discrete $\mathbb{Z}_3$ symmetry.

6.4 The Full Higgs Network

In the above examples we have shown how one can match the geometric transition in the fiber with the Higgs mechanism in the six dimensional effective theory. We can extend the calculations we have done before to the whole set of 2D polyhedra. The resulting physics and transitions are summarized in Figure 6.13. The resulting Higgs-network is the natural extension of the small version depicted in Figure 6.2 at the beginning of this chapter. Each transition is obtained by a similar procedure as we have stated above, by a match of geometrical and field theoretical expectations.
Having the full network at hand, we can make some interesting observations. For example we see, that the whole network can be obtained from Higgsings of the maximal groups of F_{16}, F_{15} and F_{13}. We

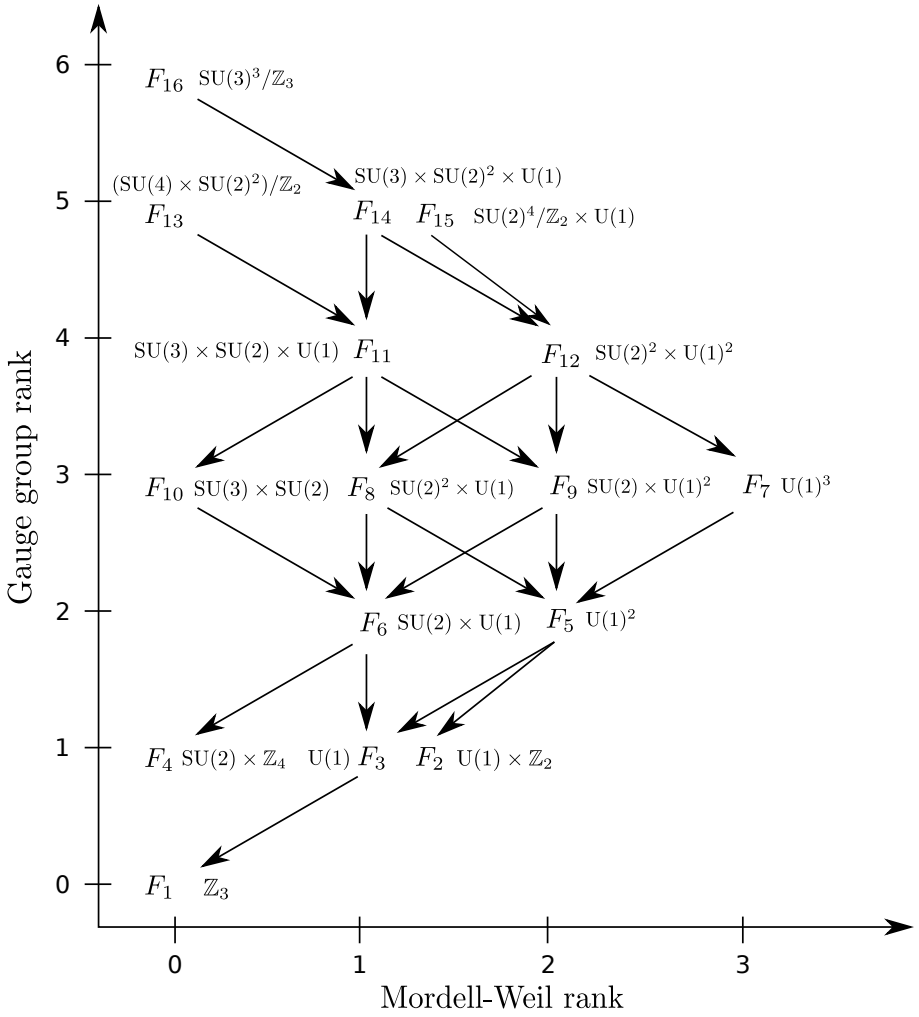

Figure 6.13: The network of Higgsings between all F-theory compactifications on toric hypersurface fibrations X_{F_i}. The axes show the rank of the MW-group and the total rank of the gauge group of X_{F_i}. Each Calabi-Yau X_{F_i} is abbreviated by F_i and its corresponding gauge group is shown. The arrows indicate the existence of a Higgsing between two Calabi-Yau manifolds.

remark that these are also exactly those fibers that exhibit Mordell–Weil torsion that acts as quotient group factors and thus have a restricted spectrum of matter representations. For the physics point of view however it is interesting to note that F_{16} and F_{13} have the exact gauge group and matter content (in 6D) of the trinification the Pati-Salam group. Moreover they are both related to F_{11} by a Higgsing that has the precise gauge group and matter content of the standard model, as we have seen in Chapter 4. It would be interesting, to see whether such a Higgsing would be possible in a 4D compactification including fluxes together with three chiral families.

Turning to the full network we observe some remarkable features and symmetries of it:

- The rank of the free Mordell-Weil group exhibited by a polyhedron F_i and its dual F_i^* are the same.

- The *rank sum rule:* The total rank of the gauge group of a polyhedron and its dual always satisfies

$$\text{Rank}(X_{F_i}) + \text{Rank}(X_{F_i^*}) = 6\,. \tag{6.51}$$

  The above rule might be explained by the fact that the sum of the area of a polyhedron and its dual are constant[8] for all 16 polyhedra.

- We find that the whole network is symmetric under *mirror symmetry* i.e. the exchange of a polyhedron and its dual. This symmetry is also satisfied by the Higgs transitions between the fibrations.

- The observed mirror symmetric structure strongly suggests that a fiber with $\mathbb{Z}_N$ Mordell-Weil torsion is mirror dual to a genus-one fiber with n-sections. Physically this implies that **discrete symmetries are mirror-dual to quotient group factors**.

Most of the points hint at a higher structure that might underlie the above toric fibrations. Especially the connection of discrete symmetries as the Mirror-dual to quotient factors is worth studying in the future and has been also observed in more general fibrations [98]. We also note, that all discrete symmetries can be understood as the remnant symmetries of local ones, as suggested by general argument of global symmetries in a theory of quantum gravity [16, 15, 102]. However the existence of a Higgs-and its mirror transition is easy to understand. As stated before a toric Higgsing acts exactly as a blow-down in the original polyhedron F_j and but as a blow-up in the dual one F_j^*:

$$(F_j\,,\,F_j^*) \overset{\text{Higgs}}{\longrightarrow} (F_j \overset{\text{blow-down}}{\longrightarrow} F_k\,,\,F_j^* \overset{\text{blow-up}}{\longrightarrow} F_k^*)\,, \tag{6.52}$$

with $j > k$. At next, we simply consider the mirror-dual elliptic fibration based on F_k^* and dual polyhedron F_k that we take to read of the monomials of the hypersurface constraint. Now we simply take the inverse map that we considered above (6.52) namely we consider the blow-down from F_k^* to F_j^* that must act as a toric blow-up in its dual to

$$(F_k^*\,,\,F_k) \overset{\text{Dual Higgs}}{\longrightarrow} (F_k^* \overset{\text{blow-down}}{\longrightarrow} F_j^*\,,\,F_k \overset{\text{blow-up}}{\longrightarrow} F_j)\,. \tag{6.53}$$

Hence by considering the toric Higgs to another polyhedron and then simply exchanging the interpretation of the fiber polyhedron with its dual, we get the unhiggsing of the dual elliptic fibration.

We have seen that the above 16 polyhedra have a great phenomenological relevance. Besides the intriguing fact that the standard model as well as grand unified groups appear very naturally in these fibers these fibers are also a great starting point to engineer additional symmetries using *tops*. The above fibrations are all interesting starting points for model building when we engineer additional symmetries using a *top*. This is exactly the avenue we want to proceed in the following chapter.

[8] We thank Albrecht Klemm for pointing this out.

CHAPTER 7

Realistic SU(5) Gut models in F-theory

In this Chapter we want to use constructions that we have encountered in the last chapter and try to embed the MSSM within them. Hence there are two basic starting points that we can choose from here on: Either we start directly to build the MSSM with gauge group SU(3) × SU(2) × U(1) for example based on the polyhedron F_{11} or we try to start from an enhanced gauge group such as SU(5) that incorporate features such as gauge coupling unification.
We will focus completely on the second alternative, as we will review in the following. The unification of the MSSM into an SU(5) has the advantage that all MSSM physics is mostly constrained to the SU(5) divisor and gets broken via fluxes [103]. We will deal with these fluxes from a bottom up perspective and analyze the properties of the resulting low energy physics. To control dangerous operators of the low energy physics it is necessary to add additional symmetries, such as U(1)'s to control them but they also restrict the fluxes on the other hand and will strongly restrict the possible models.

In the following we will first introduce the concept of fluxes in four dimensions and introduce constraints from a bottom up perspective in section 7.1. In Section 7.2 we introduce all desirable and undesirable operators of the MSSM and review model building attempts and results in the past in particular in terms of the spectral cover. In section 7.3 we present our search strategy. In section 7.4 we present our results and compare our findings. There we present a specific Benchmark model that has phenomenologically appealing features. Finally we comment on open questions concerning our flux choices and other more general models in section 7.5.

7.1 Fluxes and their constraints

A flux can be thought of a field strength that is not living in the uncompactified dimension but is confined to live within the compactification space. Fluxes add numerous new effects: It adds an internal energy contribution that can be used to create a potential for moduli fields of the compactification and gives them masses in order to stabilize the geometry. Furthermore fluxes can be used to break supersymmetries and produce a chiral spectrum. In the perturbative Type IIB setting the fluxes are distinguished as the closed-string NSNS-RR fluxes given by the three-form $C_3 = f_3 - \tau H_3$ and the brane fluxes. However these two descent from the four-form flux G_4 in the M-theory picture. The G_4-flux can be decomposed

into

$$G_4 = f^i \wedge w_i + ... , \tag{7.1}$$

with w_i describing $(1,1)$ forms of the Shioda-maps or the Cartan divisors of non-Abelian groups and f^i parametrize the flux contribution. Note that there are also other flux contributions that come from *horizontal divisors* that are not very well understood. Switching on fluxes induces in general an additional energy contribution that has an upper bound by the geometry. This constraint is given by

$$\frac{\chi(Y_4)}{24} = N_{M_2} + \frac{1}{2}\int_{Y_4} G_4 \wedge G_4 \,, \tag{7.2}$$

with the number of $M2$ branes that are dual to $D3$ branes in the Type IIB picture however we will not worry here about this constraint. The main effect for us will be to take flux as a possibility to generate chirality. For this purpose we distinguish two kinds of fluxes in an SU(5) model with additional U(1) symmetries. First there is the GUT-*universal* flux along the U(1) directions that gives a chiral net number of **5** and **10**-plets. The second type of flux is switched on along the GUT-divisor in the hypercharge direction. This flux results in a splitting of the multiplets and a breaking of the SU(5) GUT symmetry down to that of the MSSM. The net-multiplicity of a given representation specified by the curve Σ is given by the following index theorem:

$$\chi(\mathbf{R}) = \int_\Sigma c_1\left(V_\Sigma \otimes L_Y^{Y_\mathbf{R}}\right) = \int_\Sigma \left[c_1(V_\Sigma) + \mathrm{rk}(V_\Sigma)\, c_1(L_Y^{Y_\mathbf{R}})\right], \tag{7.3}$$

where the bundle V_Σ accounts for the G_4 flux and L_Y is a line bundle used to specify the hypercharge flux and $Y_\mathbf{R}$ denotes the hypercharge carried by the representation $\mathbf{R}$. We can further split this equation down to

$$\chi(\mathbf{R}) = \underbrace{\int_\Sigma c_1(V_\Sigma)}_{\mathcal{M}_\Sigma} + Y_\mathbf{R} \underbrace{\left[\mathrm{rk}(V_\Sigma)\int_\Sigma \omega_Y\right]}_{\mathcal{N}_\Sigma}, \tag{7.4}$$

introducing the $(1,1)$-form $\omega_Y \sim c_1(L_Y)$. The flux quanta $\mathcal{M}$ are exactly those that account for the SU(5) universal chirality while the $\mathcal{N}$ quanta chirality splits the SU(5) multiplets by their $Y_\mathbf{R}$ charge. Computing the resulting chiralities for $\mathbf{10}_a$ and $\mathbf{5}_i$ matter curves we first use the redefinition of the fluxes according to

$$\begin{aligned} M_a &= \mathcal{M}_a + \frac{1}{6}\mathcal{N}_a \,, & M_i &= \mathcal{M}_i + \frac{1}{3}\mathcal{N}_i \,, \\ N_a &= \frac{5}{6}\mathcal{N}_a \,, & N_i &= -\frac{5}{6}\mathcal{N}_i \,. \end{aligned} \tag{7.5}$$

This results in chiralities of all representations to

$$\begin{aligned} \Sigma_{\mathbf{10}_a}: \quad & (\mathbf{3},\mathbf{2})_{1/6} \;:\; M_a \,, \\ & (\bar{\mathbf{3}},\mathbf{1})_{-2/3} \;:\; M_a - N_a \,, \\ & (\mathbf{1},\mathbf{1})_{1} \;:\; M_a + N_a \,, \end{aligned} \qquad \begin{aligned} \Sigma_{\bar{\mathbf{5}}_i}: \quad & (\bar{\mathbf{3}},\mathbf{1})_{1/3} \;:\; M_i \,, \\ & (\mathbf{1},\mathbf{2})_{-1/2} \;:\; M_i + N_i \,, \end{aligned} \tag{7.6}$$

where the split of the representations becomes obvious.
By considering the effects of fluxes on the above spectrum, it is clear that the U(1) symmetries we put the flux on will generically be anomalous. However in a consistent string compactification these anomalies

are taken care of by the Green-Schwartz mechanism coming from the F-theory Chern-Simons terms

$$\int_{Y_4} C_4 \wedge G_4 \wedge G_4 \,, \tag{7.7}$$

that can be evaluated in M-theory. The C_4 RR four-form is can be expanded as $C_4 = c_2^M \wedge \beta_M$ with $\beta_M \in H^2(B_3)$. These bulk modes know about the whole B_3 geometry. Expanding the above expression in the four dimensional parts we are left with terms of the form

$$\mathcal{L}_4 \equiv \Pi_M^i \int d^4x\, C_2^M \wedge F_i \,, \tag{7.8}$$

with the two form C_2 that can be dualized to the 4D axion that gives a Stückelberg mass term to the $\mathrm{U}(1)^{\mathrm{i}}$ and cancels the anomaly. The prefactor is given from the dimensional reduction as

$$\Pi_M^i = \int_{Y_4} \beta_M \wedge \omega^i \wedge c_1(V_j) \wedge \omega^j \,. \tag{7.9}$$

This Stückelberg massive U(1) however stays as a global symmetry and might still be used as a selection rule in the EFT that can forbid couplings. However the same argument applies for the hypercharge when we break with hypercharge flux. Hence we have to turn on a non-trivial flux but forbid the hypercharge mass term by ensuring that its prefactor $\Pi_M^Y = 0$. As the hypercharge flux is localized along S_{GUT} we then can re express the prefactor to

$$\Pi_M^Y \equiv \int_S c_1(L^Y) \wedge i^* \beta_M = 0 \quad \forall M \,, \tag{7.10}$$

with the β_M divisors pulled back on the GUT divisor. The topological constraint that guarantees the above relation is that the divisor $c_1(L)$ is non-trivial along the GUT brane but trivial in B_3. In homology this means that the dual two-cycle $[w^Y] \in H_2(S)$ becomes the bounds of a three-chain in $\Gamma \in C_3(B_3)$ with $\Gamma = \partial w^Y$. In particular finding geometries that satisfy that constrain is in particular hard.

Again from anomaly considerations, the above fluxes and in particular the hypercharge flux is constrained not to render any non-Abelian and hypercharge gauge factor anomalous. For the universal fluxes these constraints read

$$\sum_i M_i - \sum_a M_a = 0 \,. \tag{7.11}$$

This constraint requires to have the same amount of $\overline{\mathbf{5}}$ and $\mathbf{10}$ curves in order not to render the theory inconsistent already at the GUT level and is a reminiscent of D7 tadpole cancellation [104]. Similarly to all anomalies that involve SM gauge factors we get the constraint

$$\sum_i N_i = \sum_a N_a = 0 \,, \tag{7.12}$$

which can also be derived from the homology classes in the semi-local F-theory setting. In the same setting it was first observed by [91] and then proven by [90] that also the following constraints

$$\sum_a q_a^\alpha N_a + \sum_i q_i^\alpha N_i = 0 \,, \tag{7.13}$$

with the $\overline{\mathbf{5}}_a$ and $\mathbf{10}_i$ U(1) charges q_a and q_i respectively, have to hold by considering again classes of the matter curves. It was very satisfactory that the same constraint could be derived [105] from considering the anomalies of the type $G_{\mathrm{SU}(5)} - G_{\mathrm{SU}(5)} - \mathrm{U}(1)$ that should stay unaltered after hypercharge flux breaking.
However in [106] anomalies of the type $\mathrm{SU}(5) - \mathrm{U}(1)_\mathrm{A} - \mathrm{U}(1)_\mathrm{B}$ have been considered that have to vanish due to the tracelessness of the SU(5) generators. However the hypercharge anomaly gives the constraint $\mathrm{U}(1)_\mathrm{Y} - \mathrm{U}(1)_\mathrm{A} - \mathrm{U}(1)_\mathrm{B}$

$$3\sum_a q_a^\alpha q_a^\beta N_a + \sum_i q_i^\alpha q_i^\beta N_i = 0\,, \tag{7.14}$$

that does not have a counter-part on the homology classes of the curves. This equation puts another non-trivial constrained on the fluxes in particular with raising number of additional U(1) symmetries in the theory. Up to now it is not completely clear if Eq. (7.14) should be imposed or if it could be unequal to zero[1]. In the following we comment on the implementation of the this constraints in our model search.

7.2 Model building constraints and status quo

Having introduced all flux constraints that we want to impose on our models we go on and impose the phenomenological constraints that a viable model has to satisfy. In this regard we also comment on the search strategy that has been used in other model building attempts such as [91, 108, 109, 90].

In building SU(5) GUT theories we have to face the problem that in a minimal setup we have to make triplets that accompany the Higgs doublets in the same multiplet are projected while ensuring that the Higgses stay light. Hence we need very different mechanism to give masses to these states. This is achieved by breaking the GUT group via hypercharge flux; with this flux it is possible to project out the triplets in the Higgs multiplets as one see from equation (7.6).
Moreover we need to achieve a satisfactory operator structure: We have to allow for all relevant Yukawa couplings for the SM matter fields. On the other hand we also have to suppress dangerous operators which mediate fast proton decay which we want to do by the virtue of additional U(1) symmetries[2]. Let us start the discussion on F-theory model building by introducing the MSSM superpotential at the level of SU(5) up to dimension five

$$\begin{aligned}\mathcal{W} = \;& \mu \mathbf{5}_{H_u}\overline{\mathbf{5}}_{H_d} + \beta_i \overline{\mathbf{5}}_i \mathbf{5}_{H_u} \\ & + Y^u_{ij}\mathbf{10}_i\mathbf{10}_j\mathbf{5}_{H_u} + Y^d_{ij}\overline{\mathbf{5}}_i\mathbf{10}_j\overline{\mathbf{5}}_{H_d} + W_{ij}\overline{\mathbf{5}}_i\overline{\mathbf{5}}_j\mathbf{5}_{H_u}\mathbf{5}_{H_u} \\ & + \lambda_{ijk}\overline{\mathbf{5}}_i\overline{\mathbf{5}}_j\mathbf{10}_k + \delta_{ijk}\mathbf{10}_i\mathbf{10}_j\mathbf{10}_k\overline{\mathbf{5}}_{H_d} + \gamma_i\overline{\mathbf{5}}_i\overline{\mathbf{5}}_{H_d}\mathbf{5}_{H_u}\mathbf{5}_{H_u} \\ & + \omega_{ijkl}\mathbf{10}_i\mathbf{10}_j\mathbf{10}_k\overline{\mathbf{5}}_l\,,\end{aligned} \tag{7.15}$$

in which the representations $\overline{\mathbf{5}}_i$ and $\mathbf{10}_i$ correspond to the i-th family and $\mathbf{5}_{H_u}$, $\overline{\mathbf{5}}_{H_d}$ are the SU(5) multiplets giving rise to the up- and down-type Higgs respectively. The operators in the first line of (7.15) are those leading to the μ-term and the bilinears between H_u and the lepton doublets. In the second line we have the Yukawa couplings $Y^{u,d}_{ij}$ and the Weinberg operator W_{ij}. R-parity violating dimension four and five

[1] Inspired from the Type IIB setting, there are proposals that could realize a cancellation by the orientifold-odd axion, however the F-theory uplift of that mechanism is unknown yet [107].
[2] Note that we could also control couplings by trying to *geometrically* suppress them when we go to a special point in the complex structure space of the full geometry.

operators are given in the third line, whereas the R-parity allowed dimension five operator (that leads to proton decay) is given in the fourth line. We also have dangerous proton decay operators arising from the Kähler potential [110], namely

$$\mathcal{K} \supset \kappa_{ijk}\mathbf{10}_i\mathbf{10}_j\mathbf{5}_k + \bar{\kappa}_i\bar{\mathbf{5}}_{H_u}\bar{\mathbf{5}}_{H_d}\mathbf{10}_i\,. \tag{7.16}$$

For a phenomenological relevant model we need to ensure that that all dangerous couplings in superpotential and Kähler potential as well as the μ-term are forbidden by U(1) symmetries. It is also desired that the top-quark Yukawa coupling is generated at tree level (i.e. allowed by all U(1) symmetries). These U(1) symmetries are typically GS massive such that the gauge particles do not appear but the U(1) symmetry stays as a global symmetry of the EFT. But in addition these U(1) symmetries can be broken for example by singlet VEVs i.e. see chapter 6 or by instanton effects [111]. Independent of the breaking of the U(1) symmetries, discrete remnants can survive and act as discrete symmetries in the EFT.
The crucial property is the difference in the U(1) charges for desired and undesired couplings. The breakdown of these U(1) symmetries has been used to realize a Froggatt–Nielsen (FN) type explanation [54] of the flavor structure in the quark and lepton sector.

Previous searches for models in the spectral cover constructions have been based on the idea that the three families arise from complete SU(5) representations (i.e. from curves on which the hypercharge flux acts trivially). In addition to that one has two further **5**-curves on which the hypercharge flux acts by projecting out the triplet components so that one ends up with only one pair of doublets (namely the Higgses). The couplings of the fields are determined by the extra U(1) symmetries and additional singlet fields that obtain a VEV in the spirit of FN, as described in the previous paragraph.

This strategy is realized by choosing a given split that fixes that matter charges and then distribute the flux quanta respecting the constraints (7.11)-(7.13). However these constraints, even without including (7.14), are far from trivial and the following observations have been made:

- If one insists on the exact MSSM spectrum, there is only one flavor-blind U(1) symmetry available. This symmetry corresponds to a linear combination of hypercharge and $U(1)_{B-L}$. As it allows for a μ-term as well as dimension five proton decay [90], this construction is not suitable for phenomenology.

- If one requires the presence of a U(1) symmetry which explicitly forbids the μ-term, i.e. a so-called Peccei–Quinn (PQ) symmetry, this implies the existence of exotic fields which are vector-like under the Standard Model gauge group and come as incomplete representations of the underlying SU(5) [108].

These observations suggest a strong tension between a solution to the μ-problem and the absence of light exotics in the spectrum. As already mentioned, in these models the matter arise from SU(5) representations which are not split by hypercharge flux.

However in those approaches the possibility of having split families that come from different curves has not been considered and if exotics and the above mentioned tension can be avoided.
In the following we adopt that approach and compare the results in models derived from the spectral cover and those derived from SU(5) *tops*.

7.3 Search Strategy

In order to search for models that have the chance of being of phenomenological relevance we apply the following strategy: We choose a given model that has at most two additional U(1) gauge factors in addition to the SU(5) from the available spectral cover models or from the ones with rational U(1)'s. We then distribute the GUT universal fluxes to be of the form

$$\sum_{\Sigma_{\mathbf{10}}} M^a = \sum_{\Sigma_{\bar{\mathbf{5}}}} M^i = 3 \quad \text{with} \quad M^a\,,\, M^i \geq 0\,. \tag{7.17}$$

as well as

$$\sum_{\Sigma_{\mathbf{10}}} N^a = 0 \quad \text{with} \quad -M^a \leq N^a \leq M^a\,, \tag{7.18}$$

$$\sum_{\Sigma_{\bar{\mathbf{5}}}} N^i = 0 \quad \text{with} \quad -M^i - 1 \leq N^i \leq 3\,, \tag{7.19}$$

that guarantees three chiral families and automatically satisfies the anomaly constraints (7.11) and (7.12). The additional flux constraint

$$\sum_{\Sigma_{\bar{\mathbf{5}}}} |M^i + N^i| = 5\,, \tag{7.20}$$

guarantees three lepton doublets together with **exactly one pair of Higgses**. The above constraints can be seen as constraints that restrict the length of the integral flux vectors and hence give a bound on the total amount of models such that we can perform an exhaustive scan. At last we check that the hypercharge flux satisfies the constraint (7.13). We do not take (7.14) into account at this point as it is not directly visible in the spectral cover. Moreover we argue in section 7.5 that imposing this constraint (7.14) does not allow for non-trivial flux solutions.
Imposing the above flux constraints fix the matter content to that of the MSSM, up to total MSSM gauge singlets and possible additional U(1) vectors that we expect to become GS-massive. Having fixed the spectrum we can turn to the operator structure.
We have to make sure that all dangerous operators are forbidden by virtue of some U(1) symmetry. As we are dealing with incomplete GUT multiplets we cannot use the SU(5) GUT structure to check all operators but have to do this at the level of the MSSM instead: At first we demand a heavy top quark by requiring a top quark Yukawa coupling

$$\mathbf{10}_i \mathbf{10}_j \mathbf{5}_{H_u} \supset Q_i \bar{u}_j H_u\,, \tag{7.21}$$

to be allowed by all U(1) symmetries and this its presence at tree level. In the case where all Q_i and $\bar{u}_j$ descend from only one **10**-curve the up-quark Yukawa matrix is of rank one. Nevertheless, this matrix can acquire full rank when appropriate flux or non-commutative deformations [112, 113] away from the E_6 Yukawa point are included.

In order for low energy SUSY to **solve the μ-problem** we require the μ-term

$$\mu \mathbf{5}_{H_u} \bar{\mathbf{5}}_{H_d} \supset \mu H_d H_u \tag{7.22}$$

to be forbidden by any of the U(1) symmetries. The above coupling will be generated upon breakdown of these symmetries. Let us also remark that in addition to the expected suppression in the couplings

due to singlet VEVs (or instantons) some additional suppression is expected when the couplings arise from the Kähler potential. This fact is particularly appealing for the generation of the μ-term as it can be sufficiently small, if induced from the Kähler potential along the lines of the so-called Giudice-Masiero (GM) mechanism [114].

In order to **avoid fast proton decay**, the U(1) symmetries must also forbid the following superpotential and Kähler potential couplings:

$$\begin{array}{lll}
\beta_i & \bar{\mathbf{5}}_i \mathbf{5}_{H_u} & \supset \beta_i L_i H_u \,, \\
\lambda_{ijk} \bar{\mathbf{5}}_i \bar{\mathbf{5}}_j \mathbf{10}_k & \supset \lambda^0_{ijk} L_i L_j \bar{e}_k + \lambda^1_{ijk} \bar{d}_i L_j Q_k + \lambda^2_{ijk} \bar{d}_i \bar{d}_j \bar{u}_k \,, \\
\delta_{ijk} \mathbf{10}_i \mathbf{10}_j \mathbf{10}_k \bar{\mathbf{5}}_{H_d} & \supset \delta^1_{ijk} Q_i Q_j Q_k H_d + \delta^1_{ijk} Q_i \bar{u}_j \bar{e}_k H_d \,, \\
\gamma_i & \bar{\mathbf{5}}_i \bar{\mathbf{5}}_{H_d} \mathbf{5}_{H_u} \mathbf{5}_{H_u} & \supset \gamma_i L_i H_d H_u H_u \,, \\
\kappa_{ijk} \mathbf{10}_i \mathbf{10}_j \mathbf{5}_k & \supset \kappa^1_{ijk} Q_i \bar{u}_j \bar{L}_k + \kappa^2_{ijk} \bar{e}_i \bar{u}_j d_k + \kappa^3_{ijk} Q_i Q_j d_k \,, \\
\bar{\kappa}_i & \bar{\mathbf{5}}_{H_u} \bar{\mathbf{5}}_{H_d} \mathbf{10}_i & \supset \bar{\kappa}^1_i H^*_u H_d \bar{e}_i \,.
\end{array} \tag{7.23}$$

For a consistent model we need to require that upon breakdown of the U(1) symmetries these operators are not generated. This is for example achieved by demanding the presence of an effective matter parity symmetry.
At next we have to decompose the dimension five proton decay inducing operators and check for their absence individually:

$$\omega_{ijkl} \mathbf{10}_i \mathbf{10}_j \mathbf{10}_k \bar{\mathbf{5}}_l \supset \omega^1_{ijkl} Q_i Q_j Q_k L_l + \omega^2_{ijkl} \bar{u}_i \bar{u}_j \bar{e}_k \bar{d}_l + \omega^3_{ijkl} Q_i \bar{u}_j \bar{e}_k L_l \,. \tag{7.24}$$

We demand these operators to be forbidden by the U(1) charges, keeping in mind that they can be generated in a similar fashion as the μ-term. We also expect that while the operators in (7.23) remain absent, it is possible to generate **full rank Yukawa matrices**[3]

$$\mathcal{W} \subset Y^u_{i,j} Q_i \bar{u}_j H_u + Y^d_{i,j} \bar{u}_i \bar{d}_j H_d + Y^L_{i,j} \bar{e}_i \bar{L}_j H_d \,. \tag{7.25}$$

This necessarily implies that the charges of the desired operators must differ in comparison to the undesired ones. As a consequence, one observes that the field H_d has to come from a different curve than all the other leptons and triplets to guarantee that dimension four operators (such as λ^0 and λ^1 in (7.23)) are not introduced together with the Yukawa entries.

7.4 Results of the scan

We split up the general results into the models within the spectral cover and those obtained from the *tops*. Within the spectral cover models we find that the flux restrictions of having only the MSSM spectrum an no other leptons coming from the H_d curve restricts the overall amount of models to only six models, all descending from the $2+2+1$ split. All these models have phenomenological unappealing features. We give one example model with the flux restrictions on the curves given in Table 7.1. This model suffers of the following structure of operator charges:

$$q(Q_2 \bar{u}_2 H_u) = q(H_u H_d) = q(Q_1 \bar{d}_1 L_i) = q(\bar{u}_1 \bar{u}_1 \bar{d}_k) = (-5, -5) \,. \tag{7.26}$$

[3] Recall that, as the matter fields need not to arise from complete SU(5) multiplets, so that the down and lepton Yukawas do not necessarily coincide.

Curve	q_1	q_2	M	N	Matter
$\mathbf{10}_1$	1	5	2	1	$Q_{1,2} + \bar{u}_1 + \bar{e}_{1,2,3}$
$\mathbf{10}_5$	−4	0	1	-1	$Q_3 + \bar{u}_{2,3}$
$\overline{\mathbf{5}}_{11}$	2	10	0	-1	H_u^c
$\overline{\mathbf{5}}_{15}$	−3	5	0	1	H_d
$\overline{\mathbf{5}}_{35}$	−3	−5	3	0	$(L + \bar{d})_{1,2,3}$

Table 7.1: Spectral cover model and its corresponding flux quanta along the different matter curves in the 2+2+1 splitting. The lower indices of the matter representations are family indices.

It is a notorious feature of these models that operators of competing relevance have the same charge. As we do not know of any mechanism at this point to generate a hierarchy among the above operators, we have to assume that the Yukawa coupling is generated at the same strength a the dimension four proton decay inducing operator. Even worse, we find that the μ term is generated as well.

At next we focus on the models obtained from the SU(5) *tops* given in table 5.6 and repeat the same strategy. Before we present our findings we focus on the particular feature that we have only one **10** curve in these models. It follows from (7.11) and (7.12) that there can be no flux put along these curves and the whole SU(5) structure is maintained for these curves. Furthermore, all three families come from the same **10** curve and hence have the same U(1) charge.
This structure allows us to relate the charges of all relevant operators presented above: First of all, the presence of a tree level top Yukawa fixes the H_u charge to be

$$q(H_u) = -2q(\mathbf{10})\,. \tag{7.27}$$

For the subsequent discussion, we introduce the following notation for the charges of the operators:

$$\begin{aligned} \mu &: q(H_d H_u) = q(H_d) + q(H_u) := q^{\mu}\,, \\ Y^L &: q(\bar{e} H_d L_i) := q^{Y^L_i}\,, \\ Y^d &: q(\bar{u} H_d \bar{d}_i) := q^{Y^d_i}\,, \\ \beta_i &: q(L_i H_u) = q(L_i) + q(H_u) := q^{\beta_j}\,. \end{aligned} \tag{7.28}$$

Among these operators, all but the β_i terms should be induced upon breakdown of the U(1) symmetries. Now we can express the charges of all unwanted operators in terms of the charges defined above. The dangerous dimension four proton decay operators are:

$$\begin{aligned} \lambda^0_{ij} &: q(Q\bar{d}_i L_j) = q^{Y^d_i} + q(H_d) - q(L_j) = q^{Y^d_i} + q^{\mu} - q^{\beta_j} \\ \lambda^1_{ij} &: q(\bar{e} L_i L_j) = q^{Y^L_i} + q(H_d) - q(L_j) = q^{Y^L_i} + q^{\mu} - q^{\beta_j} \\ \lambda^2_{ij} &: q(\bar{u}\bar{d}_i\bar{d}_j) = q^{Y^d_i} + q(H_d) - q(\bar{d}_j) = q^{Y^d_i} + q^{\mu} - q(H_u) - q(\bar{d}_j)\,. \end{aligned} \tag{7.29}$$

Since we want to generate the down-type Yukawa matrices, we see that the previous couplings are only forbidden due to the charge difference between the H_d - and L_j -curves in the case of the λ^0_{ij} and λ^1_{ij} couplings, and due to the charge difference between H_d - and $\bar{d}_j$ -curves in the case of the λ^2_{ij}. Thus, as already pointed out, it is necessary that the $\mathbf{5}_{H_d}$ -curve contains only the down-type Higgs, since any lepton or down-type quark with identical charge will automatically induce a dangerous operator. As we

want to induce the μ-term as well we observe that no $\bar{d}_i$ field can arise from the H_u-curve either.[4]
In general we can write the charges in terms of the β_i operators that clarifies the overall structure even more. Thus, if we find a configuration such that the Yukawa couplings and the μ-term is induced but the β_i-terms stay forbidden, the dimension four operators stay forbidden as well. Furthermore, we observe that the dimension five operators in the superpotential

$$\begin{aligned} \omega_i^1\,,\omega_i^3 \;:&\quad q(QQQL_i) = q(Q\bar{u}\bar{e}L_i) = -q^\mu + q^{Y_i^L} := q(\mathbf{10}\,\mathbf{10}\,\mathbf{10}\,L_i)\,, \\ \omega_i^2 \;:&\quad q(QQ\bar{u}\bar{d}_i) \;=\; q(\bar{u}\bar{u}\bar{e}\bar{d}_i) \;= -q^\mu + q^{Y_i^d} := q(\mathbf{10}\,\mathbf{10}\,\mathbf{10}\,\bar{d}_i)\,, \end{aligned} \tag{7.30}$$

will unavoidably be induced together with the Yukawa couplings and the μ-term. It should be noted that the μ-term charge enters with a minus sign in the previous equations. This implies that the mechanism (such as a singlet VEV) which induces the ω^i-terms in the superpotential will not induce the μ-term directly in the superpotential but can generate it from the Kähler potential after SUSY breakdown. Note also that it is possible to induce a Weinberg operator

$$W_{ij}: \quad q(L_iL_jH_uH_u) = q^{\beta_i} + q^{\beta_j} \tag{7.31}$$

without inducing the β_i-terms by using, for example, singlet VEVs with charge $q(s_i) = -2q^{\beta_i}$ which implies at least a remnant $\mathbb{Z}_{2N}$ symmetry in the VEV configuration.

In a similar fashion, we observe that the operators

$$\begin{aligned} \delta^1\,,\delta^2: &\quad q(QQQH_d) \;= q(Q\bar{u}\bar{e}H_d) = -q^{\beta_i} + q^{Y_i^L}\,, \\ \gamma_i: &\; q(L_iH_dH_uH_u) = q^\mu + q^{\beta_i}\,, \end{aligned} \tag{7.32}$$

will remain absent as long as the β_i-terms are not induced. The same holds for the Kähler potential terms

$$\begin{aligned} \kappa_i^1: &\quad q(Q\bar{u}L_i^*) \;= -q^{\beta_i}\,, \\ \bar{\kappa}: &\; q(\bar{e}H_u^*H_d) = q^\mu + q^{\beta_i}\,, \end{aligned} \tag{7.33}$$

with the exception of

$$\kappa_i^2\,,\kappa_i^3: \; q(QQ\bar{d}_i^*) = q(\bar{u}\bar{e}\bar{d}_i^*) = -q(H_u) - q(\bar{d}_j) = -q^\mu + q(H_d) - q(\bar{d}_i) := q(\mathbf{10}\,\mathbf{10}\,\bar{d}_i^*)\,, \tag{7.34}$$

for which one has to ensure that no triplets emerge from the Higgs curves as a necessary (but not sufficient) condition. Note that the above observations are independent of the number of **5**-curves and U(1) symmetries. However, there remains a crucial interplay between the Higgs charges compared to those of the down-type quarks and those of the singlet fields which have to be checked on a case by case analysis. Within the four tops and for all flux configurations, we find only four models that are based on $\tau_{5,1}$ and $\tau_{5,2}$ that meet all our phenomenological criteria. We summarize the details of one model that we call Benchmark model A in Table 7.2. There we summarize spectrum as well as the charge of all relevant operators. We indeed see, that many operators are forbidden as long as the β^i terms are not induced. We find, that the singlet s_1 induces the μ-term from the Kähler potential and induces all Yukawa couplings but also dimension five proton decay inducing operators, while dimension four

[4] Note that if H_u and $\bar{d}_j$ come from the same curve their U(1) charges carry opposite signs.

1. Spectrum

Curve	q_1	q_2	M	N	Matter
10	-1	2	3	0	$(Q+\bar{u}+\bar{e})_{1,2,3}$
$\bar{\mathbf{5}}_1$	3	-1	1	-1	$\bar{d}_1$
$\bar{\mathbf{5}}_2$	-2	4	0	-1	H_u
$\bar{\mathbf{5}}_4$	3	4	2	1	$L_{1,2,3}+\bar{d}_{2,3}$
$\bar{\mathbf{5}}_5$	-2	-1	0	1	H_d

2. Singlet VEVs: s_1 , a

$$q(s_1) = (0,-5)\,, \quad q(a) = (10,0)\,.$$

3. μ- and β_i-terms

$$q(H_u\bar{L}_i) = (5,0)\,, \quad q(H_uH_d) = (0,-5)\,.$$

4. Yukawa couplings

$$q(Q_i\bar{u}_jH_u) = (0,0)\,, \qquad q(Q_i\bar{d}_jH_d) = \begin{pmatrix}(0,0)\\(0,5)\\(0,5)\end{pmatrix}_j\,, \qquad q(\bar{e}_iL_jH_d) = (0,5)\,.$$

5. Allowed dimension five proton decay and Weinberg operators

$$q(\mathbf{10\,10\,10}\,L_i) = (0,10)\,, \qquad q(\mathbf{10\,10\,10}\,\bar{d}_i) = \begin{pmatrix}(0,5)\\(0,10)\\(0,10)\end{pmatrix}_j\,, \qquad q(L_i\,L_j\,H_u\,H_u) = (10,0)\,.$$

6. Forbidden operators

$$q(\bar{u}\bar{d}_i\bar{d}_j) = \begin{pmatrix}(5,0) & (5,0) & (5,0)\\(5,0) & (5,10) & (5,10)\\(5,0) & (5,10) & (5,10)\end{pmatrix}_{i,j}\,, \qquad q(\mathbf{10\,10}\,\bar{d}_i^*) = \begin{pmatrix}(-5,5)\\(-5,0)\\(-5,0)\end{pmatrix}.$$

Table 7.2: Details of benchmark model A. We give the charges of all relevant operators and VEV fields.

operators stay forbidden. The orders of magnitude for these couplings are

$$\begin{aligned} Y_i^L &\sim \frac{\langle s_1\rangle}{\Lambda}\,, & Y_i^d &\sim \delta_{1,i} + \frac{\langle s_1\rangle}{\Lambda}(\delta_{2,i}+\delta_{3,i})\,, \\ \omega_i^1\,, \omega_i^3 &\sim \frac{\langle s_1\rangle^2}{\Lambda^3}\,, & \omega_i^2 &\sim \frac{\langle s_1\rangle}{\Lambda^2}\delta_{1,i} + \frac{\langle s_1\rangle^2}{\Lambda^3}(\delta_{2,i}+\delta_{3,i})\,, \end{aligned} \tag{7.35}$$

where Λ is the appropriate cutoff scale which depends on the global embedding of the local model. Similarly as in [115] the only severely constrained comes the coefficients of the corresponding operators

$$\omega^1 \lesssim \frac{10^{-7}}{M_{\rm P}} \text{ and } \omega^2 \lesssim \frac{10^{-7}}{M_{\rm P}}\,. \tag{7.36}$$

All other operators that are induced stay unproblematic as long as no λ^i-terms are generated. The coupling ω^2 only leads to a constraint if there is a non-diagonal degeneracy of quark and squark masses. The ω^1-operator however, puts constraints on the size of the singlet VEV of s_1 that induces the operator after two insertions, to be

$$\frac{\langle s_1\rangle^2}{\Lambda^3} \lesssim \frac{10^{-7}}{M_{\rm P}}\,. \tag{7.37}$$

Such a size of the VEV seems compatible with down-quark and lepton-Yukawa couplings at the weak scale.

As mentioned before, it is possible to generate the Weinberg operator while keeping dangerous operators forbidden. In the matter spectrum of F_5 there exists no singlet with charge $(\pm 10, 0)$ whose VEV can introduce that operator. However, one might envision a non-perturbative effect (e.g. via instantons) which allows to generate this coupling. Note again that such an instanton resembles the effect of a singlet VEV and we will parametrize it by $\langle a\rangle$ such that the operator is introduced by[5]

$$W_{ij} \sim \frac{\langle a\rangle}{\Lambda^2}\,. \tag{7.38}$$

Another interesting question is which symmetries remain after the U(1) symmetries are broken. For this purpose it is more convenient to rotate the U(1) generators as specified in Table 7.3. There we see that after appropriate normalization, the charges of the singlet s_1 breaks the U(1) symmetry to a $\mathbb{Z}_2$ subgroup under which the charges q_1' coincide with those of R-parity. On the other hand, we see that the second U(1) with charges q_2' gets broken completely.

7.5 Anomaly constraints and models beyond toric constructions

In the previous section we have imposed only the constraints (7.11)-(7.13) but not (7.14). When we consider the rational section models, we actually note from a simple parameter counting argument, that it is not possible to satisfy all constraints simultaneously: The constraints (7.12)-(7.14) do in total give six linear constraints on the hypercharge flux quanta. Each curve contributes an degree of freedom. However in the rational section models we have only six curves and hence we find six constraints that have to be obeyed by the fluxes on the six curves. This equation can only be solved by putting a trivial flux onto the curves i.e. a non-trivial solution is not possible.

[5] Note that the expected order of magnitude for this operator is the same for all generations as all lepton doublets in this model are found to arise from the same matter curve.

	$(Q+\bar{u}+\bar{e})_{1,2,3}$	$\bar{d}_1$	H_u	$L_{1,2,3}+\bar{d}_{2,3}$	H_d	s_1	a
q_1	-1	3	2	3	-2	0	-10
q_2	2	-1	-4	4	-1	-5	0
$q_1' = (q_1 - 2q_2)/5$	-1	1	2	-1	0	2	-2
$q_2' = (2q_1 + q_1)/5$	0	1	0	2	-1	-1	-4

Table 7.3: The U(1) charges for the benchmark model in a rotated U(1) basis. After giving a VEV the charges q_1' are those of matter parity and the second U(1) with charges q_2' is broken completely.

This leaves the question on whether hypercharge flux breaking is possible in the rational section models and if the third constraint Eq. (7.14) should indeed be imposed. The best way to answer these questions is to engineer a full global geometry with a better understanding of G_4 fluxes.
As a last side remark we note that more curves give indeed more flexibility to solve for the aforementioned constraints. Hence we performed scan with more **5** curves and more diverse charges but following the charge split patterns we observed for the rational sections i.e.

$$q_{1,\bar{\mathbf{5}}} = Q_{1,\bar{\mathbf{5}}} + 5\,n_{1,i}\,, \quad q_{2,\bar{\mathbf{5}}} = Q_{2,\bar{\mathbf{5}}} + 5\,n_{2,i}\,, \tag{7.39}$$

where $Q_{1,\bar{\mathbf{5}}}$ and $Q_{2,\bar{\mathbf{5}}}$ are fixed by the splitting that is chosen for each U(1). The integer valued $n_{1,i}, n_{2,i}$ are in the range

$$n_{1,i}\,, n_{2,i} \in [-2, 2]\ . \tag{7.40}$$

The charge of the **10**-curve is chosen such that it fits the structure of a given split, see Table 5.5. The flux distribution and the search strategy in this case follows the one described in section 7.3. We find $\mathcal{O}(10^3)$ models that can solve for all anomaly constraints and especially (7.14). The models share very similar operator patterns as in the Benchmark Model A. We present a model and its features in Table **??** of Appendix **??**. Again the global construction of these charges and splits are left for future research. However we note that in [97] more general SU(5) models with two U(1) symmetries and more matter curves have been recently been constructed.

CHAPTER 8

Conclusions

O glücklich, wer noch hoffen kann,
aus diesem Meer des Irrtums aufzutauchen!
Was man nicht weiß, das eben brauchte man,
und was man weiß, kann man nicht brauchen.

-J.W. von Goethe, Faust

In this work we have considered particle physics and their phenomenological applications within two patches of the M-theory star: Once within the perturbative $E_8 \times E_8$ heterotic string and within F-theory. In both cases we have considered compactifications on singular spaces that were orbifolds and Landau-Ginzburg orbifolds on the heterotic side as well as in singular elliptic fibrations on the F-theory side. We have analyzed the theories on those singular spaces and generically found that they lead to enhanced symmetries within the effective theories. In both patches of string theory we have investigated the origin of symmetries and their breakdown throughout various phases. This general strategy provides us with new techniques to uncover symmetries and their breakdown to discrete subgroups.
Turning to the phenomenological relevance of string model building we investigate in both approaches the chances to construct the supersymmetric extension of the standard model and its embedding into a grand unified group. Here a mayor guideline was provided by the underlying higher gauge structures as well as additional symmetries to control unwanted proton decay inducing operators.

One main result of this work is the construction of $\mathbb{Z}_3$ orbifold geometries and all of its symmetries via the mirror of a Landau-Ginzburg orbifold that we have presented in Chapter 4. Here we have provided a method to obtain all discrete R-and non-R symmetries fully in terms of the world sheet fields. Using Mirror-symmetry we provide a way to keep track of all symmetries and their breakdown. In this way we propose a novel way to calculate the symmetries for non-factorizable orbifold geometries as well as geometries with freely acting involutions that extend also to the smooth Calabi-Yau phase. Having full control over all 4D symmetries enables us to match the deformation to the Higgs mechanism in 4D where the geometric Kähler moduli appear as the VEV of charged fields. This implies a chance to obtain all superpotential couplings and their Kähler moduli corrections at the orbifold point or in fully smooth phases in the spirit of the Frogatt-Nielsen mechanism. In addition we classified all A_1^9 Gepner models and constructed the full massless spectrum for the first time and observed an intriguing relation satisfied by all models.

Another main result of this work is the establishment of the network that is spanned by F-theory compactifications where the elliptic curve is constructed as a hypersurface in one of the 16 2D reflexive polyhedra. We have discussed a sub branch of the network in chapter 6 and revealed models with novel features. We provide a complete and fully consistent analysis of F-theory on all of those spaces and worked out a detailed match of geometric and field theoretic transitions in terms of the Higgs mechanism. In a concrete example we have exemplified that matching and highlighted additional geometric constraints that can be interpreted as D-flatness of the VEV configuration in the six dimensional SUGRA. The compactifications we have considered might not only be a good starting point for future model building by engineering additional gauge symmetries using *top*s but provide new conceptual features themselves: We have found the first example of a non-toric rational section that leads to matter that carries three charge quanta under a U(1) gauge symmetry. Moreover we provide explicit examples of discrete symmetries in F-theory appearing in fibrations without a section. In those cases we have computed matter charges geometrically and have established their interpretation as a discrete symmetry. Moreover we give additional examples of discrete symmetries together with U(1) gauge factors.
Finally we have observed that the overall structure of the network is beautifully mirror-symmetric and possesses some remarkable features. The most important observation is that quotient group factors are mirror-dual to discrete symmetries, an observation that was also made in more general constructions [98]. Throughout chapter 5 we clarified our methods along a specific example that yields the exact gauge and matter representations of the MSSM as a byproduct.

In addition to the conceptual advancements we made progress in the phenomenological application of string theory both within the heterotic string and F-theory. At first we have provided a systematic approach to heterotic model building within the $\mathbb{Z}_2 \times \mathbb{Z}_4$ orbifold geometry in chapter 3. Here we provided a complete and systematic way to construct the gauge embeddings. Furthermore we have worked out a general dictionary of where the MSSM matter families should be localized in the extra dimensional space to provide phenomenological viable features which we exemplified within a toy model. In this way we conjectured that the $\mathbb{Z}_2 \times \mathbb{Z}_4$ geometry is an extensive addition to the heterotic Mini-Landscape of MSSM-like models which indeed has been confirmed in greater computer based searches later on [52, 53] as well as in non-supersymmetric string searches [53].

Another result of this work is the exploration of realistic MSSM like models arising from F-theory presented in chapter 7. Those models are constructed from newly realized $SU(5) \times U(1)^2$ models based on *tops* in which we have analyzed the potential for realistic particle physics. After having imposed hypercharge flux breaking of SU(5) down to the MSSM we have found models that exhibit the exact MSSM matter content. We avoided the doublet-triplet splitting problem, have no μ-term as well as a viable Yukawa structure without dimension four proton decay inducing operators thanks to an R-parity. Furthermore we have analyzed all dimension five proton decay inducing operators that can can be suppressed sufficiently in our VEV configuration. Although the mechanism of hypercharge flux breaking is not fully understood in a global model we have shown the phenomenological potential of the SU(5) *top* constructions in F-theory.

Many of these results are subject of further investigation but provide also starting points for other future projects: First there is the exciting mirror observation in F-theory that relates quotient group factors with discrete symmetries. The mirror observation might give us a handle to investigate even more generalized discrete group structures. In this regard there is a very relevant question: What is the maximal degree of a discrete symmetry in F-theory and connected to this what the maximal U(1) charge there

can be. As there is already the Kodaira classification for non-Abelian groups it would be desirable to have something similar for U(1) groups and charges to complete the model building catalog.
As we have seen this question might be strongly connected to mirror-symmetry in the fiber. As there exists a classification for Mordell-Weil torsion, it might be possible to obtain the highest possible discrete symmetry be considering the mirror dual curve to it. Furthermore we have seen the natural appearance of non-Abelian discrete gauge symmetries in heterotic orbifolds. Hence it is natural to ask how these could arise in the F-theory context by using the heterotic duality or by trying to engineer them via fibrations with discrete groups and additional monodromies.
All of these ideas described above are relevant for F-theory model building to get interactions and gauge groups in a realistic shape. Particularly it would be desirable to find a discrete $\mathbb{Z}_6$ symmetry that can play the role of proton hexality [116] in the MSSM. But even more important for phenomenology are the effects of fluxes and in particular the hypercharge breaking that is still poorly understood. Here a clarification could help deducing the possibility to realize our models in a global completion. Furthermore the effects of fluxes combined with discrete symmetries that could have relaxed anomaly constraints might be an interesting example to consider.

In the heterotic context the use of mirror symmetry at the LGO point is a promising starting point to consider more discrete symmetries in various phases. Here we hope to get some insight into the behavior of R-symmetries on non-factorizable lattices together with freely acting involutions that are setups hard to understand within available CFT techniques. Especially the orbifold models in [42] relied on a freely acting involution and the existence of an R-symmetry there is not fully understood.
Furthermore we have full control over the whole massless spectrum and its symmetries that we can extend to other phases as well. Hence it would be intriguing to find an LGO that can be deformed to a smooth Calabi-Yau with an unbroken R-symmetry.
As another project for future directions it would be desirable to extend the LGO description to more than $\mathbb{Z}_3$ orbifold factors as well as to (0,2) models and explore various other phases. Finally it would be fascinating to explain the observed relation satisfied by all 152 LGO models. This relation hints at a common moduli space of all these models and hence might be a way to explain supersymmetry breaking from a world sheet perspective.

APPENDIX A

$\mathbb{Z}_2 \times \mathbb{Z}_4$ flavor representations

In this appendix we summarize the representation of twisted sector fields under the flavor group

$$G_{\text{Flavor}} = \frac{D_4^4 \times \mathbb{Z}_4}{\mathbb{Z}_2^4} \,. \tag{A.1}$$

- The bulk states are all flavor singlets: (A_1, A_1, A_1, A_1)
- For $T_{(0,1)}$ and $T_{(1,3)}$ the four fixed points form states transforming as $(A_1, A_1, D, D)_1$ and $(A_1, A_1, D, D)_3$
- For $T_{(0,2)}$ We have a splitting of the representations unlike in the sectors before. States transform as $(A_1, A_1, A_i, A_j)_2$ with $i, j = 1, 2, 3, 4$. However, states in the ordinary states have $i, j = 1, 2$ but for states at the special fixed points we have six possibilities. These states are exactly those, that transform non-trivially under the $\mathbb{Z}_4$ space group element such as A_4. However note that a state experiences also an gauge twist under the $\mathbb{Z}_4$ twisting. Hence only this information can decide if states transform in the even

  $$\begin{aligned} &(A_1, A_1, A_1, A_3)_2, \quad (A_1, A_1, A_2, A_3)_2, \quad (A_1, A_1, A_3, A_3)_2, \\ &(A_1, A_1, A_3, A_1)_2, \quad (A_1, A_1, A_3, A_2)_2, \quad (A_1, A_1, A_4, A_4)_2, \end{aligned}$$

  or odd

  $$\begin{aligned} &(A_1, A_1, A_1, A_4)_2, \quad (A_1, A_1, A_2, A_4)_2, \quad (A_1, A_1, A_3, A_4)_2, \\ &(A_1, A_1, A_4, A_1)_2, \quad (A_1, A_1, A_4, A_2)_2, \quad (A_1, A_1, A_4, A_3)_2, \end{aligned}$$

  flavor representations.
- For $T_{(1,0)}$ states at ordinary fixed tori transform as $(D, D, A_i, A_1)_0$ $i = 1, 2$ and at the special ones we have either $(D, D, A_3, A_1)_0$ for even or $(D, D, A_4, A_1)_0$ again fixed by the gauge transformation.
- A similar situation occurs in the $T_{(1,2)}$, where ordinary tori transform according to $(D, D, A_1, A_i)_0$ $i = 1, 2$. For the special singularities one has either $(D, D, A_1, A_3)_0$ for even or $(D, D, A_1, A_4)_0$ for odd states.
- States in $T_{(1,1)}$ or $T_{(1,3)}$ transform as $(D, D, D, D)_1$ or $(D, D, D, D)_3$, respectively.

APPENDIX B

SO(10) shifts and matter representations

In this appendix we summarize the matter spectrum in all twisted sectors for all shifts that lead to SO(10) gauge factor without any other Wilson lines in table B.1. The shifts are enumerated in the first column and can be found in appendix B of [117]. In the third column we check for couplings of the form **161610** in the untwisted sector exists which is a necessary condition for gauge-top and gauge-Higgs unification.

Table B.1: The chiral spectrum of all $\mathbb{Z}_2 \times \mathbb{Z}_4$ gauge embeddings that include an SO(10) gauge factor separated by their twisted sector contribution.

Model	Untwisted	GTU	(0,3)	(0,2)	(0,1)	(1,0)	(1,3)	(1,2)	(1,1)
4	4(**10**), 2($\overline{\mathbf{16}}$)	✓	**10**,**16**	**10**	**10**,**16**	**10**,**16**	**16**	**10**,**16**	**16**	**10**,**16**	**10**
			10,$\overline{\mathbf{16}}$	**10**	**10**,**16**	**10**,$\overline{\mathbf{16}}$	**10**	**10**,**16**	**10**	**10**,**16**	$\overline{\mathbf{16}}$
8	4(**10**), 2($\overline{\mathbf{16}}$)	✓	**10**,**16**	**10**	**10**,**16**	**10**,**16**					
			10,$\overline{\mathbf{16}}$	**10**	**10**,**16**	**10**,$\overline{\mathbf{16}}$					
16	4(**10**), 2($\overline{\mathbf{16}}$)	✓		**16**	**10**,**16**	**10**	**16**	**10**,**16**	**10**	**10**,**16**	
			10	**16**	**10**,**16**		**10**	**10**,**16**	**16**	**10**,**16**	
24	4(**10**), 2($\overline{\mathbf{16}}$)	✓		**16**	**10**,**16**	**10**					
			10	**16**	**10**,**16**						
26	4(**10**), 2($\overline{\mathbf{16}}$)	✓	**10**	$\overline{\mathbf{16}}$	**10**,$\overline{\mathbf{16}}$	**10**					
51	(**1**, **16**), (**1**, $\overline{\mathbf{16}}$), (**2**, **10**), (**2**, $\overline{\mathbf{16}}$)	✓	(**1**, **10**)		(**1**, $\overline{\mathbf{16}}$)				(**1**, **10**)		
			(**1**, **16**)		(**1**, **10**)			(**1**, **10**)	(**1**, **10**)		
52	2(**10**), 2(**16**), 2($\overline{\mathbf{16}}$)	✓2	**16**		**10**	**16**	**10**,**16**				**10**
			10		$\overline{\mathbf{16}}$	**10**	**10**,**16**				
53	2(**10**), 2(**16**), 2($\overline{\mathbf{16}}$)	✓2	**16**		**10**			**10**	**10**,$\overline{\mathbf{16}}$		
			10		$\overline{\mathbf{16}}$			$\overline{\mathbf{16}}$	**10**,$\overline{\mathbf{16}}$	**10**	
54	2(**10**), 2(**16**), 2($\overline{\mathbf{16}}$)	✓	**16**		**10**						
			10		$\overline{\mathbf{16}}$						
57	(**1**, **16**), (**1**, $\overline{\mathbf{16}}$), (**2**, **10**), (**2**, $\overline{\mathbf{16}}$)	✓	(**1**, **10**)		(**1**, **16**)	(**1**, **10**)	(**1**, **10**)				
			(**1**, $\overline{\mathbf{16}}$)		(**1**, **10**)		(**1**, **10**)				
59	(**2**, **2**, **10**),(**1**, **2**, **16**), (**2**, **1**, **16**)	✓	(**1**, **1**, **10**)	(**1**, **1**, **10**)							
				(**1**, **1**, **10**)	(**1**, **1**, **10**)						

Model	Untwisted	GTU	(0,3)	(0,2)		(0,1)	(1,0)		(1,3)	(1,2)		(1,1)
62	$(\mathbf{4},\overline{\mathbf{16}})$	X	$(\mathbf{1},\mathbf{16})$	$(\mathbf{1},\mathbf{10})$	$(\mathbf{1},\mathbf{10})$						$(\mathbf{1},\mathbf{10})$	
				$(\mathbf{1},\mathbf{10})$	$(\mathbf{1},\mathbf{10})$	$(\mathbf{1},\overline{\mathbf{16}})$				$(\mathbf{1},\mathbf{10})$	$(\mathbf{1},\mathbf{10})$	$(\mathbf{1},\overline{\mathbf{16}})$
63	$(\mathbf{4},\mathbf{16})$	X		$(\mathbf{1},\mathbf{10})$	$(\mathbf{1},\mathbf{10})$	$(\mathbf{1},\overline{\mathbf{16}})$	$(\mathbf{1},\mathbf{10})$					
			$(\mathbf{1},\mathbf{16})$	$(\mathbf{1},\mathbf{10})$	$(\mathbf{1},\mathbf{10})$		$(\mathbf{1},\mathbf{10})$	$(\mathbf{1},\mathbf{10})$				$(\mathbf{1},\mathbf{16})$
66	$(\mathbf{1},\mathbf{16})$, $(\mathbf{1},\overline{\mathbf{16}})$, $(\mathbf{2},\mathbf{10})$, $(\mathbf{2},\overline{\mathbf{16}})$	✓								$(\mathbf{1},\mathbf{10})$	$(\mathbf{1},\mathbf{10})$	
											$(\mathbf{1},\mathbf{10})$	
67_1	$2(\mathbf{10})$, $2(\mathbf{16})$, $2(\overline{\mathbf{16}})$	✓2					$\mathbf{16}$	$\mathbf{10},\mathbf{16}$				
							$\mathbf{10}$	$\mathbf{10},\mathbf{16}$				
67_2	$(\mathbf{4},\overline{\mathbf{16}})$	X	$(\mathbf{1},\mathbf{16})$	$(\mathbf{1},\mathbf{10})$	$(\mathbf{1},\mathbf{10})$					$(\mathbf{1},\mathbf{10})$	$(\mathbf{1},\mathbf{10})$	
				$(\mathbf{1},\mathbf{10})$	$(\mathbf{1},\mathbf{10})$	$(\mathbf{1},\overline{\mathbf{16}})$					$(\mathbf{1},\mathbf{10})$	
68_1	$2(\mathbf{10})$, $2(\mathbf{16})$, $2(\overline{\mathbf{16}})$	✓2								$\overline{\mathbf{16}}$	$\mathbf{10},\overline{\mathbf{16}}$	
										$\mathbf{10}$	$\mathbf{10},\overline{\mathbf{16}}$	
68_2	$(\mathbf{4},\mathbf{16})$	X		$(\mathbf{1},\mathbf{10})$	$(\mathbf{1},\mathbf{10})$	$(\mathbf{1},\overline{\mathbf{16}})$	$(\mathbf{1},\mathbf{10})$	$(\mathbf{1},\mathbf{10})$				
			$(\mathbf{1},\mathbf{16})$	$(\mathbf{1},\mathbf{10})$	$(\mathbf{1},\mathbf{10})$			$(\mathbf{1},\mathbf{10})$				
69	$2(\mathbf{10})$, $2(\mathbf{16})$, $2(\overline{\mathbf{16}})$	✓2										
												$\mathbf{10}$
70	$2(\mathbf{10})$, $2(\mathbf{16})$, $2(\overline{\mathbf{16}})$	✓2										
73	$(\mathbf{1},\mathbf{16})$, $(\mathbf{1},\overline{\mathbf{16}})$, $(\mathbf{2},\mathbf{10})$, $(\mathbf{2},\overline{\mathbf{16}})$	✓					$(\mathbf{1},\mathbf{10})$					
							$(\mathbf{1},\mathbf{10})$	$(\mathbf{1},\mathbf{10})$				
74	$(\mathbf{2},\mathbf{1},\mathbf{16})$ $(\mathbf{1},\mathbf{2},\overline{\mathbf{16}})$	X		$(\mathbf{1},\mathbf{1},\mathbf{10})$	$(\mathbf{1},\mathbf{1},\mathbf{10})$	$(\mathbf{1},\mathbf{1},\overline{\mathbf{16}})$						
			$(\mathbf{1},\mathbf{1},\mathbf{16})$	$(\mathbf{1},\mathbf{1},\mathbf{10})$	$(\mathbf{1},\mathbf{1},\mathbf{10})$							
78	$4(\mathbf{10})$, $2(\overline{\mathbf{16}})$	✓		$\mathbf{10}$	$\mathbf{10},\mathbf{16}$		$\mathbf{16}$	$\mathbf{10},\mathbf{16}$		$\mathbf{16}$	$\mathbf{10},\mathbf{16}$	
				$\mathbf{10}$	$\mathbf{10},\mathbf{16}$		$\mathbf{10}$	$\mathbf{10},\mathbf{16}$		$\mathbf{10}$	$\mathbf{10},\mathbf{16}$	
84	$4(\mathbf{10})$, $2(\overline{\mathbf{16}})$	✓		$\mathbf{10}$	$\mathbf{10},\mathbf{16}$							$\overline{\mathbf{16}}$
				$\mathbf{10}$	$\mathbf{10},\mathbf{16}$							$\mathbf{10}$
86	$4(\mathbf{10})$, $2(\overline{\mathbf{16}})$	✓		$\mathbf{10}$	$\mathbf{10},\overline{\mathbf{16}}$							
				$\mathbf{10}$	$\mathbf{10},\overline{\mathbf{16}}$							
88	$4(\mathbf{10})$, $2(\overline{\mathbf{16}})$	✓		$\mathbf{10}$	$\mathbf{10},\mathbf{16}$							
				$\mathbf{10}$	$\mathbf{10},\mathbf{16}$							
96	$(\mathbf{2},\mathbf{2},\mathbf{10})$,$(\mathbf{1},\mathbf{2},\mathbf{16})$, $(\mathbf{2},\mathbf{1},\mathbf{16})$	✓		$(\mathbf{1},\mathbf{1},\mathbf{10})$	$(\mathbf{1},\mathbf{1},\mathbf{10})$							
				$(\mathbf{1},\mathbf{1},\mathbf{10})$	$(\mathbf{1},\mathbf{1},\mathbf{10})$							$(\mathbf{1},\mathbf{1},\mathbf{16})$
97	$(\mathbf{2},\mathbf{2},\mathbf{10})$,$(\mathbf{1},\mathbf{2},\mathbf{16})$, $(\mathbf{2},\mathbf{1},\mathbf{16})$	✓		$(\mathbf{1},\mathbf{1},\mathbf{10})$	$(\mathbf{1},\mathbf{1},\mathbf{10})$							
				$(\mathbf{1},\mathbf{1},\mathbf{10})$	$(\mathbf{1},\mathbf{1},\mathbf{10})$							
107	$4(\mathbf{10})$, $2(\overline{\mathbf{16}})$	✓				$\mathbf{10}$	$\mathbf{16}$	$\mathbf{10},\mathbf{16}$				
			$\mathbf{10}$				$\mathbf{10}$	$\mathbf{10},\mathbf{16}$				
108	$4(\mathbf{10})$, $2(\overline{\mathbf{16}})$	✓				$\mathbf{10}$				$\mathbf{10}$	$\mathbf{10},\mathbf{16}$	
			$\mathbf{10}$							$\mathbf{16}$	$\mathbf{10},\mathbf{16}$	
109	$4(\mathbf{10})$, $2(\overline{\mathbf{16}})$	✓				$\mathbf{10}$						
			$\mathbf{10}$									
129	$(\mathbf{4},\overline{\mathbf{16}})$	X			$(\mathbf{1},\mathbf{10})$					$(\mathbf{1},\mathbf{10})$	$(\mathbf{1},\mathbf{10})$	
					$(\mathbf{1},\mathbf{10})$						$(\mathbf{1},\mathbf{10})$	
130	$(\mathbf{2},\mathbf{1},\mathbf{16})$ $(\mathbf{1},\mathbf{2},\overline{\mathbf{16}})$	X			$(\mathbf{1},\mathbf{1},\mathbf{10})$							$(\mathbf{1},\mathbf{1},\mathbf{10})$
					$(\mathbf{1},\mathbf{1},\mathbf{10})$							
131	$(\mathbf{2},\mathbf{1},\mathbf{16})$ $(\mathbf{1},\mathbf{2},\overline{\mathbf{16}})$	X			$(\mathbf{1},\mathbf{1},\mathbf{10})$							
					$(\mathbf{1},\mathbf{1},\mathbf{10})$							
139	$(\mathbf{4},\mathbf{16})$	X			$(\mathbf{1},\mathbf{10})$			$(\mathbf{1},\mathbf{10})$				
					$(\mathbf{1},\mathbf{10})$		$(\mathbf{1},\mathbf{10})$	$(\mathbf{1},\mathbf{10})$				

APPENDIX C

The complete spectrum of the $\mathbb{Z}_2 \times \mathbb{Z}_4$ toy model

Here we give the complete spectrum of the toy model we have defined in section 3.3. We summarize the matter content but for convenience we only give the charges under the MSSM gauge group in table C.1.

#	Rep.	label	#	Rep.	label
3	$(\overline{\mathbf{3}},\mathbf{1},\mathbf{1},\mathbf{1})_{\frac{2}{3}}$	$\overline{u}$	69	$(\mathbf{1},\mathbf{1},\mathbf{1},\mathbf{1})_{0}$	n
3	$(\mathbf{1},\mathbf{1},\mathbf{1},\mathbf{1})_{-1}$	$\overline{e}$	32	$(\mathbf{1},\mathbf{1},\mathbf{1},\mathbf{1})_{-\frac{1}{2}}$	r
3	$(\mathbf{3},\mathbf{2},\mathbf{1},\mathbf{1})_{-\frac{1}{6}}$	q	4	$(\mathbf{1},\mathbf{1},\mathbf{1},\mathbf{2})_{-\frac{1}{2}}$	b
4	$(\mathbf{1},\mathbf{2},\mathbf{1},\mathbf{1})_{\frac{1}{2}}$	l	30	$(\mathbf{1},\mathbf{1},\mathbf{1},\mathbf{1})_{\frac{1}{2}}$	$\overline{r}$
1	$(\mathbf{1},\mathbf{2},\mathbf{1},\mathbf{1})_{-\frac{1}{2}}$	$\overline{l}$	4	$(\mathbf{1},\mathbf{1},\overline{\mathbf{3}},\mathbf{1})_{0}$	s
9	$(\overline{\mathbf{3}},\mathbf{1},\mathbf{1},\mathbf{1})_{-\frac{1}{3}}$	$\overline{d}$	10	$(\mathbf{1},\mathbf{1},\mathbf{1},\mathbf{2})_{0}$	$\tilde{v}$
6	$(\mathbf{3},\mathbf{1},\mathbf{1},\mathbf{1})_{\frac{1}{3}}$	d	8	$(\mathbf{1},\mathbf{1},\mathbf{3},\mathbf{1})_{0}$	$\overline{s}$
6	$(\mathbf{3},\mathbf{1},\mathbf{1},\mathbf{1})_{-\frac{1}{6}}$	f	2	$(\mathbf{1},\mathbf{1},\overline{\mathbf{3}},\mathbf{1})_{\frac{1}{2}}$	χ
8	$(\mathbf{1},\mathbf{2},\mathbf{1},\mathbf{1})_{0}$	v	5	$(\mathbf{1},\mathbf{1},\mathbf{1},\mathbf{2})_{\frac{1}{2}}$	$\overline{b}$
1	$(\mathbf{3},\mathbf{1},\mathbf{1},\mathbf{2})_{-\frac{1}{6}}$	m	2	$(\mathbf{1},\mathbf{1},\overline{\mathbf{3}},\mathbf{1})_{-\frac{1}{2}}$	$\tilde{\chi}$
8	$(\overline{\mathbf{3}},\mathbf{1},\mathbf{1},\mathbf{1})_{\frac{1}{6}}$	$\overline{f}$			

Table C.1: Matter spectrum obtained after switching on the WLs, the numbers in parenthesis label its corresponding representation under $SU(3)_C \times SU(2)_L \times SU(3) \times SU(2)$. The subindex labels the hypercharge.

APPENDIX D

List of charges for A_1^9 classification

In this appendix we give the full classification of A_1^9 Gepner models and their discrete quotients.
In the table D.1 we list the charge vectors of the nine chiral superfields under the respective $\mathbb{Z}_3$ discrete symmetry. However note that we only list the models that are inequivalent up to mirror symmetry. All the other ones can be obtained by *mirror symmetry* specified by the $\mathbb{Z}_3^{7-N}$ discrete symmetry where the mirror map is given by equation (4.42). Moreover we compute for each model the massless fermionic fields both charged and uncharged under the E_6 gauge group. The first row we give the amount of gauginos charged in a given representation and hence the amount of additional vector multiplets. In the second row we give the left chiral superfields. Note for example that we find in the case of higher supersymmetry chiral multiplets charged in the adjoint representation as well as gauginos in the **27** plet representation.

Figure D.1: Charge assignment and matter content for all A_1^9 Fermat point. The models are inequivalent up to charge rotations and mirror symmetry and sorted by the amount of 4D supersymmetries.

S	27	$\overline{27}$	Adj.						
				$\mathcal{N}=4$					
32 96	3 9	3 9	1 3	(1,1,1,0,0,0,0,0,0) (0,0,0,1,1,1,0,0,0)	(1,1,1,0,0,0,0,0,0) (0,0,0,1,1,1,0,0,0) (0,0,0,0,0,0,1,-1,0)	(1,1,1,0,0,0,0,0,0) (0,0,0,1,1,1,0,0,0) (0,0,0,0,1,-1,1,-1,0)			
86 258	3 9	3 9	1 3	(1,1,1,0,0,0,0,0,0) (0,0,0,1,1,1,0,0,0) (1,-1,0,1,-1,0,1,1,-1,0)					
				$\mathcal{N}=2$					
14 194	1 21	1 21	1 1	(1,1,1,0,0,0,0,0,0)	(1,2,0,0,0,0,0,0,0) (0,0,0,1,1,1,0,0,0)	(1,2,0,1,2,0,0,0,0) (0,0,0,0,0,0,1,1,1)	(1,2,0,0,0,0,0,0,0) (0,0,1,1,1,1,1,1,1)		
14 194	1 21	1 21	1 1	(1,1,1,0,0,0,0,0,0) (0,0,1,1,1,0,0,0,0) (0,0,0,0,0,1,1,1,0)	(1,2,0,0,0,0,0,0,0) (0,0,0,1,2,0,0,0,0) (0,0,0,0,0,0,1,1,1)	(1,2,0,0,0,0,0,0,0) (0,2,1,0,0,0,0,0,0) (0,0,0,1,2,0,0,0,0)	(1,2,0,1,2,0,0,0,0) (0,2,1,1,2,0,0,0,0) (0,0,0,0,0,0,1,2,0)		
14 194	1 3	1 3	1 1	(1,2,0,1,1,1,0,0,0) (0,0,0,1,1,1,1,1,1)	(1,1,1,0,0,0,0,0,0) (0,0,0,1,1,1,0,0,0) (0,0,1,1,1,0,1,2,0)	(1,1,1,1,2,0,0,0,0) (0,0,0,1,1,1,0,0,0) (0,0,0,0,0,0,0,1,2,0)	(1,2,0,1,2,0,0,0,0) (0,2,1,0,2,1,0,0,0) (1,1,1,0,0,0,1,2,0)		
14 194	1 9	1 9	1 1	(1,1,1,0,0,0,0,0,0) (1,2,0,1,2,0,1,2,0)	(1,2,0,1,2,0,0,0,0) (0,1,2,0,0,0,0,0,0) (0,1,0,1,1,0,1,2,0)	(1,2,0,1,2,0,0,0,0) (0,2,1,0,2,1,0,0,0) (1,1,0,0,1,0,1,2,0)			
32 248	1 9	1 9	1 1	(1,1,1,0,0,0,0,0,0) (1,2,0,1,2,0,0,0,0)	(1,2,0,1,2,0,0,0,0) (0,0,0,1,1,1,0,0,0) (0,0,0,0,0,0,1,2,0)	(1,2,0,1,2,0,0,0,0) (1,1,1,0,0,0,0,0,0) (0,0,0,2,1,0,1,2,0)			
				$\mathcal{N}=1, \chi=0$					
8 252	0 13	0 13	1 0	(1,1,1,1,2,0,0,0,0) (0,1,0,0,0,0,1,1,0)	(1,2,0,0,0,0,0,0,0) (0,1,0,0,1,0,0,1,0) (0,0,0,1,1,1,0,0,0)	(1,2,0,0,0,0,0,0,0) (0,1,0,1,1,0,1,2,0) (0,0,0,1,1,1,0,0,0)	(1,2,0,0,0,0,0,0,0) (0,2,1,0,0,0,0,0,0) (0,1,0,1,1,0,1,2,0)		
8 252	0 9	0 9	1 0	(1,2,0,1,2,0,0,0,0) (0,1,0,0,1,1,1,2,0) (0,0,0,0,1,0,0,1,1)					
14 270	0 9	0 9	1 0	(1,1,1,1,2,0,0,0,0) (0,1,0,2,1,0,1,1,0) (1,0,0,0,0,0,0,1,1)					
8 252	0 7	0 7	1 0	(1,2,0,1,2,0,0,0,0) (2,1,0,0,0,0,1,1,1) (1,0,0,0,0,1,0,0,1)					
				$\mathcal{N}=1$ **Mirror Pairs**					
8 252	0 84	0 0	1 0	(0,0,0,0,0,0,0,0,0)	(1,2,0,0,0,0,0,0,0)	(1,2,0,0,0,0,0,0,0) (0,0,0,1,2,0,0,0,0)	(1,2,0,0,0,0,0,0,0) (0,0,0,1,2,0,0,0,0) (0,0,0,0,0,0,1,2,0)		
8 252	0 0	0 84	1 0	(1,1,1,0,0,0,0,0,0) (0,1,0,0,1,1,0,0,0) (0,1,0,0,0,0,0,1,1)					
8 252	0 40	0 4	1 0	(1,1,1,1,2,0,0,0,0)	(1,1,1,1,1,1,0,0,0) (0,0,0,0,0,0,1,1,0)	(1,2,0,1,2,0,0,0,0) (0,0,0,0,0,0,0,1,2,0)	(1,2,0,0,0,0,0,0,0) (0,2,1,1,1,1,0,0,0) (0,0,0,0,0,1,1,1,0)	(1,0,0,1,1,1,1,1,0) (0,1,0,1,1,1,1,1,0) (0,0,1,1,1,1,1,1,0)	(1,2,0,1,2,0,0,0,0) (0,0,0,0,0,0,1,2,0) (0,0,0,0,0,0,2,0,1)
8 252	0 4	0 40	1 0	(1,1,1,0,0,0,0,0,0) (0,1,0,1,1,0,0,0,0)	(1,2,0,0,0,0,0,0,0) (0,0,0,1,1,1,0,0,0) (0,0,0,0,1,0,1,1,0)	(0,0,1,1,1,0,0,0,0) (0,1,0,1,1,0,0,0,0) (1,0,0,1,1,0,0,0,0)			
14 270	0 36	0 0	1 0	(1,2,0,1,2,0,0,0,0)	(1,2,0,1,2,0,1,2,0) (0,0,1,0,0,2,0,0,0)	(1,2,0,1,2,0,0,0,0) (2,1,0,0,1,2,1,2,0)	(1,2,0,0,0,0,0,0,0) (0,1,0,1,1,0,1,2,0) (0,0,1,0,0,2,0,0,0)	(1,2,0,1,2,0,0,0,0) (2,1,0,1,2,0,0,0,0) (0,0,0,0,0,0,1,2,0)	
14 270	0 0	0 36	1 0	(1,1,1,0,0,0,0,0,0) (0,1,0,1,1,0,0,0,0) (0,0,0,0,0,1,0,1,1,0)					
32 324	0 36	0 0	1 0	(1,2,0,1,2,0,1,2,0) (2,1,2,2,1,0,0,0,1)	(1,2,0,1,2,0,0,0,0) (0,2,0,0,0,1,1,2,0) (0,1,2,0,0,2,0,0,1)				
32 324	0 0	0 36	1 0	(1,0,0,0,2,1,1,1,0) (0,1,0,1,1,1,0,2,0)	(0,0,1,2,1,1,1,0,0)				
8 252	0 24	0 12	1 0	(1,1,1,2,2,2,0,0,0)	(1,2,0,1,1,1,0,0,0) (0,0,0,0,0,0,1,2,0)	(1,2,0,0,0,0,0,0,0) (1,0,2,1,2,0,0,0,0) (0,0,0,0,0,0,1,2,0)	(1,2,0,1,2,0,0,0,0) (0,1,2,0,0,0,0,0,0) (0,1,1,0,1,0,1,2,0)	(1,2,0,0,0,0,0,0,0) (0,1,1,1,0,0,0,0,0) (0,0,0,2,1,0,0,0,0)	
8 252	0 12	0 24	1 0	(1,2,0,1,2,0,0,0,0) (0,1,0,0,1,1,2,1,0)	(1,2,0,1,2,0,0,0,0) (0,2,1,0,2,1,0,0,0) (0,0,0,0,0,1,0,1,1)				
8 252	0 18	0 6	1 0	(1,2,0,0,0,0,0,0,0) (0,0,0,1,1,1,1,2,0)	(1,2,0,1,2,0,0,0,0) (0,1,0,0,1,0,0,1,2) (0,0,1,0,0,2,0,0,0)				
8 252	0 6	0 18	1 0	(1,2,0,1,2,0,0,0,0) (0,0,1,1,0,1,0,0,0) (0,0,0,0,0,0,1,1,1,0)					
14 270	0 18	0 6	1 0	(1,0,0,0,1,2,2,0,0) (0,1,2,2,1,0,0,0,0)	(1,0,0,0,0,2,2,1,0) (0,1,0,0,2,1,1,1,0) (0,0,1,2,0,0,0,0,0)	(1,0,0,0,2,1,1,1,0) (0,1,0,0,1,1,1,2,0) (0,0,1,2,1,1,1,0,0)			
14 270	0 6	0 18	1 0	(1,0,0,1,1,0,2,1,0) (0,1,2,1,1,1,0,0,0)	(1,0,0,0,1,1,2,1,0) (0,1,0,1,0,1,0,0,0) (0,0,1,1,1,0,0,0,0)	(1,0,0,0,2,2,0,1,0) (0,1,0,0,0,1,0,2,0) (0,0,1,2,1,1,1,0,0)			
8 252	0 16	0 4	1 0	(1,0,0,2,1,0,2,0,0) (0,1,2,1,1,1,0,0,0)	(1,0,0,0,2,1,1,1,0) (0,1,0,0,0,0,0,2,0) (0,0,1,2,1,1,1,0,0)				
8 252	0 4	0 16	1 0	(1,0,0,0,2,2,1,0,0) (0,1,0,1,0,1,0,0,0) (0,0,1,1,1,0,0,0,0)	(1,0,0,0,0,2,1,2,0) (0,1,0,0,2,1,1,1,0) (0,0,1,2,1,1,1,0,0)				
8 252	0 27	0 3	1 0	(1,0,0,0,0,2,2,1,0) (0,1,0,1,0,2,1,1,0) (0,0,1,1,1,0,0,0,0)					
8 252	0 3	0 27	1 0	(1,0,0,0,1,1,0,0,0) (0,1,0,1,0,1,0,0,0) (0,0,1,1,1,0,0,0,0)					
8 252	0 12	0 0	1 0	(1,0,0,0,2,1,0,2,0) (0,1,0,0,1,1,1,2,0) (0,0,1,2,1,1,1,0,0)					

APPENDIX E

The Maximally resolved $T^6/\mathbb{Z}_3$ LGO

We present the Landau Ginzburg Phase of the maximally resolved $T^6/\mathbb{Z}_3$ GLSM. The construction is similar to the minimal case, but this time we resolve the 27 orbifold not by just one divisor with one U(1) action but by 27 independent ones. Hence we introduce 27 independent $U(1)_{\alpha,\beta,\gamma}$ actions and 27 compensating fields $C'_{\alpha,\beta,\gamma}$. The charges and fields are summarized in table E.1. Again we attain the

	$\Phi^{1,i}$	$\Phi_{2,j}$	$\Phi_{3,k}$	C_1	C_2	C_3	$C'_{\alpha,\beta,\gamma}$
$U(1)_1$	1	0	0	-3	0	0	0
$U(1)_2$	0	1	0	0	-3	0	0
$U(1)_3$	0	0	1	0	0	-3	0
$U(1)_{\alpha,\beta,\gamma}$	$\delta_{i,\alpha}$	$\delta_{j,\beta}$	$\delta_{k,\gamma}$	0	0	0	$-3\delta_{i,\alpha}\delta_{j,\beta}\delta_{k,\gamma}$

Table E.1: Charge assignment of the maximally resolved $T^6/\mathbb{Z}_3$ orbifold [56].

Landau-Ginzburg phase by a complete Higgsing of of the C fields such that all U(1)'s break down completely and only $\mathbb{Z}_3$ subgroups are left over. The resulting charges are given in Table E.2. Note that the first three charges are simply the regular three discrete U(1)'s that form the torus that we show for simplicity. However these charges are not independent and can be absorbed in the R-charge generator but we show them for convenience. Thus we should always keep in mind that we have only six independent $\mathbb{Z}_3$ actions.
The other charge generators are suitable combinations of the first three charges minus the discrete subgroups of the residual charges.

E.1 Summary of the gauginos of the maximal $T^6/\mathbb{Z}_3$ mirror

In the following we present the full spectrum of the $\mathbb{Z}_3$ mirror model. We list the twisted sector (k_0, k_1) as well as the oscillator modes that act on the vacuum. The state is identified by calculating its q_+ charge. We consider the first twisted sectors in a bit more detail, as those give the generic E_6 gauge group for all models. The $(0,0)$ state has a vacuum with $E = 0$ and charges $(q_-, q_+) = (-\frac{3}{2}, -\frac{3}{2})$. This sector has not twist, and hence we have zero modes of the fields that can act on the vacuum. However we also note, that the vacuum itself contributes a state, namely a gaugino in the **16** of SO(10).
The same happens in the vacuum $|2,0\rangle$ that also has $E = 0$ and charges $(q_-, q_+) = (\frac{3}{2}, -\frac{3}{2})$. As this is a

	$\Phi_{1,1}$	$\Phi_{1,2}$	$\Phi_{1,3}$	$\Phi_{2,1}$	$\Phi_{2,2}$	$\Phi_{2,3}$	$\Phi_{3,1}$	$\Phi_{3,2}$	$\Phi_{3,3}$
$U(1)_R$	1	1	1	1	1	1	1	1	1
$\mathbb{Z}_3^1$	1	1	1	0	0	0	0	0	0
$\mathbb{Z}_3^2$	0	0	0	1	1	1	0	0	0
$\mathbb{Z}_3^3$	0	0	0	0	0	0	1	1	1
$\mathbb{Z}_3^4$	0	1	2	0	0	0	0	0	0
$\mathbb{Z}_3^5$	0	0	0	0	1	2	0	0	0
$\mathbb{Z}_3^6$	0	0	0	0	0	0	0	1	2
$\mathbb{Z}_3^7$	1	0	0	1	0	0	1	0	0

Table E.2: The charges for the LGO phase of the maximal resolved $\mathbb{Z}_3$ orbifold.

Sector	E_{vac}	q_{vac}	Vector Multiplets	Count
(1,0)	-1	(-3/2,-3/2)	$\phi^{a,i}_{-1/6}\bar{\phi}^{a,i}_{-5/6} - 2\psi^{a,i}_{-1/3}\bar{\psi}^{a,i}_{-2/3}\vert 1;0\rangle\,, a,i = 1\ldots 3$	9
(1,1)	$-1/2$	(-1,1/2)	$\bar{\phi}^{2,1}_{-1/6}\bar{\phi}^{2,2}_{-1/6}\bar{\phi}^{2,3}_{-1/6}\,\bar{\psi}^{1,1}_{0}\bar{\psi}^{1,2}_{0}\bar{\psi}^{1,3}_{0}\vert 1;1\rangle$	1
(3,1)	$-1/2$	(-1,1/2)	$\bar{\phi}^{1,1}_{-1/6}\bar{\phi}^{1,2}_{-1/6}\bar{\phi}^{1,3}_{-1/6}\,\bar{\psi}^{3,1}_{0}\bar{\psi}^{3,2}_{0}\bar{\psi}^{3,3}_{0}\vert 3;1\rangle$	1
(5,1)	$-1/2$	(-1,1/2)	$\bar{\phi}^{3,1}_{-1/6}\bar{\phi}^{3,2}_{-1/6}\bar{\phi}^{3,3}_{-1/5}\,\bar{\psi}^{2,1}_{0}\bar{\psi}^{2,2}_{0}\bar{\psi}^{2,3}_{0}\vert 5;1\rangle$	1
(1,2)	$-1/2$	(-1,1/2)	$\bar{\phi}^{1,1}_{-1/6}\bar{\phi}^{1,2}_{-1/6}\bar{\phi}^{1,3}_{-1/6}\,\bar{\psi}^{2,1}_{0}\bar{\psi}^{2,2}_{0}\bar{\psi}^{2,3}_{0}\vert 1;2\rangle$	1
(3,2)	$-1/2$	(-1,1/2)	$\bar{\phi}^{2,1}_{-1/6}\bar{\phi}^{2,2}_{-1/6}\bar{\phi}^{2,3}_{-1/6}\,\bar{\psi}^{3,1}_{0}\bar{\psi}^{3,2}_{0}\bar{\psi}^{3,3}_{0}\vert 3;2\rangle$	1
(5,2)	$-1/2$	(-1,1/2)	$\bar{\phi}^{3,1}_{-1/6}\bar{\phi}^{3,2}_{-1/6}\bar{\phi}^{3,3}_{-1/6}\,\bar{\psi}^{1,1}_{0}\bar{\psi}^{1,2}_{0}\bar{\psi}^{1,3}_{0}\vert 5;2\rangle$	1

Table E.3: All 15 additional gauginos, that belong to the additional vector states outside of SO(10). One of them is inside E_6, 8 enhance to SU(3) and six other come from the T^6 at the LGO Fermat point.

twisted sector, there are not zero modes that can act on the vacuum and thus no additional states apart from the vacuum itself. Hence this states in the $\overline{Q}$ cohomology contributes precisely one state, that is a gaugino with charge $\overline{\mathbf{16}}$. The vacuum $|1,0\rangle$ has Energy $E = -1$ and charges $(q_-, q_+) = (0, -\frac{3}{2})$. Acting with the Mayorana Weil Fermions λ^J gives

$$\lambda^I\lambda^J|1;0\rangle\,, \tag{E.1}$$

that are $\mathbf{45}_0$ gauginos inside of SO(10). Furthermore we can act with twisted oszillator states on the vacuum and get in total 9 additional gauginos. The trace over them is precisely the U(1) that enhances SO(10) to E_6. All states contribute additional vector states outside of E_6 that we summarize in the following table E.3. Note that we explicitly give the energy and charges of the vacuum, as well as the the explicit modes that act on the vacua.

APPENDIX F

The mass matrix of the LGO orbifold deformation

In this appendix we give the full coupling (4.76) of the Landau-Ginzburg orbifold depending on the VEV insertions VEVs a, b and c that correspond to the deformation to the orbifold phase:

$$\begin{pmatrix} \Phi^2_{111} \\ \Phi^2_{211} \\ \Phi^2_{311} \\ \Phi^2_{121} \\ \Phi^2_{221} \\ \Phi^2_{321} \\ \Phi^2_{131} \\ \Phi^2_{231} \\ \Phi^2_{331} \\ \Phi^2_{112} \\ \Phi^2_{212} \\ \Phi^2_{312} \\ \Phi^2_{122} \\ \Phi^2_{222} \\ \Phi^2_{322} \\ \Phi^2_{132} \\ \Phi^2_{232} \\ \Phi^2_{332} \\ \Phi^2_{113} \\ \Phi^2_{213} \\ \Phi^2_{313} \\ \Phi^2_{123} \\ \Phi^2_{223} \\ \Phi^2_{323} \\ \Phi^2_{133} \\ \Phi^2_{233} \\ \Phi^2_{333} \end{pmatrix}^T \begin{pmatrix} 0 & 0 & 0 & 0 & 0 & 0 & 0 & 0 & 0 & 0 & 0 & 0 & 0 & a & 0 & 0 & 0 & 0 & 0 & 0 & 0 & 0 & 0 & 0 & 0 & 0 & -a \\ 0 & 0 & 0 & 0 & 0 & 0 & 0 & 0 & 0 & 0 & 0 & 0 & -a & 0 & 0 & 0 & 0 & -b & 0 & 0 & 0 & 0 & 0 & -c & 0 & 0 & 0 \\ 0 & 0 & 0 & 0 & 0 & 0 & 0 & 0 & 0 & 0 & 0 & 0 & 0 & 0 & 0 & 0 & b & 0 & 0 & 0 & 0 & 0 & c & 0 & a & 0 & 0 \\ 0 & 0 & 0 & 0 & 0 & 0 & 0 & 0 & 0 & 0 & -a & 0 & 0 & 0 & 0 & 0 & 0 & -c & 0 & 0 & 0 & 0 & 0 & 0 & 0 & -2b & 0 \\ 0 & 0 & 0 & 0 & 0 & 0 & 0 & 0 & 0 & a & 0 & 0 & 0 & 0 & 0 & 0 & 0 & 0 & 0 & 0 & c & 0 & 0 & 0 & b & 0 & 0 \\ 0 & 0 & 0 & 0 & 0 & 0 & 0 & 0 & 0 & 0 & 0 & 0 & 0 & 0 & 0 & c & 0 & 0 & 0 & -c & 0 & 0 & 0 & 0 & 0 & 0 & 0 \\ 0 & 0 & 0 & 0 & 0 & 0 & 0 & 0 & 0 & 0 & 0 & 0 & 0 & 0 & c & 0 & 0 & 0 & 0 & 0 & a & 0 & b & 0 & 0 & 0 & 0 \\ 0 & 0 & 0 & 0 & 0 & 0 & 0 & 0 & 0 & 0 & b & 0 & 0 & 0 & 0 & 0 & 0 & 0 & 0 & 0 & 0 & -b & 0 & 0 & 0 & 0 & 0 \\ 0 & 0 & 0 & 0 & 0 & 0 & 0 & 0 & 0 & 0 & -b & 0 & -c & 0 & 0 & 0 & 0 & 0 & -a & 0 & 0 & 0 & 0 & 0 & 0 & 0 & 0 \\ 0 & 0 & 0 & 0 & -a & 0 & 0 & 0 & 0 & 0 & 0 & 0 & 0 & 0 & 0 & 0 & 0 & 0 & 0 & 0 & 0 & 0 & 0 & -b & 0 & -c & 0 \\ 0 & 0 & 0 & a & 0 & 0 & 0 & 0 & b & 0 & 0 & 0 & 0 & 0 & 0 & 0 & 0 & 0 & 0 & 0 & 0 & 0 & 0 & 0 & c & 0 & 0 \\ 0 & 0 & 0 & 0 & 0 & 0 & 0 & -b & 0 & 0 & 0 & 0 & 0 & 0 & 0 & 0 & 0 & 0 & 0 & 0 & 0 & 0 & b & 0 & 0 & 0 & 0 \\ 0 & a & 0 & 0 & 0 & 0 & 0 & 0 & c & 0 & 0 & 0 & 0 & 0 & 0 & 0 & 0 & 0 & 0 & 0 & 0 & -b & 0 & 0 & 0 & 0 & 0 \\ -a & 0 & 0 & 0 & 0 & 0 & 0 & 0 & 0 & 0 & 0 & 0 & 0 & 0 & 0 & 0 & 0 & 0 & 0 & 0 & 0 & 0 & 0 & 0 & 0 & 0 & a \\ 0 & 0 & 0 & 0 & 0 & 0 & -c & 0 & 0 & 0 & 0 & 0 & 0 & 0 & 0 & 0 & 0 & 0 & b & 0 & 0 & 0 & 0 & 0 & 0 & -a & 0 \\ 0 & 0 & 0 & 0 & 0 & -c & 0 & 0 & 0 & 0 & 0 & 0 & 0 & 0 & 0 & 0 & 0 & 0 & 0 & c & 0 & 0 & 0 & 0 & 0 & 0 & 0 \\ 0 & 0 & -b & 0 & 0 & 0 & 0 & 0 & 0 & 0 & 0 & 0 & 0 & 0 & 0 & 0 & 0 & 0 & 0 & -c & 0 & 0 & 0 & 0 & -a & 0 & 0 \\ 0 & b & 0 & c & 0 & 0 & 0 & 0 & 0 & 0 & 0 & 0 & 0 & 0 & 0 & 0 & 0 & 0 & 0 & 0 & 0 & 0 & 0 & a & 0 & 0 & 0 \\ 0 & 0 & 0 & 0 & 0 & 0 & 0 & 0 & a & 0 & 0 & 0 & 0 & 0 & -b & 0 & c & 0 & 0 & 0 & 0 & 0 & 0 & 0 & 0 & 0 & 0 \\ 0 & 0 & 0 & 0 & 0 & c & 0 & 0 & 0 & 0 & 0 & 0 & 0 & 0 & 0 & -c & 0 & 0 & 0 & 0 & 0 & 0 & 0 & 0 & 0 & 0 & 0 \\ 0 & 0 & 0 & 0 & -c & 0 & -a & 0 & 0 & 0 & 0 & 0 & b & 0 & 0 & 0 & 0 & 0 & 0 & 0 & 0 & 0 & 0 & 0 & 0 & 0 & 0 \\ 0 & 0 & 0 & 0 & 0 & 0 & 0 & b & 0 & 0 & 0 & -b & 0 & 0 & 0 & 0 & 0 & 0 & 0 & 0 & 0 & 0 & 0 & 0 & 0 & 0 & 0 \\ 0 & 0 & -c & 0 & 0 & 0 & -b & 0 & 0 & 0 & 0 & 0 & 0 & 0 & 0 & 0 & 0 & -a & 0 & 0 & 0 & 0 & 0 & 0 & 0 & 0 & 0 \\ 0 & c & 0 & 0 & 0 & 0 & 0 & 0 & 0 & b & 0 & 0 & 0 & 0 & 0 & 0 & a & 0 & 0 & 0 & 0 & 0 & 0 & 0 & 0 & 0 & 0 \\ 0 & 0 & -a & 0 & -b & 0 & 0 & 0 & 0 & -c & 0 & 0 & 0 & 0 & 0 & 0 & 0 & 0 & 0 & 0 & 0 & 0 & 0 & 0 & 0 & 0 & 0 \\ 0 & 0 & 0 & b & 0 & 0 & 0 & 0 & 0 & c & 0 & 0 & 0 & 0 & a & 0 & 0 & 0 & 0 & 0 & 0 & 0 & 0 & 0 & 0 & 0 & 0 \\ a & 0 & 0 & 0 & 0 & 0 & 0 & 0 & 0 & 0 & 0 & 0 & 0 & -a & 0 & 0 & 0 & 0 & 0 & 0 & 0 & 0 & 0 & 0 & 0 & 0 & 0 \end{pmatrix} \begin{pmatrix} \Phi^3_{111} \\ \Phi^3_{211} \\ \Phi^3_{311} \\ \Phi^3_{121} \\ \Phi^3_{221} \\ \Phi^3_{321} \\ \Phi^3_{131} \\ \Phi^3_{231} \\ \Phi^3_{331} \\ \Phi^3_{112} \\ \Phi^3_{212} \\ \Phi^3_{312} \\ \Phi^3_{122} \\ \Phi^3_{222} \\ \Phi^3_{322} \\ \Phi^3_{132} \\ \Phi^3_{232} \\ \Phi^3_{332} \\ \Phi^3_{113} \\ \Phi^3_{213} \\ \Phi^3_{313} \\ \Phi^3_{123} \\ \Phi^3_{223} \\ \Phi^3_{323} \\ \Phi^3_{133} \\ \Phi^3_{233} \\ \Phi^3_{333} \end{pmatrix}.$$

APPENDIX G

Weierstrass coefficients for a general cubic

In this appendix we give f and g in terms of the coefficients s_i with $i = 1, \ldots, 10$ for the most general cubic. The discriminant Δ is easily obtained by $\Delta = -16(4f^3 + 27g^2)$. If any restricted cubic is described as an elliptic curve, the respective coefficients should be simply taken to be zero.

$$
\begin{aligned}
f = \frac{1}{48}(&-(s_6^2 - 4(s_5 s_7 + s_3 s_8 + s_2 s_9))^2 + 24(-s_6(s_{10} s_2 s_3 - 9 s_1 s_{10} s_4 + s_4 s_5 s_8 \\
&+ s_2 s_7 s_8 + s_3 s_5 s_9 + s_1 s_7 s_9) + 2(s_{10} s_3^2 s_5 + s_1 s_7^2 s_8 + s_2 s_3 s_8 s_9 + s_1 s_3 s_9^2 \\
&+ s_7(s_{10} s_2^2 - 3 s_1 s_{10} s_3 + s_3 s_5 s_8 + s_2 s_5 s_9) + s_4(-3 s_{10} s_2 s_5 + s_2 s_8^2 + (s_5^2 - 3 s_1 s_8) s_9))))
\end{aligned}
\tag{G.1}
$$

$$
\begin{aligned}
g = \frac{1}{864}(&(s_6^2 - 4(s_5 s_7 + s_3 s_8 + s_2 s_9))^3 - 36(s_6^2 - 4(s_5 s_7 + s_3 s_8 + s_2 s_9)) \\
&\times (-s_6(s_{10} s_2 s_3 - 9 s_1 s_{10} s_4 + s_4 s_5 s_8 + s_2 s_7 s_8 + s_3 s_5 s_9 + s_1 s_7 s_9) \\
&+ 2(s_{10} s_3^2 s_5 + s_1 s_7^2 s_8 + s_2 s_3 s_8 s_9 + s_1 s_3 s_9^2 + s_7(s_{10} s_2^2 - 3 s_1 s_{10} s_3 + s_3 s_5 s_8 + s_2 s_5 s_9) \\
&+ s_4(-3 s_{10} s_2 s_5 + s_2 s_8^2 + (s_5^2 - 3 s_1 s_8) s_9))) + 216((s_{10} s_2 s_3 - 9 s_1 s_{10} s_4 + s_4 s_5 s_8 \\
&+ s_2 s_7 s_8 + s_3 s_5 s_9 + s_1 s_7 s_9)^2 + 4(-s_1 s_{10}^2 s_3^3 - s_1^2 s_{10} s_7^3 - s_4^2(27 s_1^2 s_{10}^2 + s_{10} s_5^3 \\
&+ s_1(-9 s_{10} s_5 s_8 + s_8^3)) + s_{10} s_3^2(-s_2 s_5 + s_1 s_6) s_9 - s_1 s_3^2 s_8 s_9^2 \\
&- s_7^2(s_{10}(s_2^2 s_5 - 2 s_1 s_3 s_5 - s_1 s_2 s_6) + s_1 s_8(s_3 s_8 + s_2 s_9)) \\
&- s_3 s_7(s_{10}(-s_2 s_5 s_6 + s_1 s_6^2 + s_2^2 s_8 + s_3(s_5^2 - 2 s_1 s_8) + s_1 s_2 s_9) \\
&+ s_9(s_2 s_5 s_8 - s_1 s_6 s_8 + s_1 s_5 s_9)) + s_4(-s_{10}^2(s_2^3 - 9 s_1 s_2 s_3) \\
&+ s_{10}(s_6(-s_2 s_5 s_6 + s_1 s_6^2 + s_2^2 s_8) + s_3(s_5^2 s_6 - s_2 s_5 s_8 - 3 s_1 s_6 s_8)) \\
&+ (s_{10}(2 s_2^2 s_5 + 3 s_1 s_3 s_5 - 3 s_1 s_2 s_6) + s_8(-s_3 s_5^2 + s_2 s_5 s_6 - s_1 s_6^2 - s_2^2 s_8 + 2 s_1 s_3 s_8)) s_9 \\
&+ (-s_2 s_5^2 + s_1 s_5 s_6 + 2 s_1 s_2 s_8) s_9^2 - s_1^2 s_9^3 + s_7(s_{10}(2 s_2 s_5^2 - 3 s_1 s_5 s_6 + 3 s_1 s_2 s_8 + 9 s_1^2 s_9) \\
&- s_8(s_2 s_5 s_8 - s_1 s_6 s_8 + s_1 s_5 s_9))))))
\end{aligned}
\tag{G.2}
$$

APPENDIX H

The complete Spectrum of F_{11}

Representation	Multiplicity	Splitting	Locus
$(\mathbf{3},\mathbf{2})_{-1/6}$	$\mathcal{S}_9([K_B^{-1}]+\mathcal{S}_7-\mathcal{S}_9)$	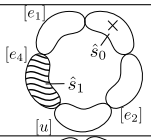	$V(I_{(1)}) := \{s_3 = s_9 = 0\}$
$(\mathbf{1},\mathbf{2})_{1/2}$	$([K_B^{-1}]+\mathcal{S}_7-\mathcal{S}_9)$ $(6[K_B^{-1}]-2\mathcal{S}_7-\mathcal{S}_9)$	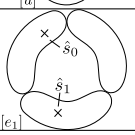	$V(I_{(2)}) := \{s_3 = 0$ $s_2 s_5^2 + s_1(s_1 s_9 - s_5 s_6) = 0\}$
$(\mathbf{3},\mathbf{1})_{-2/3}$	$\mathcal{S}_9(2[K_B^{-1}]-\mathcal{S}_7)$	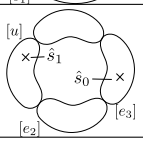	$V(I_{(3)}) := \{s_5 = s_9 = 0\}$
$(\mathbf{3},\mathbf{1})_{1/3}$	$\mathcal{S}_9(5[K_B^{-1}]-\mathcal{S}_7-\mathcal{S}_9)$	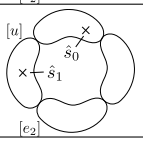	$V(I_{(4)}) := \{s_9 = 0$ $s_3 s_5^2 + s_6(s_1 s_6 - s_2 s_5) = 0\}$
$(\mathbf{1},\mathbf{1})_{-1}$	$(2[K_B^{-1}]-\mathcal{S}_7)$ $(3[K_B^{-1}]-\mathcal{S}_7-\mathcal{S}_9)$	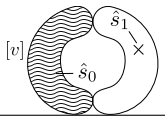	$V(I_{(5)}) := \{s_1 = s_5 = 0\}$
$(\mathbf{8},\mathbf{1})_0$	$1+\mathcal{S}_9\frac{\mathcal{S}_9-[K_B^{-1}]}{2}$	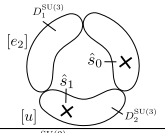	$s_9 = 0$
$(\mathbf{1},\mathbf{3})_0$	$1+\frac{\mathcal{S}_7-\mathcal{S}_9}{2}$ $\times([K_B^{-1}]+\mathcal{S}_7-\mathcal{S}_9)$	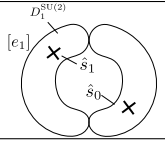	$s_3 = 0$

Table H.1: Charged matter representations under SU(3)×SU(2)×U(1) and corresponding codimension two fibers of $X_{F_{11}}$. We also include the codimension two constraints on the curve as well as the resulting multiplicities.

APPENDIX I

General base divisor classes of cubic and biquadric.

In this section we summarize the divisor classes of the cubic as well as the ones of the biquadric in terms of the base divisors classes $\mathcal{S}_7$, $\mathcal{S}_9$ and the anti-canonical class $[K_B^{-1}]$. Note that the classes have been chosen in such a way that s_9 transforms in $\mathcal{S}_9$. The divisor classes for the most general cubic i.e. the hypersurface in F_1 that is $\mathbb{P}^2$ is given as

section	Divisor Class
u	$H + \mathcal{S}_9 + [K_B]$
v	$H + \mathcal{S}_9 - \mathcal{S}_7$
w	H

section	Divisor Class
s_1	$3[K_B^{-1}] - \mathcal{S}_7 - \mathcal{S}_9$
s_2	$2[K_B^{-1}] - \mathcal{S}_9$
s_3	$[K_B^{-1}] + \mathcal{S}_7 - \mathcal{S}_9$
s_4	$2\mathcal{S}_7 - \mathcal{S}_9$
s_5	$2[K_B^{-1}] - \mathcal{S}_7$
s_6	$[K_B^{-1}]$
s_7	$\mathcal{S}_7$
s_8	$[K_B^{-1}] + \mathcal{S}_9 - \mathcal{S}_7$
s_9	$\mathcal{S}_9$
s_{10}	$2\mathcal{S}_9 - \mathcal{S}_7$

The divisor classes of the biquadric realized as F_2 or $\mathbb{P}^1 \times \mathbb{P}^1$:

section	Divisor Class
x	H_1
t	$H_1 + [K_B^{-1}] - \mathcal{S}_9$
y	H_2
s	$H_2 + [K_B^{-1}] - \mathcal{S}_7$

Section	Divisor Class
b_1	$3[K_B^{-1}] - \mathcal{S}_7 - \mathcal{S}_9$
b_2	$2[K_B^{-1}] - \mathcal{S}_9$
b_3	$[K_B^{-1}] + \mathcal{S}_7 - \mathcal{S}_9$
b_5	$2[K_B^{-1}] - \mathcal{S}_7$
b_6	$[K_B^{-1}]$
b_7	$\mathcal{S}_7$
b_8	$[K_B^{-1}] + \mathcal{S}_9 - \mathcal{S}_7$
b_9	$\mathcal{S}_9$
b_{10}	$\mathcal{S}_9 + \mathcal{S}_7 - [K_B^{-1}]$

APPENDIX J

Euler Numbers of Threefolds

In this appendix we present the Euler numbers for all elliptically fibered three-folds over a general base B and and the fiber realized as one of the 16 reflexive two dimensional polyhedra F_i. The calculations can be obtained by integrating the top Chern class c_3. The results only depend on the first Chern class c_1 of the base and presented in table J.1

Manifold	Euler number $\chi(X_{F_i})$
X_{F_1}	$-6(4c_1^2 - c_1\mathcal{S}_7 + \mathcal{S}_7^2 - c_1\mathcal{S}_9 - \mathcal{S}_7\mathcal{S}_9 + \mathcal{S}_9^2)$
X_{F_2}	$-4(6c_1^2 - 2c_1\mathcal{S}_7 + \mathcal{S}_7^2 - 2c_1\mathcal{S}_9 + \mathcal{S}_9^2)$
X_{F_3}	$-2(12c_1^2 - 3c_1\mathcal{S}_7 + 3\mathcal{S}_7^2 - 4c_1\mathcal{S}_9 - 2\mathcal{S}_7\mathcal{S}_9 + 2\mathcal{S}_9^2)$
X_{F_4}	$-4(6c_1^2 - 2c_1\mathcal{S}_7 + 3\mathcal{S}_7^2 - 2c_1\mathcal{S}_9 - 2\mathcal{S}_7\mathcal{S}_9 + \mathcal{S}_9^2)$
X_{F_5}	$-2(12c_1^2 - 4c_1\mathcal{S}_7 + 2\mathcal{S}_7^2 - 4c_1\mathcal{S}_9 - \mathcal{S}_7\mathcal{S}_9 + 2\mathcal{S}_9^2)$
X_{F_6}	$-2(12c_1^2 - 4c_1\mathcal{S}_7 + 4\mathcal{S}_7^2 - 4c_1\mathcal{S}_9 - 3\mathcal{S}_7\mathcal{S}_9 + 2\mathcal{S}_9^2)$
X_{F_7}	$-4(4c_1^2 + \mathcal{S}_7^2 - \mathcal{S}_7\mathcal{S}_9 + \mathcal{S}_9^2 - c_1(\mathcal{S}_7 + \mathcal{S}_9))$
X_{F_8}	$-2(12c_1^2 - 5c_1\mathcal{S}_7 + 3\mathcal{S}_7^2 - 4c_1\mathcal{S}_9 - 2\mathcal{S}_7\mathcal{S}_9 + 2\mathcal{S}_9^2)$
X_{F_9}	$-4(6c_1^2 - 2c_1\mathcal{S}_7 + \mathcal{S}_7^2 - 3c_1\mathcal{S}_9 + \mathcal{S}_9^2)$
$X_{F_{10}}$	$-6(4c_1^2 - 2c_1\mathcal{S}_7 + 2\mathcal{S}_7^2 - c_1\mathcal{S}_9 - 2\mathcal{S}_7\mathcal{S}_9 + \mathcal{S}_9^2)$
$X_{F_{11}}$	$-2(12c_1^2 - 4c_1\mathcal{S}_7 + 2\mathcal{S}_7^2 - 7c_1\mathcal{S}_9 - \mathcal{S}_7\mathcal{S}_9 + 3\mathcal{S}_9^2)$
$X_{F_{12}}$	$-2(12c_1^2 - 6c_1\mathcal{S}_7 + 2\mathcal{S}_7^2 - 6c_1\mathcal{S}_9 + \mathcal{S}_7\mathcal{S}_9 + 2\mathcal{S}_9^2)$
$X_{F_{13}}$	$-4(6c_1^2 - 2c_1\mathcal{S}_7 + \mathcal{S}_7^2 - 5c_1\mathcal{S}_9 + 2\mathcal{S}_9^2)$
$X_{F_{14}}$	$-2(12c_1^2 - 9c_1\mathcal{S}_7 + 3\mathcal{S}_7^2 - 6c_1\mathcal{S}_9 + 2\mathcal{S}_7\mathcal{S}_9 + 2\mathcal{S}_9^2)$
$X_{F_{15}}$	$-4(4c_1^2 - 2c_1\mathcal{S}_7 + \mathcal{S}_7^2 - 2c_1\mathcal{S}_9 + \mathcal{S}_9^2)$
$X_{F_{16}}$	$-6(4c_1^2 - 3c_1\mathcal{S}_7 + \mathcal{S}_7^2 - 3c_1\mathcal{S}_9 + \mathcal{S}_7\mathcal{S}_9 + \mathcal{S}_9^2)$

Table J.1: Summary of the Euler numbers of the three folds for the 16 F_i-fibered threefolds with general base B. c_1 denotes the first Chern class of the base and is given by its canonical class $[K_B]$.

APPENDIX K

Section redefinitions of F_2 in cubic form

In this appendix we give the sections $\tilde{s}_i$ of the restricted cubic in terms of the sections b_i of the biquadric that allow for the mapping. Note that the $\tilde{s}_i$ have square root factors of the b_i showing that this is not a birational map.

$$
\begin{aligned}
\tilde{s}_1 &= b_1\,, \\
\tilde{s}_2 &= \frac{1}{b_8}\left(b_2 b_8 - b_1 b_9 - b_1\sqrt{-4b_{10}b_8 + b_9^2}\right), \\
\tilde{s}_3 &= \frac{1}{b_8^2}\left(-2b_1 b_{10} b_8 + 2b_3 b_8^2 - b_2 b_8 b_9 + b_1 b_9^2 - b_2 b_8\sqrt{-4b_{10}b_8 + b_9^2} + b_1 b_9\sqrt{-4b_{10}b_8 + b_9^2}\right), \\
\tilde{s}_5 &= b_5\,, \\
\tilde{s}_6 &= \frac{1}{b_8}\left(b_6 b_8 - b_5 b_9 - b_5\sqrt{-4b_{10}b_8 + b_9^2}\right), \\
\tilde{s}_7 &= \frac{1}{b_8^2}\left(-2b_{10} b_5 b_8 + 2b_7 b_8^2 - b_6 b_8 b_9 + b_5 b_9^2 - b_6 b_8\sqrt{-4b_{10}b_8 + b_9^2} + b_5 b_9\sqrt{-4b_{10}b_8 + b_9^2}\right), \\
\tilde{s}_8 &= b_8\,, \\
\tilde{s}_9 &= -\sqrt{-4b_{10}b_8 + b_9^2}\,.
\end{aligned}
\tag{K.1}
$$

APPENDIX L

A Benchmark model beyond toric sections

1. Spectrum

Curve	q_1	q_2	M	N	Matter
10	-3	-1	3	0	$(Q+\bar{u}+\bar{e})_{1,2,3}$
$\overline{\mathbf{5}}_1$	9	-2	0	1	L_1
$\overline{\mathbf{5}}_2$	9	-7	1	-1	$\bar{d}_1$
$\overline{\mathbf{5}}_3$	-1	8	2	-1	$L_2+\bar{d}_{1,2}$
$\overline{\mathbf{5}}_4$	-1	-7	0	1	L_3
$\overline{\mathbf{5}}_5$	-6	8	0	1	H_d
$\overline{\mathbf{5}}_6$	-6	-2	0	-1	H_u

2. Singlet VEVs: s_1 , s_2

$$q(s_1) = (0, \pm 5)\,, \quad q(s_2) = (\pm 10, 0)\,.$$

3. μ- and β_i-terms

$$q(H_u L_i) = \begin{pmatrix} (15,0) \\ (5,10) \\ (5,-5) \end{pmatrix}, \quad q(H_u H_d) = (0,10)\ .$$

4. Yukawa couplings

$$q(Q\bar{u}H_u) = (0,0)\,, \qquad q(Q\bar{d}_j H_d) = \begin{pmatrix} (0,0) \\ (-10,15) \\ (-10,15) \end{pmatrix}, \qquad q(\bar{e}L_j H_d) = \begin{pmatrix} (0,5) \\ (-10,15) \\ (-10,0) \end{pmatrix}.$$

5. Allowed dimension five proton decay and Weinberg operators

$$q(\mathbf{10\,10\,10}\,L_i) = \begin{pmatrix} (0,-5) \\ (-10,5) \\ (-10,-10) \end{pmatrix}, \quad q(\mathbf{10\,10\,10}\,\bar{d}_i) = \begin{pmatrix} (0,-10) \\ (-10,5) \\ (-10,5) \end{pmatrix},$$
$$q(L_i\,L_j\,H_u\,H_u) = \begin{pmatrix} (30,0) & (20,10) & (20,-5) \\ (20,10) & (10,20) & (10,5) \\ (20,-5) & (10,5) & (10,-10) \end{pmatrix}.$$

6. Forbidden operators

$$q(\bar{u}\bar{d}_i\bar{d}_j) = \begin{pmatrix} (15,-15) & (5,0) & (5,0) \\ (5,0) & (-5,15) & (-5,15) \\ (5,0) & (-5,15) & (-5,15) \end{pmatrix}, \qquad q(\mathbf{1010}\bar{d}_i^*) = \begin{pmatrix} (-15,5) \\ (-5,-10) \\ (-5,-10) \end{pmatrix}.$$

Table L.1: Details of a benchmark model beyond the toric sections including the charges of all relevant operators

Bibliography

[1] Gerard 't Hooft. Renormalization of Massless Yang-Mills Fields. *Nucl.Phys.*, B33:173–199, 1971.

[2] Peter W. Higgs. Broken symmetries, massless particles and gauge fields. *Phys.Lett.*, 12:132–133, 1964.

[3] F. Englert and R. Brout. Broken Symmetry and the Mass of Gauge Vector Mesons. *Phys.Rev.Lett.*, 13:321–323, 1964.

[4] Georges Aad et al. Observation of a new particle in the search for the Standard Model Higgs boson with the ATLAS detector at the LHC. *Phys.Lett.*, B716:1–29, 2012.

[5] Serguei Chatrchyan et al. Observation of a new boson at a mass of 125 GeV with the CMS experiment at the LHC. *Phys.Lett.*, B716:30–61, 2012.

[6] S.L. Glashow. Partial Symmetries of Weak Interactions. *Nucl.Phys.*, 22:579–588, 1961.

[7] Abdus Salam. Weak and Electromagnetic Interactions. *Conf.Proc.*, C680519:367–377, 1968.

[8] Steven Weinberg. A Model of Leptons. *Phys.Rev.Lett.*, 19:1264–1266, 1967.

[9] K.A. Olive et al. Review of Particle Physics. *Chin.Phys.*, C38:090001, 2014.

[10] Y. Fukuda et al. Evidence for oscillation of atmospheric neutrinos. *Phys.Rev.Lett.*, 81:1562–1567, 1998.

[11] P.A.R. Ade et al. Planck 2013 results. XVI. Cosmological parameters. *Astron.Astrophys.*, 571:A16, 2014.

[12] Gerard 't Hooft and M.J.G. Veltman. One loop divergencies in the theory of gravitation. *Annales Poincare Phys.Theor.*, A20:69–94, 1974.

[13] S. Perlmutter et al. Measurements of Omega and Lambda from 42 high redshift supernovae. *Astrophys.J.*, 517:565–586, 1999.

[14] H. Georgi and S.L. Glashow. Unity of All Elementary Particle Forces. *Phys.Rev.Lett.*, 32:438–441, 1974.

[15] Tom Banks. Effective Lagrangian Description of Discrete Gauge Symmetries. *Nucl.Phys.*, B323:90, 1989.

[16] Lawrence M. Krauss and Frank Wilczek. Discrete Gauge Symmetry in Continuum Theories. *Phys.Rev.Lett.*, 62:1221, 1989.

[17] Renata Kallosh, Andrei D. Linde, Dmitri A. Linde, and Leonard Susskind. Gravity and global symmetries. *Phys.Rev.*, D52:912–935, 1995.

[18] Xian O. Camanho, Jose D. Edelstein, Juan Maldacena, and Alexander Zhiboedov. Causality Constraints on Corrections to the Graviton Three-Point Coupling. 2014.

[19] Hans Peter Nilles. Supersymmetry, Supergravity and Particle Physics. *Phys.Rept.*, 110:1–162, 1984.

[20] Michael B. Green and John H. Schwarz. Anomaly Cancellation in Supersymmetric D=10 Gauge Theory and Superstring Theory. *Phys.Lett.*, B149:117–122, 1984.

[21] Petr Horava and Edward Witten. Heterotic and type I string dynamics from eleven-dimensions. *Nucl.Phys.*, B460:506–524, 1996.

[22] Edward Witten. String theory dynamics in various dimensions. *Nucl.Phys.*, B443:85–126, 1995.

[23] Cumrun Vafa. Evidence for F theory. *Nucl.Phys.*, B469:403–418, 1996.

[24] Oleg Lebedev, Hans Peter Nilles, Stuart Raby, Saul Ramos-Sanchez, Michael Ratz, et al. A Mini-landscape of exact MSSM spectra in heterotic orbifolds. *Phys.Lett.*, B645:88–94, 2007.

[25] Maximilian Fischer, Michael Ratz, Jesus Torrado, and Patrick K.S. Vaudrevange. Classification of symmetric toroidal orbifolds. *JHEP*, 1301:084, 2013.

[26] Hans Peter Nilles, Saúl Ramos-Sánchez, Michael Ratz, and Patrick K.S. Vaudrevange. A note on discrete R symmetries in $\mathbb{Z}_6$-II orbifolds with Wilson lines. *Phys.Lett.*, B726:876–881, 2013.

[27] Nana G. Cabo Bizet, Tatsuo Kobayashi, Damian Kaloni Mayorga Pena, Susha L. Parameswaran, Matthias Schmitz, et al. Discrete R-symmetries and Anomaly Universality in Heterotic Orbifolds. *JHEP*, 1402:098, 2014.

[28] Shamit Kachru and Edward Witten. Computing the complete massless spectrum of a Landau-Ginzburg orbifold. *Nucl.Phys.*, B407:637–666, 1993.

[29] Paul S. Aspinwall, Ilarion V. Melnikov, and M. Ronen Plesser. (0,2) Elephants. *JHEP*, 1201:060, 2012.

[30] Jacques Distler and Shamit Kachru. Quantum symmetries and stringy instantons. *Phys.Lett.*, B336:368–375, 1994.

[31] Mikio Nakahara. *Geometry, topology, and physics*. Graduate student series in physics. Institute of Physics Publishing, Bristol, Philadelphia, 2003.

[32] Paul S. Aspinwall. K3 surfaces and string duality. pages 421–540, 1996.

[33] J. Polchinski. String theory. Vol. 2: Superstring theory and beyond. 1998.

[34] L. Dixon, J. A. Harvey, C. Vafa, and E. Witten. Strings on orbifolds. *Nuclear Physics B*, 261:678–686, 1985.

[35] L. Dixon, J. Harvey, C. Vafa, and E. Witten. Strings on orbifolds (ii). *Nuclear Physics B*, 274(2):285 – 314, 1986.

[36] Sebastian J.H. Konopka. Non Abelian orbifold compactifications of the heterotic string. *JHEP*, 1307:023, 2013.

[37] S. Hamidi and C. Vafa. Interactions on orbifolds. *Nuclear Physics B*, 279:465–513, January 1987.

[38] Florian Beye, Tatsuo Kobayashi, and Shogo Kuwakino. Gauge Origin of Discrete Flavor Symmetries in Heterotic Orbifolds. *Phys.Lett.*, B736:433–437, 2014.

[39] Tom Banks and Nathan Seiberg. Symmetries and Strings in Field Theory and Gravity. *Phys.Rev.*, D83:084019, 2011.

[40] Tatsuo Kobayashi, Hans Peter Nilles, Felix Ploger, Stuart Raby, and Michael Ratz. Stringy origin of non-Abelian discrete flavor symmetries. *Nucl.Phys.*, B768:135–156, 2007.

[41] Hans Peter Nilles, Saul Ramos-Sanchez, Patrick K.S. Vaudrevange, and Akin Wingerter. The Orbifolder: A Tool to study the Low Energy Effective Theory of Heterotic Orbifolds. *Comput.Phys.Commun.*, 183:1363–1380, 2012.

[42] Michael Blaszczyk, Stefan Groot Nibbelink, Michael Ratz, Fabian Ruehle, Michele Trapletti, et al. A Z2xZ2 standard model. *Phys.Lett.*, B683:340–348, 2010.

[43] Yasuhiko Katsuki, Yoshiharu Kawamura, Tatsuo Kobayashi, Yasuji Ono, Kazutaka Tanioka, et al. $Z(4)$ and $Z(6)$ Orbifold Models. *Phys.Lett.*, B218:169–175, 1989.

[44] L.E. Ibáñez, H.P. Nilles, and F. Quevedo. Reducing the rank of the gauge group in orbifold compactifications of the heterotic string. *Physics Letters B*, 192(3–4):332 – 338, 1987.

[45] Arthur Hebecker, Alexander K. Knochel, and Timo Weigand. A Shift Symmetry in the Higgs Sector: Experimental Hints and Stringy Realizations. *JHEP*, 1206:093, 2012.

[46] Pierre Hosteins, Rolf Kappl, Michael Ratz, and Kai Schmidt-Hoberg. Gauge-top unification. *JHEP*, 0907:029, 2009.

[47] S. Ferrara, L. Girardello, and Hans Peter Nilles. Breakdown of Local Supersymmetry Through Gauge Fermion Condensates. *Phys.Lett.*, B125:457, 1983.

[48] Hans Peter Nilles. Dynamically broken supergravity and the hierarchy problem. *Physics Letters B*, 115(3):193 – 196, 1982.

[49] Oleg Lebedev, Hans-Peter Nilles, Stuart Raby, Saul Ramos-Sanchez, Michael Ratz, et al. Low Energy Supersymmetry from the Heterotic Landscape. *Phys.Rev.Lett.*, 98:181602, 2007.

[50] Valeri Lowen and Hans Peter Nilles. Mirage Pattern from the Heterotic String. *Phys.Rev.*, D77:106007, 2008.

[51] Sven Krippendorf, Hans Peter Nilles, Michael Ratz, and Martin Wolfgang Winkler. The heterotic string yields natural supersymmetry. *Phys.Lett.*, B712:87–92, 2012.

[52] Hans Peter Nilles and Patrick K. S. Vaudrevange. Geography of Fields in Extra Dimensions: String Theory Lessons for Particle Physics. 2014.

[53] Michael Blaszczyk, Stefan Groot Nibbelink, Orestis Loukas, and Saul Ramos-Sanchez. Non-supersymmetric heterotic model building. *JHEP*, 1410:119, 2014.

[54] C.D. Froggatt and Holger Bech Nielsen. Hierarchy of Quark Masses, Cabibbo Angles and CP Violation. *Nucl.Phys.*, B147:277, 1979.

[55] Edward Witten. Phases of N=2 theories in two-dimensions. *Nucl.Phys.*, B403:159–222, 1993.

[56] Michael Blaszczyk, Stefan Groot Nibbelink, and Fabian Ruehle. Gauged Linear Sigma Models for toroidal orbifold resolutions. *JHEP*, 1205:053, 2012.

[57] Edward Witten. On the Landau-Ginzburg description of N=2 minimal models. *Int.J.Mod.Phys.*, A9:4783–4800, 1994.

[58] M. B. Green, J. H. Schwarz, and E. Witten. *Superstring Theory*. Cambridge University Press, 1987.

[59] Doron Gepner. Space-Time Supersymmetry in Compactified String Theory and Superconformal Models. *Nucl.Phys.*, B296:757, 1988.

[60] E.J. Chun, J. Mas, J. Lauer, and Hans Peter Nilles. Duality and Landau-ginzburg Models. *Phys.Lett.*, B233:141, 1989.

[61] A. Font, Luis E. Ibanez, and F. Quevedo. String Compactifications and $N = 2$ Superconformal Coset Constructions. *Phys.Lett.*, B224:79, 1989.

[62] C.A. Lutken and Graham G. Ross. Taxonomy of Heterotic Superconformal Field Theories. *Phys.Lett.*, B213:152, 1988.

[63] Brian R. Greene and M.R. Plesser. Duality in Calabi-Yau Moduli Space. *Nucl.Phys.*, B338:15–37, 1990.

[64] Paul S. Aspinwall and M. Ronen Plesser. Elusive Worldsheet Instantons in Heterotic String Compactifications. *Proc.Symp.Pure Math.*, 85:33–51, 2012.

[65] Timo Weigand. Lectures on F-theory compactifications and model building. *Class.Quant.Grav.*, 27:214004, 2010.

[66] C.M. Hull and P.K. Townsend. Unity of superstring dualities. *Nucl.Phys.*, B438:109–137, 1995.

[67] Ashoke Sen. Orientifold limit of F theory vacua. *Phys.Rev.*, D55:7345–7349, 1997.

[68] Frederik Denef. Les Houches Lectures on Constructing String Vacua. pages 483–610, 2008.

[69] Maximilian Kreuzer and Harald Skarke. On the classification of reflexive polyhedra. *Commun.Math.Phys.*, 185:495–508, 1997.

[70] Vincent Bouchard and Harald Skarke. Affine Kac-Moody algebras, CHL strings and the classification of tops. *Adv.Theor.Math.Phys.*, 7:205–232, 2003.

[71] Volker Braun, Thomas W. Grimm, and Jan Keitel. Geometric Engineering in Toric F-Theory and GUTs with U(1) Gauge Factors. *JHEP*, 1312:069, 2013.

[72] Jean-Pierre Serre. *Lectures on the Mordell-Weil theorem*. Aspects of Mathematics, E15. Friedr. Vieweg & Sohn, Braunschweig, 1989. Translated from the French and edited by Martin Brown from notes by Michel Waldschmidt.

[73] Christoph Mayrhofer, David R. Morrison, Oskar Till, and Timo Weigand. Mordell-Weil Torsion and the Global Structure of Gauge Groups in F-theory. *JHEP*, 1410:16, 2014.

[74] Volker Braun, Thomas W. Grimm, and Jan Keitel. New Global F-theory GUTs with U(1) symmetries. *JHEP*, 1309:154, 2013.

[75] Mirjam Cvetic, Denis Klevers, and Hernan Piragua. F-Theory Compactifications with Multiple U(1)-Factors: Constructing Elliptic Fibrations with Rational Sections. *JHEP*, 1306:067, 2013.

[76] Volker Braun and David R. Morrison. F-theory on Genus-One Fibrations. *JHEP*, 1408:132, 2014.

[77] David R. Morrison and Washington Taylor. Sections, multisections, and U(1) fields in F-theory. 2014.

[78] Noboru Nakayama. On weierstrass models. *Algebraic geometry and commutative algebra,*, Vol. II:pp. 405–431. Kinokuniya, 1988.

[79] Christoph Mayrhofer, Eran Palti, Oskar Till, and Timo Weigand. On Discrete Symmetries and Torsion Homology in F-Theory. 2014.

[80] Mirjam Cvetič, Ron Donagi, Denis Klevers, Hernan Piragua, and Maximilian Poretschkin. F-Theory Vacua with Z3 Gauge Symmetry. 2015.

[81] Kunihiko Kodaira. On compact analytic surfaces: Ii. *The Annals of Mathematics*, 77(3):563–626, 1963.

[82] Mboyo Esole, James Fullwood, and Shing-Tung Yau. D_5 elliptic fibrations: non-Kodaira fibers and new orientifold limits of F-theory. 2011.

[83] Craig Lawrie and Sakura Schäfer-Nameki. The Tate Form on Steroids: Resolution and Higher Codimension Fibers. *JHEP*, 1304:061, 2013.

[84] Hirotaka Hayashi, Craig Lawrie, David R. Morrison, and Sakura Schafer-Nameki. Box Graphs and Singular Fibers. *JHEP*, 1405:048, 2014.

[85] Daniel S. Park. Anomaly Equations and Intersection Theory. *JHEP*, 1201:093, 2012.

[86] David R. Morrison and Daniel S. Park. F-Theory and the Mordell-Weil Group of Elliptically-Fibered Calabi-Yau Threefolds. *JHEP*, 1210:128, 2012.

[87] Edward Witten. Phase transitions in M theory and F theory. *Nucl.Phys.*, B471:195–216, 1996.

[88] Washington Taylor. TASI Lectures on Supergravity and String Vacua in Various Dimensions. 2011.

[89] Ron Donagi and Martijn Wijnholt. Higgs Bundles and UV Completion in F-Theory. *Commun.Math.Phys.*, 326:287–327, 2014.

[90] Matthew J. Dolan, Joseph Marsano, Natalia Saulina, and Sakura Schafer-Nameki. F-theory GUTs with U(1) Symmetries: Generalities and Survey. *Phys.Rev.*, D84:066008, 2011.

[91] Emilian Dudas and Eran Palti. Froggatt-Nielsen models from E(8) in F-theory GUTs. *JHEP*, 1001:127, 2010.

[92] Ralph Blumenhagen, Mirjam Cvetic, Shamit Kachru, and Timo Weigand. D-Brane Instantons in Type II Orientifolds. *Ann.Rev.Nucl.Part.Sci.*, 59:269–296, 2009.

[93] Philip Candelas and Anamaria Font. Duality between the webs of heterotic and type II vacua. *Nucl.Phys.*, B511:295–325, 1998.

[94] Jan Borchmann, Christoph Mayrhofer, Eran Palti, and Timo Weigand. SU(5) Tops with Multiple U(1)s in F-theory. *Nucl.Phys.*, B882:1–69, 2014.

[95] Philip Candelas, Duiliu-Emanuel Diaconescu, Bogdan Florea, David R. Morrison, and Govindan Rajesh. Codimension three bundle singularities in F theory. *JHEP*, 0206:014, 2002.

[96] Denis Klevers, Damian Kaloni Mayorga Pena, Paul-Konstantin Oehlmann, Hernan Piragua, and Jonas Reuter. F-Theory on all Toric Hypersurface Fibrations and its Higgs Branches. *JHEP*, 1501:142, 2015.

[97] Hirotaka Hayashi, Craig Lawrie, and Sakura Schafer-Nameki. Phases, Flops and F-theory: SU(5) Gauge Theories. *JHEP*, 1310:046, 2013.

[98] Volker Braun, Thomas W. Grimm, and Jan Keitel. Complete Intersection Fibers in F-Theory. 2014.

[99] Christoph Mayrhofer, Eran Palti, Oskar Till, and Timo Weigand. Discrete Gauge Symmetries by Higgsing in four-dimensional F-Theory Compactifications. *JHEP*, 1412:068, 2014.

[100] Iñaki García-Etxebarria, Thomas W. Grimm, and Jan Keitel. Yukawas and discrete symmetries in F-theory compactifications without section. *JHEP*, 1411:125, 2014.

[101] Gabriele Honecker and Michele Trapletti. Merging Heterotic Orbifolds and K3 Compactifications with Line Bundles. *JHEP*, 0701:051, 2007.

[102] Luis E. Ibanez and Graham G. Ross. Discrete gauge symmetries and the origin of baryon and lepton number conservation in supersymmetric versions of the standard model. *Nucl.Phys.*, B368:3–37, 1992.

[103] Ron Donagi and Martijn Wijnholt. Breaking GUT Groups in F-Theory. *Adv.Theor.Math.Phys.*, 15:1523–1604, 2011.

[104] Erik Plauschinn. The Generalized Green-Schwarz Mechanism for Type IIB Orientifolds with D3- and D7-Branes. *JHEP*, 0905:062, 2009.

[105] Joseph Marsano. Hypercharge Flux, Exotics, and Anomaly Cancellation in F-theory GUTs. *Phys.Rev.Lett.*, 106:081601, 2011.

[106] Eran Palti. A Note on Hypercharge Flux, Anomalies, and U(1)s in F-theory GUTs. *Phys.Rev.*, D87:085036, 2013.

[107] Christoph Mayrhofer, Eran Palti, and Timo Weigand. Hypercharge Flux in IIB and F-theory: Anomalies and Gauge Coupling Unification. *JHEP*, 1309:082, 2013.

[108] Emilian Dudas and Eran Palti. On hypercharge flux and exotics in F-theory GUTs. *JHEP*, 1009:013, 2010.

[109] Christoph Ludeling, Hans Peter Nilles, and Claudia Christine Stephan. The Potential Fate of Local Model Building. *Phys.Rev.*, D83:086008, 2011.

[110] R. Barbier, C. Berat, M. Besancon, M. Chemtob, A. Deandrea, et al. R-parity violating supersymmetry. *Phys.Rept.*, 420:1–202, 2005.

[111] Max Kerstan and Timo Weigand. Fluxed M5-instantons in F-theory. *Nucl.Phys.*, B864:597–639, 2012.

[112] Jonathan J. Heckman and Cumrun Vafa. Flavor Hierarchy From F-theory. *Nucl.Phys.*, B837:137–151, 2010.

[113] Anamaria Font, Luis E. Ibanez, Fernando Marchesano, and Diego Regalado. Non-perturbative effects and Yukawa hierarchies in F-theory SU(5) Unification. *JHEP*, 1303:140, 2013.

[114] G.F. Giudice and A. Masiero. A Natural Solution to the mu Problem in Supergravity Theories. *Phys.Lett.*, B206:480–484, 1988.

[115] Ian Hinchliffe and Thomas Kaeding. B+L violating couplings in the minimal supersymmetric Standard Model. *Phys.Rev.*, D47:279–284, 1993.

[116] Herbi K. Dreiner, Christoph Luhn, and Marc Thormeier. What is the discrete gauge symmetry of the MSSM? *Phys.Rev.*, D73:075007, 2006.

[117] Damian Kaloni Mayorga Pena, Hans Peter Nilles, and Paul-Konstantin Oehlmann. A Zip-code for Quarks, Leptons and Higgs Bosons. *JHEP*, 1212:024, 2012.

List of Figures

List of Tables